Modelling Contaminant Transport In Saturated Pumice Sand and Alluvial Gravel Aquifer Media

A thesis
Submitted in partial fulfilment
of the requirements for the
degree of
Doctor of Philosophy
in Civil Engineering
in the
University of Canterbury

by

Liping Pang

Department of Civil Engineering
University of Canterbury
Christchurch, New Zealand

December 2002

Abstract

The objective of the studies presented in this thesis is to use modelling and experimental analyses to elucidate the important processes and mechanisms affecting contaminant transport in various groundwater systems and to establish values of transport parameters that could be used to describe these processes. The important contaminant transport processes and mechanisms explored in these studies include scale-dependent dispersion, interaction between sorption and first-order degradation, effects of pore-water velocity on chemical-nonequilibrium sorption, degradation and sorption of pesticides, die-off and filtration of microbes, and velocity-enhanced microbial transport (i.e. faster transport of microbes than conservative solute tracers).

Specifically, this thesis includes studies which (1) develop and validate solutions for a scale-dependent dispersion model, (2) validate a novel method of temporal moments, (3) model nonequilibrium transport of Cd, Zn and Pb in an alluvial gravel aquifer medium, (4) explore attenuation and transport of atrazine, hexazinone, procymidone, faecal bacteria and F-RNA phages in pumice sand aquifer media, (5) quantify setback distances between septic tanks and the shoreline of Lake Okareka based on transport of microbial indicators in a pumice sand aquifer and worst-case values for aquifer properties and effluent discharge, (6) introduce methods related to modelling non-linear equilibrium sorption, and (7) discuss other important issues involving contaminant transport in groundwater (e.g. preferential flow, maximum groundwater velocity, velocity enhancement due to size/anion exclusion) as well as issues related to contaminant transport modelling.

By calibrating a number of transport models with observed data, we have obtained descriptive parameters that characterize contaminant attenuation and transport in the selected aquifer systems. The methods presented in this work will allow researchers and groundwater resource managers to better understand, and therefore quantitatively predict, the fate and transport of contaminants in the subsurface. In addition, gaps in the current literature that are identified in this thesis and some of the ideas presented herein could be used for planning future research.

Acknowledgments

I would like to express my sincere appreciation to those who have assisted me during the course of this study. Firstly, I thank my employer, Institute of Environmental Science & Research Ltd. (ESR), for providing the research projects and funding for the study. I would like to thank my supervisor, Dr. Bruce Hunt, for his advice, encouragement, guidance, and for his genuine support. He has always made the effort to be available to answer my questions, help me understand the mathematics involved with contaminant transport models, and to review my manuscripts. His patience, particularly during my course work in the first year, is greatly appreciated. It has been a great experience working closely with Murray Close, my co-supervisor and immediate manager at ESR. I wish to express my gratitude to Murray for his supervision, valuable comments, suggestions, communications and association, and for the fun groundwater projects that he leads. Without his support, this study would be impossible. I am very lucky to have Professor Mark Goltz of the Air Force Institute of Technology, USA, as my co-supervisor. I am indebted to him for his consistent support, ideas and frequent discussions over the years. Working with him side-by-side for two weeks during his visit to New Zealand has brought a great deal to this study. I am also indebted to Greg Stanton, Mark Flintoft, Carollyn Hall and Daniela Schneider for their technical support. Without their assistance, this study would be impossible.

Thanks are also given to Dr. Rien van Genuchten of USSL and Dr. Tim Ginn of UC Davis for their recommendation to commence a Ph.D study through publications during my trip to California at the end of 1999. Their encouragement and inspiration initiated my motivation, without which, I may never have embarked upon this path. I also wish to acknowledge journal referees (Dr. Peter Wierenga, Dr. Hilaire De Smedt, Dr. Edward Sudicky, Dr. Rien van Genuchten, Dr. Mustafa Aral and other anonymous reviewers), and two external examiners (Dr. Markus Flury and Dr. Vince Bidwell) for their valuable comments that have significantly helped in improving the quality of this study.

Finally, I would like to thank my family for their unconditional love and my dear friends for their warm friendships, and for all the mental support they have given me.

Preface

The major content presented in this thesis is based on work that is part of ESR's project for the Foundation for Research, Science and Technology (FRST) "Reducing Contamination of Groundwaters". An exception is Chapter 6, estimation of septic tank setback distances, which is based on a sub-contract from the National Institute of Water & Atmospheric Research Ltd. (NIWA) and funded by the Rotorua District Council.

The core of this thesis comprises individual chapters that are organised in the form of scientific publications for refereed journals, although some additional studies are also included in each chapter. The publications are those that have been prepared after enrolment for the Ph.D study. As each publication is a team effort, the individual contributions are stated below:

(1)Chapter 2: Scale-dependent dispersion model. The model and solutions presented in this paper are credited to Dr. Bruce Hunt. With his guidance, I have learnt to derive the solutions of the model step by step. I carried out the column experiments with help from Greg Stanton; applied the model in simulating the experimental data; and drafted the manuscript. Bruce carefully polished the manuscript, putting it into good shape. Comments were also received from Mark Goltz and Murray Close.

(2)Chapter 3: Method of temporal moments. Both Mark Goltz and I independently derived the same solutions, but my work was aided by Bruce Hunt. Greg Stanton carried out the column experiment with supervision from Murray Close and myself. I completed the method validation using different models and drafted the manuscript. Mark thoroughly edited the draft manuscript and improved its organisation. Murray also gave comments and suggestions on the manuscript.

(3) Chapter 4: Chemical nonequilibrium transport of heavy metals. Murray Close and I supervised Daniela Schneider (a student from Germany) on the performance of column experiments, with some input from Greg Stanton. I carried out the experimental design using model predictions, completed model simulations, and drafted the manuscript. Analysis of the heavy metal samples was carried out by Daniela with assistance from Greg. Murray gave valuable comments and suggestions on the draft manuscript. Mark Goltz reviewed the manuscript prior to its

submission and discussed some issues mentioned in the additional study of the chapter.

(4) Chapter 5: Pesticide transport in pumice sand groundwater. My contribution to this paper is designing the tracer experiment using model predictions, carrying out the tracer experiment with Murray Close and staff of Landcare Research, completing data analysis and model simulations, and drafting the manuscript. Murray Close gave valuable advice throughout the study and reviewed the manuscript. Mark Goltz also gave detailed review comments on the manuscript. The additional study in this chapter is the result of a discussion with Mark Goltz.

(5) Chapter 6. Septic tank setback distances. This is based on a technical report prepared by Pang, L.; Davies, H.; Hall, C.; and Stanton, G. (2001) and reviewed by Close, M. and Sinton, L. My contribution to this paper is designing project and experiments, carrying out field experiments (assisted by a staff from NIWA), field sampling and laboratory batch tests, supervising Greg Stanton on column experiments, completing data analysis and model simulations, and writing up the manuscript. Microbial samples were analysed by Carollyn Hall, and Br samples were analysed by Greg Stanton. Helen Davies reviewed the setback distances used by regional councils in New Zealand (Table 1). Murray Close and Lester Sinton reviewed the manuscript and discussed the project proposal and experiments. I had frequent discussions with Mark Goltz on the details of modelling microbial transport. The additional study of the chapter is also a result of the discussion with Mark. Bruce Hunt proofread the first draft of the manuscript.

Others who are not among the co-authors but have also made contributions have been acknowledged in the individual papers. It should be noted that ESR's FRST project includes (a) pesticide leaching through soils and transport in groundwater, (b) transport of contaminants (heavy metals, micro-organisms and pesticides) in groundwater, and (c) preferential flow in unsaturated zones. Only a small fraction of the above project, mainly (b), is presented in this thesis. Other works have been presented by Murray Close and Lester Sinton. During my Ph.D study, I have also carried out modelling work and been a co-author in a number of papers drafted by Murray and Lester. However, this thesis only includes the manuscripts that I was principal author.

Table of contents

Chapter 1

Introduction

1.1 Background

Soil and groundwater contamination (for example, by microbes, heavy metals, organics, and pesticides) from municipal, industrial, and agricultural activities is a world-wide environmental problem. Modelling the processes of attenuation and transport of contaminants in subsurface systems is a very important specialization in the new field of contaminant hydrogeology. The use of transport models helps us to gain an understanding of the processes that govern the movement and fate of contaminants in the subsurface; knowing that it is critical to protect human and environmental receptors from the deleterious effects of these contaminants.

By calibrating transport models with observed data, we can characterise contaminant attenuation and transport in a specific system using descriptive parameters, such as groundwater flow velocity, dispersivity, sorption coefficient (or retardation factor), degradation rate, mass transfer rates, and so on. These calibrated parameter values together with transport models could then be used by others (e.g. government agencies, regional authorities, and consultants) to manage similar systems for various purposes (e.g. resource management, land-use planning, design of monitoring programs, risk analysis, choosing alternatives in feasibility studies, and cleanup). Compared to actual measurements in the field, model simulations using realistic parameter values are a much more cost and time effective way of obtaining the understanding necessary to make decisions on how best to manage very complex systems

1.2 Scope and objectives

This study focuses on model simulations of data measured in both laboratory and field experiments for a range of contaminants in pumice sand (Chapters 3, 5, and 6) and alluvial gravel (Chapters 2 and 4). The work presented in this study deals with contaminant transport in fully-saturated groundwater flow.

The contaminants involved in this study include conservative solute tracers (tritiated water and bromide), heavy metals (Cd, Zn, Pb), microbes (*E. coli*, F-RNA phages), and pesticides (atrazine, hexazinone, and procymidone).

The objective of this study is to use modeling and experimental analyses to elucidate the important processes and mechanisms of subsurface contaminant transport for the systems investigated and to establish values of transport parameters that could be used to describe these processes. The selected contaminants and aquifer media commonly occur in New Zealand, and the results are expected to be applicable both in New Zealand and at other locations having similar conditions.

1.3 Contaminant transport models

The study involves the use of established transport models (Chapters 2-6), development of a scale-dependent dispersion model (Chapter 2), and validation of new temporal moment solutions (Chapter 3).

A number of transport models are used in this study. The specific model employed in each situation depended on the nature of the problem and capabilities of the model. CXTFIT (Toride et al., 1995) is used to simulate equilibrium and nonequilibrium transport for the data obtained from column experiments (Chapters 2, 3, 4 and 6). AT123D (Yeh, 1981) is used to predict microbial transport under equilibrium conditions for the determination of septic tank setback distances in a pumice sand aquifer (Chapter 6). N3DADE (Leij and Toride, 1997) is used to describe nonequilibrium transport of pesticides and conservative tracers for the data obtained from a field experiment (Chapter 5). The scale-dependent dispersion model, SDM, is used to simulate solute transport along an 8-m long column with multiple sampling locations (Chapter 2). The method of temporal moments, MOM, is applied to transport of organic solutes with concurrent sorption and degradation (Chapter 3).

Calibration of models is achieved through inverse modelling. However, of the models used in this study only CXTFIT contains an inverse modelling capability. For the models without this capability, a powerful optimization package, PEST (Doherty et al., 1994), which can optimize parameters for any model, is used. An exception is that calibration of SDM is carried out using the Solver function of Excel.

1.4 Thesis outline

The work presented in this thesis is organized chronologically (i.e. earliest work to latest work). In Chapter 2, analytical solutions are developed for a one-dimensional scale-dependent dispersion model and the solutions are experimentally verified for a pulse source using an 8-m long pea-gravel column. In Chapter 3, we apply and validate solutions for breakthrough curve temporal moments where advective/dispersive solute transport is affected by concurrent sorption and degradation. Analyses are carried out using experimental data obtained from a pumice sand column as well as some data obtained from the literature. In Chapter 4, we examine the effect of pore-water velocity on non-equilibrium transport of heavy metals (Cd, Zn, and Pb) in alluvial gravel aquifer material. In Chapter 5, non-equilibrium transport of pesticides (atrazine, hexazinone, and procymidone) in a pumice sand aquifer under field conditions is investigated. In Chapter 6, we determine septic tank setback distances based on transport of *E. coli* and F-RNA phages in a pumice sand aquifer.

The core of each chapter is a paper that has been prepared for publishing in the peer-reviewed literature. After examiners' comments, some of these core chapters have some minor revisions even though four of them had been published by the time of thesis examination. At the end of each chapter, additional studies relevant to the paper are presented. The problems and issues discussed in the additional studies were not included in the publications. Some of these additional studies were completed after publication of the paper, while others were not included in the paper due to constraints on journal article length or suitability for inclusion.

In Chapter 7, I further discuss the topics investigated in the previous chapters and provide additional linkage between the chapters. I also discuss some other important contaminant transport issues, which are relevant to the previous chapters. Applications of the study and ideas for future research are also presented. Finally, a summary and conclusions are presented in Chapter 8.

Chapter 2

Solutions and verification of a scale-dependent dispersion model

Liping Pang[1], Bruce Hunt[2]. 2001. Solution and verification of a scale-dependent dispersion model. Journal of Contaminant Hydrology 53(1-2): 21-39.

Minor revision was made after the publishing (mainly Section 2.2.4).

Author affiliations:

[1] Institute of Environmental Science & Research Ltd., PO Box 29181, Christchurch, New Zealand

[2] Department of Civil Engineering, University of Canterbury, Private Bag 4800, Christchurch, New Zealand

Journal Referees:

Dr. Rien van Genuchten, George E. Brown, Jr. Salinity Laboratory, USDA-ARS, Riverside, California, USA.

Professor Mustafa M. Aral, School of Civil & Environmental Engineering Georgia Institute of Technology, Atlanta, Georgia, USA.

Abstract

In this paper, analytical solutions are derived for a one-dimensional scale-dependent dispersion model (SDM) considering linear equilibrium sorption and first-order degradation for continuous and pulse contaminant sources with a constant input concentration in a semi-infinite uniform porous medium. In the SDM model, dispersivity α_x is replaced with a constant ε multiplied by the transport distance x. The solution for a pulse source is verified experimentally in the analysis of tritium data obtained from an 8-m long homogenous pea-gravel column with multiple sampling locations, and the results are compared with those analysed by a commonly used solution of a constant dispersion model (CDM). The SDM predicts concentrations satisfactorily at all sampling locations, while the CDM fits the experimental data well for only one location. Both models are then calibrated for each individual concentration breakthrough curve using local values for either ε in the SDM or α_x in the CDM. Both models give equally good fits for appropriate choices of individual ε and α_x values, and both indicate a linear increase in α_x with distance. The ε values tend to change little as x increases and are expected to approach a constant at relatively large distances downstream. Hence, predictions from the SDM should become more accurate as x increases.

Keywords: Scale-dependent dispersion; Analytical solution; Equilibrium transport; Groundwater

2.1. Introduction

It is well known that dispersivity generally increases with transport distance in groundwater systems (Molz et al., 1983; Domenico and Robbins, 1984; Gelhar et al., 1992; Rajaram and Gelhar, 1993). However, most commonly used groundwater contaminant transport analytical models are based on governing equations with constant dispersion coefficients. When applying a constant dispersion model to simulate data at multiple locations for a multi-location system, model predictions often under or overestimate the

experimental data when a single dispersion coefficient is used for all locations, for example, as shown in a study of Sinton et al. (2000). An alternative approach for modelling a multi-location system is to fit the model to data from each sampling location. Thus, for each location a different constant dispersion coefficient is used (e.g., Ptak and Teutsch 1994; Zhang et al., 1994; Pang and Close, 1999).

Researchers have also evaluated other approaches to deal with scale-related dispersion problems, for example, the use of numerical solutions (Pickens and Grisak, 1981a; Jayawardena and Lui, 1984; Mishra and Parker, 1989) and stochastic analysis (Wheatcraft and Tyler, 1988; Roco et al., 1989; Zhang et al., 1994). The finite element model developed by Pickens and Grisak (1981a) allows dispersivity to vary temporally as a function of the mean travel distance. Similarly, the numerical model of Jayawardena and Lui (1984) considers the dispersion coefficient a function of time. Zhang et al. (1994) use a stochastical convection-dispersion equation based on travel time probability density functions as modified by Jury and Roth (1990), in which a distance-dependent dispersion coefficient is defined. Wheatcraft and Tyler (1988) developed Lagrangian models for dispersion in a single fractal streamtube and for a set of fractal streamtubes and allow dispersivity to be proportional to the travel distance. Scale-dependent dispersion is also incorporated in the model of Mishra and Parker (1989).

Relatively few researchers have developed analytical solutions for scale-dependent dispersion. Yates (1990, 1992) obtained one-dimensional solutions for uniform flow with constant concentration or constant flux boundary conditions when the medium has a linearly or exponentially increasing dispersion coefficient. Huang et al. (1996) also presented analytical solutions for scale-dependent dispersion, assuming dispersivity increases linearly with distance until some distance after which dispersivity reaches an asymptotic value. Logan (1996) derived an analytical solution for the one-dimensional equations incorporating rate-limited sorption and first-order decay under time varying boundary conditions, assuming an exponentially increasing dispersion coefficient. However, the solutions given by Yates (1990, 1992), Huang et al. (1996), and Logan (1996) are complex and difficult to

evaluate. These authors consider molecular diffusion, which increases the complexity of their solutions. In many groundwater problems, this additional complexity is unnecessary since molecular diffusion is generally insignificant. Ignoring molecular diffusion, Hunt (1998) developed one-, two-, and three-dimensional analytical solutions of a scale-dependent dispersion equation for unsteady flow with an instantaneous source and for steady flow with a continuous source. However, solutions obtained by Hunt (1998) are for infinite model domains, while some groundwater problems require solutions for semi-infinite domains. Furthermore, only a conservative solute is considered in Hunt's solution. Alternatively, Aral and Liao (1996) developed analytical solutions for two-dimensional advection-dispersion equation with a time-dependent dispersion coefficient. None of these studies have compared their analytical solutions with experimental data.

This paper presents exact solutions in relatively simple form for both continuous and pulse sources in a semi-infinite domain. Molecular diffusion is assumed negligible and mechanical dispersion is assumed to increase linearly with distance downstream. The solutions also include first-order degradation together with linear equilibrium sorption that is instantaneous and reversible. The solution for a pulse source is verified by comparing model simulations with actual experimental data for a nonsorbing and nondegrading tracer.

2.2. Theory

2.2.1. Governing equations and solutions of the scale-dependent dispersion model (SDM)

One dimensional solute transport in saturated, homogenous porous media with linearly increasing dispersion, linear equilibrium sorption, and first-order degradation in the dissolved phase can be described by

$$\frac{\partial}{\partial x}\left(\varepsilon x V \frac{\partial c}{\partial x}\right) = V\frac{\partial c}{\partial x} + R\frac{\partial c}{\partial t} + \lambda c \qquad (2.1)$$

where c = contaminant concentration in solution (M/L^3), V = average pore-water velocity (L/T), x = longitudinal distance (L), R = retardation factor, t = time (T), ε = dispersivity/distance ratio (L/L), and λ = first-order degradation rate constant (T^{-1}). Equation 2.1 can be compared with the constant dispersion equation

$$D\frac{\partial^2 c}{\partial x^2}=V\frac{\partial c}{\partial x}+R\frac{\partial c}{\partial t}+\lambda c \tag{2.2}$$

The only difference between Eq.2.1 and Eq.2.2 is that the variable mechanical dispersion coefficient, εxV, in Eq.2.1 has been replaced with the constant mechanical dispersion coefficient D (L^2/T) in Eq.2.2. In other words, εx has been replaced with dispersivity α_x (L). A more general form is given by Yates (1990), who used $\varepsilon xV + D_0$ to replace εxV in Eq.2.1, where D_0 is a constant molecular diffusion coefficient (L^2/T). However, as noted earlier, molecular diffusion is often insignificant compared with mechanical dispersion and can be ignored in many groundwater problems. Experimental data presented in this paper will verify that the assumption $D_0 << \varepsilon xV$ is valid for the experimental conditions of this study. Thus, molecular diffusion is neglected in Eq.2.1.

The solution for a continuous source in a semi-infinite system must satisfy Eq.2.1 and the following initial and boundary conditions:

$$c(x,0)=0 \qquad 0<x<\infty \tag{2.3}$$

$$c(0,t)=c_0 \qquad 0<t<\infty \tag{2.4}$$

$$c(\infty,t)=0 \qquad 0<t<\infty \tag{2.5}$$

in which c_0 = constant source concentration (M/L^3). Setting

$$c(x,t)=e^{-\lambda t/R}\varphi(x,t) \tag{2.6}$$

we find that $\varphi(x, t)$ is a solution of the following problem:

$$\frac{\partial}{\partial x}\left(\varepsilon x V\frac{\partial \varphi}{\partial x}\right)=V\frac{\partial \varphi}{\partial x}+R\frac{\partial \varphi}{\partial t} \tag{2.7}$$

$$\varphi(x, 0)=0 \qquad 0<x<\infty \tag{2.8}$$

$$\varphi(0,t)=c_0 e^{\lambda t/R} \qquad 0<t<\infty \tag{2.9}$$

$$\varphi(\infty,t)=0 \qquad 0<t<\infty \tag{2.10}$$

The Duhamel superposition integral (Hildebrand, 1976) gives the solution for φ in the following form:

$$\varphi(x,t)=c_0\psi(x,t)+\int_0^t \psi(x,t-\tau)\frac{d(c_0 e^{\lambda\tau/R})}{d\tau}d\tau \tag{2.11}$$

where τ is a dummy integration variable and $\psi(x, t)$ is the solution of the following problem:

$$\frac{\partial}{\partial x}\left(\varepsilon x V\frac{\partial\psi}{\partial x}\right)=V\frac{\partial\psi}{\partial x}+R\frac{\partial\psi}{\partial t} \tag{2.12}$$

$$\psi(x, 0)=0 \qquad 0<x<\infty \tag{2.13}$$

$$\psi(0,t)=1 \qquad 0<t<\infty \tag{2.14}$$

$$\psi(\infty,t)=0 \qquad 0<t<\infty \tag{2.15}$$

Introducing the dimensionless variables $\Psi(X, T) = \psi(x, t)$, $X = x/L$ and $T = Vt/L$, where L is some unspecified length scale, transforms the problem for ψ into the following problem for Ψ:

$$\frac{\partial}{\partial X}\left(\varepsilon \mathrm{X}\frac{\partial\Psi}{\partial \mathrm{X}}\right)=\frac{\partial\Psi}{\partial X}+R\frac{\partial\Psi}{\partial T} \tag{2.16}$$

$$\Psi(X,0)=0 \qquad 0<X<\infty \tag{2.17}$$

$$\Psi(0,T)=1 \qquad 0<T<\infty \tag{2.18}$$

$$\Psi(\infty,T)=0 \qquad 0<T<\infty \tag{2.19}$$

Since rewriting the solution for $\Psi(X, T)$ in dimensional variables must lead to a solution for $\psi(x, t)$ in which L does not appear, we see that X and T must appear in $\Psi(X, T)$ in a combination that causes L to cancel. This will occur if $\Psi(X, T)$ is obtained from the following similarity transformation

$$\Psi(X,T)=f(\beta) \tag{2.20}$$

where

$$\beta = RX/T = Rx/(Vt) \tag{2.21}$$

Introduction of Eqs.2.20-2.21 into Eqs.2.16-2.19 gives the following problem for $f(\beta)$:

$$(\varepsilon\beta f')' - f'(1-\beta) = 0 \tag{2.22}$$

$$f(0) = 1 \tag{2.23}$$

$$f(\infty) = 0 \tag{2.24}$$

where primes are used to denote differentiation with respect to β. Solution of Eqs. 2.22-2.24 gives the following result for $f(\beta)$:

$$f(\beta) = 1 - \frac{\gamma(\frac{1}{\varepsilon}, \frac{\beta}{\varepsilon})}{\Gamma(\frac{1}{\varepsilon})} \qquad \beta = \frac{Rx}{Vt} \tag{2.25}$$

where Γ is the gamma function and γ is the incomplete gamma function, which are defined by

$$\Gamma(\frac{1}{\varepsilon}) = \int_0^{\infty} y^{(\frac{1}{\varepsilon}-1)} e^{-y}\, dy \tag{2.26}$$

$$\gamma(\frac{1}{\varepsilon}, \frac{\beta}{\varepsilon}) = \int_0^{\beta/\varepsilon} y^{(\frac{1}{\varepsilon}-1)} e^{-y}\, dy \tag{2.27}$$

Mathematical details for the derivation of Eq.2.25 are given in Appendix A.

An integration by parts in Eq.2.11, using Eq.2.13 allows φ(x,t) to be rewritten in the form

$$\varphi(x,t) = c_0 \int_0^t \frac{\partial\psi(x, t-\tau)}{\partial t} e^{\lambda\tau/R} d\tau \tag{2.28}$$

Since $\psi(x, t) = \Psi(X, T) = f(\beta)$, where β is given by Eq.2.21, calculation of $\partial\psi(x, t-\tau)/\partial t$ from Eq.2.25 and 2.27 and substitution of the result in Eqs.2.28 and 2.6 gives the solution for $c(x, t)$.

$$\frac{c(x,t)}{c_0}=\frac{1}{\Gamma(1/\varepsilon)}\int_0^t e^{-\frac{\lambda\tau}{R}-\frac{xR}{\varepsilon V\tau}}\left(\frac{xR}{\varepsilon V\tau}\right)^{1/\varepsilon}\frac{d\tau}{\tau} \tag{2.29}$$

Equation 2.29 is the solution for a constant, continuous source of concentration C_0. This solution has a much simpler form and therefore is easier to use than the solutions obtained by Yates (1990) and Huang et al. (1996).

Finally, since the governing equations are linear with coefficients that are time independent, the principles of superposition and time translation can be applied to Eq. 2.29 to obtain the following solution for a pulse source:

$$\frac{c(x,t)}{c_0}=\frac{1}{\Gamma(1/\varepsilon)}\int_0^t e^{-\frac{\lambda\tau}{R}-\frac{xR}{\varepsilon V\tau}}\left(\frac{xR}{\varepsilon V\tau}\right)^{1/\varepsilon}\frac{d\tau}{\tau} \qquad 0<t\le t_0 \tag{2.30a}$$

$$\frac{c(x,t)}{c_0}=\frac{1}{\Gamma(1/\varepsilon)}\int_0^t e^{-\frac{\lambda\tau}{R}-\frac{xR}{\varepsilon V\tau}}\left(\frac{xR}{\varepsilon V\tau}\right)^{1/\varepsilon}\frac{d\tau}{\tau}-\frac{1}{\Gamma(1/\varepsilon)}\int_0^{t-t_0} e^{-\frac{\lambda\tau}{R}-\frac{xR}{\varepsilon V\tau}}\left(\frac{xR}{\varepsilon V\tau}\right)^{1/\varepsilon}\frac{d\tau}{\tau}$$

$$t_0\le t<\infty \tag{2.30b}$$

in which t_0 is the time duration of the pulse (T). Equation 2.30 satisfies the following initial and boundary conditions:

$$c(x,0)=0 \qquad 0<x<\infty \tag{2.31}$$

$$c(0,t)=c_0 \qquad 0<t\le t_0 \tag{2.32}$$

$$c(0,t)=0 \qquad t_0\le t<\infty \tag{2.33}$$

$$c(\infty,t)=0 \qquad 0<t<\infty \tag{2.34}$$

2.2.2. Numerical evaluation of the SDM solutions

The numerical evaluation of Eqs.2.29 and 2.30 must be carried out carefully to avoid round-off errors that occur for small values of ε. Introducing the dimensionless variables $C^* = c/c_0$, $t^* = t\ V/(x\ R)$, $\tau^* = \tau\ V/(R\ x)$, $\lambda^* = \lambda\ x\ /\ V$ in Eq.2.29 results in the following dimensionless equation:

$$c^* = \frac{1}{\varepsilon^{1/\varepsilon}\Gamma(1/\varepsilon)} \int_0^{t^*} e^{-\lambda^*\tau^* - \frac{1}{\varepsilon\tau^*}} \frac{d\tau^*}{\tau^{*1/\varepsilon+1}} \tag{2.35}$$

Using Stirling's asymptotic formula for the gamma function

$$\varepsilon^{1/\varepsilon}\Gamma(1/\varepsilon) = e^{-1/\varepsilon} F(\varepsilon) \tag{2.36}$$

where

$$F(\varepsilon) = \sqrt{2\pi\varepsilon}\left(1 + \frac{\varepsilon}{12} + \frac{\varepsilon^2}{288} - \frac{139\varepsilon^3}{51840} - \frac{571\varepsilon^4}{2488320} + \ldots\ldots\right) \tag{2.37}$$

The error of approximation in using an asymptotic series such as Eq.2.37 has the same order of magnitude as the first neglected term provided that this neglected term has a smaller magnitude than the last term retained (Hildebrand, 1976). Therefore, the truncation series expansion in Eq.2.37 becomes more accurate as ε becomes smaller, and use of a value for ε =1 in Eq.2.37 can be expected to give an error of only about 0.02% in the calculation of $F(\varepsilon)$.

The use of Eq.2.36 and the identity $\tau^{*-1/\varepsilon} = e^{-1/\varepsilon \ln(\tau^*)}$ in Eq.2.35 leads to the following result:

$$c^* = \frac{1}{F(\varepsilon)} \int_0^{t^*} e^{-\lambda^*\tau^* - \frac{1}{\varepsilon}[1/\tau^* + \ln(\tau^*) - 1]} \frac{d\tau^*}{\tau^*} \tag{2.38}$$

The integrand in Eq.2.38 has finite values that become confined to a smaller and smaller region near $\tau^* = 1$ as ε approaches zero. Therefore, the integration interval $0 \le \tau^* \le t^*$ may be divided up into n equal steps where the number of steps is determined by

$$n = 2\,Integer\left(\frac{5t^*}{\sqrt{\varepsilon}} + 1\right) \tag{2.39}$$

The numerical integration was carried out using Simpson's rule. The numerical approximation of Eq.2.30 for a pulse source is obtained based on Eq.2.38 using the principles of superposition and time translation as below:

$$c^* = \frac{1}{F(\varepsilon)} \int_0^{t^*} e^{-\lambda^* \tau^* - \frac{1}{\varepsilon}[1/\tau^* + \ln(\tau^*) - 1]} \frac{d\tau^*}{\tau^*} \qquad 0 < t^* \le t_0^* \tag{2.40a}$$

$$c^* = \frac{1}{F(\varepsilon)} \int_0^{t^*} e^{-\lambda^* \tau^* - \frac{1}{\varepsilon}[1/\tau^* + \ln(\tau^*) - 1]} \frac{d\tau^*}{\tau^*} - \frac{1}{F(\varepsilon)} \int_0^{t^* - t_0^*} e^{-\lambda^* \tau^* - \frac{1}{\varepsilon}[1/\tau^* + \ln(\tau^*) - 1]} \frac{d\tau^*}{\tau^*} \qquad t_0^* \le t^* < \infty \tag{2.40b}$$

Equations 2.28 and 2.30a-2.30b are mathematically exact solutions of the stated problems. Numerical accuracy of the integration was tested by the usual method of increasing n until two successive calculations gave nearly identical results. The solutions of Yates (1990) and Huang et al. (1996) were judged to be too complicated to evaluate for comparisons with the solutions obtained herein.

2.2.3. Solutions of the constant dispersion model

As a conservative tracer was used in this study for experimental verification, the solution for a constant dispersion model without sorption and degradation was needed for purposes of comparison. According to Freeze and Cherry (1979) and Domenico and Schwartz (1990), the solution of Eq.2.2 for a continuous source with a non-reactive solute is

$$\frac{c}{c_0} = \frac{1}{2}\left[erfc\left(\frac{x - Vt}{2\sqrt{Dt}}\right) + \exp\left(\frac{Vx}{D}\right) erfc\left(\frac{x + Vt}{2\sqrt{Dt}}\right)\right] \tag{2.41}$$

in which *erfc* is the complementary error function, and $D = V\alpha_x$. The solution for a pulse source with a non-reactive solute for the CDM could be found in van Genuchten and Alves (1982) as below:

$$\frac{c}{c_0}=\frac{1}{2}\left[erfc\left(\frac{x-Vt}{2\sqrt{Dt}}\right)+\exp\left(\frac{Vx}{D}\right)erfc\left(\frac{x+Vt}{2\sqrt{Dt}}\right)\right] \qquad 0<t\le t_0 \qquad (2.42a)$$

$$\frac{c}{c_0}=\frac{1}{2}\left[erfc\left(\frac{x-Vt}{2\sqrt{Dt}}\right)+\exp\left(\frac{Vx}{D}\right)erfc\left(\frac{x+Vt}{2\sqrt{Dt}}\right)\right]$$
$$-\frac{1}{2}\left[erfc\left(\frac{x-V(t-t_0)}{2\sqrt{D(t-t_0)}}\right)+\exp\left(\frac{Vx}{D}\right)erfc\left(\frac{x+V(t-t_0)}{2\sqrt{D(t-t_0)}}\right)\right]$$

$$t_0\le t<\infty \qquad (2.42b)$$

The solution for a sorbing, nondegrading solute, where linear equilibrium sorption is assumed, may be obtained by replacing t with t/R in Eqs.2.42a and 2.42b (van Genuchten and Alves, 1982).

2.2.4. Extension

The above solutions are based on the assumption that degradation occurs only in the dissolved phase. For some contamination problems, this assumption may be true. For example, Zhao and Voice (2000) determined experimentally that the first-order degradation rate for the sorbed naphthalene is zero as when the contaminant is sorbed, it could become inaccessible to the bacteria that can biodegrade it. However, a more general case is that degradation occurs in both dissolved and sorbed phases. Hence, Eq.2.1 should be expressed as

$$\frac{\partial}{\partial x}\left(\varepsilon x V\frac{\partial c}{\partial x}\right)=V\frac{\partial c}{\partial x}+R\frac{\partial c}{\partial t}+\lambda c+\mu\frac{\rho_b}{\eta}S \qquad (2.43)$$

in which, μ is the degradation rate in the solid phase (T^{-1}), ρ_b is the bulk density (M/L^3), η is the porosity (L^3/L^3), and S is the concentration in the solid phase (M/M). For linear

equilibrium sorption, there is $S = K_d C$ and $R = 1+K_d \rho_b/\eta$, where K_d is the partitioning coefficient (L^3/M). For linear equilibrium sorption, Eq. 43 could be rewritten as

$$\frac{\partial}{\partial x}\left(\varepsilon x V \frac{\partial c}{\partial x}\right) = V\frac{\partial c}{\partial x} + R\frac{\partial c}{\partial t} + [\lambda + \mu(R-1)]c \qquad (\lambda \neq \mu \neq 0) \qquad (2.44a)$$

$$\frac{\partial}{\partial x}\left(\varepsilon x V \frac{\partial c}{\partial x}\right) = V\frac{\partial c}{\partial x} + R\frac{\partial c}{\partial t} + R\lambda c \qquad (\mu = \lambda \neq 0) \qquad (2.44b)$$

$$\frac{\partial}{\partial x}\left(\varepsilon x V \frac{\partial c}{\partial x}\right) = V\frac{\partial c}{\partial x} + R\frac{\partial c}{\partial t} + \lambda c \qquad (\lambda \neq 0, \mu = 0) \qquad (2.44c)$$

$$\frac{\partial}{\partial x}\left(\varepsilon x V \frac{\partial c}{\partial x}\right) = V\frac{\partial c}{\partial x} + R\frac{\partial c}{\partial t} + \mu(R-1)c \qquad (\lambda = 0, \mu \neq 0) \qquad (2.44d)$$

From Eq. 2.44, one can see that the effects of degradation in the sorbed phase can be included in the solutions given in this paper simply by replacing λ with $\lambda + \mu(R-1)$ if $\mu \neq \lambda$, replacing λ with λR if $\mu = \lambda$, and replacing λ with $\mu(R-1)$ if $\lambda = 0$ and $\mu \neq 0$. For most organic and microbial contaminants, it is likely $\mu \neq \lambda$. However, for radioactive contaminants, it is possible for $\mu = \lambda$ as it does not matter whether the contaminant is sorbed or dissolved, it still decays with a constant rate. It is less common for $\lambda = 0$ and $\mu \neq 0$.

2.3. Experimental verification

2.3.1. Methods

The solutions given by Eqs.2.40 and 2.42 were used for analysing experimental results obtained from a large column. The column was 8 m long with a 30 cm internal diameter and had sampling points at 1 m intervals. The column was inclined upward at a 30 degree angle. Pea-gravel of uniform grain size, 5-7 mm in diameter, was filled from the top of the inclined column and compacted during the packing with a shower-head attached to a PVC pipe. Tapwater, sourced from the Canterbury alluvial gravel groundwater, was then introduced from the bottom of the column from a constant head-tank and kept flushing constantly. Any gap in the top end of the column was filled after gravel within the column had fully settled.

The upward water movement helped to remove entrapped air and to minimise preferential flow. Tritiated water (henceforth referred to as tritium), a non-reactive tracer, was used as the solute. In both experiments, a pulse of tritium solution at an injection rate approximately equal to the flow rate (33.3 L/hr and 40 L/hr for Experimental One and Two, respectively) was applied. In Experiment One, about seven litres of solution containing tritium at 21,666 dpm/10ml was injected for 13 minutes. In Experiment Two, five litres of solution containing tritium at 10,000 dpm/10ml was injected for 9 minutes. Samples were collected from 8 m downstream of the injection point during Experiment One and at 2, 4, 6, and 8 m downstream during Experiment Two. Tritium samples were analysed at the University of Canterbury using a liquid scintillation counter.

Typical pore-water velocities for the two experiments were 28-34 m/day, giving Darcy velocities of about 10-12 m/day and Reynolds numbers of 0.6-0.7 for the flow. The Reynolds numbers are within the range for which Darcy's law applies. At these velocities, contaminant fronts extended only 0.2-0.3 m downstream at the end of the injections, suggesting that the downstream concentration measurements taken in these experiments should be nearly independent of the history of the injection process.

As the location of the sample point x, the input concentration c_o, and the injection time t_o were known, the unknown parameters in Eqs.2.40 and 2.42 were the mean pore-water velocity V, the dispersivity/distance ratio ε for the SDM, and the dispersivity α_x for the CDM. The solutions were computed with EXCEL spreadsheets that incorporated modules with Visual Basic programs. Data analysis included three procedures, as follows:

- The analytical solutions of the SDM and CDM were first applied to the tritium data of Experiment One. The parameters optimised were V and ε for the SDM and V and α_x for the CDM. For the SDM, α_x was calculated from $\alpha_x = \varepsilon x$ and was not optimised. The method of least squares was used to achieve the best fit between predicted and observed tritium concentrations. Low weights were given for the noisy data of low concentration measurements to minimise their influence. The noisy tritium data were mainly due to

variable natural background levels in the source water, which were measured to vary between 62 and 97 dpm/10ml.

- Using the ε and α_x values estimated from Experiment One for the SDM and CDM respectively, concentrations of tritium for Experiment Two were predicted and compared with their observed values. The mean pore-water velocity (V) of Experiment Two was optimised based on concentration breakthrough curve at x = 8 m using the SDM, and the same V value was also used in the CDM. This V value was assumed to be constant along the column.
- The values of ε and α_x were then calibrated for each breakthrough curve for Experiment Two using the SDM and CDM respectively with an aid of the least square method, as described above. Subsequently, comparison was made between models. The same mean pore-water velocity was used for all locations in both models, as described previously.

2.3.2. Results and discussion

Observed and model simulated relative concentrations for Experiment One are compared in Fig.2.1, and the optimised parameter values are listed in Table 2.1. Table 2.1 shows that the ε value estimated from the SDM is 6.8 x 10^{-3}, which gives an equivalent dispersivity value of 5.4 x 10^{-2} m at x =8 m. This is two times greater than the dispersivity estimated from the CDM.

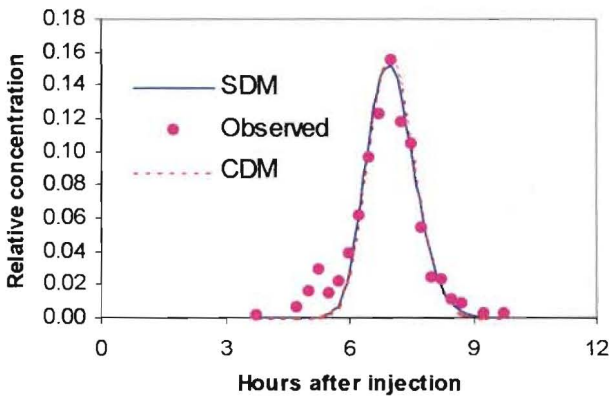

Fig. 2.1 Observed and simulated relative tritium concentrations for Experiment One. SDM - scale-dependent dispersion model. CDM - constant dispersion model

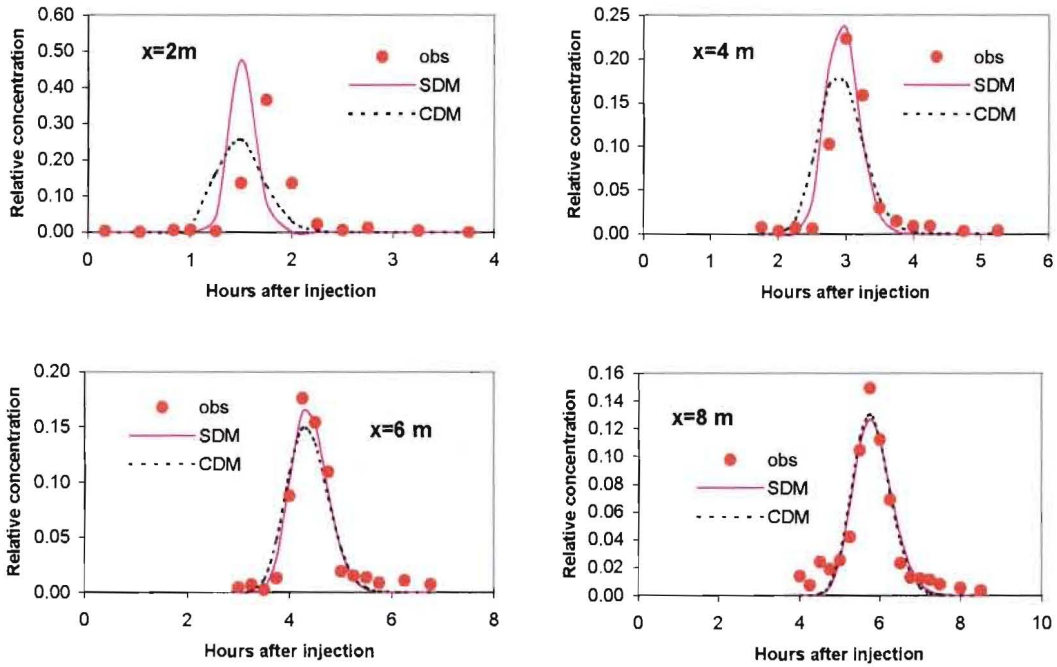

Fig. 2.2 Observed and simulated relative tritium concentrations (without calibration) for Experiment Two
SDM - scale-dependent dispersion model using ε value = 6.8×10^{-3} estimated from Experiment One, x =8 m
CDM - constant dispersion model using α_x value = 2.6×10^{-2} m estimated from Experiment One, x =8 m
A mean pore-water velocity of 33.58 m/day was used in all simulations.

Table 2.1

Parameter values optimised from the scale-dependent dispersion model (SDM) and constant dispersion model (CDM) for Experiment One

Model used	SDM	CDM
Pore-water velocity, v (m/day)	27.9	27.7
Dispersivity/distance ratio, ε	6.8×10^{-3}	
Dispersivity, α_x (m)	5.4×10^{-2} [a]	2.6×10^{-2}

[a] α_x value was estimated from $\alpha_x = \varepsilon x$

Using the above estimated values of $\varepsilon = 6.8 \times 10^{-3}$ in the SDM and $\alpha_x = 2.6 \times 10^{-2}$ m in the CDM, we can simulate breakthrough curves for a range of x values (2, 4, 6, 8 m) and compare with experimental data for Experiment Two (Fig.2.2). Compared to the observed concentrations, the SDM better predicts concentrations over a range of x values, while the CDM prediction provides a good estimate of the experimental data only toward the end of the column (x = 8m). This is because the dispersivity used in the CDM for Experiment Two was derived from x = 8 m of Experiment One. For smaller values of x, the CDM underestimates concentrations (overestimates dispersion). These results suggest that the use of a dispersivity/distance ratio in a transport model makes a definite improvement over the use of a constant dispersivity in predicting concentrations for a range of x values. Extending the predictions to x =16 and 32 m (Fig.2.3), one can expect that the difference between SDM and CDM predicted concentrations become greater with increasing distance. Although the column used in this study was not long enough to obtain observations at such distances, it is expected that predictions from the CDM would be significantly overestimated.

Fig.2.4 shows observed and simulated concentration breakthrough curves using individually calibrated values of ε in the SDM and α_x in the CDM for each sampling location for Experiment Two. The optimised parameter values are listed in Table 2.2 and plotted in Fig.2.5. Fig.2.4 shows that the SDM and CDM models give equally good fits for appropriate choices of individual ε and α_x values. Fig.2.5(b) clearly shows that dispersivities increase

linearly with transport distances for both SDM and CDM results. Similar like results of Experiment One, equivalent dispersivity values estimated from the SDM are about two times greater than those estimated from the CDM. Variation in the α_x values at x = 8 m between Experiments One and Two is almost the same as that of the ε values. Variations in ε and α_x values between experiments for the same location could be a result of data analysis errors and different flow rates, as dispersivity could be pore-water velocity related (Gerritse and Singh, 1988; Brusseau, 1993; Pang and Close, 1999).

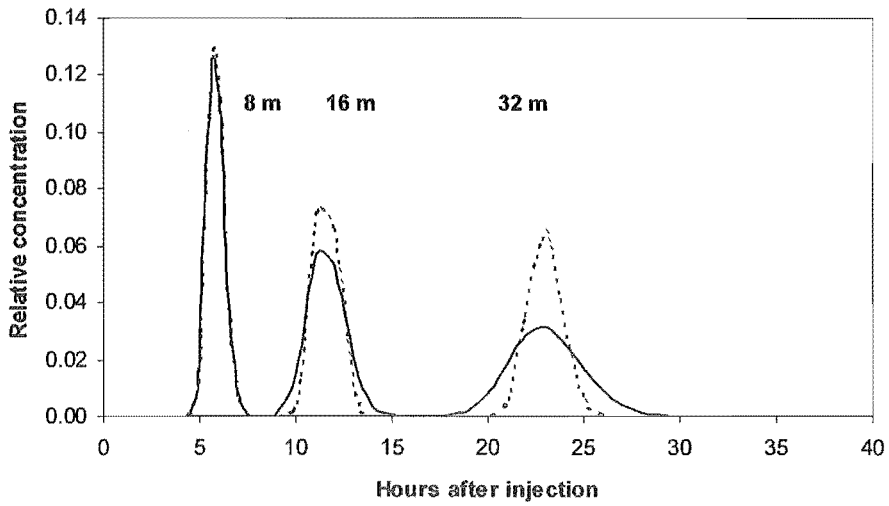

Fig.2.3. Simulated relative tritium concentrations for Experiment Two assuming a 32-m-long column. A mean pore-water velocity of 33.58 m/day was used in all simulations. SDM (solid line) - scale-dependent dispersion model using $\varepsilon = 6.8 \times 10^{-3}$. CDM (dashed line) - constant dispersion model using $\alpha_x = 2.6 \times 10^{-2}$ m.

Table 2.2

Parameter values optimised from the scale-dependent dispersion model (SDM) and constant dispersion model (CDM) for Experiment Two. A mean pore-water velocity of 33.58 m/day was used in all simulations.

Method	x (m)	ε	α_x (m)
SDM	2	1.20×10^{-2}	2.40×10^{-2} [a]
	4	8.00×10^{-3}	3.20×10^{-2} [a]
	6	5.70×10^{-3}	3.42×10^{-2} [a]
	8	4.90×10^{-3}	3.92×10^{-2} [a]
CDM	2		1.30×10^{-2}
	4		1.55×10^{-2}
	6		1.75×10^{-2}
	8		2.00×10^{-2}

[a] α_x values were estimated from $\alpha_x = \varepsilon x$

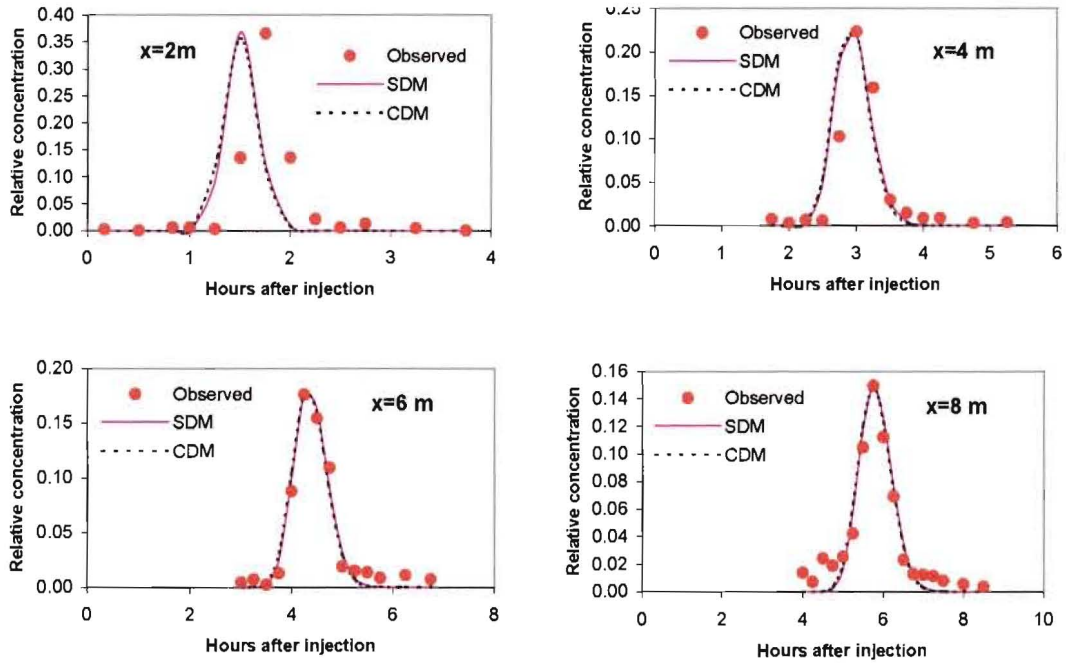

Fig. 2.4 Observed and simulated relative tritium concentrations (with calibration) for Experiment Two. Models were calibrated individually for ε values in the SDM and α_x values in the CDM for each of the concentration breakthrough curves.
SDM - scale-dependent dispersion model.
CDM - constant dispersion model.
A mean pore-water velocity of 33.58 m/day was used in all simulations.

Fig.2.5(a) shows that ε values seem to be approaching a constant as x increases. If this is true, this would agree with the interpretation of the analytical argument given by Hunt (1999a, b). In Hunt's analytical argument, ε will approach a constant at relatively large distances downstream when dispersion is dominated by advection within the pore spaces rather than molecular diffusion. Fig.2.5(a) also shows that the value of ε is a function of distance x for small x. In order to evaluate the effect of variations in ε on the concentration prediction, values of ε listed in Table 2.2 for different values of x were used to predict concentrations at x = 6 m. The results are shown in Fig.2.6. We chose x = 6 is because it shows a comparatively better data set. Fig.2.6 suggests that the error caused by ε variations on the concentration prediction reduces when using ε values derived from large x. This implies that, in practice, representative ε values for the aquifer systems should be obtained at large distances.

Figs. 2.2 and 2.4 show that predicted breakthrough curves for x =2 m are earlier than the experimentally observed curves. This is because a uniform pore-water velocity was used in the simulation for all locations. The observed flow rates (Fig.2.7) indicate that flow rates were lower than the average in the first two hours and then remained constant afterwards. As hydraulic residence time of the column, L/V, at location x = 2 is only 1.4 hours, the lower flow rate in the first two hours had a greater impact on the breakthrough curves at smaller values of x. The sudden drop and rise of flow rates in the first two hours were because the inflow pipe valve was accidentally shut when changing over from tracer solution to fresh water at the end of the injection.

Let us now look at the validity of the assumption that molecular diffusion, D_o, is negligible. According to Daily and Harleman (1966), the molecular diffusion coefficient (D_o) of tritium at 25 °C is 1.61 x 10^{-9} m^2/sec. Using an ε value of 0.01 and typical pore-water velocities of 28-33 m/day, the values of mechanical dispersion $D = \varepsilon x V$ for all sampling locations are greater than 6.48 x 10^{-6} m^2/sec. As $D >> D_o$, the use of a SDM solution that ignores molecular diffusion is appropriate for the experimental conditions herein.

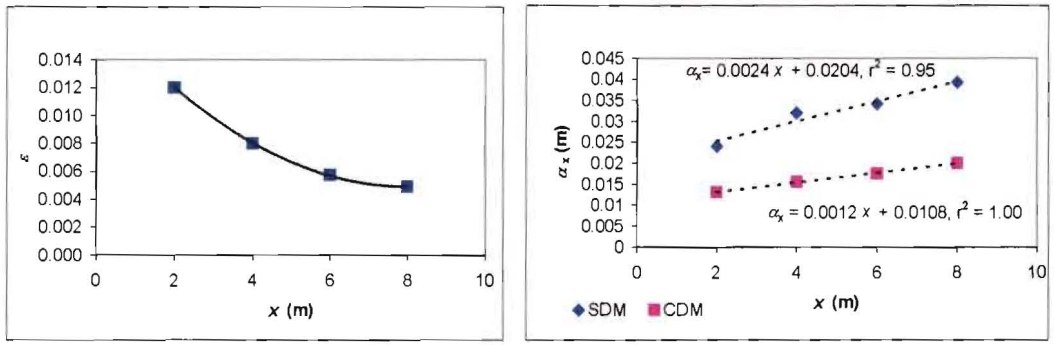

Fig. 2.5 ε - x and α_x - x relationships summarised from the individually optimised results for Experiment Two; α_x value for SDM was calculated from $\alpha_x = \varepsilon x$

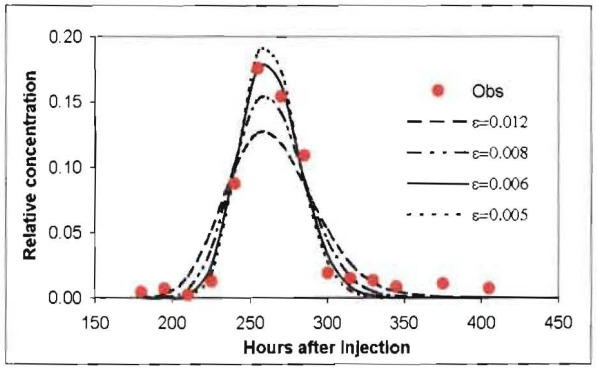

Fig. 2.6 Effect of variations in ε on the concentration prediction (using x =6 m as an example). The ε values of 0.012, 0.008, 0.006, and 0.005 are derived from x =2, 4, 6, and 8 m, respectively.

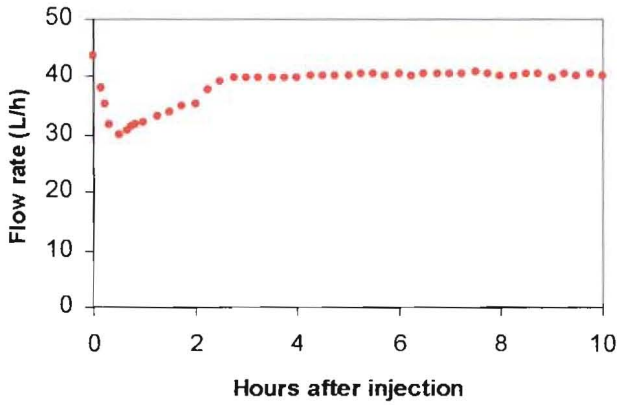

Fig.2.7 Observed flow rates for Experiment Two. The sudden drop and rise of flow rates in the first two hours were because the inflow pipe valve was accidentally shut when changing over from tracer solution to fresh water at the end of the injection.

Similar to dispersivity, the dispersivity/distance ratio ε is expected to be medium- and site-specific. Since dispersivity values generally increase with increasing degree of heterogeneity as a result of a wide distribution of pore-water velocities (Singh and Kanwar, 1991; Li and Ghodrati, 1995), ε will also be expected to increase with heterogeneity. The approximate value of ε =0.01 derived above for a uniformly packed 8 m column is expected to be much lower than the value derived from data for heterogeneous aquifers. A dispersivity/distance ratio of about 0.1 for the field scale was reported in a few studies (Lallemand-Barres and Peaudecerf 1978; De Marsily 1986; Pickens and Grisak, 1981a & b). Gelhar et al (1992) summarised that longitudinal dispersivities ranged from 10^{-2} to 10^{4} m for scales ranging from 10^{-1} to 10^{5} m, but, at a given scale, the longitudinal dispersivity values could vary by 2-3 orders of magnitude. It should be noted that comparison of these general ranges of dispersivity with the dispersivities reported in this study should be made with caution, as these ranges of dispersivity are predominately derived using CDMs, and, therefore, are not entirely comparable with values derived using a SDM.

The usual explanation for scale-dependent dispersion in heterogeneous media is given by Fetter (1993). As the flow path gets longer, groundwater encounters greater and greater variations in hydraulic conductivity and porosity. This suggests that the dispersivity will reach a maximum at large enough distances downstream when all possible variations in hydraulic conductivity have been encountered. However, few studies have explained the cause of scale-dependent dispersion in homogenous media, which has been observed both in this study and in a study by Zhang et al. (1994) using a 12.5 m long sandy soil column. Since the above explanation does not explain scale-dependent dispersivity in homogenous media, where variations in hydraulic conductivity and porosity are small, an asymptotic dispersivity value may not exist at large distances downstream in such a system.

An analytical argument given by Hunt (1999a, b) may explain scale-dependent dispersion in homogenous media. If his argument is correct, then the dispersion coefficient will continue to increase indefinitely with distance downstream and the limiting asymptotic value suggested by Fetter (1993) will never be reached. Similarly, Molz et al. (1983) state that if the local transverse dispersivity is zero, the convective component of longitudinal dispersivity continues to grow indefinitely with distance downstream.

2.4. Summary and conclusions

Analytical one-dimensional solutions are obtained for continuous and pulse contaminant sources in a semi-infinite saturated porous medium when the dispersion coefficient increases linearly with distance downstream. Experiments were carried out in an 8-m long homogenous pea-gravel column to verify the solution for a pulse source. The SDM solution describes accurately the experimental data over a range of x values for which samples were taken. The experimental data were also analysed using the solution of a constant dispersion model. The CDM solution fits the experimental data well for only one value of x. Predictions from the CDM underestimate experimental values upstream from this location, and calculations suggest that the CDM overestimates experimental values downstream from this location.

Both models are then calibrated for each individual breakthrough curve using local values for either the ε in the SDM or the α_x in the CDM. Both models give equally good fits for appropriate choices of individual ε and α_x values and both indicate a linear increase in α_x. The ε values tend to change little as x increases and is expected to approach a constant at relatively large distances downstream. Hence predictions from the SDM should become more accurate as x increases.

This study suggests that the use of a constant dispersivity/distance ratio in a transport model is more appropriate than the use of a constant dispersivity. Scale-dependent dispersion may be an important mechanism to take into account when designing monitoring programs and experiments.

2.5. Appendix A. Detailed derivation procedures between Eqs.2.20 and 2.25

Equations 2.20 and 2.21 allow us to calculate the following derivatives that appear in Eq.2.16:

$$\frac{\partial \Psi}{\partial X} = \frac{\partial \Psi}{\partial \beta}\frac{\partial \beta}{\partial X} = f'\frac{R}{T} \tag{2.A1}$$

$$R\frac{\partial \Psi}{\partial T} = R\frac{\partial \Psi}{\partial \beta}\frac{\partial \beta}{\partial T} = -\frac{\beta f' R}{T} \tag{2.A2}$$

$$\frac{\partial}{\partial X}\left(\varepsilon X\frac{\partial \Psi}{\partial X}\right) = \frac{\partial \beta}{\partial X}\frac{\partial}{\partial \beta}\left(\frac{\varepsilon \beta T}{R}\frac{f' R}{T}\right) = -\frac{R}{T}(\varepsilon \beta f')' \tag{2.A3}$$

where primes are used to denote differentiation with respect to β. Inserting 2.A1-2.A3 in Eq.2.16 gives an equation for f:

$$(\varepsilon \beta f')' - f'(1-\beta) = 0 \tag{2.A4}$$

Let $p = f'$ in 2.A4, separate variables and integrate once to obtain p.

$$p = \frac{df}{d\beta} = C_1 \beta^{(\frac{1}{\varepsilon}-1)} e^{-\frac{\beta}{\varepsilon}} \tag{2.A5}$$

A second integration gives f:

$$f = C_1 \int_0^{\beta} \theta^{(\frac{1}{\varepsilon}-1)} e^{-\frac{\theta}{\varepsilon}} d\theta + C_2 \tag{2.A6}$$

Make the substitution $y = \theta/\varepsilon$ in 2.A6 to obtain

$$f = C_3 \int_0^{\beta/\varepsilon} y^{(\frac{1}{\varepsilon}-1)} e^{-y} \, dy + C_2 \tag{2.A7}$$

where $C_3 = C_1 \, \varepsilon^{1/\varepsilon}$. The constants C_2 and C_3 are found by imposing Eqs.2.23 and 2.24 to obtain the following result for f:

$$f(\beta) = 1 - \frac{\int_0^{\beta/\varepsilon} y^{(\frac{1}{\varepsilon}-1)} e^{-y} \, dy}{\int_0^{\infty} y^{(\frac{1}{\varepsilon}-1)} e^{-y} \, dy} = 1 - \frac{\gamma(\frac{1}{\varepsilon}, \frac{\beta}{\varepsilon})}{\Gamma(\frac{1}{\varepsilon})} \tag{2.A8}$$

where Γ= Gamma function and γ= Incomplete gamma function.

Acknowledgements

We would like to thank Murray Close of ESR for valuable discussion and review, Lester Sinton of ESR for design and construction of the column apparatus, Greg Stanton of ESR for technical assistance, and John Milne and Peter Carran of Lincoln Ventures for their assistance during construction and operation of the column. Valuable and detailed peer review comments were also received from Professor Mark Goltz of Air Force Institute of Technology and journal referees. This study was funded by the Foundation for Research, Science and Technology (New Zealand) under contract number CO3802.

2.6. Additional study

2.6.1. Theoretical explanation of scale-dependent dispersion in homogenous media

The usual explanation for scale-dependent dispersion coefficients is that the dispersion coefficient is proportional to the scale of aquifer heterogeneity, and this heterogeneity scale increases with distance downstream as the flow samples a larger and larger region. This explanation implies that the dispersion coefficient would not increase with distance downstream for a homogeneous aquifer, and the dispersion coefficient for a heterogeneous aquifer will approach an upper limit at a far enough distance downstream. We have briefly mentioned in our paper that an analytical argument given by Hunt (1999a, b) may explain the observation of scale-dependent dispersion in homogenous media but we did not elaborate on it further. In this section, we will provide a theoretical explanation.

Considering dispersion of a finite mass of conservative tracer (M) that has been released instantaneously at $x = 0$ in a one-dimensional aquifer, we have the following transport equation, with initial/boundary conditions:

$$\frac{\partial}{\partial x}\left(D(x)\frac{\partial c}{\partial x} \right) = V\frac{\partial c}{\partial x} + \frac{\partial c}{\partial t} \qquad (-\infty < x < \infty,\ 0 < t < \infty) \tag{2.45}$$

$$c(x,0) = \frac{M}{\eta}\delta(x) \tag{2.46}$$

$$\int_{-\infty}^{\infty} c(x,t)\, dx = \frac{M}{\eta} \qquad \text{for } 0 < t < \infty \tag{2.47}$$

$$c(\pm\infty, t) = 0 \tag{2.48}$$

where η = aquifer porosity, $\delta(x)$ is the Dirac delta function, and M = contaminant mass per unit area that is normal to the x-axis (M/L^2).

Let Δ = base width (defined empirically, e.g. concentration = 5% peak concentration) of a contaminant pulse moving downstream with an average pore-water velocity, V, as shown in Fig. 2.8. Since $x = Vt + \zeta$, we have $x \approx Vt$ as $t \to \infty$. This assumes that $\Delta << Vt$. Under these conditions, the previous problem reduces to

$$D(Vt)\frac{\partial^2 c}{\partial \zeta^2} = \frac{\partial c}{\partial t} \qquad (-\infty < \zeta < \infty, 0 < t < \infty) \tag{2.49}$$

$$c(\zeta, 0) = \frac{M}{\eta}\delta(\zeta) \tag{2.50}$$

$$\int_{-\infty}^{\infty} c(\zeta, t)\, d\zeta = \frac{M}{\eta} \qquad \text{for } 0 < t < \infty \tag{2.51}$$

$$c(\pm\infty, t) = 0 \tag{2.52}$$

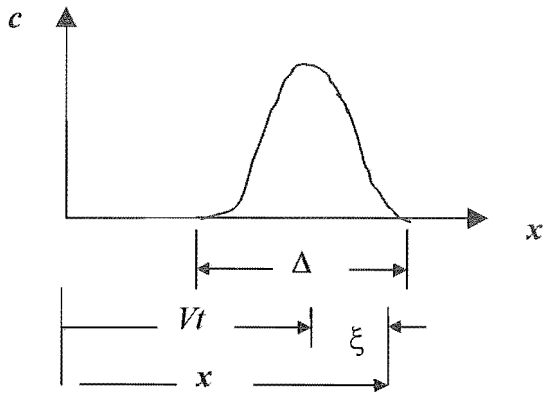

Fig. 2.8 Downstream movement of a contaminant pulse

The analytical solution of this problem has been given by Hunt (1999a, b) as below

$$D \approx \frac{1}{47.9}\frac{d\Delta^2}{dt} \qquad \left(t \to \infty,\ t = \frac{x}{V}\right) \tag{2.53}$$

If dispersion due to advection is assumed to dominate molecular diffusion within the pores, then the spreading process is due almost entirely to velocity differences. Therefore, it is reasonable to assume that

$$\Delta \propto (V_{max} - V)\, t \tag{2.54}$$

where V_{max} = maximum pore-water velocity. Inserting Eq. 2.54 into Eq. 2.53 gives

$$D(Vt) \propto (V_{max} - V)^2\, t \tag{2.55}$$

Since $Vt \approx$ x as $t \rightarrow \infty$, replacing t with x/V gives the following asymptotic expression for $D(x)$:

$$D(x) = \varepsilon x V \tag{2.56}$$

where ε = constant proportional to $\left(\frac{V_{max}}{V} - 1\right)^2$.

The above argument suggests that the dispersion coefficient will continue to increase indefinitely with distance downstream and the limiting asymptotic value suggested by Fetter (1993) will never be reached.

2.6.2. Relationship between dispersivity derived from CDM and apparent dispersivity estimated from SDM

In the publication (Section 2.3.2), we mentioned that values of equivalent dispersivity (εx) estimated from the SDM are consistently about two times greater than dispersivity (α_x) values estimated from the CDM, such as shown in Tables 2.1 and 2.2. There seems to be a relationship, $\alpha_x = \varepsilon x/2$. We did not give explanation for this in the original paper. In this section, we will explain it from the solutions of the SDM and CDM.

A SDM for a finite mass of conservative tracer released instantaneously (Fig. 2.8) could be expressed as

$$\frac{\partial}{\partial x}\left(\varepsilon\, x\, V\frac{\partial c}{\partial x}\right)=V\frac{\partial c}{\partial x}+\frac{\partial c}{\partial t} \qquad (-\infty < x < \infty, 0 < t < \infty) \tag{2.57}$$

$$\int_{-\infty}^{\infty} c(x,t)\,dx=\frac{M}{\eta} \qquad (0 < t < \infty) \tag{2.58}$$

$$c(\pm\infty,t)=0 \qquad (0 < t < \infty) \tag{2.59}$$

Rewrite this problem so that

$$c(x,t)=\varphi(\zeta,t) \qquad (\zeta = x - Vt) \tag{2.60}$$

$$\frac{\partial c}{\partial x}=\frac{\partial \varphi}{\partial \zeta}\frac{\partial \zeta}{\partial x}=\frac{\partial \varphi}{\partial \zeta} \tag{2.61}$$

$$\frac{\partial c}{\partial t}=\frac{\partial \varphi}{\partial \zeta}\frac{\partial \zeta}{\partial t}+\frac{\partial \varphi}{\partial t}=-V\frac{\partial \varphi}{\partial \zeta}+\frac{\partial \varphi}{\partial t} \tag{2.62}$$

Eqs. 2.57-2.59 become

$$\frac{\partial}{\partial \zeta}[\varepsilon V(\zeta + Vt)\frac{\partial \varphi}{\partial \zeta}] = \frac{\partial \varphi}{\partial t} \tag{2.63}$$

$$\int_{-\infty}^{\infty} \varphi(\zeta,t)\,d\zeta=\frac{M}{\eta} \tag{2.64}$$

$$\varphi(\pm\infty,t)=0 \tag{2.65}$$

Far downstream, $Vt >> \zeta$ and $\zeta + Vt \approx Vt$, therefore

$$\varepsilon V^2 t\frac{\partial^2 \varphi}{\partial \zeta^2} = \frac{\partial \varphi}{\partial t} \tag{2.66}$$

$$\int_{-\infty}^{\infty} \varphi(\zeta,t)\,d\zeta=\frac{M}{\eta} \tag{2.67}$$

$$\varphi(\pm\infty,t)=0 \tag{2.68}$$

Solve this by using the transformation $\tau=\varepsilon V^2 t^2/2$. Then

$$\frac{\partial\varphi}{\partial t}=\frac{\partial\varphi}{\partial\tau}\frac{\partial\tau}{\partial t}=\varepsilon V^2 t^2\frac{\partial\varphi}{\partial\tau}$$

$$\frac{\partial^2\varphi}{\partial\zeta^2}=\frac{\partial\varphi}{\partial\tau} \tag{2.69}$$

$$\int_{-\infty}^{\infty}\varphi(\zeta,\tau)\,d\zeta=\frac{M}{\eta} \tag{2.70}$$

$$\varphi(\pm\infty,\tau)=0 \tag{2.71}$$

The solution for this problem is

$$\varphi(\zeta,\tau)=\frac{M}{2\eta\sqrt{\pi\tau}}\exp\left(-\frac{\zeta^2}{4\tau}\right) \tag{2.72}$$

Rewrite this result as $c(x,t)$ to obtain

$$c(x,t)=\frac{M}{2\eta\sqrt{\pi\,\varepsilon V^2 t^2/2}}\exp\left(-\frac{(x-Vt)^2}{4\varepsilon V^2 t^2/2}\right) \tag{2.73}$$

A CDM can be expressed as

$$\alpha_x V\frac{\partial^2 c}{\partial x^2}=V\frac{\partial c}{\partial x}+\frac{\partial c}{\partial t} \qquad (-\infty<x<\infty,\ 0<t<\infty) \tag{2.74}$$

$$\int_{-\infty}^{\infty}c(x,t)\,dx=\frac{M}{\eta} \qquad (0<t<\infty) \tag{2.75}$$

$$c(\pm\infty,t)=0 \qquad (0<t<\infty) \tag{2.76}$$

Using the similar procedure as above, we could derive the solution for this problem as

$$c(x,t)=\frac{M}{2\eta\sqrt{\pi\,\alpha_x Vt}}\exp\left(-\frac{(x-Vt)^2}{4\alpha_x Vt}\right) \tag{2.77}$$

Comparing these two solutions (Eqs. 2.73 and 2.77) shows that for the same c value, there is a relationship between parameters of the two models:

$$\alpha_x=\frac{\varepsilon V t}{2}=\frac{\varepsilon x}{2} \tag{2.78}$$

Chapter 3

Application of the method of temporal moments to interpret solute transport with sorption and degradation

Liping Pang[1], Mark Goltz[2], Murray Close[1]. 2003. Application of the method of temporal moments to interpret solute transport with sorption and degradation. Journal of Contaminant Hydrology 60(1-2): 123-134.

Author affiliations:

[1] Institute of Environmental Science & Research Ltd., PO Box 29181, Christchurch, New Zealand

[2] Department of Systems and Engineering Management, Air Force Institute of Technology Wright-Patterson Air Force Base, OH 45433-7765, USA

Journal Referees:

Professor Edward A. Sudicky, Department of Earth Sciences, University of Waterloo, Canada.

Two other anonymous referees.

Abstract

In this note, we applied the temporal moment solutions of Das and Kluitenberg (1996) for one-dimensional advective-dispersive solute transport with linear equilibrium sorption and first-order degradation for time pulse sources to analyse column experimental data. Unlike most other moment solutions, these solutions consider the interplay of degradation and sorption. This permits estimation of a first-order degradation rate constant using the zeroth moment of column breakthrough data, as well as estimation of the retardation factor or sorption distribution coefficient of a degrading solute using the first moment. The method of temporal moment (MOM) formulae were applied to analyse breakthrough data from a laboratory column study of atrazine, hexazinone, and rhodamine WT transport in volcanic pumice sand, as well as experimental data from the literature. Transport and degradation parameters obtained using the MOM were compared to parameters obtained by fitting breakthrough data from an advective-dispersive transport model with equilibrium sorption and first-order degradation, using the non-linear least-square curve-fitting program CXTFIT. The results derived from using the literature data were also compared with estimates reported in the literature using different equilibrium models. The good agreement suggests that the MOM could provide an additional useful means of parameter estimation for transport involving equilibrium sorption and first-order degradation. We found that the MOM fitted breakthrough curves with tailing better than curve fitting. However, the MOM analysis requires complete breakthrough curves and relatively frequent data collection to ensure the accuracy of the moments obtained from the breakthrough data.

Key words: Temporal moments; Retardation; First-order degradation; Equilibrium sorption

3.1. Introduction

The method of temporal moments (MOM) is often used for analysing concentration breakthrough curves (BTCs) in contaminant transport studies. The MOM may be used to

estimate the parameters of a contaminant transport model by comparing the moments of concentration breakthrough data to the theoretical moments predicted using the model. These theoretical moments may be derived using a Laplace transformed version of the model (Kučera, 1965; Cho, 1971; Valocchi, 1985). The MOM is convenient to use as there is no need to solve the transport model in real time and space (only the Laplace solution is required) and depending on the complexity of the transport model and the number of model parameters that are needed, only the zeroth, first, and perhaps second, moment solutions are necessary. The MOM is commonly used to estimate pore-water velocities and dispersion coefficients for laboratory column BTC data for conservative tracers (Maloszewski et al., 1994; Pang et al., 1998; Yu et al., 1999), and retardation factors for sorbing solutes under both equilibrium and non-equilibrium transport conditions (Jacobsen et al., 1992; Ptak and Schmid, 1996; Rubin et al., 1997). However, there has been little work published demonstrating its use to simultaneously estimate degradation rates and retardation factors for sorbing and degrading solutes. Instead, curve fitting procedures (e.g Toride et al., 1995) have typically been used for parameter estimation under these conditions. This is probably due to the fact that many of the published MOM solutions (e.g. Valocchi, 1985, 1986; Leij and Dane, 1992; Espinoza and Valocchi, 1998; Young and Ball, 2000) do not incorporate contaminant degradation.

The interplay between degradation and sorption has become of increasing interest, as issues such as the bioavailability of subsurface contaminants are explored. It is known that sorption and degradation are related (Matthess, 1994). Jury and Roth (1990) and Gamerdinger et al. (1993) showed that degradation shifts the apparent center-of-mass of a breakthrough curve to the left. Many subsurface contaminants, such as pesticides, hydrocarbons, and microorganisms, undergo simultaneous degradation and sorption. To our knowledge, the only published MOM solutions considering solute transport undergoing both sorption and degradation are those given by Das and Kluitenberg (1996). However, Das and Kluitenberg (1996) did not apply their theoretical results to experimental data.

The MOM solutions of Das and Kluitenberg (1996) are based on the assumptions that local equilibrium is established instantaneously during solute transport in a homogenous porous medium, and that sorption is linear and reversible. Although real systems are rarely homogenous, and sorption may be kinetic, these assumptions are reasonable when sorption kinetics are significantly faster than the hydraulic residence time (Brusseau, 1992; Kookana et al., 1993), such as found in relatively homogenous media systems with slow flow rates (Lee et al., 1988; Bajracharya et al., 1996).

We carried out a column experiment using degradable sorbing solutes (atrazine, hexazinone, and rhodamine WT) and applied the MOM solutions of Das and Kluitenberg (1996) to our data as well as to data from Langner et al. (1998) and Casey et al. (2000). MOM-estimated parameters were compared to parameters obtained from fitting a transport model that assumes advective-dispersive transport, equilibrium sorption, and first-order degradation to the BTC data, using the non-linear least-square curve-fitting program, CXTFIT (version 2, Toride et al., 1995). The results derived from using the data of Langner et al. (1998) and Casey et al. (2000) were also compared with the independent estimates reported in these studies using different equilibrium models.

3.2. Theory

3.2.1. Governing solute transport equations

Solute transport through saturated, homogenous porous media, in a one-dimensional uniform flow field, considering advection, dispersion, linear equilibrium sorption, and first-order degradation may be described by the following partial differential equation (Toride et al., 1995):

$$R\frac{\partial c}{\partial t} = D\frac{\partial^2 c}{\partial x^2} - V\frac{\partial c}{\partial x} - \lambda c \qquad (3.1)$$

where c is the contaminant concentration (M/L^3), D is the dispersion coefficient (L^2/T), R is the retardation factor, V is the average pore-water velocity (L/T), x is the longitudinal distance (L), t is the time (T), and λ is a combined first-order degradation rate constant (T^{-1}) that accounts for degradation of solute in both liquid and solid phases. In this study we are interested in a pulse source of duration t_0 with the following initial and boundary conditions:

$$c(x,0)=0 \qquad 0<x<\infty \tag{3.2}$$

$$c(0,t)=c_0 \qquad 0<t\le t_0 \tag{3.3}$$

$$c(0,t)=0 \qquad t_0<t<\infty \tag{3.4}$$

$$c(\infty,t)=0 \qquad 0<t<\infty \tag{3.5}$$

λ is defined as (van Genuchten and Alves, 1982; Toride et al., 1995) $\lambda=\lambda_l+\frac{\rho_b K_d}{\theta}\lambda_s$,

where λ_l is the first-order degradation rate constant in the liquid phase (T^{-1}), λ_s is the first-order degradation rate constant in the solid phase (T^{-1}), ρ_b is the bulk density of the porous material (M/L^3), K_d is the sorption distribution coefficient (L^3/M), and θ is the porosity of the porous material (L^3/L^3). For linear instantaneous sorption $R=1+\frac{\rho_b K_d}{\theta}$. Therefore, replacing $\rho_b K_d/\theta$ with $(R\text{-}1)$ give $\lambda=\lambda_l+(R-1)\lambda_s$.

3.2.2. Temporal moments

The nth temporal moment of a concentration distribution at a location, x, is defined as (Kučera, 1965; Valocchi, 1985):

$$M_n=\int_0^\infty t^n\, c(x,t)\, dt \tag{3.6}$$

and the nth normalized moment of the distribution is defined as:

$$\mu_n = \frac{M_n}{M_0} = \frac{\int_0^\infty t^n c(x,t)\,dt}{\int_0^\infty c(x,t)\,dt} \tag{3.7}$$

Eqs. 3.6 and 3.7 may be used to obtain experimental temporal moments from concentration breakthrough curves. Das and Kluitenberg (1996) derived the following theoretical zeroth and first temporal moments using a Laplace transformed version of the transport model (Eqs. 3.1-3.5):

$$M_0 = c_0 t_0 \exp\left[\frac{Vx}{2D}\left(1-\sqrt{1+\frac{4D\lambda}{V^2}}\right)\right] \tag{3.8}$$

$$\mu_1 = \frac{M_1}{M_0} = \frac{t_0}{2} + \frac{xR}{\sqrt{V^2+4D\lambda}} \tag{3.9}$$

By setting the experimentally determined moments equal to the theoretical moments, we can estimate the degradation rate and retardation factor, as follows:

$$\lambda = \frac{V^2}{4D}\left[\left(1-\frac{2D}{xV}\ln\frac{M_o}{c_o t_o}\right)^2 - 1\right] \tag{3.10}$$

$$R = \frac{(\mu_1 - 0.5t_0)\sqrt{V^2+4D\lambda}}{x} \tag{3.11}$$

where M_0 and μ_1 are as defined in Eqs.3.6 and 3.7.

The pore-water velocity (V) and dispersion coefficient (D) must be known in order to calculate λ and R from Eqs.3.10 and 3.11. These parameters can be obtained using the

experimentally determined moments of the concentration BTC of a non-reactive tracer. Since R=1 and λ=0 for a non-reactive tracer, we can use Eq.3.11 to calculate V from first moment data:

$$V = \frac{x}{\mu_1 - 0.5t_0} \tag{3.12}$$

Following Valocchi (1985) and Goltz and Roberts (1987), we could define the contaminant effective velocity, V_c, calculated from the first moment of a breakthrough curve obtained at location x, as x/μ_1. We can then use Eq.3.11 to determine that the effective velocity of a sorbing, degrading contaminant that is instantaneously injected into the medium (t_0=0) is:

$$V_c = \frac{x}{\mu_1} = \frac{\sqrt{V^2 + 4D\lambda}}{R} \tag{3.13}$$

Eq.3.13 confirms the relationship presented in Cho (1971) who found that the effective velocity of a degrading but non-sorbing solute, V_c, is related to the first-order degradation rate constant, by the expression $\sqrt{V^2 + 4D\lambda}$. Eq.3.13 also is consistent with Gamerdinger et al. (1993) and Jury and Roth (1990) who showed that an increasing degradation rate results in a shift of the BTC center-of-mass to the left (that is, λ and μ_1 are inversely related).

The dispersion coefficient needed in Eqs. 3.10 and 3.11 can also be independently determined using the first and second moments of a non-reactive tracer BTC by applying the following formula (adapted from Leij and Dane, 1992; Young and Ball, 2000):

$$D = \frac{V^3}{2x}(\mu_2 - \mu_1^2 - \frac{t_0^2}{12}) \tag{3.14}$$

with the pore-water velocity, V, and the second normalized moment, μ_2, in Eq.3.14 determined from experimental data, using Eqs.3.12 and 3.7, respectively.

3.3. Experimental verification

3.3.1 Column experiment

A column experiment was carried out to test the applicability of the MOM solutions using atrazine, hexazinone, and rhodamine WT dye. The material used in the experiment was taken from 0.5 m below the water table while drilling a well at Hamilton, New Zealand. Analysis of the pumice sand aquifer material showed a mean cation exchange capacity of 2.49 cmol/kg and total carbon content of 0.11% with an estimated allophane content of approximately 0.8%.

The column used was an acrylic tube with a length of 200 cm and a 19 cm internal diameter. The aquifer material, stored at residual saturation after being taken from the field, was uniformly repacked under saturation. Tapwater sourced from the Canterbury deep gravel aquifer was used.

The experiment was undertaken at room temperatures (20 °C ±1). A flow rate (Q) of 7.3 ml/min was applied to the column. Knowing the cross-sectional area of the column (A=283 cm^2), along with the bulk density (ρ_b=1.37 g/ml), particle density (ρ_s=2.35 g/ml), and porosity ($\theta = 1- \rho_b / \rho_s = 0.42$) of the pumice sand, the average pore-water velocity (V) in the column could be estimated ($V = Q /(A\theta)$) at 0.89 m/day. This velocity is typical for a pumice sand aquifer. After extensively flushing the column with tapwater prior to the experiment, 29 l of solution containing atrazine (960 µg/l), hexazinone (350 µg/l), and rhodamine WT (310 µg/l) along with tritiated water ^3H_2O (4423 dpm/10ml) and bromide (4.5 mg/l) were introduced into the column. ^3H_2O and Br were used as conservative tracers in order to characterise the physical transport properties (advection and dispersion). The column was then flushed with tapwater until chemical concentrations in the effluent were

reduced to the background level of the tapwater. Effluent flow rates were measured regularly, and the cumulative volume was recorded using a flow-meter.

Pesticide samples were analysed by gas chromatography-mass spectrometry with detection limits of 0.3 and 0.5 μg/l for atrazine and hexazinone, respectively. Rhodamine WT samples were analysed fluorimetrically (detection limit 0.05 μg/l). ^3H_2O samples were analysed using a liquid scintillation counter and bromide samples were analysed by ion chromatography (detection limit 0.1 mg/l).

3.3.2 Experimental data from literature

To further test the applicability of the MOM, we applied the MOM solutions to the experimental data of Langner et al. (1998) and Casey et al. (2000). Langner et al. (1998) obtained experimental data showing degradation and sorption of 2,4-dichlorophenoxyacetic acid (2,4-D) using a series of unsaturated soil columns with varying column lengths and pore-water velocities. The experimental data of Casey et al. (2000) were obtained from column experiments with pulses of trichloroethylene (TCE) flowing through zerovalent metals at three pore-water velocities, resulting in simultaneous breakthrough curves of TCE and its reduction daughter product, ethylene. According to Casey et al. (2000), the concentration detection limit for both chemicals was approximately 0.01 mg/l.

3.3.3 Parameter estimation

For the pumice sand column, the pore-water velocity (V) and dispersion coefficient (D) were first estimated from the ^3H_2O and Br data using Eqs.3.12 and 3.14, respectively. The experimental moments in the equations were calculated from the BTCs using the trapezoidal rule. Compared to ^3H_2O (total of 97 observations), Br samples were collected less frequently (total of 24 observations), and consequently the MOM analysis of the Br BTC was less accurate. Therefore, the V and D values estimated from the ^3H_2O data were used in subsequent analyses. Values of λ and R for the reactive solutes were estimated using Eqs.3.10 and 3.11. Due to premature termination of the atrazine experiment, the atrazine

BTC was truncated. Use of the truncated data would have resulted in underestimation of the zeroth and first moments of the BTC, leading to underestimation of R and overestimation of λ when applying Eqs.3.10 and 3.11. To obtain better estimates of the BTC moments, we extrapolated the atrazine BTC according to the slope of the tail, resulting in an estimated data point of 0.0 relative concentration at 400 h (see Fig.3.1).

For the experimental data of Langner et al. (1998) and Casey et al. (2000), we used values of V and D given in their papers, and estimated values of λ and R using Eqs.3.10 and 3.11. Langner et al. (1998) estimated the V values for their system based on Darcy velocity and water content. Casey et al. (2000) did not indicate how the reported V values were determined. Both Langner et al. (1998) and Casey et al. (2000) estimated the D values from fitting BTCs of conservative solutes.

For comparison purposes, parameter values were also estimated independently by fitting the experimental BTCs with analytical solutions of the transport model (Eqs.3.1-3.5) using CXTFIT (version 2, Toride et al., 1995). The results reported in Langner et al. (1998) and Casey et al. (2000), derived from different equilibrium models, served as independent estimates to compare with the parameter estimates from applying the MOM in this study.

3.4. Results and discussion

Table 3.1 lists values of V and D for the conservative solutes and R and λ for the reactive solutes estimated from the MOM and from curve fitting. Fig.3.1 shows BTCs observed and simulated using both approaches. We see from the table and figure that the parameter values and the simulated BTCs obtained from applying the two methods are very similar except for atrazine. Also note that the values of V that were obtained using the two methods were very similar to the independently determined value of V based on a flow rate of 0.89 m/day (see Section 3.3.1). Statistically, the MOM and curve fitting values for R and λ were found to be well correlated ($r \geq 0.95$, $P = 0.000$). Using a modified coefficient of deviation,

Table 3.1
Comparison of results obtained from method of moments and curve-fitting using CXTFIT

(1) Experimental data of this study (pumice sand column)

Tracer	V (m/day)			D (m^2/day)		
	MOM	CXTFIT	ε	MOM	CXTFIT	ε
Tritiated water	0.87	0.90	-0.03	0.18	0.09	0.53
Br	0.93	0.95	-0.02	0.14	0.07	0.52
	R			λ (per day)		
	MOM	CXTFIT	ε	MOM	CXTFIT	ε
Atrazine	3.03	2.22	0.27	0.27	0.47	-0.76
Hexazinone	1.60	1.34	0.16	0.12	0.23	-0.94
Rhodamine WT	1.50	1.28	0.14	0.39	0.43	-0.12

(2) Experimental data of Langner et al. (1998)

2,4-D column	R			λ (per min)		
	MOM	CXTFIT	ε	MOM	CXTFIT	ε
RT05-L09	3.03	2.78	0.08	0.60	0.73	-0.22
RT16-L09	2.96	3.15	-0.06	0.79	0.76	0.04
RT48-L09	3.97	3.95	0.01	1.59	1.62	-0.02
RT05-L28	3.01	2.77	0.08	0.44	0.61	-0.39
RT16-L28	3.71	3.59	0.03	0.46	0.51	-0.11
RT48-L28	3.84	3.75	0.02	0.92	0.92	0.00
RT16-L85	3.00	2.84	0.06	0.27	0.35	-0.29
RT48-L85	3.22	3.18	0.01	0.22	0.21	0.05

RT-residence time (h), L- column length (cm)

(3) Experimental data of Casey et al. (2000)

Experiment	R			λ (per min)		
Column-solute-flow rate	MOM	CXTFIT	ε	MOM	CXTFIT	ε
FeCu-TCE-fast	4.38	3.45	0.21	0.18	0.19	-0.05
FeCu-TCE-intermediate	4.30	3.69	0.14	0.13	0.14	-0.04
FeCu-TCE-slow	12.06	11.23	0.07	0.20	0.20	0.01
Fe-TCE-fast	2.69	2.10	0.22	0.15	0.18	-0.20
Fe-TCE-intermediate	2.75	2.57	0.07	0.12	0.12	0.02
Fe-TCE-slow	7.12	5.43	0.24	0.12	0.14	-0.14
FeCu-Ethylene-fast	5.36	5.59	-0.04	0.02	0.02	0.13
FeCu-Ethylene-intermediate	4.66	4.70	-0.01	0.01	0.01	0.09
Fe-Ethylene-fast	3.70	3.48	0.06	0.04	0.04	-0.21
Fe-Ethylene-intermediate	3.32	3.44	-0.03	0.01	0.01	-0.38

ε = (MOM value-CXTFIT value) /MOM value

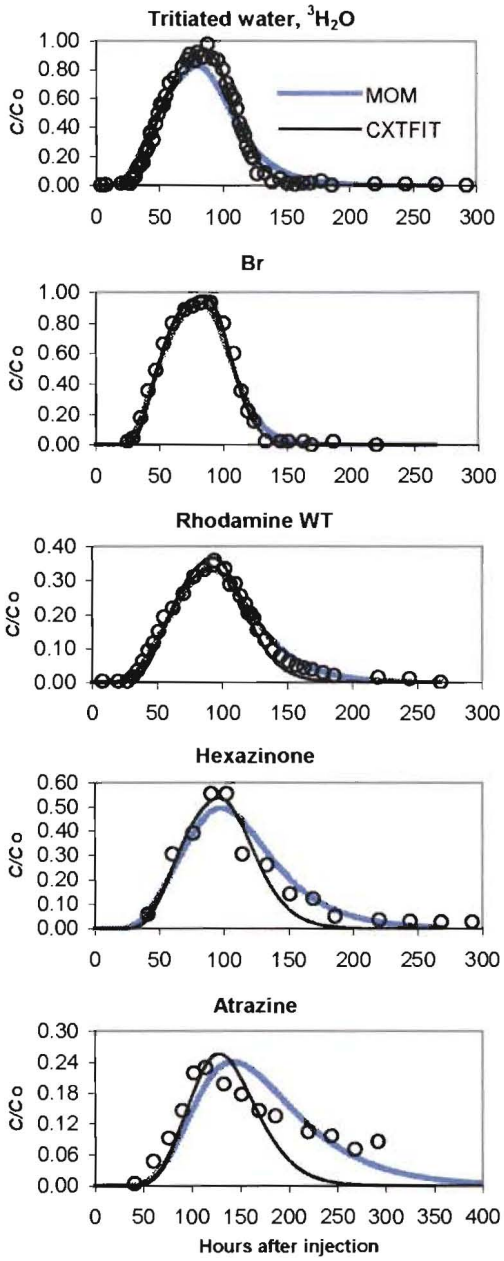

Fig. 3.1. Comparison of MOM- and CXTFIT-simulated concentration breakthrough curves with experimental data for the pumice sand column (observed data in circles). Every second observations are plotted for tritiated water and every third observations are plotted for rhodamine WT.

ε= (MOM value-CXTFIT value) /MOM value, the similarity of the results between the methods for each parameter could be compared. Table 3.1 shows that the ε-values for V are one order of magnitude smaller than the values for D, R, and λ for the experiment with the pumice sand column. As only the first moment is needed to estimate V for a non-reactive tracer, it is not surprising that the MOM estimate is quite close to the curve-fitting estimate. In contrast, first and second moments are required to estimate R, D and λ, so the estimates for these parameters exhibit more deviation. This is expected, as the higher the order of the moment, the less stable the calculation (Leij and Dane, 1992).

Table 3.1 shows that dispersion coefficients estimated from the MOM are higher (by about twofold) than the curve-fitting estimates. A similar finding was also reported by Pang et al. (1998). This is not surprising, as the MOM-estimated value of D is a function of the difference between the second moment and the first moment squared (Eq.3.14). Thus, even small concentrations that are measured at times distant from the first moment (i.e. the BTC tail) will have a large impact on the dispersion estimate. In contrast, CXTFIT curve-fitting results that are based on minimizing the sum of square deviations are dominated by the high-concentration data points (as all the data points are assigned an equal weight by CXTFIT); hence curve-fitting-derived dispersion coefficients are comparatively low. For a similar reason, there is a tendency for the MOM to estimate slightly higher R-values than least square curve fitting, as the first moment calculation is positively influenced by concentrations in the BTC tail, thus, resulting in increased estimates for R (Eq.3.11). Because of the higher D-value estimated using the MOM in comparison with curve-fitting, the MOM appears to do a better job fitting the tails for atrazine, hexazinone and rhodamine WT. It should be noted that neither the MOM nor curve-fitting could adequately describe the atrazine BTC, which exhibits significant tailing (Fig.3.1), suggesting that atrazine sorption may be kinetic. To adequately describe a BTC with significant tailing due to kinetic sorption, a model that accounts for kinetic sorption would be needed, but this is beyond the scope of this note.

Table 3.2
Comparison of results estimated in this study and those reported by Langner et al (1998) and Casey et al. (2000) obtained from the equilibrium models.

Column with 2,4-D	R			λ (per h)		
	This study		Langner et al.	This study		Langner et al.
	MOM	CXTFIT	(1998)	MOM	CXTFIT	(1998)
RT05-L09	3.03	2.78	4.23	0.025	0.030	0.031
RT16-L09	2.96	3.15	3.79	0.033	0.032	0.035
RT48-L09	3.97	3.95	4.35	0.066	0.068	0.071
RT05-L28	3.01	2.77	3.49	0.018	0.025	0.015
RT16-L28	3.71	3.59	4.17	0.019	0.021	0.021
RT48-L28	3.84	3.75	4.91	0.038	0.038	0.038
RT16-L85	3.00	2.84	3.42	0.011	0.015	0.015
RT48-L85	3.22	3.18	3.55	0.009	0.009	0.007

The λ values of Langner et al. (1998) were given in Table 3 of the original paper, but the R values were not directly given and hence were calculated from the given values of K_d, ρ_b, and θ.

Column	K_d (ml/g)			$K_{s,sa}$ ($l\ h^{-1}\ m^{-2}$) x 10^{-5}		
	This study		Casey et al	This study		Casey et al
	MOM	CXTFIT	(2000)	MOM	CXTFIT	(2000)
FeCu-TCE-fast	0.56	0.40	0.46 (+/-0.07)	14	21	18 (+/-1.8)
FeCu-TCE-intermediate	0.54	0.44	0.50 (+/-0.08)	11	14	14 (+/-1.3)
FeCu-TCE-slow	1.83	1.69	1.77 (+/-0.94)	4.9	5.2	6 (+/-0.79)
Fe-TCE-fast	0.46	0.30	0.40 (+/-0.44)	25	47	19 (+/-11.0)
Fe-TCE-intermediate	0.48	0.43	0.40 (+/-0.04)	19	21	21 (+/-1.5)
Fe-TCE-slow	1.67	1.21	1.36 (+/-0.75)	5.9	8.8	8.9 (+/-2.0)

K_d and $K_{s,sa}$ were presented in Table 1 of Casey et al. (2000).
The K_d values estimated in this study were converted from the R values together with the given values of ρ_b and θ.
$K_{s,sa}$ was the normalized sorbed reaction rate constant, and was defined as $K_{s,sa} = \lambda\ \theta\ /\ (\rho_b K_d S_a)$
S_a is the surface area concentration, and was given as 21,147 m^2/l for the Fe columns and 22,417 m^2/l for the FeCu columns.
The $K_{s,sa}$ values estimated in this study were converted from the λ and K_d values of this study together with given θ, ρ_b and S_a values.

Table 3.2 shows the results obtained in this study using data of Langner et al. (1998) and Casey et al. (2000) compared to the results reported in those studies. Table 3.2 shows that the λ values derived from the 2,4-D data of Langner et al. (1998) are almost the same between the studies. In addition, the values of R calculated from the K_d, θ, and ρ_b values given in Langner et al. (1998) are similar to the values of R estimated in this study using the MOM and curve fitting. In the equilibrium model used by Casey et al. (2000), sorption was described using K_d and degradation was described using a normalised sorbed reaction rate constant, $K_{s,sa}$. Converting R and λ values estimated in this study to the corresponding K_d and $K_{s,sa}$ values, the results are shown to also be similar between the studies. This analysis of the results of Langner et al. (1998) and Casey et al. (2000) offers further support of the applicability of the MOM to describe transport with equilibrium sorption and degradation.

In using the MOM, a note of caution is needed. In order to obtain exact moments, data must theoretically be collected for an infinite time, as a precise mechanistic interpretation of the transport requires a complete recovery of injected solute (Young and Ball, 2000). To minimize integration errors in the MOM analysis, frequent data collection is also required, which may be impractical, due to time and cost constraints. Hence, the accuracy of MOM results is very much affected by the degree of data truncation and frequency of data collection.

3.5. Conclusions

The temporal moment solutions of Das and Kluitenberg (1996) were satisfactorily verified in this note using breakthrough data obtained from column experiments. The MOM estimates agreed very well with curve-fitting estimates for the BTCs with little tailing. For BTCs with tailing, the MOM appeared to fit the tail better than the curve-fitting approach. These results suggest that the MOM could be used as an additional useful tool to estimate pore-water velocity, dispersivity, degradation rate and retardation factor for transport with equilibrium sorption and degradation. However, like other equilibrium models, the moment solutions of Das and Kluitenberg (1996) are unable to describe BTCs with significant tailing. Also, like other temporal moment solutions, the

above MOM analysis requires complete breakthrough curves and relatively frequent data collection.

Acknowledgements

We express our great gratitude to Dr. Heiko Langner of Montana State University and Dr. Francis Casey of North Dakota State University for generously providing us with their published experimental data. Technical assistance from Mr. Maitland Manning and Dr. Cliff Randall of Institute of Environmental Science & Research is acknowledged. Dr. Bruce Hunt of Canterbury University and Dr. Feike Leij of U.S. Salinity Laboratory are also thanked for their helpful discussions. This study was funded by the Foundation for Research, Science and Technology (New Zealand) under contract number CO3X001.

3.6. Additional study: Derivation of theoretical MOM solutions

In this section, we will demonstrate the procedure of deriving the MOM solutions presented in equations 3.8 and 3.9. The procedure was not included in the publication that constitutes the core of Chapter 3, as Das and Kluitenberg (1996) had derived equivalent solutions previously, using a different procedure.

3.6.1. Laplace transformation of governing solute transport equations

Applying the Laplace transform to Eqs. 3.1 and 3.2 changes the partial differential equation to the following ordinary differential equation:

$$D\frac{d^2C}{dx^2}-V\frac{dC}{dx}-(\lambda+Rs)C=0 \tag{3.15}$$

where s denotes the Laplace transform variable and $C(x,s)$ is the concentration in the Laplace domain, expressed as

$$C(x,s)=\int_0^\infty e^{-st}\,c(x,t)\,dt \tag{3.16}$$

Boundary conditions (3.3) – (3.5) are similarly transformed to:

$$C(0,s)=\frac{c_0(1-e^{-st_0})}{s} \tag{3.17}$$

$$C(\infty,s)=0 \tag{3.18}$$

Solution of the ordinary differential equation (3.15), with boundary conditions (3.17) and (3.18), is straightforward. The solution for concentration in the Laplace domain is:

$$C(x, s) = \frac{c_0}{s}\left(1 - e^{-st_0}\right) e^{m_2 x} \tag{3.19}$$

where m_2 is defined as:

$$m_2 = \frac{V}{2D}\left(1 - \sqrt{1 + \frac{4D(Rs + \lambda)}{V^2}}\right) \tag{3.20}$$

3.6.2. Temporal moments

The following well-known property of the Laplace transformation relates the temporal moments of a concentration distribution with its representation in the Laplace domain (Aris, 1958; Kučera, 1965):

$$M_n = \int_0^\infty t^n c(x,t)\, dt = (-1)^n \lim_{s \to 0} \frac{d^n C(x, s)}{ds^n} \tag{3.21}$$

As indicated in the paper, Eqs. 3.6 and 3.7 may be used to obtain experimental temporal moments from breakthrough data. For a given model, Eq. 3.21 may be used to obtain the theoretical temporal moments, using the solution of the model in the Laplace domain. For

the given model, transport parameters may be estimated by setting the theoretical moments calculated from Eq. 3.21 equal to the experimental moments estimated from Eq. 3.6.

3.6.2.1. Zeroth moment

We can develop a formula for the zeroth moment of a BTC by substituting Eq. 3.19 into Eq. 3.21 with n=0:

$$M_0 = (-1)^0 \lim_{s\to 0} \frac{d^0 C(x,s)}{ds^0} = \lim_{s\to 0} C(x,s) = \lim_{s\to 0}\left[\frac{c_0}{s}(1-e^{-st_0})e^{m_2 x}\right] \tag{3.22}$$

Using L'Hospital's rule to evaluate the right hand side of Eq. 3.22 as $s \to 0$, we obtain Eq. 3.8.

3.6.2.2. First moments

To derive the first moment formula, we use Eq. 3.21 with n=1:

$$M_1 = (-1)^1 \lim_{s\to 0} \frac{d^1 C(x,s)}{ds^1} = (-1) \lim_{s\to 0} \frac{dC(x,s)}{dm_2}\frac{dm_2}{ds} \tag{3.23}$$

From the definition of m_2 in Eq. 3.19, we obtain

$$\frac{dm_2}{ds} = -\frac{R}{\sqrt{V^2 + 4D(Rs+\lambda)}} \tag{3.24}$$

Taking the natural log of both sides of Eq. 3.19 gives

$$\ln C = \ln c_0 - \ln s + \ln (1 - e^{-st_0}) + m_2 x \tag{3.25}$$

Differentiating Eq. 3.25 with respect to s yields

$$\frac{1}{C}\frac{dC}{ds} = -\frac{1}{s} + \frac{t_0 e^{-st_0}}{1 - e^{-st_0}} + \frac{x\,dm_2}{ds} \tag{3.26}$$

where the terms $-\frac{1}{s} + \frac{t_0 e^{-st_0}}{1 - e^{-st_0}}$ are indeterminant as $s \to 0$.

A Taylor series expansion about s =0 gives

$$\frac{t_0 e^{-st_0}}{1 - e^{-st_0}} = \frac{1}{s} - \frac{t_0}{2} + O(s) \tag{3.27}$$

where O(s) represents terms of order s. Inserting Eqs. 3.24 and 3.27 in Eq. 3.26, and taking the limit as $s \to 0$ gives

$$\begin{aligned} \lim_{s\to 0}\left(\frac{1}{C}\frac{dC}{ds}\right) &= \lim_{s\to 0}\left(-\frac{t_0}{2} + O(s) + \frac{x\,dm_2}{ds}\right) \\ &= -\frac{t_0}{2} - \frac{xR}{\sqrt{V^2 + 4D\lambda}} \end{aligned} \tag{3.28}$$

Therefore, Eqs. 3.22, 3.23, and 3.28 give

$$-M_1 = \lim_{s\to 0}\frac{dC}{ds} = -\left(\frac{t_0}{2}+\frac{xR}{\sqrt{V^2+4D\lambda}}\right)\lim_{s\to 0} C(x,s)$$
$$= -\left(\frac{t_0}{2}+\frac{xR}{\sqrt{V^2+4D\lambda}}\right)M_0 \qquad (3.29)$$

Finally, Eq. 3.29 and the definition of the normalized first moment from Eq. 3.7 results in Eq. 3.9.

We have now derived the theoretical zeroth and first temporal moments (Eqs. 3.8 and 3.9) of a concentration distribution simulated at position x using the model described by Eq. 3.1-3.5, as presented in the paper.

As our M_0/c_0t_0 corresponds to the *MRF* given by Das and Kluitenberg (1996), we can see that our Eq. 3.8 is the same as their Eq. 30. Likewise, our Eq. 3.11 could be derived from Eq. 24 of Das and Kluitenberg (1996) and their comments below the equation.

Chapter 4

Effect of pore-water velocity on chemical nonequilibrium transport of Cd, Zn, and Pb in alluvial gravel columns

Liping Pang, Murray Close, Daniela Schneider, Greg Stanton. 2002. Effect of pore-water velocity on chemical nonequilibrium transport of Cd, Zn, and Pb in alluvial gravel columns. Journal of Contaminant Hydrology 57(3-4): 241-259.

Author affiliations:

Institute of Environmental Science & Research Ltd., PO Box 29181, Christchurch, New Zealand

Journal Referees:

Professor Peter Wierenga, Department of Soil, Water and Environmental Sciences, University of Arizona, Tucson, USA.

Professor Hilaire De Smedt, Department of Hydrology and Hydraulic Engineering, Free University of Brussels, Belgium.

Commented by Editor Dr. Grathwohl

Abstract

This paper investigates the effects of pore-water velocity on chemical nonequilibrium during transport of Cd, Zn, and Pb through alluvial gravel columns. Three pore-water velocities ranging from 3 to 60 m/day were applied to triplicate columns for each metal. Model results for the symmetric breakthrough curves (BTCs) of tritium (^3H_2O) data suggest that physical nonequilibrium components were absent in the uniformly packed columns used in these studies. As a result, values of pore-water velocity and dispersion coefficient were estimated from fitting ^3H_2O BTCs to an equilibrium model. The BTCs of metals display long tailing, indicating presence of chemical nonequilibrium in the system, which was further supported by the decreased metal concentrations during flow interruption. The BTCs of the metals were analysed using a two-site model, and transport parameters were derived using the CXTFIT curve-fitting program. The model results indicate that the partitioning coefficient (β), forward rate (k_1), and backward rate (k_2) are positively correlated with pore-water velocity (V); while the retardation factor (R), mass transfer coefficient (ω), and ratio of k_1/k_2 are inversely correlated with V. There is no apparent relationship between the fraction of exchange sites at equilibrium (f) and V. The influence of V on k_2 is much greater than on R, β, ω, and k_1. A one-order-of-magnitude change in V would cause a two-order-of-magnitude change in k_2 while resulting in only a one order-of-magnitude change in R, β, ω, and k_1. The forward rates for the metals are found to be two to three orders-of-magnitude greater than the corresponding backward rate. However, the difference between the two rates reduces with increasing pore-water velocity. Model results also suggest that Cd and Zn behave similarly, while Pb is much more strongly sorbed. At input concentrations of about 4 mg/L and pore-water velocities of 3-60 m/day in the groundwater within alluvial gravel, this study suggests retardation factors of 26-289 for Cd, 24-255 for Zn, and 322-6377 for Pb.

Key words: Pore-water velocity; Chemical nonequilibrium; Heavy metals; Alluvial gravel; Groundwater

4.1. Introduction

Transport of contaminants in groundwater systems could be affected by physical nonequilibrium processes (e.g. caused by aquifer heterogeneity, preferential flow, and kinetic diffusion) or/and chemical nonequilibrium processes (e.g. caused by kinetic sorption/ion exchange and hysteretic sorption). Local equilibrium establishes only when solute transport is under simple and ideal conditions, for example, when sorption is linear, instantaneous and reversible. The effect of pore-water velocity on contaminant transport, particularly on sorption/desorption, is receiving increased interest. It has been reported that pore-water velocity influences kinetic sorption/desorption (Akratanakul et al., 1983; Lee et al., 1988; Bouchard et al., 1988; Brusseau, 1992a; Ptacek and Gillham, 1992; Maraqa et al., 1999) but it does not influence sorption/desorption under equilibrium conditions (Lee et al., 1988; Bajracharya et al., 1996).

Kinetic sorption/desorption is commonly described by a two-site model, which assumes that the sorption sites can be partitioned into instantaneous sites and kinetic (i.e. rate-limited) sites (van Genuchten, 1981). Most studies focus on evaluating the effect of pore-water velocity on the rate of mass transfer between the two sites, and a positive relationship between the two parameters is commonly reported (Kookana et al., 1993; Maraqa et al., 1999). Comparatively less is known about the effect of pore-water velocity on other nonequilibrium parameters. For example, conflicting findings are reported in the literature for whether the fraction of instantaneous sorption sites is dependent on pore-water velocity (Brusseau et al., 1991; Kookana et al., 1993; Maraqa et al., 1999).

Parameter relationships are related to experimental conditions. The pore-water velocities reported in the above cited studies are generally low (predominantly <1 m/day) as fine materials (sand and silt) are usually used in these experiments. The findings derived from such conditions may not be applicable for coarse aquifer materials such as alluvial gravel. Pore-water velocities in alluvial gravel groundwater systems are higher than the velocities

reported in most studies in the literature, and velocity variations in alluvial gravel systems are typically large, varying between 5 and 104 m/day (Pang and Close, 1999a).

Many of the laboratory studies of reactive contaminant sorption/desorption reported in the literature were conducted with both physical and chemical nonequilibrium processes affecting transport, thereby complicating interpretation of the experimental results. It is relatively easy to study physical nonequilibrium transport alone by applying a conservative tracer to a heterogeneous medium, as has been shown by studies of Nkedi-Kizza et al. (1983), De Smedt and Wierenga (1984), Brusseau et al. (1994), Bajracharya and Barry (1997), and Pang and Close (1999a). However, it is difficult to distinguish chemical nonequilibrium processes from physical nonequilibrium transport when the experimental media is heterogeneous, and a multifactor nonideality model (Brusseau, 1992b) is needed. Hence, relatively fewer studies have investigated the effect of pore-water velocity on chemical nonequilibrium transport alone. It is possible to conduct such a study in homogeneous media as physical nonequilibrium effects are found to be minor in uniformly packed columns (Brusseau et al., 1991; Pang and Close, 1999b; Maraqa et al., 1999).

Most studies on the effect of pore-water velocity on sorption/desorption have investigated the transport of organic contaminants (e.g. Lee et al., 1988; Bouchard et al., 1988; Brusseau et al., 1991, Brusseau, 1992a; Ptacek and Gillham, 1992; Kookana et al., 1993; Maraqa et al., 1999). Few studies have investigated the effect of pore-water velocity on nonequilibrium transport of heavy metals (Akratanakul et al., 1983). Groundwater contamination by heavy metals occurs in many countries throughout the world, to a greater or lesser extent. Reliable prediction of metal movement in groundwater requires an understanding of the sorption/desorption of metals with aquifer materials. Cd, Zn, and Pb are often detected in groundwater contaminated from mining and other industrial activities as well as from landfills. Many researchers have reported that rate-limited sorption is observed for Cd (Selim, 1989; Kookana et al., 1994), Zn (Hinz and Selim, 1994), and Pb (Wilczak and Keinath, 1993) in porous media. This rate-limited sorption is characterised by rapid initial sorption followed by slow uptake. Considering the gaps in the current literature discussed

above, the objective of this paper is to investigate the effect of pore-water velocity on rate-limited sorption/desorption of Cd, Zn, and Pb in a high-pore water velocity alluvial gravel aquifer under conditions of chemical nonequilibrium.

4.2. Material and methods

4.2.1. Two-site sorption-desorption model

A one-dimensional two-site sorption-desorption transport model can be expressed as (adopted from Bales et al. 1991; McCaulou et al. 1994):

$$\frac{\partial C}{\partial t} + \frac{\phi}{\theta}\left(\frac{\partial S_1}{\partial t} + \frac{\partial S_2}{\partial t}\right) = D\frac{\partial^2 C}{\partial x^2} - V\frac{\partial C}{\partial x} \tag{4.1}$$

$$\frac{\partial S_1}{\partial t} = K_{p1}\frac{\partial C}{\partial t} \tag{4.2}$$

$$\frac{\partial S_2}{\partial t} = \frac{\theta}{\phi}k_1 C - k_2 S_2 \tag{4.3}$$

where C = solute concentration in solution (M/L^3); t = time after injection (T); x = transport distance (L); V = pore-water velocity (L/T); D = dispersion coefficient (L^2/T); ϕ = bulk density of the aquifer material (M/L^3); θ = porosity of the aquifer material (L^3/L^3); S_1 = sorbed concentration on instantaneous sites (M/M); S_2 = sorbed concentration on kinetic sites (M/M); K_{p1} = equilibrium partition coefficient for the instantaneous sites (L^3/M); k_1 = first-order sorption rate coefficient (T^{-1}); k_2 = first-order desorption rate coefficient (T^{-1}). In the above two-site sorption/desorption transport model, sorption for the instantaneous sites is represented by the sorption isotherm equation (Eq.4.2) and sorption for the kinetic sites by a first-order rate equation (Eq.4.3).

Three dimensionless coefficients are introduced to define inter-parameter relationships in the studies of Bales et al. (1991) and McCaulou et al. (1994) as follows:

$$R = 1 + \frac{\phi\left(K_{p1} + K_{p2}\right)}{\theta} = 1 + \frac{\phi K_{p1}}{\theta} + \frac{k_1}{k_2} \tag{4.4}$$

$$\omega = \frac{L/V}{1/k_1} = \frac{k_1 L}{V} \tag{4.5}$$

$$\beta = 1 - \frac{k_1}{k_2 R} = 1 - \frac{\omega V}{k_2 L R} \tag{4.6}$$

where, R= retardation factor; K_{p2}= equilibrium partition coefficient for the kinetic sites (L^3/M); ω= mass transfer coefficient; β= partitioning coefficient between the equilibrium and nonequilibrium phases; L= characteristic length (L). The degree of chemical nonequilibrium is reflected in the magnitude of β and ω. A small value for β indicates a relatively large amount of solute resides in the nonequilibrium phase, while β=1 indicates equilibrium conditions (Toride et al., 1995). From Eq.4.5, we can see that ω is the ratio of hydrodynamic residence time (L/V) to the characteristic time of sorption ($1/k_1$). The degree of nonequilibrium increases as the magnitude of ω decreases. When $\omega \geq 100$, transport is at equilibrium (Toride et al., 1995), and when $\omega \geq 10$, the local equilibrium assumption appears to be reasonably approximated (Brusseau et al., 1991).

The parameters R, β, and ω may be estimated from column breakthrough curve (BTC) data using the computer program CXTFIT (Toride et al., 1995) since the basic transport equation (Eq.4.1) is the same as the two site model given in CXTFIT. CXTFIT includes an inverse modelling capability that uses a nonlinear least-squares parameter optimisation method. The program solves the inverse problem by fitting mathematical solutions of the theoretical transport models to experimental results. In the CXTFIT program, definitions of S_1, S_2, R, β, and ω, in terms of parameters slightly different than those defined above, are given below:

$$\frac{\partial S_1}{\partial t} = f K_d \frac{\partial C}{\partial t} \tag{4.7}$$

$$\frac{\partial S_2}{\partial t} = \alpha\left((1-f)K_d C - S_2\right) \tag{4.8}$$

$$R = 1+\frac{\phi K_d}{\theta} \tag{4.9}$$

$$\beta = \frac{\theta + f\phi K_d}{\theta + \phi K_d} \tag{4.10}$$

$$\omega = \frac{\alpha(1-\beta)RL}{v} \tag{4.11}$$

where, K_d is the partition coefficient for linear sorption (L^3/M); α is the rate of mass transfer (T^{-1}); and f is the fraction of instantaneous sorption sites. Using Eqs.4.9 and 4.10, f can be calculated as:

$$f = \frac{\beta R - 1}{R - 1} \tag{4.12}$$

Comparing the CXTFIT parameters defined in Eqs.4.7-4.11 with the parameters defined in Eqs.4.2-4.6, the following equivalence formulas could be derived:

$$K_{p1} = fK_d \tag{4.13}$$

$$k_2 = \alpha = \frac{\omega V}{(1-\beta)RL} \tag{4.14}$$

$$k_1 = k_2(1-\beta)R \tag{4.15}$$

As the mass transfer rate is the same as the desorption rate ($k_2=\alpha$), we will only refer to k_2 in the remainder of the paper. Therefore, from CXTFIT-estimated values for R, β, and ω, we can calculate values for f, k_1 and k_2 using Eqs.4.12, 4.14, and 4.15, as well as residence time, T, using the formula:

$$T = \frac{RL}{V} \tag{4.16}$$

It is assumed that any reversible precipitation/dissolution processes which occurred for the metals could be lumped into sorption/desorption of the two-site model. Therefore, for the rest of this paper, we will refer to k_1 and k_2 as forward and backward rates, respectively. These rates will include any reversible precipitation/dissolution that may have occurred.

4.2.2. Experiments

The material used in the laboratory columns was taken during well drilling from below the water table at Burnham, Canterbury, New Zealand, the same field site as used in the study of Pang and Close (1999a). The aquifer material has a low cation exchange capacity (0.96 meq/100 g) and low organic carbon content (0.04%). The fine fraction (particle size <0.063 mm) contains mainly SiO_2 and Al_2O_3 with very little clay mineral content. There is a coating material, predominantly iron oxides (6-13 μm thick), on the gravel surfaces.

The columns used were acrylic tubes with a length of 18 cm and a 10 cm internal diameter. The column experiments were carried out in triplicates to assess the reproducibility of the results. The columns were packed under saturated conditions. The weight of gravel used and the water volume required to saturate the column were measured. The repacked gravel in the columns had a mean bulk density and mean effective porosity of 1.9 g/cm^3 and 0.27, respectively. This gives a mean pore volume of 382 ml for each column. The material used consisted of particle sizes as follows: 12% < 0.5 mm, 5% 0.5-2 mm, and 83% 2-20 mm. This composition reflects the average particle size distribution observed in the bulk field material with stones greater than 20 mm replaced by material from 2-20 mm. Flow was supplied from the bottom of each column to remove any entrapped air and to minimise the possibility of preferential flow. The bottom cap consisted of an acrylic plate with small holes, covered with fine mesh to distribute the inflow. All columns were covered with black coats to prevent algae growth caused by daylight.

The experiments took place at room temperature (20°C ± 1). Tap-water which was untreated and sourced from groundwater in Christchurch gravel aquifers was used as the water source. To examine the influence of pore-water velocity on metal transport, high-, intermediate-, and low-flow rates, ranging from 3-60 m/day, were applied to the columns. This velocity range is typical for Canterbury alluvial aquifers (Pang and Close, 1999a). First the columns were flushed with tap-water at the desired flow rate. Then a continuous pulse of chemical solution, containing a metal and tritiated water (^3H_2O), was injected into the columns until the ratio between metal inflow- and outflow-concentrations was significantly high (refer to Fig.4.2 in Section 4.3.2). Then the columns were flushed with tap-water again until the metal concentration in the effluent had dropped down to the tap-water background level. The experiments were conducted in a sequence of high-, intermediate-, and low-flow rates. Experiments on Cd were carried out first, followed by Zn, and finally Pb in order of assumed decreasing mobility. ^3H_2O was used as a conservative tracer to provide an independent estimation of pore-water velocity and dispersion, and to examine any physical nonequilibrium processes in the experimental system. Effluent flow rates were measured regularly and the cumulative volume recorded using a flow-meter. Samples were frequently taken from the outflow, particularly during times of rapid concentration change, and twice a day from the inflow. Inflow and outflow samples were also measured for pH. The designed input concentrations of the chemical solution were about 5000 decays per minute/10 ml for ^3H_2O and about 4 mg/l for the metals. As Pb precipitation was significant, tap-water that had been treated using reverse osmosis, which had a pH of 5.9 and total dissolved ion concentration 0.4-0.5% of the tapwater, was used in the Pb experiment at intermediate flow conditions. No experiment was conducted for Pb at low flow. This is because Pb is strongly sorbed and the long time required to conduct the experiment would result in varying input concentrations due to precipitation reactions. Table 4.1 lists the experimental conditions and properties of the chemicals used. The metal samples were acidified and analysed using a Flame Atomic Absorption Spectrometer with a detection limit of 20 μg/l. ^3H_2O samples were analysed using a liquid scintillation counter.

Table 4.1
Experimental conditions for the column experiments

a) chemical concentrations of the pulses and pulse duration

Chemical	Molecular formula	Net input concentration[a]			Pulse duration, hour, (PVs[b])		
		high flow	intermediate flow	low flow	high flow	intermediate flow	low flow
Cd	$Cd(NO_3)_2 * 4 H_2O$	4.69 (4.61-4.75)	4.22 (4.05-4.34)	2.67 (1.26-3.93)	6 (79)	19 (74)	117 (97)
Zn	$Zn(NO_3)_2 * 6 H_2O$	3.88 (3.82-3.91)	3.64 (3.52-3.70)	2.57 (1.72-3.15)	7 (86)	26 (105)	113 (98)
Pb	$PbNO_3$	3.62 (3.14-4.64)	3.17 (2.51-3.92)		19 (220)	339 (1554)	
Tritiated water$_{-Cd}$	^3H_2O	3409 (3283-3825)	3355 (3072-3579)	3329 (3310-3608)	6 (79)	19 (74)	117 (97)
Tritiated water$_{-Zn}$	^3H_2O	5656 (5340-5854)	6029 (5784-6220)	4667 (4333-5078)	7 (86)	26 (105)	113 (98)
Tritiated water$_{-Pb}$	^3H_2O	6224 (5943-6464)	5106 (4620-5523)		19 (220)	339 (1554)	

[a]Concentration units: mg/l for Cd, Zn, Pb; and decays per minute/10 ml for ^3H_2O.
Background levels of ^3H_2O due to scintillant and Zn in the tap-water were taken off.

[b]PVs = average number of pore volumes
Values in parentheses with hyphens are the minimum and maximum.

b) Chemical composition of the tap-water
(from Canterbury gravel aquifers)

Parameter	Concentration (mean of 8 samples)
*p*H	7.2
Ionic strength	1.7
Conductivity	12.0
HCO_3	65
Cl	4.9
NO_2-N	0.00
NO_3-N	0.91
NH_4-N	0.01
Na	7.4
K	0.7
Ca	13.7
Mg	1.9
SO_4	5.6
Fe	0.04
Mn	0.02
Total organic carbon	<1

Concentration units: ionic strength in mmol/l, conductivity in mS/m, major ions in mg/l

c) Mean pH values of inflow and outflow

Metal	*p*H-inflow	*p*H-outflow
Zn @ low flow	7.9	7.8
Zn @ intermediate flow	8.0	7.9
Zn @ high flow	7.9	7.6
Cd @ low flow	8.2	7.9
Cd @ intermediate flow	8.0	7.6
Pb @ intermediate flow	5.9	5.9 **
Pb @ high flow	7.9	7.9

**Tap-water treated using reverse osmosis was used.

A flow interruption method (Brusseau et al., 1989) was used to discern nonequilibrium conditions during solute transport. If nonequilibrium conditions exist, an arrival wave interruption of the flow during breakthrough would result in a decrease in aqueous concentrations. In contrast, if equilibrium conditions exist, the flow interruption should have no effect on outflow concentrations. For each experiment, flow was stopped for 2 hours during the early period of pulse supply. The effluent was sampled several times rapidly in succession once the flow resumed.

4.2.3. Parameter estimation

A two-region model incorporated in the CXTFIT program was first applied to the ^3H_2O data to examine any physical nonequilibrium processes in the system. However, as model results gave β values of unity, i.e. all the water in the system was essentially mobile, the program suggested to us the equilibrium model for the ^3H_2O data. Hence the equilibrium model was used for the ^3H_2O data to estimate pore-water velocity (V) and dispersion coefficient (D). As only two parameters are optimised in the equilibrium model, the V and D results can be determined uniquely. Then, holding V and D constant for the metal, values of R, β, and ω for the metal were optimised using the two-site model of the CXTFIT program. As three parameters are optimised in the two-site model, model results are not unique and, hence, a few model runs were undertaken using different initial parameter value guesses until the results converged. Values of f, k_1, k_2, k_1/k_2, and T were then calculated from model-derived parameters based on formulas given previously.

It should be noted that the R-values derived from the CXTFIT program correspond to the K_d values for linear isotherms (Eq.4.9). However, sorption is generally not linear for Cd (Pekdeger et al. 1988; Pang and Close, 1999b), Zn (Mandal and Hazra, 1997), and Pb (Hinton and Close, 1998). For solutes with nonlinear isotherms to be used in the CXTFIT program, van Genuchten (1981) introduced two linearization methods. These methods allow obtaining an equivalent K_d value for linear sorption from nonlinear isotherms and input concentration of the column experiment. An example could be seen in Pang and Close (1999b). However, as we did not actually determine isotherms of the metals in this study,

calculation of K_d and K_{pl} values and their corresponding nonlinear parameters was hence not carried out. Therefore, the retardation factor, R, is the only parameter used herein to express the relative sorption capacity of the aquifer material.

4.3. Results and discussion

4.3.1. ^3H_2O

The results obtained from the two-region model for the ^3H_2O data suggest that all the water in the system was essentially mobile (β=1) and the equilibrium model should be used for analysing the ^3H_2O data. Further evidence of equilibrium ^3H_2O transport could be seen from the results of the flow interruption experiments. After flow interruption, ^3H_2O concentrations were the same as concentrations prior to flow interruption, indicating equilibrium transport. Table 4.2 lists D and V values obtained from curve-fitting of ^3H_2O BTCs. Comparison of the experimental results of triplicates (Table 4.2 and Fig.4.1) shows that the reproducibility of the miscible-displacement method is excellent.

4.3.2. Heavy metals

Fig.4.2 shows observed and model-simulated BTCs of Cd, Zn, and Pb at three pore-water velocities, and Table 4.3 lists parameter values for the metals derived from the curve-fitting and calculated from model-derived parameters. It should be noted that for the low-flow Cd experiment only the rising part of the BTCs was used for the optimization and presentation. This is because the input concentration changed significantly during injection and it was difficult to match the metal concentrations in the effluent to the varying injected concentrations, particularly at later times in the experiment. Fig.4.2 shows that all the metal BTCs that were completed exhibit significant tailing suggesting chemical nonequilibrium processes affected transport. Other evidence of nonequilibrium transport for the metals are the decreasing concentrations during flow interruption and very small β (<0.05) and ω values (<2.4).

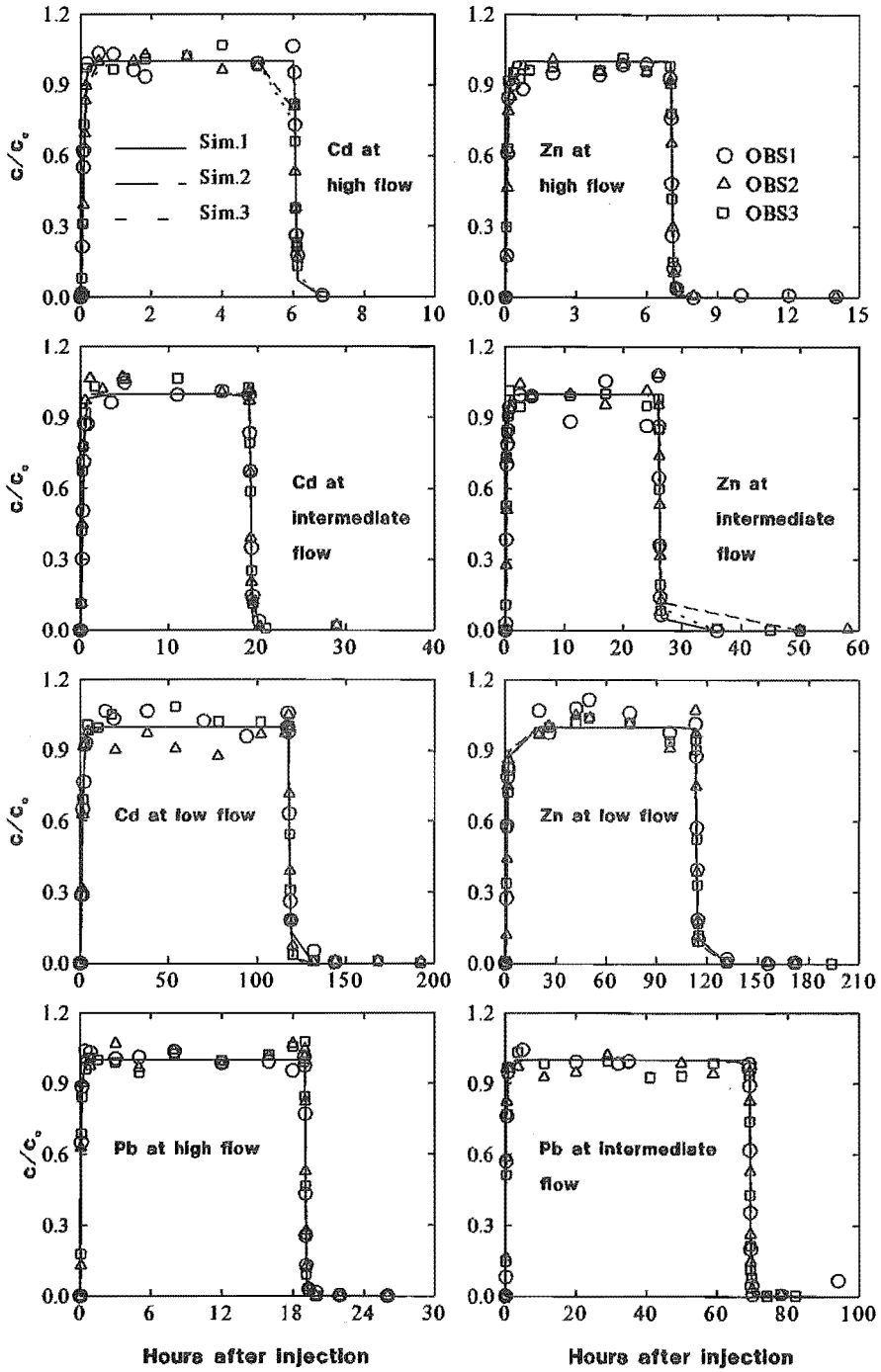

Fig.4.1. Observed and CXTFIT-simulated concentration breakthrough curves of ^3H_2O for the triplicate columns.

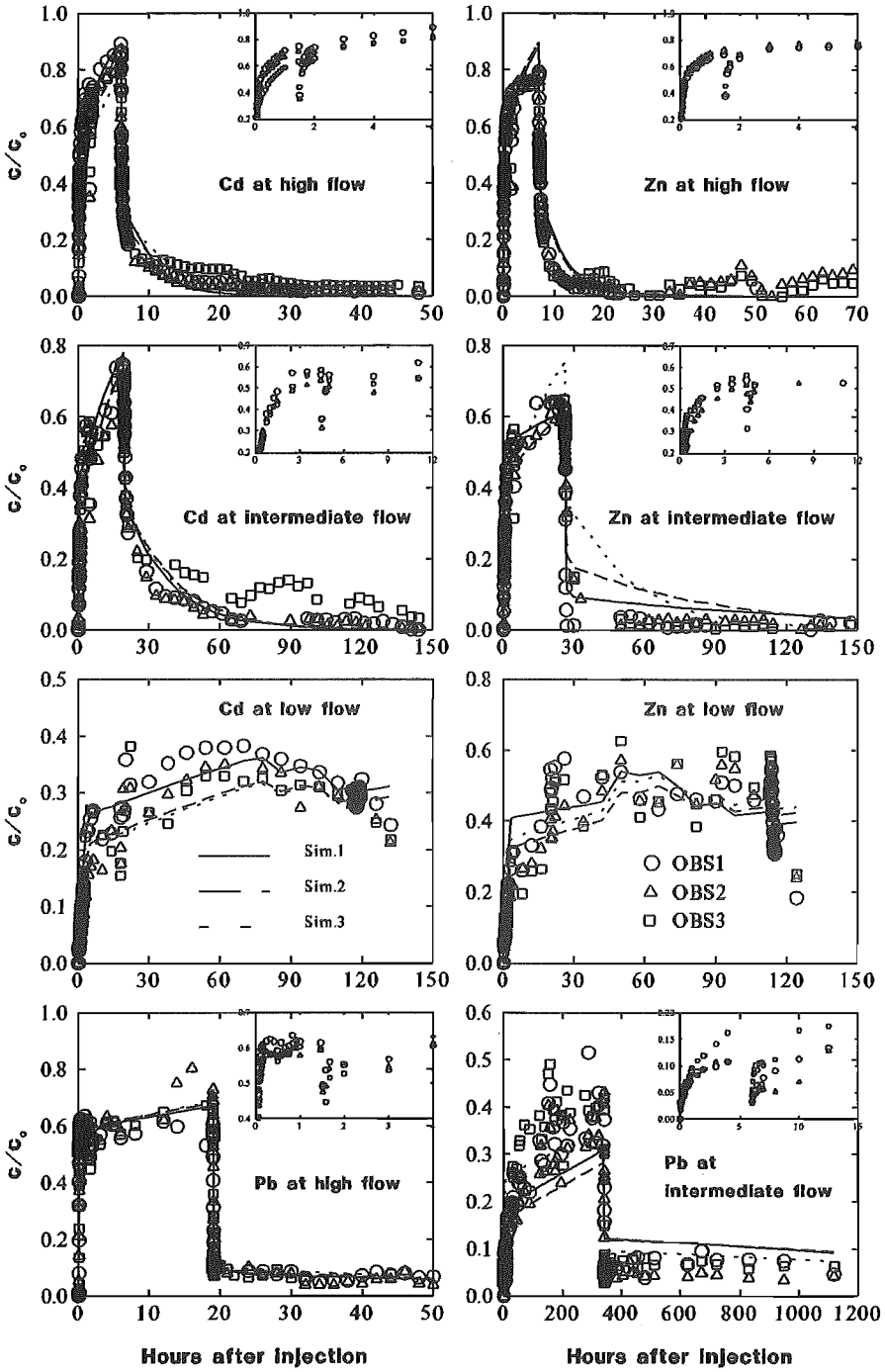

Fig.4.2. Observed and CXTFIT-simulated concentration breakthrough curves of Cd, Zn, and Pb for the triplicate columns. Plots in the small boxes show concentration changes during flow interruption.

Table 4.2
Equilibrium model-derived pore-water velocity and dispersion coefficient estimated from the ^3H_2O data

Experiment with	Column	V (m/day)	D (m^2/day)
Cd	1	3.51 (0.17)	0.12 (0.02)
Cd	2	3.42 (0.16)	0.08 (0.02)
Cd	3	3.79 (0.20)	0.10 (0.03)
Cd	1	15.1 (0.60)	0.45 (0.08)
Cd	2	17.8 (0.75)	0.42 (0.08)
Cd	3	17.7 (1.61)	1.06 (0.33)
Cd	1	58.6 (3.09)	1.40 (0.36)
Cd	2	52.1 (1.78)	2.04 (0.32)
Cd	3	59.7 (2.95)	2.17 (0.46)
Zn	1	3.79 (0.18)	0.14 (0.03)
Zn	2	3.62 (0.11)	0.07 (0.01)
Zn	3	3.82 (0.17)	0.16 (0.03)
Zn	1	18.4 (0.94)	0.58 (0.13)
Zn	2	14.6 (0.53)	0.52 (0.07)
Zn	3	19.2 (3.24)	1.93 (0.74)
Zn	1	55.4 (3.25)	1.79 (0.46)
Zn	2	44.7 (2.12)	1.57 (0.27)
Zn	3	59.0 (1.89)	1.96 (0.27)
Pb	1	18.9 (1.03)	0.56 (0.14)
Pb	2	16.3 (0.97)	0.39 (0.11)
Pb	3	16.3 (1.41)	0.56 (0.19)
Pb	1	51.1 (1.81)	1.34 (0.30)
Pb	2	48.8 (2.05)	1.15 (0.26)
Pb	3	50.3 (2.39)	1.27 (0.32)

Values in parentheses give standard errors of the model estimation.

Student's *t*-test results suggest that Cd and Zn are similar in the values of their transport parameters. This is probably because they are within the same group in the periodic table and thus share similar chemical properties. The only exception is the greater values of f calculated for Cd than for Zn (P=0.02, where P= the probability that the two paired test parameters have the same mean), suggesting more sorption sites are instantaneous for Cd than for Zn. Compared to Cd and Zn, values of R, T, and k_1/k_2 for Pb are generally one-order-of-magnitude greater ($P \leq 0.07$), values of β and k_2 are generally one order-of-magnitude smaller ($P \leq 0.04$), while values of ω and k_1 are similar. This finding suggests that, compared to Cd and Zn, Pb is much more strongly sorbed, with a correspondingly longer residence time. Although forward rates, k_1, for Pb are not much different from those of Cd and Zn, backward rates, k_2, for Pb are much slower than those of Cd and Zn.

Reversible sorption is observed for Cd at the high- and intermediate-flows, and for Pb at the intermediate flow, as indicated from their total mass recovery. The total mass recovery for these experiments also indicates that precipitation/dissolution, if any, is also reversible. Reversible sorption of Cd has also been observed by others (Pekdeger et al., 1988; Al-Hashimi et al. 1994). It is unclear if Zn sorption is also reversible. The estimated mass recovery for Zn is 84-89% for the high-flow and 72-76% for the intermediate-flow. However, Zn mass balance was confounded by the fact that Zn had significantly fluctuating background concentrations in the tap-water and it was impossible to obtain a representative background level. As the net Zn concentrations were simply obtained by subtracting the average background Zn concentration from the measured Zn concentrations, Zn data may not be reliable. Other factors, such as inaccuracy in representative flow rates and input concentrations, sampling frequency and data truncation, as well as errors in numerical integration of BTC data could have also contributed to the errors in the estimated Zn mass recoveries. For the low-flow of the Cd and Zn experiments and intermediate flow of the Pb experiment, it was impractical to obtain complete BTCs due to the prolonged duration of experiments, hence mass recovery for these incomplete BTCs is only 69-81% for Cd, 75-85% for Zn, and 47-67% for Pb.

Table 4.3
Chemical nonequilibrium transport parameters derived from the two-site model and parameters calculated from the model results

Metal	Column	V (m/day)	R	β	ω	T (day)	f	k_1 (per day)	k_2 (per day)	k_1/k_2
Cd	1	3.51	254 (12.3)	0.008 (0.000)	1.71 (0.05)	13.0 (0.63)	0.005 (0.001)	33.3 (0.96)	0.13 (0.00)	251 (2.31)
Cd	2	3.42	251 (13.3)	0.009 (0.001)	1.89 (0.06)	13.2 (0.70)	0.005 (0.001)	33.3 (0.96)	0.13 (0.00)	251 (0.86)
Cd	3	3.79	289 (15.3)	0.004 (0.000)	1.98 (0.05)	13.7 (0.73)	0.000 (0.001)	41.7 (1.15)	0.14 (0.00)	288 (0.71)
Cd	1	15.1	39.7 (1.58)	0.050 (0.002)	0.96 (0.04)	0.47 (0.02)	0.025 (0.003)	80.1 (3.61)	2.12 (0.02)	37.7 (1.42)
Cd	2	17.8	55.2 (2.51)	0.033 (0.002)	1.11 (0.05)	0.56 (0.03)	0.015 (0.002)	109 (5.21)	2.05 (0.01)	53.4 (2.33)
Cd	3	17.7	55.1 (3.41)	0.045 (0.003)	1.21 (0.09)	0.56 (0.03)	0.027 (0.004)	119 (8.37)	2.26 (0.03)	52.7 (3.10)
Cd	1	58.5	26.0 (1.71)	0.044 (0.003)	0.54 (0.02)	0.08 (0.01)	0.027 (0.006)	175 (7.50)	7.03 (0.14)	24.8 (0.56)
Cd	2	52.1	37.5 (1.76)	0.035 (0.002)	0.58 (0.02)	0.13 (0.01)	0.009 (0.003)	168 (6.06)	4.64 (0.04)	36.2 (0.97)
Cd	3	59.6	50.4 (2.51)	0.032 (0.002)	0.87 (0.03)	0.15 (0.01)	0.012 (0.003)	289 (10.7)	5.91 (0.06)	48.8 (1.28)
Zn	1	3.79	255 (53.6)	0.004 (0.001)	1.05 (0.09)	12.1 (2.55)	0.000 (0.002)	22.2 (1.87)	0.09 (0.01)	254 (12.1)
Zn	2	3.52	158 (15.8)	0.006 (0.001)	1.28 (0.09)	8.07 (0.81)	0.000 (0.001)	22.2 (1.87)	0.09 (0.00)	254 (7.69)
Zn	3	3.82	158 (21.7)	0.006 (0.002)	1.32 (0.13)	7.45 (1.02)	0.000 (0.002)	28.1 (2.75)	0.18 (0.01)	157 (9.32)
Zn	1	18.4	233 (47.8)	0.010 (0.002)	0.72 (0.04)	2.28 (0.47)	0.006 (0.003)	73.7 (4.58)	0.32 (0.05)	230 (20.2)
Zn	2	14.6	125 (11.3)	0.019 (0.005)	0.98 (0.05)	1.54 (0.14)	0.011 (0.006)	79.0 (4.30)	0.65 (0.02)	122 (2.78)
Zn	3	19.2	81.2 (4.98)	0.025 (0.002)	1.46 (0.09)	0.76 (0.05)	0.012 (0.003)	156 (9.54)	1.97 (0.00)	79.2 (5.01)
Zn	1	55.4	32.0 (2.33)	0.039 (0.003)	0.79 (0.03)	0.10 (0.01)	0.008 (0.006)	244 (10.6)	7.95 (0.21)	30.7 (0.53)
Zn	2	44.7	23.5 (1.91)	0.045 (0.004)	0.75 (0.04)	0.09 (0.01)	0.003 (0.008)	188 (8.80)	8.34 (0.25)	22.5 (0.38)
Zn	3	59.0	31.0 (2.39)	0.035 (0.003)	0.76 (0.03)	0.09 (0.01)	0.003 (0.006)	248 (10.4)	8.26 (0.26)	29.9 (0.31)
Pb	1	18.9	5377 (806)	0.002 (0.001)	2.52 (0.16)	51.3 (7.68)	0.001 (0.001)	264 (16.3)	0.05 (0.00)	5369 (153)
Pb	2	15.3	5778 (741)	0.001 (0.000)	2.26 (0.12)	67.9 (8.71)	0.001 (0.000)	264 (16.3)	0.05 (0.00)	5369 (60.6)
Pb	3	15.3	5301 (549)	0.004 (0.001)	1.72 (0.10)	62.3 (6.45)	0.003 (0.001)	147 (8.55)	0.03 (0.00)	5282 (69.6)
Pb	1	51.5	415 (57.3)	0.002 (0.000)	0.57 (0.02)	1.45 (0.20)	0.000 (0.001)	164 (6.44)	0.40 (0.04)	414 (25.6)
Pb	2	48.8	352 (34.2)	0.003 (0.000)	0.55 (0.02)	1.30 (0.13)	0.000 (0.001)	151 (4.10)	0.43 (0.03)	351 (15.2)
Pb	3	50.3	322 (25.1)	0.003 (0.000)	0.58 (0.06)	1.15 (0.09)	0.000 (0.001)	162 (15.5)	0.51 (0.01)	321 (24.9)

Values of R, β, and ω are derived from the model simulation, and the rest parameters are calculated from the model results.
Values in parentheses give standard errors.

There was generally 0.1-0.2 units reduction in the effluent pH, compared with the input pH. Sorption of heavy metal ions onto iron oxides, the coating material of the gravel, can cause the release of hydrogen ions into solution, resulting in the reduction of the pH. Dissolution or precipitation reactions are generally slower than reactions (including sorption) among dissolved species (Stumm and Morgan, 1981). For example, in the laboratory, Cd precipitation has been found to occur much more slowly than sorption (Fuller and Davis 1987; Pang and Close 1999b). Because it is difficult to generalize the rates of precipitation and dissolution from literature sources (Stumm and Morgan, 1981), rates of any precipitation and dissolution have been lumped into forward and backward sorption rates, respectively. Together with desorption, dissolution of precipitated metals may have also contributed to the slow decrease in metal concentrations as exhibited by the tailing of the BTCs. This tailing also results in elevated R values estimated by the model.

4.3.3. Effect of pore-water velocity

Fig.4.3 displays the relationship between pore-water velocity and chemical nonequilibrium parameters. Considering the similarity of Cd and Zn, the results for Cd and Zn are plotted together. The results of Pb are plotted separately, as its parameter values are very different from those of Cd and Zn. Although stronger relationships can be seen when using residence time, T, than using V with the above parameters, the calculated T values from Eq.4.16 involve the use of two model estimated parameters (V and R), hence, the uncertainty for T values is higher than for V values. In addition, it is more convenient to use V for comparing results of other studies. Therefore, we will focus on presentation and discussion of V. Parameter relationships are generally expressed well in log-log plots.

4.3.3.1. Retardation factor (R)

Fig.4.3 shows that pore-water velocity is inversely related with R. This has been also reported by others (Nkedi-Kizza et al., 1983; Schulin et al., 1987; Ptacek and Gillham, 1992; Shimojima and Sharma, 1995). The velocity dependence of R is an indication of

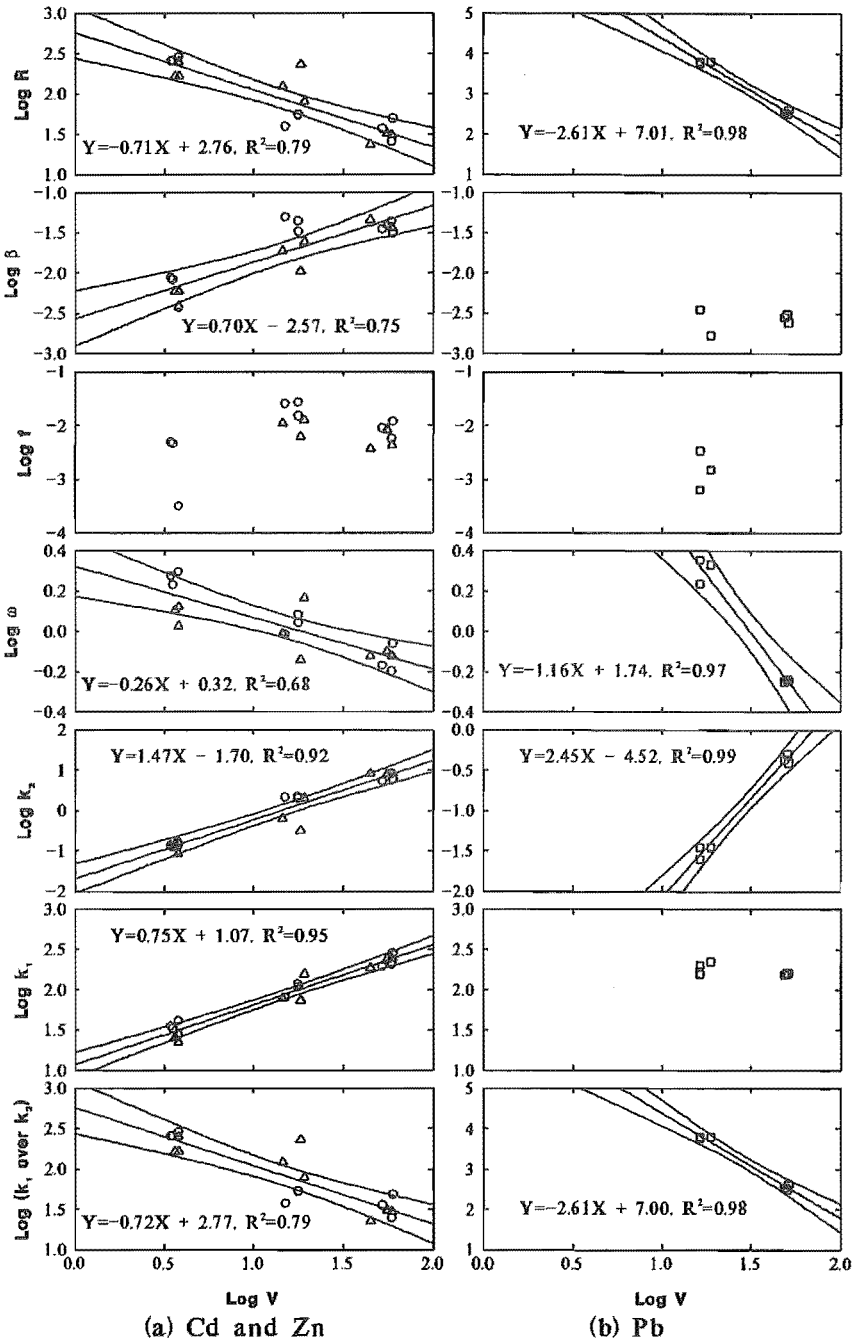

Fig.4.3. The effects of pore-water velocity on chemical nonequilibrium parameters. Results from the triplicate columns are shown.

nonequilibrium conditions. The inverse *R-V* relationship could be explained in terms of the retention time of the metals in the columns. At the low flows, longer retention times of the metals in the columns allow more complete sorption. Table 4.3 shows that the *R* values increase significantly when the flow is dropped from the intermediate-flow to the low-flow, but do not increase much when the flow is dropped from the high flow to the intermediate-flow. For Zn, most differences can be found when changing the high flow to the intermediate flow, whereas a further decrease of the flow rate does not affect the retardation factor significantly.

It should be noted that as sorption/desorption of metals is highly dependent on pH and metal concentrations, the retardation factors estimated in this study (*R*=26-289 for Cd, *R*=24-255 for Zn, and *R*=322-6377 for Pb) are applicable only to the specific conditions of this study. This paper focuses on the effect of pore-water velocity on chemical nonequilibrium parameters, and does not intend to determine the sorption characteristics of the metals, for which batch isotherms would be needed.

4.3.3.2. Nonequilibrium transport parameters (β, ω, and f)

Fig.4.3 shows that pore-water velocity is positively related with β, inversely related with ω, and not related to f. The inverse relationship between V and ω indicates that, as expected, the degree of nonequilibrium transport increases with pore-water velocity, which is also observed by Bouchard et al. (1988). The explanation is that a higher velocity leads to more nonequilibrium, hence a smaller value for ω. Similar relationships between V-β and V-ω have been also found for physical nonequilibrium (Pang and Close, 1999a). The observed independence of f on V is consistent with findings of Maraqa et al. (1999) and Brusseau et al. (1991) but in conflict with findings of Kookana et al. (1993) and Hu and Brusseau (1996). Whether f is velocity related seems to depend on the process involved. Physical nonequilibrium was absent in the experimental systems of this study and studies of Maraqa et al. (1999) and Brusseau et al. (1991), while physical and chemical nonequilibrium coexisted in the experimental systems of Kookana et al. (1993) and Hu and Brusseau

(1996). Schwarzenbach and Westall (1981) indicated that f would be dependent on V for a chemical nonequilibrium process involving a number of different reaction times. For nonequilibrium caused by a diffusion process, f is found to be independent of V (Brusseau et al., 1991). If this is the case, the lack of dependence of f on V observed in this study suggests that sorption nonequilibrium of the metals may be due to a diffusion process.

The very small β (< 0.05) and f values (<0.03) suggest that sorption/desorption of the metals is predominantly kinetic and less than 3% of sorption sites are instantaneous. However, results obtained from the one-site model (not shown) are not better than those obtained from the two-site model. Compared to the literature studies (Nkedi-Kizza et al., 1984; Brusseau et al., 1991; Brusseau, 1992a; Maraqa et al., 1999), the β and f values derived in this study (Table 4.3) are two-orders-of-magnitude lower, while the ω values are of a similar order, or one-order-of-magnitude higher. This is probably because β and f are related to retardation factors (Eqs.4.10 and 4.12) which are high for the heavy metals in this study. Hence, values of β and f are probably contaminant and media specific. In contrast, the ω values do not seem to vary much between studies, even though flow rates, porous media, and contaminants are different.

4.3.3.3. Forward and backward rates (k_1, k_2, k_1/k_2)

Fig.4.3 demonstrates that forward/backward rates (k_1 and k_2) are positively correlated with V, suggesting both sorption and desorption rates increase with increasing pore-water velocity. A possible interpretation for this finding is a hypothesis of "film-mass transfer". Increases in pore-water velocity may decrease the thickness of an immobile water film between mobile water and sorption sites and hence speed mass transport across the film in both forward and backward directions. Akratanakul et al. (1983) also observed that the rate of Cd sorption increased with increasing pore-water velocity. They interpret that the high flow rate brings a greater mass of ions during the same span of time and thus maintains a higher ion concentration in the bulk solution, which drives more ions toward the surfaces of the media particles. The positive relationship between pore-water velocity and backward

rate has been reported for chemical nonequilibrium (Maraqa et al., 1999) and physical nonequilibrium (Pang and Close, 1999a), as well as for transport with interplay of both processes (Kookana et al., 1993; Hu and Brusseau, 1996). The k_1 values for the metals are two to three orders-of-magnitude greater than their corresponding k_2 values (Table 4.3). Fig.4.3 shows that k_1/k_2 ratio reduces with increasing V, indicating that the difference between k_1 and k_2 reduces with increasing pore-water velocity. This is expected, as k_1/k_2 is proportional to R (Eq.4.4) while R is inversely related to V as described in Section 4.3.3.1.

The influence of V on k_2 is much greater than on R, β, ω, and k_1. For both Cd and Zn, a one-order-of-magnitude increase in pore-water velocity (from the low flow to the high flow) leads to two-orders-of-magnitude increase in the k_2 values while only same-order-of-magnitude increases in β and k_1 values, and same-order-of-magnitude decreases in the R and ω values. Hu and Brusseau (1996) also report a similar finding.

The pore-water velocities used in this study are generally higher than those used in other studies reported in the literature. Comparing studies that used the same order-of-magnitude values of V, the k_2 values derived herein for the metal-alluvial gravel interaction are generally lower than the literature values for organic compound-fine porous media interaction, by two-orders-of-magnitude (Lee et al., 1988; Ptacek and Gillham, 1992; Brusseau, 1992a) or one-order-of-magnitude (Kookana et al., 1993; Maraqa et al., 1999). This may be explained by the lower sorption capacity for the alluvial gravel than for fine porous media as k_2 is found to be inversely correlated to the sorption partition coefficient, K_d (Karickhoff and Morris, 1985; Brusseau and Rao, 1989; Brusseau et al., 1991; Brusseau, 1992a).

4.4. Conclusions

This study investigates metal sorption in uniformly packed columns, where physical nonequilibrium effects are minimal, so metal sorption/desorption was affected by chemical nonequilibrium phenomena. The study investigates the effect of pore-water velocity on chemical nonequilibrium transport for Cd, Zn, and Pb. As has been found for physical

nonequilibrium transport in alluvial gravel aquifers (Pang and Close, 1999a), pore-water velocity (V) was found to be positively corrected with partitioning coefficient (β) and the first-order backward rate constant (k_2) but inversely correlated with mass transfer coefficient (ω), although these parameters have different meanings for chemical and physical nonequilibrium transport. In contrast to what is observed for the systems with interplay of physical and chemical nonequilibrium processes (e.g. Kookana et al., 1993; Hu and Brusseau, 1996), we found that, at chemical nonequilibrium conditions, the fraction of exchange sites at equilibrium (f) is independent of pore-water velocity. The independence of f on V observed in this study suggests that sorption nonequilibrium of Cd, Zn, and Pb is due to a diffusion process.

Values of β, f, and k_2 derived in this study for the metal-alluvial gravel interaction are much lower than the literature values for organic compound-fine porous media interaction, probably due to the poor sorption capacity of the alluvial gravel used in this study. However, ω values derived from this study are similar to those reported in other studies. This suggests that β, f, and k_2 are closely related to the contaminant and media while ω is relatively independent of contaminant and media characteristics.

Acknowledgements

This study was funded by the Foundation for Research, Science and Technology (New Zealand) under contract number CO3410. Professor Mark Goltz of Air Force Institute of Technology (USA) is acknowledged for his valuable and detailed comments.

4.5. Additional study: Non-linear equilibrium sorption

4.5.1. Transport equation and retardation factor for non-linear sorption

In Chapter 4, instantaneous sorption (i.e. equilibrium sorption) in the two-site sorption/desorption model is described by a linear sorption isotherm equation. More generally, equilibrium reversible sorption isotherms could be represented by a non-linear function, such as the Freundlich equation,

$$S = K C^n \tag{4.17}$$

where S = sorbed concentration (M/M), K = non-linear equilibrium partition coefficient $(L^3/M)^n$, and n = Freundlich exponent constant. Neglecting degradation and kinetic sorption, contaminant transport in a one-dimensional flow field could be described by

$$\frac{\partial C}{\partial t} = D\frac{\partial^2 C}{\partial x^2} - v\frac{\partial C}{\partial x} - \frac{\phi}{\theta}\frac{\partial S}{\partial t} \tag{4.18}$$

Incorporating non-linear sorption, differentiation of (Eq. 4.17) with respect to time gives,

$$\frac{\partial S}{\partial t} = K n C^{n-1}\frac{\partial C}{\partial t} \tag{4.19}$$

Inserting Eq. 4.19 into Eq. 4.18 yields

$$\frac{\partial C}{\partial t} = D\frac{\partial^2 C}{\partial x^2} - v\frac{\partial C}{\partial x} - \frac{\phi}{\theta} K n C^{n-1}\frac{\partial C}{\partial t} \tag{4.20}$$

Equation 4.20 may be rewritten as:

$$R\frac{\partial C}{\partial t} = D\frac{\partial^2 C}{\partial x^2} - v\frac{\partial C}{\partial x} \tag{4.21}$$

where R is defined as

$$R = 1 + \frac{\phi}{\theta} K n C^{n-1} \tag{4.22}$$

Note that in this more generic version of the retardation factor, R is concentration dependent. When n <1, the retardation factor decreases with increasing concentrations, when n > 1, the retardation factor increases with increasing concentrations, and when n =1, the retardation factor is a constant. The expression for R in Eq. 4.22 has also been presented by others (Fetter, 1993; Spurlock et al. 1995; Clothier et al. 1996). Many contaminants (e.g. heavy metals, organics) have a value of n < 1, particularly at high concentrations (e.g. Pang and Close, 1999b). The situation where n > 1 occurs less often (e.g. some pesticides and ion exchange). However, as the retardation factor is a function of concentration and not a constant, the transport equation is non-linear and it is difficult to model. Therefore, for simplicity, most models (including all the models used in this thesis) deal with linear equilibrium sorption (n =1) which is typically seen in the literature in the form of Eq. 4.9 of the publication: $R = 1 + \frac{\phi}{\theta} K_d$ where $K_d = K$.

4.5.2. Linearization of non-linear sorption isotherms

Sorption is generally not linear for the metals investigated in this chapter. If using non-linear isotherm parameter values to calculate the R-values that could be used in the CXTFIT program, the non-linear isotherm must first be linearized. This is because CXTFIT, like other analytical models, can only handle linear sorption for both equilibrium and non-

equilibrium transport. Two linearization methods, described by van Genuchten (1981), could be used to obtain an equivalent K_d value if a non-linear isotherm ($S= KC^n$) and the input concentration of an experiment (C_o) are given.

Linearization method 1 assumes that the area under the linearized isotherm ($S= K_d C$) is the same as the area under the nonlinear isotherm ($S= KC^n$) over the range of concentration values. For an initial concentration C_i =0 (note $C_i \neq C_o$), this gives:

$$K_d = \frac{2KC_o^{n-1}}{n+1} \tag{4.23}$$

where C_o is the input solute concentration and n is the exponent from the Freundlich isotherm. Linearization method 2 assumes that K_d can be approximated by the average slope of the non-linear isotherm. For C_i =0, this gives:

$$K_d = KC_0^{n-1} \tag{4.24}$$

An example of linearizing the Freundlich isotherm for Cd sorption determined from batch tests (to determine K_d and R-values for use in CXTFIT) can be seen in a previous study of Pang and Close (1999b). They found that Method 1 generally gave a slightly better fit to the observed column data than Method 2.

4.5.3. Determination of a non-linear sorption isotherm using column data

4.5.3.1. Using a conservative tracer

Traditionally, sorption isotherms are determined from batch tests. Inventively, Clothier et al. (1996) proposed using a permeameter with both a conservative tracer and reactive chemical to resolve the sorption isotherm in the field. This method could be also applied to column

experiments. The retardation factor can be determined either from the lag of the reactive solute front behind a conservative tracer at time t, or the lag time in peak concentration (or centre of mass) at location x for the two compounds, or their velocity ratio:

$$R = \frac{x_{conservative}}{x_{reactive}} = \frac{t_{reactive}}{t_{conservatiev}} = \frac{v_{conservative}}{v_{reactive}} \tag{4.25}$$

At the same pore-water velocity, for inflow concentration C_1, there is a retardation factor value R_1; and for inflow concentration C_2, there is a retardation factor value R_2 as below:

$$R_1 = 1 + \frac{\phi}{\theta} K n C_1^{n-1} \tag{4.26}$$

$$R_2 = 1 + \frac{\phi}{\theta} K n C_2^{n-1} \tag{4.27}$$

Solving Eqs. 4.26 and 4.27 simultaneously give the value of the exponent:

$$n = 1 + \frac{\ln\left(\frac{R_1 - 1}{R_2 - 1}\right)}{\ln\left(\frac{C_1}{C_2}\right)} \tag{4.28}$$

Then from either Eq. 4.26 or Eq. 4.27, we can solve for the value of K. Hence, the non-linear sorption isotherm expressed in Eq. 4.17 can be determined.

In the paper we have demonstrated that at nonequilibrium conditions, R is a function of pore-water velocity. Therefore, to avoid the influence of nonequilibrium transport on the determination of R, we must use the same pore-water velocity when determining R and C with the above method.

4.5.3.2. Without use of a conservative tracer

A non-linear isotherm can be also determined using column data without the use of a conservative tracer. In a column experiment with a continuous source of concentration C_o and when all the sorption sites of a non-degrading contaminant (e.g. a heavy metal) are filled, the outflow concentration (C) will be equal to the inflow concentration (C_o), i.e. $C = C_o$. For non-linear equilibrium, this implies:

$$S = K C^n = K C_o^n \tag{4.29}$$

From the definition of S, we have

$$S = \frac{m_{ads}}{m} \tag{4.30}$$

where m_{ads} = mass sorbed (M) and m = mass of the solid phase (M). m_{ads} could be estimated from integration of the breakthrough curve, if we begin injecting contaminant at V=0:

$$m_{ads} = C_o V_{ads} - C_o V_o - \int_0^{V_{ads}} C\, dV \tag{4.31}$$

where C_o = inflow concentration (M/L^3), C = outflow concentration (M/L^3), V_{ads} = total volume of solution applied (L^3), V_o = pore volume of the column (L^3), and V = volume of the outflow sampled (L^3). The mass of the aquifer material in the column (m) can be estimated from the bulk density and column volume (W),

$$m = \phi W \tag{4.32}$$

This same experiment can be repeated at the same pore-water velocity for different inflow concentrations C_0 to provide an S versus C_0 plot. Uisng a power function to fit the S - C_0 data, we can then obtain values of K and n. Knowing K and n, the retardation factor, R, can be estimated using Eq. 4.22.

For the column experiment discussed in this section (4.5.3.2), Eq. 4.22 can be alternatively expressed as

$$R = 1 + \frac{\phi}{\theta} K n C_o^{n-1} = 1 + \frac{m_{ads}\, n}{C_o V_o} \tag{4.33}$$

This is because from Eqs. 4.29 and 4.30, we have

$$K = \frac{m_{ads}}{m C_0^{\,n}} \tag{4.34}$$

Porosity (θ) can be estimated from the pore volume (V_0) and column volume (W), $\theta = V_0/W$, and from Eq. 4.32, we have $\phi = m/W$.

Eq. 4.33 could be used for an independent estimate of R for non-degradable contaminants when outflow concentration is the same as the inflow concentration under a continuous source.

It should be noted that there are some limitations in this approach. Firstly, it would take a long time to reach equilibrium in a column system. Secondly, its accuracy is limited by error in integrating m_{ads} and estimating m.

4.5.4. Differentiating breakthrough curve tailing caused by non-linear equilibrium sorption from tailing caused by rate-limited sorption

Non-linear Freundlich isotherms are sometimes misunderstood and misinterpreted as a non-equilibrium phenomenon. By definition, a Freundlich isotherm describes non-linear reversible sorption equilibrium between sorbed and dissolved concentrations. It is not a kinetic phenomenon. Looking at a concentration breakthrough curve, it may be easy to confuse non-linear equilibrium sorption with linear, rate-limited sorption because both phenomena produce "tailing" (Spurlock et al. 1995; Brusseau et al., 1997) and asymmetry (Brusseau and Srivastava, 1999). Below are methods that could be used to differentiate tailing caused by non-linear equilibrium sorption from tailing due to rate-limited linear sorption.

4.5.4.1 Long-pulse

Brusseau et al. (1997) indicate that for a BTC resulting from a long pulse of solute, the BTC influenced by nonlinear sorption exhibits tailing only for the receding limb; while a BTC influenced by rate-limited sorption is self-similar, in that tailing is exhibited in the approach to a relative concentration of 1 and 0 (i.e. both the arrival and receding limbs, respectively). This is illustrated in Fig. 4.4 (a).

The above observation of Brusseau et al. (1997) could be more clearly explained by considering how the retardation factor for non-linear equilibrium sorption changes with concentration. As indicated previously, when n <1, the retardation factor decreases with increasing concentrations. This means sorption at low concentrations is greater, and the solute is more retarded. Thus, for an arrival wave, as a result of greater retardation for the low concentrations at the front of the wave than the higher concentrations behind the front, the wave exhibits so-called "self-sharpening" behaviour. For such an arrival wave, no tailing would be observed. Conversely, for a receding wave, the low concentrations at the rear of the wave are retarded more than the higher concentrations in front of them, and hence tailing

is increased. Similarly, for a continuous step input, the Freundlich curve will be "sharpened" all the way up to C/C_o =1, while the rate-limited curve will slowly approach C/C_o =1. However, for $n > 1$, the opposite occurs as retardation increases with increasing concentrations. Therefore, we would expect some tailing when the BTC approaches C/C_o =1 (sorption step) and a sharp drop when it approaches C/C_o =0 (desorption step).

4.5.4.2 Short-pulse: flow interruption

The difference between tailing caused by non-linear instantaneous sorption and rate-limited linear sorption (Fig. 4.4a) is apparent for a long-pulse. However, it is not apparent for BTCs obtained with a short pulse or influenced by mass loss since both breakthrough curves exhibit tailing only for the receding wave (Brusseau et al., 1997) as shown in Fig. 4.4(b). For this case, a flow-interruption technique used in the publication (section 4.2.2) is perhaps the most effective way to identify if tailing is caused by non-linear equilibrium sorption or rate-limited sorption. As mentioned in the publication, during a flow interruption, aqueous concentrations would decrease if nonequilibrium conditions exist but would not change if equilibrium conditions exist. This is true for the arrival portion of the pulse. The opposite would be true for the receding leg of the pulse (that is, aqueous concentrations would increase under nonequilibrium conditions). As short pulses are more often used than large pulses in column experiments, it is good practice to always perform a flow interruption during the experiments to ascertain the controlling process. For BTCs obtained in column experiments that were conducted without any flow interruption, one thing that can be done is to compare the pore volume value at which the arrival wave "arrives" to the independently calculated retardation factor (personal communication with Dr. Brusseau, 2002). If sorption is relatively strongly rate-limited, the arrival wave will be shifted leftward. Thus, the "early arrival" effect will evidence rate-limited sorption. However, one needs to have calculated the R-value independently to use this method.

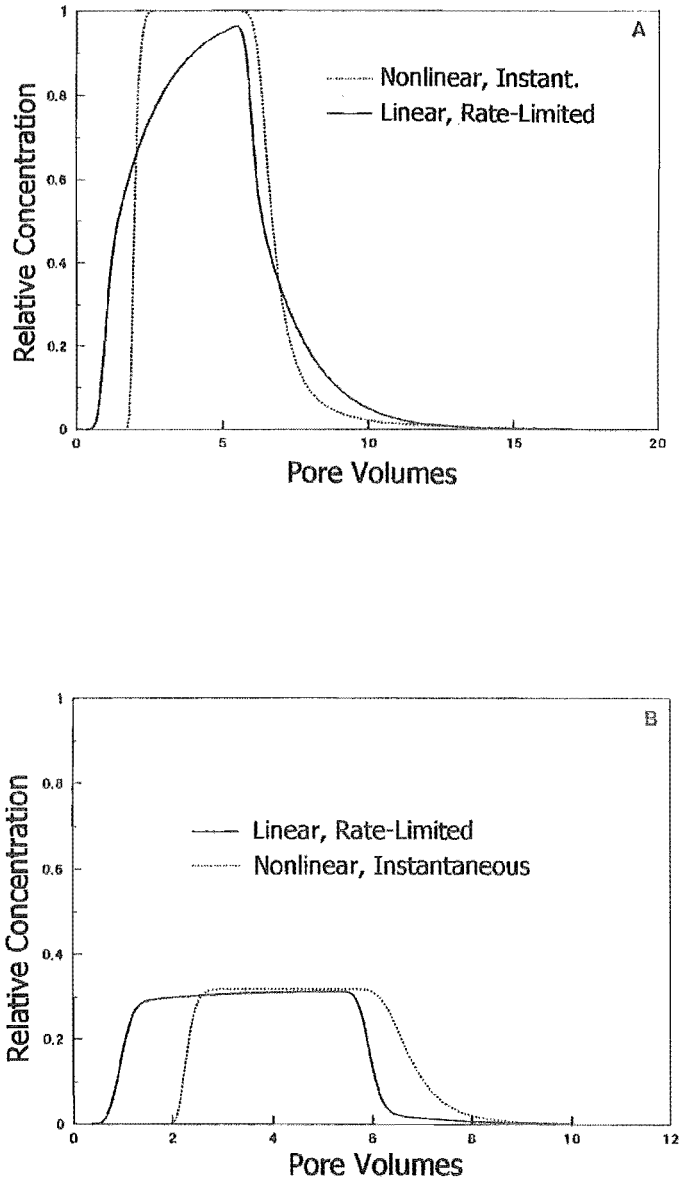

Fig. 4.4 Simulations for transport influences by instantaneous, non-linear sorption and rate-limited, linear sorption. (from Brusseau et al. 1997).

A. Large volume breakthrough curves

B. Small-volume breakthrough curves

Chapter 5

A field tracer study of attenuation of atrazine, hexazinone and procymidone in a pumice sand aquifer

Liping Pang, Murray Close. 2001. A field tracer study of attenuation of atrazine, hexazinone and procymidone in a pumice sand aquifer. Pest Management Science 57 (12): 1142-1150.

Author affiliations:

Institute of Environmental Science & Research Ltd., PO Box 29181, Christchurch, New Zealand

Journal referees:

Two anonymous referees

Abstract

A field tracer experiment, simulating point source contamination, was conducted to investigate attenuation and transport of atrazine, hexazinone and procymidone in a volcanic pumice sand aquifer. Preliminary laboratory incubation tests were also carried out to determine degradation rates. Field transport of the pesticides was observed to be significant under non-equilibrium conditions. Therefore, a two-region/two-site nonequilibrium transport model, N3DADE, was used for analysis of the field date. A lumped reduction rate constant was used in this paper to encompass all the irreversible reduction processes (e.g. degradation, irreversible sorption, complexation and filtration for the pesticides sorbed into particles and colloids) which are assumed to follow a first-order rate law. Results from the field experiment suggest that (a) hexazinone was the most mobile (retardation factor R=1.4) and underwent least mass reduction; (b) procymidone was the least mobile (R=9.26) and underwent the greatest mass reduction; (c) mobility of atrazine (R=4.45) was similar to that of rhodamine WT (R=4.10). Hence, rhodamine WT could be used to delimit the appearance of atrazine in pumice sand groundwater. Results from the incubation tests suggest that (a) hexazinone was degraded only in the mixture of groundwater and aquifer material (degradation rate constant = 4.36×10^{-3} d^{-1}); (b) procymidone was degraded not only in the mixture of groundwater and aquifer material (rate constant =1.12×10^{-2} d^{-1}) but also in the groundwater alone (rate constant = 2.79×10^{-2} d^{-1}); (c) atrazine was not degraded over 57 days incubation in either the mixture of aquifer material and groundwater or the groundwater alone. Degradation rates measured in the batch tests were much lower than the total reduction rates. This finding suggests that not only degradation but also other irreversible processes are important in attenuating pesticides under field conditions. Hence, the use of laboratory-determined degradation rates could underestimate reduction of pesticides in the field conditions.

Key words: pesticides; attenuation; solute transport; modelling; groundwater; point source

5.1. Introduction

Groundwater contamination by pesticides from agricultural activities, either from non-point and point sources, is a world-wide environmental problem. Information on mobility and persistence of pesticides is essential in modelling pesticide transport in groundwater. However, available literature data such as those reviewed and summarised by Wauchope et al. (1992) are predominately derived from soils, and only limited information is available for aquifers. Groundwater systems are low in temperature, organic materials, microbes and sometimes oxygen. Hence, sorption and degradation of pesticides in aquifers are expected to be generally less than in soils.

Of the reported groundwater studies, little work has been done in pumice sand aquifers, which are a major aquifer type in volcanic regions. Pumice sand materials have some specific physical and chemical characteristics, such as high specific surface area, the presence of allophane clay minerals and a slightly acidic environment, which may have an important impact on the attenuation of pesticides.

Atrazine, hexazinone and procymidone are three pesticides commonly used world-wide. Atrazine is a herbicide primarily used in arable cropland and forests. Hexazinone is an organonitrogen herbicide primarily used in forestry. Procymidone is a dicarboximide fungicide used on vegetables (particularly onions), strawberries and stone-fruits. These pesticides have been found in New Zealand groundwaters in areas where they are heavily used and where vulnerable hydrogeological conditions exist (Close et al., 2001).

World-wide, atrazine has been detected in groundwater more frequently than any other herbicide (Ritter et al., 1990) because of its frequent usage and leaching properties, and this is also true in New Zealand (Close et al., 1995). Compared with most other pesticides in soils, hexazinone is very mobile (Peterson et al., 1997). Hence, hexazinone has a high potential for leaching into groundwater. It is often found in surface runoff and groundwater (Miller et al., 1995). Procymidone is more strongly sorbed in soils, and its potential for

leaching into groundwater is relatively low. However, its detection in New Zealand groundwater (Close and Rosen, 2001) prompted its inclusion in this study. There is some information scattered in the literature on the mobility and persistence of atrazine in groundwater, but no information is available for the attenuation of hexazinone or procymidone in groundwater.

Groundwater contamination by pesticides could result from both non-point sources (e.g. application of pesticides on farmland) and point sources (e.g. accidental spills, offal hole disposal of agrochemical wastes and farm dumps set on permeable substrata). Groundwater could be considered more vulnerable to point-source contamination, as much higher concentrations could be present in point sources.

Considering the limited information available in the literature on the attenuation and transport of the three pesticides involved, particularly under the specific conditions encountered in pumice sand aquifers, the primary objective of this study was to determine attenuation and transport characteristics of atrazine, hexazinone and procymidone in a pumice sand aquifer for a scenario of point-source contamination.

5.2. Materials and methods

5.2.1. Properties of selected pesticides

Atrazine (6-chloro-N^2-ethyl-N^4-isopropyl-1,3,5,-triazine-2,4-diamine) is moderately mobile with a water solubility of 33 mg/l (Tomlin, 1994) and an organic carbon distribution coefficient, K_{oc}, of 100 ml/g (The ARS Pesticides Property Database, 2000). Degradation rate constants of atrazine in groundwater reported in the literature are of the order of 10^{-3} to 10^{-4} d^{-1} as shown in Table 5.1. There is relatively less information available concerning atrazine mobility in groundwater. Hexazinone (3-cyclohexyl-6-dimethylamino-1-methyl-1,3,5,-triazine-2,4(1H,3H)-dione) is highly soluble with a solubility of 33,000 mg/l, and is stable in aqueous media between pH 5 and 9 (Tomlin, 1994). It is less sorbed than atrazine with K_{oc}=54 ml/g (The ARS Pesticides Property Database, 2000). Procymidone (N-(3,5-

Table 5.1
Literature information on atrazine degradation and retardation in groundwater

(a) Degradation

Method of determination	Reaction	Half life	Degradation rate, λ, (per day)	Reference
Hydrogeologic analysis	Shallow aquifer in the Harvey County Experiment Field near Hesston, Kansas		$<=6.9 \times 10^{-4}$	Sinclair and Lee, 1992
Batch incubation	Groundwater from pristine sandy aquifer		Not degraded over 539 days	Klint et al., 1993
Batch incubation	A mixture of groundwater and aquifer sediment from a pristine sandy aquifer		Not degraded over 174 days	Klint et al., 1993
Batch incubation	Groundwater from five sites in the London Basin	Half-life of 15-20 weeks	$6.6\text{x}10^{-3}$ - $4.95\text{x}10^{-3}$	Wood et al., 1991
Batch incubation	A mixture of groundwater and aquifer sediments		Rates varied	Wood et al., 1991
Model estimation	A sandy-till aquifer		2×10^{-4}	Levy and Chesters, 1995
Batch incubation	A mixture of groundwater and alluvial gravel from Canterbury, New Zealand		$3.4\text{x}10^{-3}$	Pang and Close, 1999

(b) Sorption or retardation

Method of determination	Reaction	Distribution coefficient, K_d, (ml/g)	Retardation factor, R	
Batch experiments	A mixture of groundwater and alluvial gravel from Canterbury, New Zealand	0.04		Pang and Close, 1999
Column experiments	Sand aquifer material with an organic matter content of 0-3.65%.		1.34- 4.77	Jernlas, 1990

dichlorophenyl)-1,2-dimethylcyclopropane-1,2-dicarboximide) is relatively insoluble, with water solubility of 4.5 mg/l (Rittter et al., 1990) and K_{oc}=1,500 ml/g (The ARS Pesticides Property Database, 2000).

5.2.2. Field site and tracer experiment

The field site was located near Hamilton, in the North Island of New Zealand. The site had been used for a pesticide leaching trial (Magesan et al., 1999). The material in the underlying unconfined aquifer consists of alluvial pumice sand derived from volcanic deposit. The overlying allophanic soils are formed from silty/sandy alluvium of volcanic origin. A 30-cm silt layer occurs 5.45 m below ground level, forming an aquitard layer.

The aquifer material has a mean cation exchange capacity of 2.49 cmol/kg and total carbon content of 0.11%. Inorganic carbon (mainly carbon dioxide) was assumed to be negligible in the aquifer material. X-ray diffraction analysis indicated that the crystalline materials were composed of equal amounts of quartz and albite (a feldspar). Oxalate Al and pyrophosphate Si were 0.21% and 0.11%, respectively, with an estimated allophane content of approximately 0.8%, which is about seven times higher than the carbon content in the aquifer material. Although allophane clay minerals are present in the aquifer materials, their content is much lower than in the top 2 m of the soil profile at the site, where allophane content varies from 2-12%.

Five 15-mm diameter piezometers, spaced at 0.65 m intervals, were placed in an arc 1.5 m down-gradient of an injection well (diameter 50 mm). The depth of the piezometers was just above the silt layer (5.45 m). The injection well was located at the centre of the pesticide leaching plot. Water column depths in the piezometers varied with piezometer location from 0.23 to 0.7 m, indicating non-uniform aquifer thickness. The depth to the water-table varied with time from 3.95 to 5.10 m below the ground surface and was 4.75 m at the time of the field experiment. The native groundwater had a pH of 6.8 and an ionic strength of 0.003 mol/l with a very low microbial population. Concentrations of major components are listed in Table 5.2.

Table 5.2 Chemistry of the native groundwater

Parameter	Units	Values
pH		6.8
Ionic strength	mmol/l	2.7
Conductivity	mS/m	27
HCO_3	mg/l	46
Cl	mg/l	9.5
NO_2-N	mg/l	0.007
NO_3-N	mg/l	16
NH_4-N	mg/l	<0.04
Na	mg/l	10.0
K	mg/l	6.6
Ca	mg/l	19.0
Mg	mg/l	9.6
SO_4	mg/l	13
Fe	mg/l	0.33
Mn	mg/l	0.02
Total organic carbon	mg/l	5.0
Microbial population[a]	cfu/ml	3

[a]Determined by heterotrophic plate counts, after being incubated for three days at 12 °C (similar to groundwater temperature)

Six litres of a solution containing atrazine (1080 mg/l), hexazinone (1450 mg/l), procymidone (1320 mg/l), tritiated water (30,173 dpm/10ml), bromide (1600 mg/l) and rhodamine WT (1681 mg/l), was injected through a perforated tube from the water table to the bottom of the injection well. The pesticide solutions were made up from commercially available formulations: hexazinone 200 g/kg WG (Velpar 20G), atrazine 500 g/l SC (Gesaprim 500 FW) and procymidone 250 g/kg SC (Sumisclex 25 Flowable). The injection solution was made by mixing one litre concentrated chemical solution with the native groundwater. The injection was spread over 30 min so that there was minimal disturbance of the natural hydraulic gradient.

Tritiated water (^3H_2O) was used as a conservative tracer to indicate groundwater flow and the physical characteristics of the aquifer. Bromide was tested for conservative behaviour in the pumice sand aquifer since a significant sorption of this had been found in shallow soils at the same site (Close et al., 1999). Rhodamine WT was used as a visual aid for detecting peak concentrations and the main flow line. Another reason for using rhodamine WT was to determine whether it could delimit the appearance of atrazine in

groundwater, as suggested by Sabatini and Austin (Sabatini and Austin, 1991). Previous work has indicated that rhodamine WT is sorbed in pumice sand aquifers (Pang et al., 1996).

Groundwater samples were taken from all the down-gradient piezometers 20 cm above the well bases using a vacuum pump with dedicated Teflon tubing for each piezometer. The samples were stored in a chilly-bin (at about 4 °C) to minimise the effect of temperature and light on concentration change, and were transported to the laboratory on the same day, where they were stored in a refrigerator at 4 °C until analysed. The sampling continued for 23 days.

As indicated in the Introduction, the field experiment was meant to be representative of point-source contamination, and pesticide loading into groundwater at a point source could be very high. In addition, a high-concentration injection solution was used in the experiment for other reasons:

(a) From the pesticide leaching trial, it was found that after leaching through a 1.5-m soil profile, concentrations of pesticide and bromide were 10^{-4}-10^{-7} of their initial concentrations (Magesan et al., 1999). It is known that pumice sand aquifer material has a high attenuation capacity because of its high specific surface area and allophane clay minerals. Although attenuation of pesticides in groundwater would be less, it was unsure how much difference there would be. Hence, to ensure detection of pesticides at the observation points, high concentrations in the injection solution were used.

(b) In the original experimental design, we proposed to install two additional piezometers along the flow line further downstream once tracers were detected so that transport of pesticides could be better investigated. The use of high-input concentrations would allow the detection of pesticides at greater distances. However, the solutes were transported more slowly than anticipated and so, due to time limitations, this was not carried out.

(c) A minimal volume was injected to avoid perturbation of the groundwater flow. However, as a consequence, high-input pesticide concentrations were needed to provide sufficient solute mass.

5.2.3. Sample analysis

^3H_2O and rhodamine WT samples were analysed first in order to determine the primary flow direction. The results enabled selection of samples from the well along the main flow line for subsequent pesticide and bromide analysis. ^3H_2O samples were analysed using a liquid scintillation counter. The rhodamine WT samples were analysed using a Shimadzu RF-1501 spectrofluorimeter with a detection limit of 0.05 µg/l, an excitation wavelength of 543 nm and an emission wavelength of 573 nm. The selected pesticide samples were buffered with sodium sulphate. The sample was then extracted with ethyl acetate. The target analytes in the extract were measured by gas chromatography-mass spectrometry with detection limits of 0.3, 0.5 and 0.2 µg/l for atrazine, hexazinone and procymidone, respectively. The gas chromatography-mass spectrometry was carried out on a HP5890 gas chromatograph – HP 5970 mass spectrometer using a 30 m x 0.25 mm x 0.25 µm DB5 MS capillary column at 750 mm Hg. The recoveries were 98, 87 and 97% for atrazine, hexazinone and procymidone, respectively. Bromide samples were analysed by ion chromatography with a detection limit of 0.1 mg/l.

5.2.4. Incubation tests

Field experiments provide results only on total reduction of the pesticides. To supplement the field study, two batch incubation tests were carried out to determine pesticide degradation rates in native groundwater and aquifer material:

(1) Test one: Atrazine, hexazinone and procymidone, with initial concentrations of about 500 µg/l, were incubated with the native groundwater and a mixture of 100 g aquifer material to 80 ml groundwater. The glass bottles were covered with black plastic to minimise photo-decomposition and incubated at room temperature (20 (±1) ^oC), which is the likely maximum groundwater temperature. Samples were only taken after 57 days incubation.

(2) Test Two: Atrazine, hexazinone and procymidone, at initial concentrations of about 200 µg/l, were dissolved in the native groundwater. Incubation tests for degradation of rhodamine WT, at an initial concentration of about 280 µg/l in the native groundwater, were also carried out separately. The glass bottles were placed in the

dark at 12 °C, which is the likely minimum groundwater temperature. Duplicates were set for incubation with the pesticides and the dye. Samples were taken every 5(±2) days over a period of 28 days.

5.2.5. Estimation of relative mass recovery

Relative mass recovery is used in this paper to describe mass reduction of the solutes during transport. All irreversible processes, such as biological and chemical degradation (predominantly hydrolysis), irreversible sorption onto aquifer material, complexation and filtration (if sorbed into organic/inorganic particles and colloids), are possible causes of mass reduction. Relative mass recovery, M_{re}, is defined as the percentage of mass recovery of a reactive solute to mass recovery of the conservative tracer ^3H_2O, as given in Eqs. 5.1 and 5.2.

$$M_{re} = \frac{MRF_{reactive}}{MRF_{^3H_2O}} x\,100\% \tag{5.1}$$

and

$$MRF = \frac{vA\theta \int_0^\infty c(x,y,z,t)\,dt}{M_0} \tag{5.2}$$

where MRF is the mass recovery of a tracer (M/M); M_0 is the initial mass injected (M); c is the concentration of the solute (M/L^3); x, y and z are the co-ordinates of the sampling point (L); v is the pore-water velocity (L/T); θ is the effective porosity of the aquifer material (L^3/L^3); t is the time since injection (T); and A is the cross-sectional area of the measuring volume perpendicular to the direction of the flow (L^2). As no well packer was used in the sampling wells, the value of A was calculated from the well screen length (L) and radius (r), i.e. $A=2rL$. This approach assumed that the solute was evenly distributed over the whole length of the well screen. By measuring concentrations over time, the integral may be evaluated using the trapezoidal rule.

When M_{re}=100%, the solute has the same mass recovery as that of ^3H_2O and, if there were any sorption, the sorption process would be reversible. In contrast, if M_{re}<100% for a well-defined concentration breakthrough curve (BTC), the solute would have undergone some irreversible reduction process.

5.2.6. Simulation using two region/site non-equilibrium model

A three-dimensional two-region/site non-equilibrium model, N3DADE, developed by Leij and Toride (1997) was used to estimate transport parameters. The two-region model (TRM) was used for the conservative solutes, assuming that the liquid phase could be partitioned into mobile and immobile regions. Likewise, a two-site model (TSM) was used for the reactive solutes, assuming that the sorption sites could be partitioned into instantaneous and kinetic sites. Solute exchange between the two liquid regions and two sorption sites was modeled as a first-order process. The TRM and TSM have the same dimensionless forms (Leij and Toride, 1997):

$$\beta R\frac{\partial C_1}{\partial T}=\frac{1}{P_x}\frac{\partial^2 C_1}{\partial X^2}-\frac{\partial C_1}{\partial X}+\frac{1}{P_y}\frac{\partial^2 C_1}{\partial Y^2}+\frac{1}{P_Z}\frac{\partial^2 C_1}{\partial Z^2}+\omega(C_2-C_1)-U_1C_1 \tag{5.3}$$

$$(1-\beta)R\frac{\partial C_2}{\partial T}=\omega(C_1-C_2)-U_2C_2 \tag{5.4}$$

in which, R is the retardation factor; β is a partition coefficient between the equilibrium and non-equilibrium phases; C is resident concentration; T is time; P_x, P_y and P_z are the Peclet numbers in the x, y, z directions; X, Y and Z are the dimensionless distances in x, y and z directions; ω is a mass transfer coefficient; U is first-order reduction term; and the subscripts 1 and 2 refer to the equilibrium and non-equilibrium phases, respectively. All parameters are in dimensionless forms.

The retardation factor R is defined as

$$R=1+\frac{\rho_b K_d}{\theta} \tag{5.5}$$

in which ρ_b is the bulk density of the aquifer material (M/L^3) and K_d is the distribution coefficient (L^3/M). From undisturbed core samples, we obtained a mean value of ρ_b =1.02 g /cm^3 for the pumice sand aquifer material. A value of θ = 0.3 was considered reasonable for this particular pumice sand aquifer.

As TRM was used only for the conservative solutes in this study, Eqs. 5.3 and 5.4 were simplified by letting R=1 and U=0 when analysing conservative solutes. In the TRM, β represents the fraction of mobile water and ω is an indication of kinetic mixing/diffusion between the two regions. In the TSM, β represents the fraction of fast-sorption sites and ω is an indication of mass transfer or reaction rate of the kinetically controlled sorption sites. Both β and ω are indicative of the degree of non-equilibrium. High ω values correspond to fast mass exchange and vice versa. When β = 1 or $\omega \geq 100$, transport is regarded to be at the equilibrium condition (Toride et al., 1995) and when $\omega \geq 10$, the local equilibrium assumption appears to be approximated reasonably well (Brusseau et al., 1991).

The N3DADE model requires inputs of dimensional parameters v, t, L, x, y, z, D_x, D_y and D_z, which are incorporated into the following dimensionless forms:

$$T = \frac{vt}{L} \qquad X = \frac{x}{L} \qquad Y = \frac{y}{L} \qquad Z = \frac{z}{L} \qquad P_x = \frac{vL}{D_x} \qquad P_y = \frac{vL}{D_y} \qquad P_z = \frac{vL}{D_z} \tag{5.6}$$

in which L is the characteristic length (L); x, y and z are spatial coordinates (L); and D_x, D_y and D_z are dispersion coefficients in the x, y, z directions (L^2/T^1), respectively. Values of x=1.5 m, y = z =0 m were used in the model, assuming that the main flowline went through the well with maximum tracer concentrations. However, model-given results for the reduction terms, U, are dimensionless. In order to make comparisons with degradation rates, we converted U values into a dimensional form (T^{-1}) by multiplying U with v/L. It should be noted that we use U in this paper to encompass all the irreversible reduction processes of pesticide transport (e.g. degradation, irreversible sorption, complexation and filtration, if sorbed into particles and colloids) which are assumed to follow a first-order rate law. This assumption is reasonable. For example, Matthess

(1994) used a filter factor to describe filtration of pesticides sorbed onto particles and colloids, which also follows a first-order law.

Keeping D_x/D_y=15 and D_y/D_z =10 as adopted from Hadfield et al (1999) for the field site, values of v and D_x were first estimated from a conservative tracer and then applied to other solutes. Compared to the length of injection time, the release time of the injected tracer from the well would be much longer due to residence of tracer in the well and/or upstream movement of tracer due to injection. Therefore, an effective pulse duration of the field experiment, T_o, was also determined from the conservative tracer. This same value was used for hexazinone and rhodamine WT. However, as injected concentrations of atrazine and procymidone were much higher than their water solubility values, T_o was used as a fitting parameter for these two pesticides. This allows for a longer effective injection period, which reflects solubility limitations, i.e. the more saturated the injection solution, the longer the expected duration of T_o. For reactive solutes, values of β, ω, R and U were used as fitting parameters.

N3DADE does not include an inverse modelling capability. Hence, model parameter fits were obtained using a non-linear optimisation package, PEST (Doherty et al., 1994). PEST is a model-independent parameter estimator and is able to interface with any model through that model's own input and output files, thus requiring no alternations to the model.

5.3. Results and discussion

It is impossible to obtain a total mass recovery from a single well in the field experiment because of three-dimensional movement of the groundwater combined with the small cross-sectional area of the well screen. Although ^3H_2O was also detected in wells that were not along the main flowline, concentrations in these wells were only 2-3% of the well that was in the main flowline. The mass captured by the well in the main flowline was 3% of that injected. Hence, all the results presented in this paper were obtained from this selected well. Values of transport parameters estimated from the field data are listed in Table 5.3. Observed and model-simulated BTCs are shown in Fig.5.1. These results are discussed below.

5.3.1. Conservative solutes

The shape of the bromide BTC (Fig.5.1), and the values of transport parameters and relative mass recovery estimated from bromide (Table 5.3) are very similar to those of ^3H_2O. The slight differences in the results between bromide and ^3H_2O are probably due to sample analytical errors (particularly the noisy background of ^3H_2O) and uncertainty in the model simulation. The similar behaviour of bromide to that of ^3H_2O suggests that the former can be used as a conservative tracer in the pumice sand aquifer investigated. This finding is different from that in the top 2 m soil of the same study site as described in Section 5.2.2. This is probably because of the significantly lower content of allophane clay minerals in the aquifer material than in the soils.

BTCs of ^3H_2O and bromide display early breakthrough and long tailings, indicating the presence of physical non-equilibrium conditions. The skewed ^3H_2O and Br BTCs may be explained by the heterogeneity of the aquifer and presence of zones of immobile water. It should be noted that the slow release of tracer from the injection well could result in a gradual decrease in the input concentration. However, this effect has been largely encompassed in the effective pulse length T_o, which was determined from the optimisation procedure. Hence, the slow mixing between zones of contrasting permeability and exchange between mobile and immobile water is considered to be the major cause of tailing in ^3H_2O and Br BTCs. The TRM-derived β values estimated from ^3H_2O and Br suggest that about 45-48% of water is mobile and the rest is immobile. The ω values estimated from ^3H_2O and Br are about one, indicating a slow mass exchange between mobile and immobile waters (see Section 5.2.6).

5.3.2. Reactive solutes

5.3.2.1. Mobility

Table 5.3 suggests that, among all pesticides investigated, hexazinone is the most mobile (R=1.38) and procymidone is the most immobile (R=9.26). This conclusion is consistent with information reported in the literature. The value of R=4.45 for atrazine estimated from this study for pumice sand is at the upper end of the range of R=1.34-4.77 reported by Jernlas (Jernlas, 1990) for sandy aquifer material (Table 5.1). In

Table 5.3

Transport parameters[a] estimated from the field tracer experimental data (sampling well at x =1.5 m)

(a) Conservative tracers

Tracer	Model[b]	v (m/day)	D (m^2/day)	β	ω	T_o (day)	M_{re} (%)
^3H_2O	TRM	0.44	0.01	0.45	1.18	0.97	100
Br	TRM	0.47	0.01	0.48	0.90	0.94	96

(b) Reactive solutes

Tracer	Model	R	K_d (ml/g)	μ_{lump} (per day)	β	ω	T_o (day)	M_{re} (%)
Hexazinone	TSM	1.30	0.94	assigned as zero	0.51	1.08	fixed as 0.94	96
Atrazine	TSM	4.45	1.01	0.33	0.17	3.57	1.66	25
Procymidone	TSM	9.26	2.43	0.71	0.05	5.08	1.97	5
Rhodamine WT	TSM	4.10	0.91	1.37	0.20	4.99	fixed as 0.94	0.3

[a]Values of v, D, β, ω, T_o and R are directly estimated from model-curve-fitting. K_d values are calculated from Eq. 5.5. M_{re} is estimated from Eqs. 5.1-5.2.

[b]TRM - two region nonequilibrium model; TSM - two site nonequilibrium model.

μ_{lump} is calculated from model-derived reduction rate U multiplied with v/L.

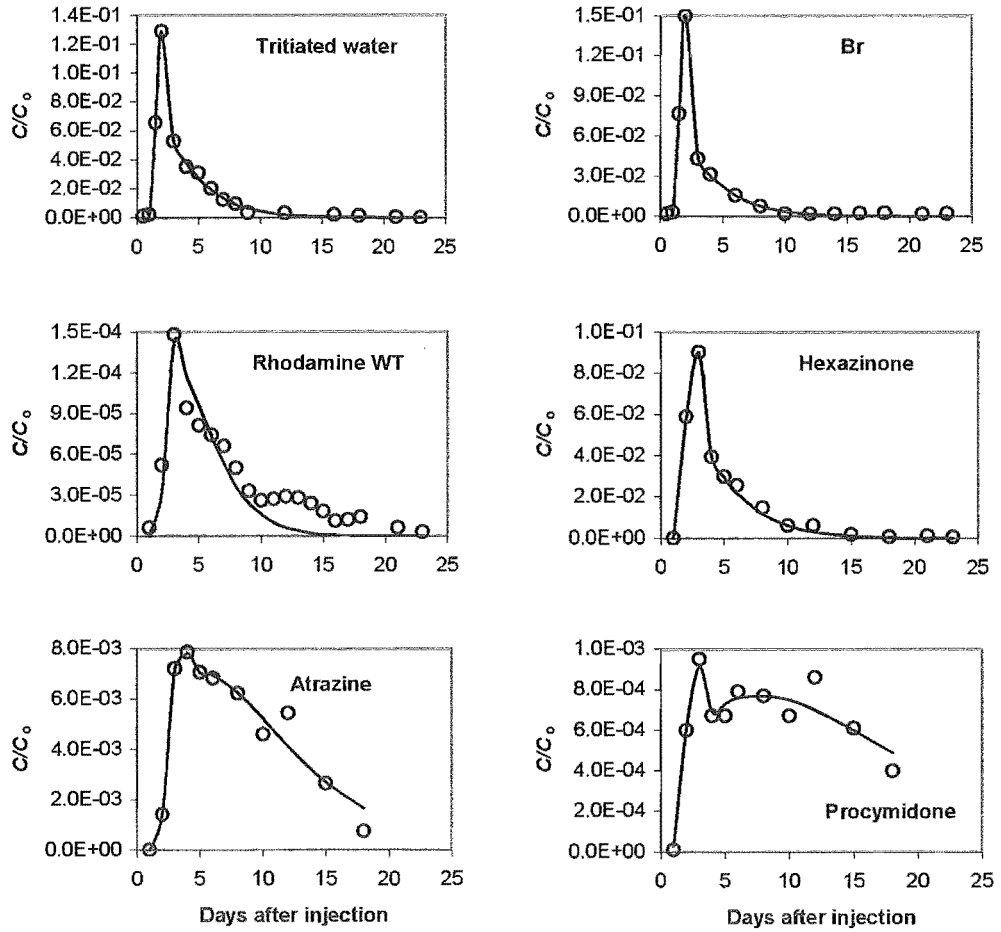

Fig.5.1 Observed (circles) and N3DADE-simulated (solid lines) concentration breakthrough curves for the field tracer experiment

contrast, the calculated equivalent value of K_d=1.01 ml/g for atrazine is about 25 fold higher than K_d=0.04 ml/g reported by Pang and Close (1999) for alluvial gravel material (Table 5.1). This suggests that sorption of atrazine is much greater in pumice sand aquifer than in alluvial gravel aquifer, as would be expected.

Literature K_{oc} values (Section 5.2.1) and a measured organic carbon content (OC) of 0.11% (Section 5.2.2) would give K_d values (calculated from $K_d = K_{oc} \times OC$) of 0.06, 0.11 and 1.65 ml/g for hexazinone, atrazine and procymidone, respectively. Compared with these values, the K_d values given in Table 5.3 are about two fold higher for hexazinone and procymidone, and about nine times higher for atrazine. This suggests that organic carbon is not the only sorbent in the pumice sand aquifer, and allophane clay has also played an important role in pesticide sorption.

Mobility of rhodamine WT (R=4.10) is similar to that of atrazine in the pumice sand aquifer investigated. This finding is similar to that of Sabatini and Austin (Sabatini and Austin, 1991). The calculated equivalent value of K_d =0.91 ml/g for rhodamine WT is similar to the value of K_d =0.60 ml/g reported by Pang et al. (1996) based on a batch test conducted with pumice sand of the same geological origin from an adjacent region (Rotorua, North Island of New Zealand).

5.3.2.2. Mass recovery/reduction

Table 5.3 shows that, of all pesticides investigated, relative mass recovery of hexazinone (M_{re}=96%) is the greatest and is the same as bromide. The recovery of M_{re}=96% is not significantly different from that of ^3H_2O (M_{re}=100%). The small difference could be within the errors of sample analysis. Hence, a zero reduction rate for hexazinone was assigned in the model simulation. In contrast, relative mass recovery of procymidone is the smallest (M_{re}=5%). It should be noted that mass recoveries estimated for atrazine and procymidone are less accurate due to their incomplete BTCs (Fig.5.1). Compared with the pesticides, there was very little mass of rhodamine WT recovered (M_{re}=0.3%).

5.3.2.3. Degradation rates

Results from the incubation Test One suggest that, after 57 days incubation, (1) similar to that found by Klint et al. (1993) as shown in Table 5.1, atrazine concentration did not decline when incubated with either the groundwater or a mixture of groundwater and aquifer material; (2) hexazinone concentration did not decrease when incubated with the groundwater but declined 22% when incubated with the mixture, giving an approximate degradation rate constant of 4.36 x 10^{-3} d^{-1}; (3) procymidone concentration decreased by 62% when incubated with the groundwater but only by 47% when incubated with the mixture. This gives procymidone degradation rate constants of approximately 1.70 x 10^{-2} d^{-1} for the groundwater and 1.12 x 10^{-2} d^{-1} for the mixture.

Results from incubation Test Two are consistent with the results of Test One, i.e. no detectable degradation for atrazine and hexazinone but procymidone was degraded significantly. No degradation was also observed for rhodamine WT. The frequent sampling allowed good definition of the degradation rate for procymidone. Fig.5.2 shows that procymidone was degraded exponentially in the groundwater at a rate constant of 2.79×10^{-2} d^{-1} (n=14, r^2=0.94), i.e. a half-life of 25 days. This value is very similar to that determined from the Test One (1.70×10^{-2} d^{-1}, i.e. a half-life of 40 days). The rapid degradation of procymidone at the site may be due to acclimatisation of the microbial population. According to our unpublished data, procymidone was detected in the soil profile depth between 1.5 and 2.5 m, suggesting that it has been used previously at the site. The zero degradation of atrazine, hexazinone and dye in the groundwater during the period of incubation observed in this study is not surprising because microbial populations of the groundwater examined are very small (Table 5.2). Little degradation of atrazine in groundwater is reported in the literature, as reviewed in Table 5.1.

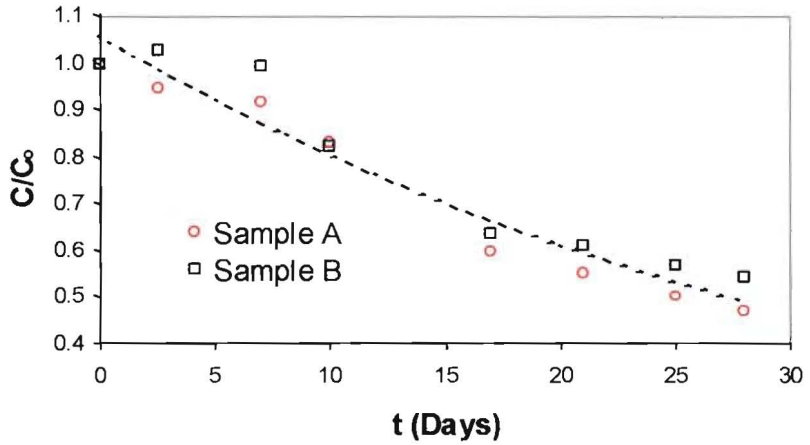

Fig.5.2 Degradation of procymidone with time in the native pumice sand groundwater

5.3.2.4. Total reduction rates

As indicated in Section 5.2.6, model-derived total reduction rates encompass not only degradation but also all other irreversible reduction processes such as irreversible sorption, complexation and filtration. Table 5.3 suggests that reduction rate is in an order of rhodamine WT > procymidone > atrazine ≥ hexazinone (the latter as zero). This order

is consistent with results of relative mass recovery, which are independently estimated from the BTCs. On the basis of the findings described in Section 5.3.2.3, reduction due to degradation in the field experiment is considered not to be the dominant reduction process, as the experimental period was only 23 days. Compared with the degradation rates given in Section 5.3.2.3, total reduction rates are much greater. This suggests that other irreversible processes could also have contributed to the reductions of pesticides and dye. This is particularly true for atrazine and rhodamine WT, which showed high mass losses and reduction rates yet without any observed degradation. This implies that the use of laboratory-determined degradation rates could underestimate reduction of contaminants in the field conditions, and degradation rates alone are not representative for field loss, which involve other irreversible processes. Apart from degradation, other irreversible processes are possible in the pumice sand aquifer for the following reasons:

(a) Many sorption processes are not reversible, particularly for organic compounds. In addition, many pesticides could form partially irreversible complexes with organic carbon in particulate, colloidal or dissolved forms. A previous batch study (Pang et al., 1996) indicated that 36-47% of rhodamine WT could be sorbed onto the pumice sand. It is possible that irreversible sorption is the predominant reduction process for rhodamine WT. The presence of allophane clay mineral may have increased this.

(b) Filtration of pesticides may occur if the pesticides are sorbed into organic/inorganic particles and colloids, which could be removed from water by filtration within the aquifer. Reduction of pesticides by filtration may be important in the pumice sand aquifer, as pumice sand is a natural filter due to its high surface area.

(c) Pesticides could also come out of solution in aquifers when their solubilities are exceeded. Concentrations of atrazine and procymidone in the tracer solution injected in the field experiment were much higher than their water solubilities, as mentioned previously. However, their effective solubilities in the field are unknown. The solubility of a pesticide given in the literature is related to an active ingredient in neutral water at 20-26 °C, while the pesticides used in this study are active ingredients in formulations, which include surface-active agents and other additives.

The effect of the latter would decrease with increasing dilution/mixing down-gradient of the injection well. The native groundwater is slightly more acidic and at a lower temperature than the literature conditions. As indicated by Matthess (1994), the solubilities of non-polar organic substances can be significantly higher in natural water than in pure water due to their interaction with dissolved organic compounds. The ionic strengths of the native groundwater and of the tracer solution are much higher than that of the pure water. This would have a positive impact on solubility as solubility increases with increasing ionic strength (Stumm and Morgan, 1981). The effect of solubility for atrazine and procymidone is reflected in the results of T_0 (Table 5.3). Procymidone was more super-saturated than atrazine in the injection solution. Hence, a longer duration of T_0 was estimated for procymidone than for atrazine.

5.3.2.5. Nonequilibrium transport

The field-data-derived ω values are all less than 10, suggesting that transport of the reactive solutes was under non-equilibrium conditions in the field. The β values shown in Table 5.3 suggest that the instantaneous sorption sites are about 51% for hexazinone, 20% for rhodamine WT, 17% for atrazine and only 5% for procymidone.

It should be noted that, although a non-equilibrium model is capable of describing asymmetrical BTCs, because of the introduction of additional parameters, the uncertainty of the modelling results also increases as a result of parameter inter-relationship. Another drawback of the non-equilibrium model used in this paper is that it is unable to distinguish individual effects of physical and chemical non-equilibrium processes on transport of reactive solutes because of their mathematical equivalence in the model. To identify the individual processes, a multifactor non-ideality model (Hu and Brusseau, 1996) is needed, which incorporates more non-equilibrium parameters, and independent estimation of some parameters is required. However, this is beyond the scope of this paper. Nevertheless, transport of hexazinone in the field experiment is probably dominated by physical non-equilibrium conditions, as its BTC shape and values of transport parameters are not greatly different from those of ^3H_2O and Br.

5.4. Conclusions and implications

Of the three pesticides investigated in the field tracer experiment, we found that hexazinone was the most mobile and underwent little mass reduction; while procymidone was the least mobile and underwent the greatest mass reduction. Mobility of atrazine was similar to that of a commonly used dye tracer, rhodamine WT. Hence, rhodamine WT could be used as a sorbing tracer in a monitoring program to delimit the appearance of atrazine in pumice sand groundwater. However, mass reduction of rhodamine WT in the pumice sand was much greater than that of the pesticides and cannot be used for indicating reduction of the pesticides. The sorption distribution coefficients estimated in this study are a few-fold higher than those estimated based on the assumption that pesticide sorption is entirely due to organic matter, indicating that allophane clay has also played an important role in pesticide sorption in pumice sand aquifer.

Degradation rates derived from the incubation tests are much lower than the total reduction rates derived from the field data. Compared with degradation in the groundwater alone, degradation in a mixture of groundwater and aquifer material was enhanced for hexazinone but decreased slightly for procymidone. Finding much greater total reduction rates than degradation rates suggest that reductions of pesticides observed in the field tracer experiment were induced not only by degradation but also by other irreversible processes such as irreversible sorption, filtration and complexation.

Acknowledgements

We thank Dr Cliff Randall of Institute of Environmental Science & Research, John Hadfield of Environment Waikato and staff of Landcare Research for their assistance during the course of this work. Professor Mark Goltz of Air Force Institute of Technology (USA) is acknowledged for his valuable and detailed comments. This study was funded by the Foundation for Research, Science and Technology (New Zealand) under contract number CO3X0001.

5.5. Additional study

Use of a two-region model to simulate transport of reactive solutes

In the publication, we have concluded that transport of hexazinone in the field experiment conducted in a pumice sand aquifer is probably dominated by physical non-equilibrium conditions caused by heterogeneity in permeability. We came to this conclusion based upon the similarity between the hexazinone and conservative tracer breakthrough curves. From Chapter 3, we could see that an equilibrium model could well describe transport of hexazinone through a homogeneously packed pumice sand column, suggesting negligible kinetic sorption process within the system.

Two-region models exclude kinetic sorption and assume all sorption sites are instantaneous in both mobile and immobile regions. For solute transport with equilibrium sorption in heterogeneous media (hence physical nonequilibrium exists), the assumption of the two-region model is valid. Hence, for the field hexazinone data, a two-region model is conceptually more correct than a two-site model as the two-site model does not consider the influence of mass exchange between mobile and immobile water on the transport of reactive solutes. In addition, the two-site model assumes rate-limited sorption, which appears not to be the case for the hexazinone and pumice sand system, based upon Chapter 3 results. Two-region models have been applied in the literature to simulate non-ideal transport of reactive solutes where rate-limited sorption has been assumed to be insignificant (e.g. Goltz and Roberts 1986; Gamerdiner et al., 1990; Spurlock et al. 1995).

Similar to the two-site model, the same V, D, and T_o values as those of Br (estimated from the two-region model, as shown in Table 3) are used in the two-region model. As in the publication, we assume zero degradation for hexazinone. In the two-region model, ω is defined as $\omega = \frac{\alpha L}{\theta v}$ in which α is first-order mass exchange rate between mobile and immobile regions (T^{-1}). Using the same approach as Goltz and Roberts (1986), we

assume that the α values (hence the ω values) for the conservative tracer and reactive solutes are approximately equal.

The results for hexazinone optimised using the two-region model (R =1.05, β=0.63) are very similar to those from the two-site model (R =1.30, β=0.51), though the BTC simulated using the two-region model with two-parameter optimisation has a slightly worse fit to the data than that of the two-site model with three-parameter optimisation, as shown in Fig. 5.3. Also note, however, that the two-region model, using an approach similar to the approach used for hexazinone, fails to simulate other reactive solutes. This suggests that rate-limited sorption was significant in the transport of other pesticides in the pumice sand aquifer investigated.

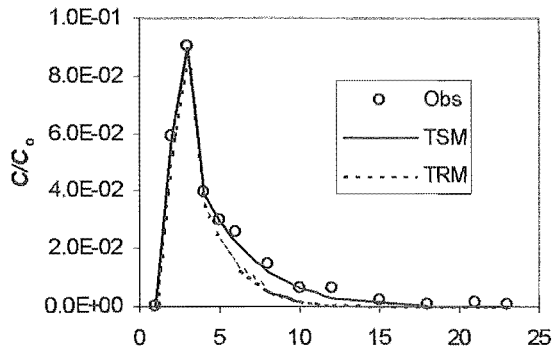

Fig. 5.3. Comparison of hexazinone BTCs simulated from TRM and TSM with observed data.

Chapter 6

Estimation of septic tank setback distances based on transport of *E. coli* and F-RNA phages

Liping Pang [1], Murray Close [1], Mark Goltz [2], Lester Sinton [1], Helen Davies [1], Carollyn Hall[1], Greg Stanton [1]. 2002. Estimation of septic tank setback distances based on transport of *E. coli* and F-RNA phages. N.Z. J. of Marine & Freshwater Research. Revised.

Author affiliations:

[1] Institute of Environmental Science & Research Ltd., PO Box 29181, Christchurch, New Zealand

[2] Department of Systems and Engineering Management, Air Force Institute of Technology, Wright-Patterson Air Force Base, OH 45433-7765, USA

Journal referees:

Two anonymous referees

Abstract

Setback distances between septic tanks and the shorelines of Lake Okareka near Rotorua, New Zealand, were determined from model simulation for a worst-case scenario, using the highest hydraulic conductivity and gradient measured in the field, removal rates of the microbial indicators (*E. coli* and F-RNA phages) determined from a column experiment, and maximum values of the design criteria for the disposal system, and assuming the absence of an unsaturated zone, a continuous discharge of the raw effluent (both indicators at concentrations of $1x10^7$ counts/100 ml) into the groundwater and no sorption of pathogens in the aquifer. Modelling results suggest that the minimal setback distances were 16 m to satisfy the Recreational Water Quality Guidelines for *E.coli* < 126 per 100 ml, and 48 m to meet the Drinking-Water Standards For New Zealand for enteric virus <1 per 100 L. These distances may be applicable for other lakeshores in pumice sand aquifers with groundwater velocities < 7 m/day.

Findings of laboratory column and batch experiments provided an insight into the microbial attenuation and transport processes in pumice sand aquifers: (a) Bacterial removal was predominately through filtration (87-88%) and partially by die-off (12-13%), while viral removal was by both die-off (45%) and filtration (55%). (b) Microbial die-off in groundwater without aquifer material (i.e., free microbes) was much lower than that in groundwater with aquifer material (i.e., sorbed microbes) and contributed only 2-6% to the total removal. This implies that the setback distances estimated from die-off rates for the free microbes, determined in the laboratory without involving aquifer media and considering other removal processes as those often reported in the literature, could be larger than necessary.

Key words septic tanks; setback distance; groundwater; lake; modelling; microbial transport

6.1. Introduction

The water quality of the Rotorua Lakes in the Central North Island of New Zealand has been of concern to both government authorities and the public. Of particular concern is contamination from septic tanks directly upstream of the lakes as they are a potential source for contaminating the shallow groundwater and surface runoff that feed into the lakes. Septic tank effluent often contains many pathogens and contamination of lake water poses a health risk for the downstream users and near-shore bathers.

Rotorua District Council has been investigating the potential for septic tank leachate contamination of several of the lake margins adjacent to urban developments. The institute of Environmental Science & Research, ESR, was contracted to carry out an assessment of the acceptable setback distances for septic tanks from shorelines directly 'downstream' of the septic tank location. The lake-side community of Lake Okareka (Fig.6.1) is one of the identified problem areas and was selected as the focus of our study.

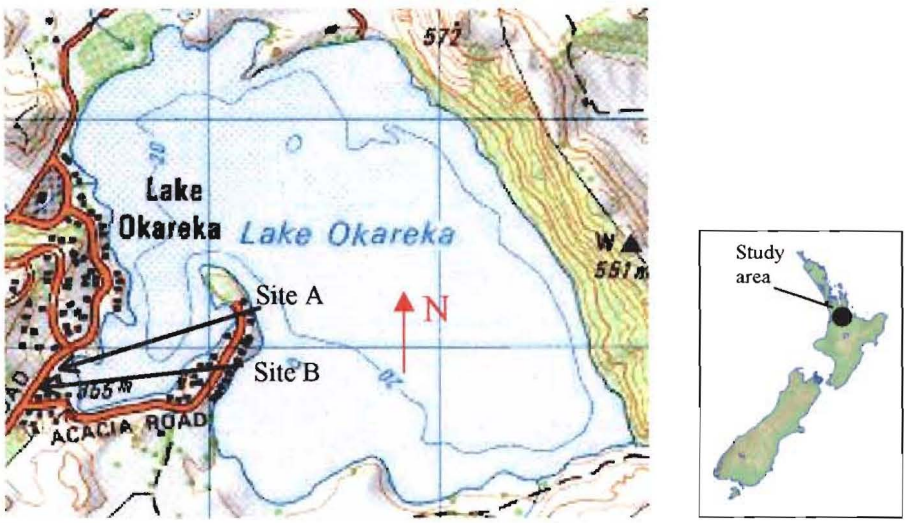

Fig.6.1 Lake-side community of Lake Okareka.
The grids are in 1 km x1 km scale.

Similar to other lake margins in the Rotorua district, as well as many rural areas of the central North Island, disposal of septic tank effluent through pumice sand soils is a common practice in the Lake Okareka area. The project conducted by ESR included (a) a site characterisation of hydraulic conductivity of the underlying pumice sand aquifer, groundwater table gradient, and concentration of the septic tank effluent, (b) a field filtration experiment investigating microbial attenuation in the unsaturated zone, (c) laboratory column and batch experiments using sewage effluent and native groundwater to investigate attenuation and transport of microbial indicators in the pumice sand aquifer material under saturated conditions, (d) model estimation of horizontal setback distances, and (e) a review of both horizontal and vertical separation distances used by authorising institutions. These are documented in a technical report by Pang et al. (2001). This paper focuses on presenting the laboratory study of microbial transport and model estimation of the setback distances.

Nation-wide, regional and district councils often need to set up safe setback distances between septic tanks and either drinking water wells or recreational surface water bodies. Currently, councils have used arbitrary values, mostly 20-30 m for surface water and 30-50 m for groundwater, as shown in Table 6.1. However, little has been reported about how these arbitrary values were determined. Gunn (2001) commented that many setback distances used today appear to be based on the values established in 1958 by the US Public Health Service (USPHS 1958), i.e. 15 m from any surface-water body and 30 m from any water-supply well. These arbitrary distances may under- or over-protect the water resources. Taking a step further, Environment Canterbury established setback distances for drinking water wells between 20-1000 m (Fietje 1991) using the results from a microbial contaminant transport study conducted in Canterbury (Sinton 1986), together with local information. This work has recently been complemented with groundwater modelling of viral and bacterial transport (ECAN 1999) using results of the recent studies of Sinton et al. (1997) and Pang et al. (1998).

Table 6. 1.

Horizontal setback distances used by some regional councils in New Zealand

Organisation	Horizontal distance (m)	
	Surface water body	Drinking water well
Auckland Regional Council	15-20	
Environment Waikato	30	30
Hawkes Bay Regional Council	20	30
Environment Bay of Plenty	5	15
Taranaki Regional Council	25	50
Marlborough District Council	30	30
Environment Canterbury	20	20-1000
West Coast Regional Council	50	100
Otago Regional Council	50	50
Environment Southland	20	50

Setback distances are site-specific. For adequate determination of setback distances, information on attenuation and transport of pathogens or microbial indicators in groundwater systems is needed. Although a few studies have been carried out on the attenuation of microbes in unsaturated pumice sand soils (Aislabie et al. 2001; McLeod et al. 2001), little is known about microbial attenuation in pumice sand groundwater systems, either in New Zealand or overseas. Some information is available in the literature on viral transport in alluvial and beach sand aquifers (Sobsey et al. 1986; Schijven et al. 1999; Schijven & Hassanizadeh 2000). However, pumice sand media have specific physical and chemical properties that are different from other sand aquifer materials. Its highly porous nature makes the media ideal for attenuation and removal of microbes. The large specific surface area and the frequent presence of allophanic clay minerals would enhance microbial sorption. The sorption of the microbes, together with the high water storage capacity of the media, would provide more opportunity for contact of microbes with the pumice sand and increase the time length for microbial residence. Consequently, this would facilitate further sedimentation and filtration, also chemical and biochemical reaction.

The objective of this paper was to (1) obtain an insight into microbial attenuation and transport processes in pumice sand aquifers, and (2) to estimate acceptable setback distances for septic tanks from the bathing shores of Lake Okareka, based on model simulations using results from field and laboratory experiments and assumptions for a worst-case scenario.

6.2. Materials and methods

6.2.1. Experimental sites

Two representative septic tank systems, serving permanently-occupied dwellings near Lake Okareka, were selected for the study. Site A (U16: 034-307) was 47 m upstream from the lake edge. The underlying aquifer was composed of non-uniform, coarse gravelly pumice sand. According to results from laboratory analysis, the aquifer material contained 0.31% total carbon and 0.88% allophane with a bulk density of 1.00 (0.98-1.12) g/cm^3 and a total porosity of 0.58 (0.55-0.64). The median value of effective porosity of the aquifer material, determined from the fraction of drainable water for the undisturbed core samples in triplicate, was 0.20 (0.17-0.27). Discharge of the septic tank effluent was through a free-drained soakage bed. The water table was very close to the bottom of the disposal bed, with a separation distance 0.2 m in March 2001 and zero m in winter and after heavy rainfall. Site B (U16: 032-307) was 155 m upstream of the lake edge. In comparison with Site A, the pumice soils at this site contained finer materials (ash and clay) and less gravel, with a bulk density of 1.17 (1.16-1.18) g/cm^3 and a total porosity of 0.52 (0.49-0.55). Discharge of the septic tank effluent was through a well-drained soakage bed. In March 2001, the separation distance between the disposal depth and the water table at this site was 1.05 m.

Five small diameter wells (25-50 mm) were installed at each site for the purpose of site characterisation. Initial water levels in the wells were about 1.6 m below ground level (b.g.l) at Site B and 1.1-1.2 m b.g.l at Site A. The well depths were up to a few tens of centimetres below the water table. The results from a surface survey suggest that the shallow groundwater flowed towards the lake at an overall hydraulic gradient of 0.005 at Site A and 0.008 at Site B. According to results from rising-head borehole tests (Pang et al. 2001), hydraulic conductivity of the underlying aquifer was 41-172 m/day for Site A and 11-17 m/day for Site B. Using an effective porosity of 0.20 given above, the estimated groundwater velocity was 1.01-4.29 m/day at Site A and 0.45-0.66 m/day at Site B.

6.2.2. Septic tank effluent and microbial indicators

Septic tank effluent often contains many viral, bacterial and protozoan pathogens. According to the reviews of Keswick (1984) and Rose & Gerba (1991), viruses and protozoa generally have much lower infectious doses than bacteria, and for some viruses, as little as one organism could cause infection. However, protozoans are expected to have lower input concentrations and generally larger particle size than bacteria and viruses (and hence are more likely to be filtered out), thus they are unlikely to control the setback distances. Therefore we excluded protozoans from this study.

It is impossible to examine all types of viruses and bacteria in septic tank effluent. Commonly, indicators of viruses and bacteria are used to study the attenuation and transport of pathogens in groundwater and soils. In this study, we used faecal coliforms and *E. coli* as faecal bacterial indicators and F-RNA bacteriophages as viral indicators. Both faecal coliforms and *E. coli* (a species within the faecal coliform group) are consistently present in human wastes, and large numbers of F-RNA bacteriophages are also excreted in faeces. Faecal coliform dimensions are typically 0.3-1 μm in diameter and 0.6-6 μm in length. *E. coli* is a species within the faecal coliform group. F-RNA bacteriophages are a group of viruses that attack and replicate inside *E. coli* bacterial cells. F-RNA bacteriophages have similar physical properties to important enteric viruses, especially with respect to size (Goyal & Gerba 1979; Bitton 1980; Havelaar 1993). The size of F-RNA phages ranges from 21-30 nm in diameter (Havelaar 1993). As F-RNA bacteriophages are very persistent (Nasser et al. 1993) and poorly sorbed to soil particles (Goyal & Gerba 1979), the use of F-RNA bacteriophages as viral indicators is a conservative approach. Concentrations of faecal bacteria are commonly expressed as cfu/100 ml, and that of F-RNA bacteriophages as pfu/100 ml, where cfu stands for colony forming units and pfu stands for plaque forming units.

Table 6.2
Concentrations of micro-organisms in septic tank and sewage effluent

Micro-organisms	Concentration (count/100ml)	Effluent description	Reference Reference
Faecal coliforms:	$2.3x10^6$	Septic tank effluent from Site B	This study
	$7.39x10^6$-$8.4x10^6$	Christchurch raw sewage	This study
	$4x10^5$	Septic tank effluent from Rotorua	Pang et al. 1996
	$7.5x10^5$-$3.9x10^6$	Christchurch raw sewage	Pang et al. 1996
	$4.2 x10^5$		Ziebell et al. (1974)
	$2.3x10^6$-$5.1x10^6$	Septic tank effluent	Sinton 1986
Total coliforms:	$3.4x10^6$		Ziebell et al. (1974)
	$3.7x10^6$-$1.2x10^7$	Septic tank effluent	Unpublished data from Brent Gilpin, ESR
E. coli:	$1.2x10^6$	Septic tank effluent from Site B	This study
	$7.16x10^6$-$8.0x10^6$	Christchurch raw sewage	This study
	$2.0 x10^6$-$9.3x10^6$	Raw and primary treated sewage	Unpublished data from Brent Gilpin, ESR
F-RNA phages:	$5.26x10^5$-$1.1x10^6$	Christchurch raw sewage	This study
	$1.01x10^6$	Septic tank effluent from Rotorua	Pang et al. 1996
	$8.5x10^5$-$1.05x10^6$	Christchurch raw sewage	Pang et al. 1996
Faecal *streptococci:*	$3.8 x10^3$	-	Ziebell et al. (1974)
Pseudomonas aeruginosa:	$1.0 x10^4$	-	Ziebell et al. (1974)

Summarising available information, the typical concentrations of faecal bacteria and F-RNA phages in raw human effluent are of the order of 10^6 cfu or pfu/100 ml, and total coliforms could be up to 10^7 cfu/100 ml, as shown in Table 6.2. A concentration level of 10^6 cfu/100 ml for faecal coliforms and *E. coli* was found both in the sample taken at the septic tank outlet of Site B and also in some contaminated shallow groundwater in the Rotorua region (pers. comm., John McIntosh of Environment B.O.P). This indicates that septic tank effluent may enter the groundwater at similar concentrations to raw effluent, especially for those sites where the water table rises to flood the disposal trench/bed of a septic tank system.

6.2.3. Laboratory experiments

In order to obtain insight into attenuation and transport of microbial indicators and establish parameter values for modelling setback distances, laboratory column and batch experiments were carried out. The pumice sand used in the experiments was excavated from a pit at Site A. The pit was excavated to a depth just above the groundwater table, which was 1.2 m below the ground level. The material taken was typical of the shallow pumice sand aquifers in the central North Island. The pumice sand material was sieved through a 1.1 x 1.1 cm mesh to exclude large gravels and well mixed prior to the experiments.

Column experiments

The well-mixed material was uniformly packed under saturated conditions into a stainless-steel column 1 m long and 20 cm in diameter. The amount of water used to saturate the sand column and the weight of solids used were recorded, giving bulk density of 1.48 g/cm^3 and porosity of 0.50. As large pumice stones were excluded in the column, the bulk density of the packed material was significantly greater than that measured in the field. Shallow groundwater taken from the study area was used. The flow was supplied from the base of the column to remove any trapped air and to minimise the development of preferential flow pathways. The experiments were undertaken at room temperature.

Two experiments using native groundwater (total dissolved solids = 25.64 mg/l) spiked with the raw sewage taken from a sewage treatment plant, together with bromide, were carried out. Bromide was used to indicate water flow, as results of a batch sorption test and a column experiment using tritiated water and Br show that Br is conservative in the pumice sand material used in the study (Pang et al. 2001). Prior to spiking, the undiluted raw effluent was filtered through a piece of 340 μm pore size coarse cloth to exclude large organic particles. The pH value (7.38) of the filtered effluent was slightly higher than that of the native groundwater (6.99-7.28) and that of the column outflow (6.5).

Two different scenarios of septic tank effluent discharge were simulated: (a) Continuous-Source Experiment: faster flow velocity (1.34 m/day) and an injection period equal to the experimental duration (52 hours i.e. 2.90 pore volumes); (b) Pulse-Source Experiment: slower flow velocity (0.31 m/day), a pulse injection (51 hours, i.e. 0.66 pore volumes), and longer experimental duration (284 hours). The initial inflow concentrations for the Continuous-Source Experiment were: faecal coliforms 5.30×10^4 cfu/100 ml, *E.coli* 3.60×10^4 cfu/100 ml, F-RNA phages 6.30×10^3 pfu/100 ml, and Br 3.63 mg/l. The initial inflow concentrations for the Pulse-Source Experiment were faecal coliforms 4.20×10^4 cfu/100 ml, *E.coli* 4.00×10^4 cfu/100 ml, F-RNA phages 5.50×10^3 pfu/100 ml, and Br 3.75 mg/l.

Batch tests

The column experiments provided information on the total removal rates for the microbial indicators but not on their die-off (or inactivation) rates. The die-off of the microbial indicators in the injection solution of the column experiments was measured during the column experiments to obtain estimates of their die-off rates in the groundwater (without aquifer material), i.e. die-off of the free microbes.

In order to examine the die-off of the microbes in the groundwater with the aquifer material, i.e. the die-off of the sorbed microbes, a preliminary batch test was conducted. The injection solution of the Continuous-Source Experiment (164 ml) was mixed with aquifer material (370 g) in a glass bottle. The above solid-to-solution ratio used was similar to the bulk density in the column after correcting for water content. In order to

avoid filtration, the test was carried out in a static condition with gentle hand shaking a few times at the beginning. The vessel was covered with black plastic to minimise the effect of sunlight and incubated at a similar room temperature (20 °C ±1) to that of the column experiments. Samples were taken at 0, 24, and 48 hours. It should be noted that this test did not directly measure die-off of the sorbed microbes but the effective concentration reduction due to a combination of sorption, die-off of the sorbed microbes, and die-off of the dissolved microbes. The method for deducing die-off of the sorbed microbes from the result of this test will be discussed later.

Sample analysis

The microbial samples were assayed for bacteria by membrane filtration (Millipore EZ-Pak™, 0.45 μm pore size). The enumeration of faecal coliforms was by incubation on mFC agar (BBL) at 44.5 °C ± 0.2 °C for 24 ± 2 hours (APHA 1998). Typical blue faecal coliform colonies were counted, and all other colonies were marked. The membranes were transferred to nutrient agar containing 4-methylumbelliferyl-β-D-glucuronide (nutrient agar with MUG; Difco), incubated at 35 °C for 4 hours, and exposed to a UV-A lamp. Faecal coliform colonies exhibiting a ring of fluorescence were counted as *E. coli* (USEPA 1991). F-RNA phages were assayed by replicate overlay pour plates (APHA 1998), on host *E. coli* HS(pFamp)R (Debartolomeis & Cabelli 1991). The bromide samples were analysed by a bromide ion selective electrode.

6.2.4. Estimation of transport parameters using conceptual models

Column experimental data

Adapting the model of Harvey and Garabedian (1991) to include die-off, contaminant transport through saturated, homogeneous porous media, in a one-dimensional flow field, considering advection, dispersion, reversible sorption, first-order die-off (for both free and sorbed microbes), filtration (i.e., irreversible attachment, including irreversible sorption) may be described by the following equation:

$$\frac{\partial c}{\partial t} = D\frac{\partial^2 c}{\partial x^2} - v\frac{\partial c}{\partial x} - \frac{\rho_b}{\theta}\frac{\partial S}{\partial t} - \mu_l c - \mu_s \frac{\rho_b}{\theta} S - k_{att} c \qquad (6.1)$$

in which c = contaminant concentration in the liquid phase (M/L^3), t = time (T), D = dispersion coefficient (L^2/T), x = longitudinal distance (L), v = mean pore-water velocity (L/T), ρ_b = bulk density (M/L^3), θ = porosity (L^3/L^3), S = contaminant concentration in the solid phase (M/M), μ_l = first-order die-off rate for the free microbes (1/T), μ_s = first-order die-off rate for the sorbed microbes (1/T), and k_{att} = first-order filtration rate coefficient or the irreversible attachment rate constant (1/T).

The attachment rate constant k_{att} is known to depend on flow and diffusion characteristics as well as surface properties of microbes and solid grains (Schijven and Hassanizadeh, 2000). k_{att} is a function of the pore-water velocity, v, as described by the colloid filtration model (Yao et al., 1971; Bales et al., 1991; McCaulou et al., 1994):

$$k_{att} = \frac{3(1-\theta)}{2\ d_c}\alpha\eta v \qquad (6.2)$$

in which, d_c = average diameter of grain (L), α = collision efficiency, and η = single collector efficiency. Various theoretical and experimental methods have been presented for estimating α and η (e.g. Harvey and Garabedian, 1991). However, these parameters are not relevant to this study so those methods will not be discussed here.

Harvey and Garabedian (1991) indicated that the reversible sorption term could be described assuming sorption is (a) linear and instantaneous (at equilibrium), or (b) rate-limited, with sorption/desorption kinetics described as first-order processes. These two approaches are 'the basis for the quantitative modelling of the bacterial breakthrough and explanation of the bacterial transport' (Harvey and Garabedian, 1991).

In this study we have chosen the first approach and we assume linear reversible equilibrium sorption in our model. Other researchers (Jin et al., 1997; Matthess et al., 1988, Yates and Ouyang, 1992; Schijven and Hassanizadeh, 2000) have also presented the same approach for modelling microbial transport in porous media. The major reasons for our choice of an equilibrium model rather than a kinetic model are: (a) the pore-water velocities involved in the column experiments were slow (0.3-1.3 m/day), and under slow

velocities equilibrium models are often applicable; and (b) we wish to demonstrate an example of a methodology for estimation of septic tank setback distances that may be applied by groundwater scientists and managers in regional councils and other professionals in New Zealand, and we desire to use a model, such as the equilibrium model, that is easily learned, used, and accessed, as well as being generally accepted.

For linear reversible equilibrium sorption,

$$S = K_d c \qquad \frac{\partial S}{\partial t} = K_d \frac{\partial c}{\partial t} \qquad R = 1 + K_d \rho_b / \theta \tag{6.3}$$

Where K_d is a sorption partitioning coefficient (L^3/M), and R is the retardation factor, which is the ratio of mean pore-water velocity to the mean contaminant transport velocity. Eq. 6.1 may be rewritten as:

$$R\frac{\partial c}{\partial t} = D\frac{\partial^2 c}{\partial x^2} - v\frac{\partial c}{\partial x} - [\mu_l + \mu_s (R-1) + k_{att}]c \tag{6.4}$$

Eq. 6.4 could then be simplified as:

$$R\frac{\partial c}{\partial t} = D\frac{\partial^2 c}{\partial x^2} - v\frac{\partial c}{\partial x} - \lambda c \tag{6.5}$$

where λ = first-order total removal rate (1/T), and is defined as the sum of the combined die-off rate (μ) and filtration rate (k_{att}):

$$\lambda = \mu + k_{att} \qquad \text{where} \quad \mu = \mu_l + \mu_s (R-1) \tag{6.6}$$

Eq. 6.5 has the same form as the common Advection-Dispersion Equation, ADE, with a first-order reduction term. However, in this case, the first-order reduction term encompasses die-off in the liquid phase, die-off in the sorbed phase and removal by filtration (including irreversible sorption). We assumed that filtration is a first-order irreversible process. This assumption is commonly made to model filtration (e.g., Iwasaki 1937; Matthess et al. 1988). We have also modeled filtration and sorption as distinct

processes. Sorption is assumed to be a reversible, equilibrium process while filtration is an irreversible process, controlled by first-order kinetics.

Transport parameters, v, D, R, and λ, were estimated by fitting the experimental data to data simulated by Eq. 6.5 using the CXTFIT curve-fitting program (Toride et al. 1995). The values of v and D were first estimated from the bromide data. These values were then kept constant when optimising R and λ values for the microbial indicators. The combined die-off rate, μ, could be determined from a batch test after adjusting for sorption (as will be described in Section 6.2.4). Knowing the values of μ and λ, we could then estimate the filtration rate (k_{att}) using Eq. 6.6. Consequently, the ratios of μ/λ and k_{att}/λ allow us to deduce the relative contribution of die-off and filtration to total removal. The errors of model estimation were also considered in the calculations.

It should be noted that due to the die-off of microbial indicators in the injection solution, the input concentration was observed to have changed with time. Therefore, variable input concentrations were used in the model. For the times when we did not take samples of the input solution, the estimation of input concentrations was based on first-order die-off.

In addition to the above parameters, the mass removal and the concentration reduction could also be determined to describe the attenuation of the microbes. The mass removal of the microbes, M_{re}, could be estimated from the integration of the concentration breakthrough curves as follows:

$$M_{re} = \left[1 - \frac{\int_0^{\infty} Q(t)c(t)dt}{\int_0^{T_0} Q(t)c_0(t)dt} \right] x\,100\% \qquad (6.7)$$

where, Q = flow rate (L^3/T), c_0 = inflow concentration (M/L^3), and T_0 = duration of the pulse (T). The log-reduction of concentration could be calculated from the formula:

$$\log\text{-}reduction = -\log_{10}\left(\frac{c_{\max}}{c_{o\max}}\right) \tag{6.8}$$

The surface coverage of the microbes in the column could supply some information on whether clogging by the microbes would occur. This is estimated from the equation below:

$$SC = \frac{\left(\int_0^{T_0} Q(t)c_0(t)dt - \int_0^{\infty} Q(t)c(t)dt\right)A_{microbe}}{n\,A_{sand}} x\,100\% \quad \text{where} \quad n = \frac{\rho_b W}{\rho_s W_p} \qquad A_{sand} = \pi\Phi^2 \tag{6.9}$$

where A_{microbe} is the surface area of the microbe (L^2), $A_{\text{microbe}} = \pi d^2$ for the F-RNA phages and $A_{\text{microbe}} = \pi d(L+d/2)$ for faecal bacteria, in which d and L is the diameter and length of the microbe (L), respectively; Φ = mean diameter of the sand particle (L); A_{sand} = surface area of a sand particle (L^2); $W_p = 1/6\ \pi\Phi^3$ is the volume of the each sand particles (L^3); n is the total number of sand particles; W is the column volume (L^3); and ρ_s is the particle density of the sand (M/L^3).

Batch test data

In a static batch system, there is no hydrodynamic dispersion ($D = 0$) and advection ($v = 0$). As k_{att} is a function of v as indicated previously (Eq. 6.2), we could then assume $k_{att} = 0$ in the static batch system. Hence, Eq. 6.5 could be reduced to:

$$R\frac{\partial c}{\partial t} = -\mu c = -[\mu_l + (R-1)\mu_s]\,c \quad \text{with a solution of} \quad c = c_o\,Exp\left[-\frac{\mu_l + (R-1)\mu_s}{R}t\right] \tag{6.10}$$

in which, c_0 is the initial concentration. When there is no solid involved in the batch system (i.e. $R = 1$, $\mu_s = 0$), Eq. 6.10 could be further reduced to:

$$\frac{\partial c}{\partial t} = -\mu_l c \quad \text{with a solution of} \quad c = c_o\,Exp[-\mu_l t] \tag{6.11}$$

The μ_l value could be determined by fitting the experimental data of the die-off batch tests (with liquid phase only) with an exponential function. As the R-value could be estimated from the column data, there is now only one parameter, μ_s, unknown in Eq. 6.6. This parameter could be solved from the batch test data with the mixture of groundwater and aquifer material.

The batch test with the mixture measured the effective reduction caused by sorption and die-off in the mixture, which could be described using an effective reduction rate, λ_{eff}, as given by Schijven and Hassanizadeh (2000):

$$\lambda_{eff} = -\frac{1}{t}\ln\left(\frac{c}{c_o}\right) \tag{6.12}$$

Similar to the approach of estimating μ_l, the λ_{eff} values could be determined by fitting the experimental data of the batch test (with the mixture) with an exponential function. From Eqs. 6.10 and 6.12, we could solve for μ_s as below (Schijven and Hassanizadeh, 2000):

$$\mu_s = \frac{R\lambda_{eff} - \mu_l}{R-1} \tag{6.13}$$

We should note that there is some uncertainty in applying the R-value estimated from the column data to the batch system. However, this is acceptable for a system at equilibrium conditions, which is assumed in our model. At equilibrium conditions, the R-value determined from a column experiment should be the same as that determined from a batch test and should not vary with pore-water velocity. The similar R-values determined from the column experiments with different flow rates (see Section 6.3.1) suggest that the column system was approximately under equilibrium conditions. The reason for us to have used this approach was because it is difficult to independently determine the R-value using batch data as other processes could be also interacted with sorption in a batch system.

6.2.5. Model estimation of setback distances

Choice of water quality criteria

The current guidelines for fresh water bathing are the Recreational Water Quality Guidelines (RWQG) set by the Ministry for the Environment (1999). These guidelines have adopted *E. coli* as the preferred indicator organism for freshwater water quality. The guidelines require that for 'Acceptable/Green Mode', the running median (estimated monthly) of *E. coli* must be less than 126 cfu/100 ml.

However, viruses are also of a health concern. Compared to bacteria, viruses have lower infectious doses as stated previously and a longer survival time in soils and aquifer materials. Allowing for *E. coli* concentrations 126 cfu/100 ml in the bathing water, viral concentrations could be very high. Considering the possibility for ingestion of pathogens during recreational use of lake water, the Drinking-Water Standards For New Zealand (DWSNZ) set by the Ministry of Health (2000) were also considered. The DWSNZ require less than one *E. coli* in 100 ml of sample and less than one enteric virus in 100 L sample (i.e., $<1x10^{-3}$ pfu/100 ml). If recreational contact with lake-water is the only concern, this approach will be conservative as the amount ingested while swimming would be minor compared to use as a drinking water supply. However, it would be relevant if the lake water was considered as a drinking water supply.

As typical concentrations of the viral indicators, F-RNA phages, in human effluents are in the order of 10^6 pfu/100 ml (Table 6.2), a 10-log reduction would ensure viral concentrations below 1 pfu/100 L. Similarly, in a recent work on the determination of protection zones for Dutch groundwater well systems, a 9-log reduction was used for preventing viral contamination (Schijven 2001). However, with a 9-log reduction, the groundwater may still contain a few viruses/100 L if viral concentrations in the raw effluent are of the order of 10^6 pfu/100 ml and there is no reduction in levels before entry to the groundwater.

For *E. coli* concentrations <126 cfu/100 ml, it is possible to determine the setback distance through a field sampling program and through model prediction. A field-

sampling program would have to address the timing when there would be the most problems, e.g. after heavy rainfall, and require a detailed investigation on the main flow path. Even then, there are still some other uncertainties and one would have to apply some safety factor in designing the sampling program. In addition to these difficulties, compliance with enteric viruses less than 1 pfu/100 L can only be assessed by analysing a very large volume of the sample, i.e. of the order of 100-1000 litres. This is often difficult and therefore, model simulation is an essential approach.

Transport model and model inputs

A three-dimensional contaminant transport model, AT123D (Yeh 1981), was used to determine the minimum septic tank setback distances that would comply with RWQG and DWSNZ for a worst-case scenario. AT123D is an analytical solution for solute transport in an homogeneous aquifer with uniform flow. It considers advection, dispersion, linear equilibrium sorption, and first-order decay. The first-order decay term was adopted as the total removal in this study. Model inputs for a worst-case scenario are described below and summarised in Table 6.3.

Contaminant source

Inputs for dimension, flow rate, and loading rate of the disposal trench/bed were based on the maximum values of design criteria from "On-site domestic wastewater management" (AS/NZS 1547 2000). Considering the worst case, we assumed the effective depth for the disposal trench/bed to be within the saturated zone. Although in reality the discharge of septic tank effluent into the groundwater is intermittent, we assumed a continuous discharge (1-year) in the model. A steady-state situation will occur when the input of viruses is continuous over a sufficiently long period of time.

Aquifer characteristics

Inputs for aquifer characteristics were mainly based on the results from field and laboratory experiments. To consider scale-dependent dispersion, the values of dispersivity at various transport distances were calculated using the ratio of longitudinal dispersivity/distance, $\varepsilon = 0.06$, determined from the Continuous-Source Experiment. The lateral dispersivity, α_y, was assumed to be 0.1 α_x and the vertical dispersivity, α_z, was

assumed to be 0.1 α_y (Gelhar et al. 1992). According to the well log data that Environment B.O.P provided, the depth of pumice sand aquifer could be up to 31-42.7 m in the Lake Okarea area. Therefore, a depth of 43 m was used in the model.

Inputs for attenuation and transport characteristics of microbial indicators

A worst case was considered in the model, i.e. the entry of the raw effluent into the groundwater. Typical microbial concentrations in the raw septic tank effluent are of the order of 10^6 cfu or pfu/100 ml (Table 6.2), and we used the maximum concentration from the table of 10^7 cfu or pfu/100 ml as inputs to the model. Although microbial indicators were slightly sorbed in the experiments of our study (Table 6.4), they may not be sorbed in many cases (i.e. sorption coefficient $K_d = 0$). For example, Goyal and Gerba (1979) reported a zero K_d value for coliphage f2 (a subgroup of F-RNA phages) and Coxsackievirus type B4 in loamy sand. Bales et al. (1995) and Pieper et al. (1997) reported that PRD1, a viral indicator, was transported at about the same rate as a conservative tracer in the field studies, where preferential flow was absent. For a conservative approach, the sorption coefficient, K_d, was set equal to zero. In other words, it was assumed that average velocities of the pathogens and groundwater were identical. Removal rates used in the model were based on the lower 95% confidence limits of the model estimations, determined from the Continuous-Source Experiment.

It should be noted that the possibility of microbial growth was not considered in the model as the temperature of the groundwater is generally not favourable for microbial growth. This is particularly true for F-RNA phages. According to Havelaar et al. (1993) and IAWPRC (1991), F-RNA phages are widely considered to be highly unlikely to replicate in natural waters, because production by host bacteria of the F-pili necessary for phage attachment does not occur below 30°C.

6.3. Results and discussion

6.3.1. Laboratory experiments

Fig.6.2 shows the concentration breakthrough curves observed in the Continuous-Source Experiment and simulated concentrations generated from the curve fitting. For showing the magnitude of relative reduction, concentrations were converted to c/c_{omax} in

Table 6.3
Model inputs for determining the minimum septic tank setback distance for a worst-case scenario

Model parameter	Symbol and formula	Units	Value
1. Contaminant source			
Designed maximum disposal trench/bed width	W	m	4
Designed maximum daily flow for a 10-person system	Q	L/day	2000
Designed maximum loading rate	DLR	mm/day	35
Designed effective depth for disposal trench/bed		m	0.25 (allowed to be within the saturated zone)
Calculated standard length of disposal trench/bed (parallel to the groundwater flow-direction in the model)	$L = Q/(DLRxW)$	m	14 (along groundwater flow direction)
2. Aquifer characteristics			
Longitudinal dispersivity/distance ratio	ε		0.06
Longitudinal dispersivity	$\alpha_x = \varepsilon x$	m	ε x distance
Lateral dispersivity	$\alpha_y = 0.1\alpha_x$	m	0.1 x α_x
Vertical dispersivity	$\alpha_z = 0.1\alpha_y$	m	0.1 x α_y
Depth of the pumice sand aquifer		m	43
Effective porosity of the aquifer material	θ		0.20
Bulk density of the aquifer material	ρ_b	g/cm^3	1.17
Maximum hydraulic gradient measured in the field	I		0.008
Maximum hydraulic conductivity measured in the field	K	m/day	172
Equivalent maximum pore-water velocity	$v = KI/\theta$	m/day	6.88
3. Microbial indicators			
Maximum input concentration of microbial indicators	c_o	count/100ml	1x10^7
Input microbial mass flux	$M = Qc_o$	count/day	2.0 x10^{11}
Source of microbial input			Continuous
Sorption coefficient of microbial indicators	K_d	ml/g	0
Removal rate of F-RNA phages	λ	per day	8.41 (lower limit of the estimate in Table 6.4)
Removal rate of *E. coli*	λ	per day	13.6 (lower limit of the estimate in Table 6.4)

Fig.6.2. Table 6.4 lists the estimated parameter values for the attenuation and transport of the microbial indicators and bromide in the pumice sand aquifer material.

It should also be noted that in the Pulse-Source Experiment, due to the long residence time in the column at low flow rate, the die-off of the microbial indicators in the column was significant and hence the concentrations in the outflow were very low (1-5 counts detected in 10 ml) and F-RNA phages were detected in only one sample. Therefore, no model-simulation was carried out on the phage data. The *R*-value for the F-RNA phages was simply defined from the ratio of peak-concentration-time of the phages to the peak-concentration-time of the bromide.

Retardation/sorption

Fig.6.2 and Table 6.4 suggest that the microbial indicators investigated were retarded in both experiments compared to the bromide, with the bacteria slightly less sorbed than the phages. Retardation factors of the bacteria were not significantly different at high and low flow rates, indicating that the column system was approximately under equilibrium conditions.

The *R*-values of 2.1-2.5 for the F-RNA phages determined in this study are very similar to $R = 1.4$ for MS2 and $R = 2.2$ for PRD1 as reported by Powelson and Gerba (1994). The attenuation and transport of MS2 (a subgroup of F-RNA phages) and PRD1 are regarded as being very similar with nearly equal removal rates (Schijven et al. 1999). The *R*-values of the F-RNA phages determined in this study are lower than the $R = 5.2$ for poliovirus reported by Powelson and Gerba (1994). This is expected, as F-RNA phages are less sorbed than most other viruses (Goyal & Gerba 1979). The calculated values of the sorption coefficient for the F-RNA phages (K_d = 0.36-0.52 ml/g) are similar to K_d = 0.20 ml/g for MS2 reported by Goyal and Gerba (1979). As there is a lack of information in the literature on the sorption of faecal coliforms and *E. coli*, no comparison can be made for the bacterial results between this study and other studies.

Removal

In both column experiments, the bacteria underwent a 4-log reduction and the F-RNA phages a 3-log reduction. A 3-log viral reduction in sandy materials was also found in

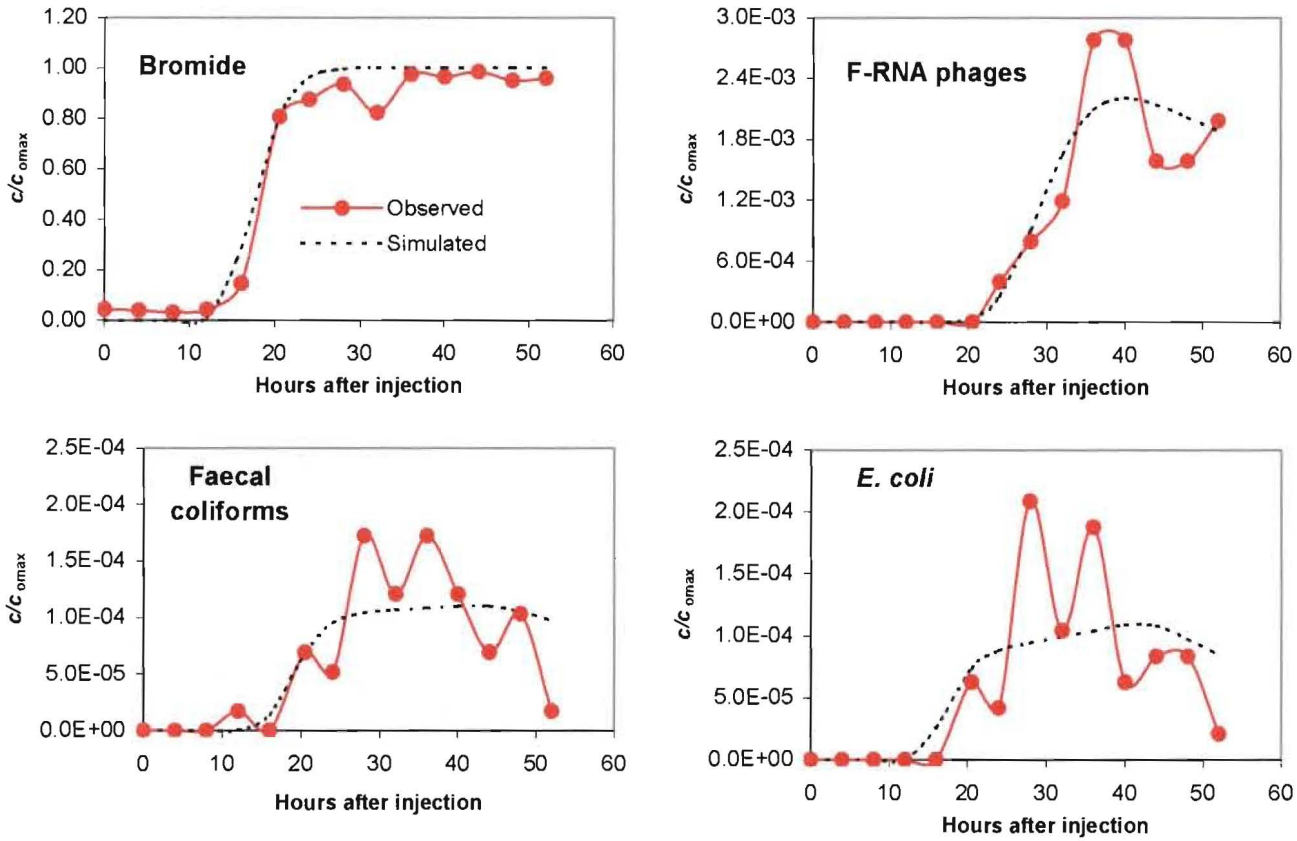

Fig. 6.2. Observed and CXTFIT-simulated concentration breakthrough curves for the Continuous-Source Experiment

Table 6.4
Attenuation and transport parameters derived from the column experiments with pumice sand aquifer material

Experiment	v (m/day)	D (m^2/day)	Tracer and microbes	R	K_d (ml/g)	λ (per day)	M_{re} (%)	log-reduction =-Log(c_{max}/c_{omax})	SC (%)
Continuous-Source	1.34	0.02	Bromide	1.00	0.00	0.00	-	0	-
	(1.25-1.43)	(0.00-0.04)	F-RNA phages	2.06 (1.78-2.34)	0.36 (0.26-0.45)	8.81 (8.41-9.21)	99.83	3	4.64E-08
			Faecal coliforms	1.44 (0.95-1.94)	0.15 (0-0.32)	14.2 (13.6-14.8)	99.99	4	2.18E-03
			E. coli	1.31 (0.56-2.06)	0.1 (0-0.36)	14.2 (13.6-15.1)	99.99	4	1.56E-03
Pulse-Source	0.31	0.02	Bromide	1.00	0.00	0.00	-	0	
	(0.29-0.32)	(0.01-0.02)	F-RNA phages	2.53[a]	0.52		99.96	3	5.44E-09
			Faecal coliforms	1.87 (0.97-2.76)	0.29 (0-0.59)	5.37 (5.14-5.61)	99.98	4	2.53E-04
			E. coli	1.92 (1.02-2.81)	0.31 (0.01-0.61)	5.25 (5.02-5.49)	99.97	4	2.20E-04

[a]The R value for F-RNA phages in the Pulse-Source Experiment was simply defined from the ratio of peak-concentration-time of the phages to the peak-concentration-time of the bromide.

Values of v and D were estimated from the bromide data. Values in parentheses give 95% confidence limits of the model estimations.

K_d values were calculated from $K_d=(R-1)\theta/\rho_b$, where $\theta=0.50$ and $\rho_b=1.48$ g/cm^3.

other laboratory studies (i.e. similar transport scales) of Moore et al. (1982) for reovirus, Dizer et al. (1985) for coxsackievirus B1, Goyal and Gerba (1979) for rotavirus SA-11, Echovirus 1-7, and poliovirus 1.

The degree of microbial removal in pumice sand observed in this study is consistent with the findings of a similar experiment carried out by Pang et al. (1996) using pumice sand and septic tank effluent. In that study, the same stainless steel column used in this study was driven into a pumice sand-pit in the same study area and an undisturbed core sample of pumice sand was extracted. The experimental conditions were very similar to those of the Pulse-Source Experiment in the present study: about one pore volume of 10% (by volume) septic tank effluent with input concentrations of 10^5 cfu/100 ml for faecal coliforms and 10^3 pfu/100 ml for F-RNA phages was injected at a pore-water velocity of 0.5 m/day. The results of the 1996 study are similar to the present study. Faecal coliforms were detected in only a few outflow samples at about a 4-log reduction from the original values. F-RNA phages were not detected in the 1996 study, and were detected only in one sample in this study. These similar findings observed in both studies imply that in a normal situation of intermittent discharge of septic tank effluent (similar to the pulse injection in the above column experiments), the breakthrough of pathogens is likely to be of an abrupt nature, occurring and disappearing quickly. Contamination events may not be identifiable if the sampling frequency is insufficient.

Very few studies reported in the literature have presented information on removal rates for microbes in aquifer systems. From a field tracer experiment in an alluvial gravel aquifer over 385-401 m distance, Sinton et al. (1997) estimated the following removal rates: 1.14 per day for faecal coliforms, 0.99 per day for *E. coli,* 1.92 per day for F-RNA phages, and 1.42 per day for MS2. Schijven and Hassanizadeh (2000) reported removal rates for MS2 and PRD1: 0.30-5.53 per day based on experiments with 1.5 m long sand columns at pore-water velocity 1.6-3.3 m/day, and 0.25-4.15 per day based on a field experiment within 30 m travel distance in a coastal sand aquifer. Compared to these values, the removal rates for the microbial indicators determined from the 1-m long column in this study are higher. This suggests that pumice sand aquifer material is superior to alluvial gravel and coastal sand aquifer materials in attenuating microbial contaminants.

Table 6.5
Die-off rates for the free and adsorbed microbes estimated from the batch tests

	λ_{eff}	μ_l (per day)			R		μ_s (per day)		μ_s/μ_l		μ (per day)	
	per day	CSE	PSE	mean	CSE	PSE	CSE	PSE	CSE	PSE	CSE	PSE
F-RNA phages	1.93	0.55	0.69	0.62	2.06	2.53	3.24	2.75	5.89	3.96	3.99	4.89
Faecal coliforms	1.28	0.22	0.14	0.18	1.44	1.87	3.68	2.60	16.5	18.1	1.85	2.40
E. coli	1.28	0.30	0.09	0.19	1.31	1.92	4.47	2.59	15.2	28.4	1.68	2.46

λ_{eff} Effective reduction rate measured in the batch test with the mixture of groundwater and aquifer material,
μ_l Die-off rate for the free microbes,
R Mean retardation factor estimated from the column experiment (Table 6.4),
μ_s Mean die-off rate for the adsorbed microbes, calculated from Eq. 6.13,
μ Mean combined die-off rate, calculated from Eq. 6.6,
CSE Continuous-Source Experiment,
PSE Pulse-Source Experiment.

According to Schijven (2001), the removal rate for F-RNA phages in sandy aquifers is lower than for most other viruses and viral indicators as follows: Poliovirus 1 > ϕX174 > Coxsackievirus B4 ≈ PRD1 ≈ MS2 (F-RNA phages). Therefore, F-RNA phages are relatively conservative indicators of viral movement through saturated materials.

Table 6.4 suggests that removal rates of the faecal bacteria derived from the high flow Continuous-Source Experiment were greater than those derived from the low flow Pulse-Source Experiment. This is expected as filtration theory predicts that increased pore-water velocity will normally result in an increase in the first-order filtration rate (Rajagopolan and Tien 1976; Rijnaarts et al. 1996; Goltz et al. 2001). Thus, the finding that the removal rate increased with increasing pore-water velocity suggests that removal of bacteria by filtration may dominate.

Die-off

Table 6.5 lists measured die-off rates for the free microbes in the groundwater (μ_l), die-off rates for the sorbed microbes (μ_s, calculated from values of μ_l, R, and λ_{eff}), and calculated combined die-off rates (μ). Table 6.5 shows that the μ_l values for the F-RNA phages and faecal coliforms were reasonably similar between experiments, but there was a factor of 3 difference in the *E. coli* results between experiments. This is considered to be due to the variable nature of the microbial die-off experiments, and/or errors in the sample analysis and data simulation. However, the average μ_l and λ_{eff} values were very similar between the bacterial indicators. This is expected because *E. coli* comprises a large proportion of the faecal coliform population.

The mean die-off rates for the free microbes in the groundwater (μ_l) derived from this study are consistent with some studies reported in the literature. The mean μ_l value of 0.18 per day for the faecal coliforms (Table 6.5) was the same as that reported by Pang et al. (1996), and was only two times lower than that estimated by Martin and Noonan (1977). The mean μ_l value of 0.19 per day for *E. coli* was not much different from the value of 0.37 per day reported by Bitton et al. (1983) and the lowest value of 0.32 per day (ranging 0.32-1.12 per day) derived from the data of Thorpe et al. (1982). The mean μ_l value of 0.62 per day for the F-RNA phages determined at 20 °C in this study was also

similar to the value of 0.90 per day for coliphage f2 reported by Keswick et al. (1982), to the values of 0.58-1.3 per day for MS2 at 23 °C reported by Yahya et al. (1993), and to the value of 0.73 for MS2 at 23 °C reported by Yates et al. (1985). Both coliphage f2 and MS2 are members of the F-RNA phage groups.

Relatively less information is available in the literature for die-off rates for the sorbed microbes in groundwater with aquifer materials, μ_s. This could be seen in a review by Schijven and Hassanizadeh (2000). The calculated μ_s values of 2.75-3.24 per day for the F-RNA phages determined in this study were higher than the μ_s values reported by Blanc and Nasser (1996) for MS2 at 23 °C. They reported μ_s = 0.46 per day in groundwater with loamy sand, μ_s = 1.34 per day in secondary effluent with loamy sand, μ_s = 0.44 per day in groundwater with sand, and μ_s = 0.64 per day in secondary effluent with sand. The higher die-off rate for F-RNA phages determined in this study compared to the die-off rates for MS2 reported in the literature is perhaps due to the superior attenuation capability of the pumice sand than other materials or/and the presence of a different predominant subgroup of F-RNA phages (rather than MS2) with a higher die-off rate. Sobsey et al. (1986) reported μ_s = 1.0 per day for hepatitis A virus at 25 °C in groundwater with Corolla sand. No information on the μ_s values has been found in the literature for the bacterial indicators.

Table 6.5 suggests that the F-RNA phages were inactivated faster than the faecal bacteria. There are wide ranges of inactivation rates reported in the literature. Apart from different die-off mechanisms between viruses and bacteria, there are also other possible reasons: (1) There was some apparent increase in bacterial counts at room temperature (20 °C ± 1) in the first 24 hours. Thus, the die-off rates of the faecal indicators were relatively lower than that of F-RNA phages. (2) The possible separation of aggregates ("de-clumping") of faecal bacteria could also result in the lower die-off rates of the faecal indicators. (3) The faecal bacteria could be attached to other organic particles in the effluent and the possible detachment of the faecal bacteria from these particles may also have contributed to the lower die-off rates of the faecal indicators. (4) Although F-RNA phages inactivate slowly at temperatures less than 10 °C, they could inactivate faster at higher temperatures (Schijven & Hassanizadeh 2000). Together with the growth of

bacteria, this resulted in higher die-off rates of the F-RNA phages compared to the faecal indicators. The reason for measuring the die-off rates at room temperature in this study was to keep the same temperature between experiments/tests so that we were able to identify the relative contribution of individual processes.

Table 6.5 shows that compared to the die-off for the free microbes (μ_l), the die-off for the sorbed microbes (μ_s) was 4-6 times greater for the F-RNA phages and 15-28 times greater for the bacteria. Higher μ_s values compared to the relevant μ_l values are also often reported in the literature (Blanc & Nasser 1996, Schijven & Hassanizadeh 2000). The ratio of μ_s/μ_l for the F-RNA phages determined in this study was similar to the ratio μ_s/μ_l = 2-3 for MS2 (a subgroup of F-RNA phages) and PRD1 reported by Blanc and Nasser (1996). However, there is no information available on the μ_s/μ_l values for faecal coliforms and *E. coli*.

Relative contribution of filtration and die-off to total removal

Having established the total removal rates (from model simulation of the column data) and combined die-off rates, we can now calculate the filtration rates from Eq. 6.6. From these reaction rates, we are able to quantify the relative contribution of filtration and die-off to total removal. The results are listed in Table 6.6. As a continuous microbial input was considered in estimating setback distances, the calculations were based on data derived from the Continuous-Source Experiment.

Table 6.6 suggests that filtration was the major removal process for the bacteria, contributing 87-88% of their total removal with the remaining 12-13% contributed from the combined die-off for both free and sorbed microbes. In other words, the filtration rates for the faecal bacteria were over 7 times that of their combined die-off rates. This finding suggests that bacteria could be largely filtered out in the pumice sand aquifer material. For the F-RNA phages, both filtration (contributing 55% of the total removal) and die-off (contributing 45% of the total removal) were important. Although the phages have much smaller particle size, they could be sorbed onto large colloid particles in the effluent and hence could be filtered out.

The ratio of the die-off rate for the free microbes to the removal rate was 0.02 for the faecal bacteria and 0.06 for the phages, suggesting that the die-off of the free microbes contributed little to the total removal. This implies that the setback distances determined from the die-off rates in the liquid phases, established in the laboratory survival tests without involving any aquifer material, could be much larger than those determined from the total removal rates. Unfortunately, most available data in the literature are subject to die-off rates in the liquid phase, and there is relatively little reported information on total removal rates.

It should be noted that we observed a gradual decrease in flow rate with time in both column experiments. It was interpreted as the result of grain surfaces becoming progressively clogged by the filtered particles. However, the clogging was believed to be caused by other large colloid particles in the septic tank effluent rather than from the microbes themselves as the calculated surface coverage of the microbes in the column was negligible compared with the sand surface area (Table 6.4). It should be noted that this is based on the assumption there is no microbial growth during the column experiments.

6.3.2. Model-estimated setback distances

Simulation results

The model-estimated maximum *E. coli* concentrations along the main flowline were 75 cfu/100 ml at 16 m, 0.73 cfu/100ml at 20 m, and 0.03 cfu/100 ml at 25 m. Thus, in order to meet the RWQG for *E. coli* <126 cfu/100 ml, only 16 m distance is required for the setback distance. The above model-estimated *E. coli* results generally agree with results from the field monitoring. Ray et al. (2000) analysed 20 groundwater samples taken from 10-35 m downstream of the septic tanks on the shorelines of Okareka. *E. coli* bacteria were not detected in 17 of these samples. The remaining 3 samples only contained 2-5 *E. coli* /100 ml.

However, to meet the DWSNZ for viral concentrations < 1 pfu/100 L, a minimum distance of 48 m is suggested as the model-simulated maximum viral concentration in the groundwater was 0.85 pfu/100 L at 48 m, about a 10-log reduction from the initial

Table 6.6
Relative contribution of filtration and die-off to total removal of the microbial indicators using data derived from the Continuous-Source Experiment

Parameter	Symbol	Units	F-RNA phages	Faecal coliforms	*E. coli*
Total removal rate (Table 6.4)	λ	per day	8.81 (8.41-9.21)	14.2 (13.6-14.8)	14.2 (13.6-15.1)
Die-off rate for the free microbes (Table 6.5)	μ_l	per day	0.55 -	0.22 -	0.30 -
Die-off rate for the adsorbed microbes (Table 6.5)	μ_s	per day	3.24 (2.97-3.71)	3.68 a	4.47 a
Combined die-off rate (Table 6.5)	μ	per day	3.99 (3.44-4.53)	1.85 (1.22-2.49)	1.68 (0.72-2.65)
Filtration rate (attachment rate)	$k_{att} = \lambda - \mu$	per day	4.82 (4.68-4.97)	12.4 (12.3-12.4)	12.5 (12.5-12.9)
Ratio of filtration rate / total removal rate	k_{att} / λ		0.55 (0.51-0.59)	0.87 (0.83-0.91)	0.88 (0.82-0.95)
Ratio of filtration rate / combined die-off rate	k_{att} / μ		1.21 (1.03-1.44)	6.68 (4.96-10.1)	7.44 (4.70-17.9)
Ratio of combined die-off rate / total removal rate	μ/λ		0.45 (0.41-0.49)	0.13 (0.09-0.17)	0.12 (0.05-0.18)
Ratio of die-off rate for the free microbes/total removal rate	μ_l / λ		0.06 (0.06-0.07)	0.02 (0.02-0.02)	0.02 (0.02-0.02)

Values in parentheses give 95% confidence limits of the estimations.
a - negative μ_s values for R<1

concentration. Fig.6.3 shows model-estimated maximum F-RNA phage concentrations in the downstream groundwater along the flow-line. At the distance that satisfies the RWQG, i.e. 16 m, model-estimated F-RNA phage concentration is 312 pfu/100ml (4.5-log reduction), which is 312,000 times above the DWSNZ.

It is interesting to compare our results from the model simulations with those observed in a field tracer experiment of Schijven et al. (1999). In their field study, groundwater velocity in a sand dune aquifer varied 1.19-1.59 m/day with effective porosity of 0.35. Schijven et al. (1999) used MS2 and PRD1 as viral indicators in their experiment, which are similar to F-RNA phages. The log-reductions in viral concentrations, calculated on the basis of $-\log(C_{max}/C_o)$, increased almost linearly with transport distances in both studies of Schijven et al. (1999) and ours, as shown in Fig.6.3. The similar slopes of the plots indicate that the removal rates, if expressed as the ratio of log-reduction to distance, were similar between the field-determined by Schijven et al. (1999) and the model-simulated in this study.

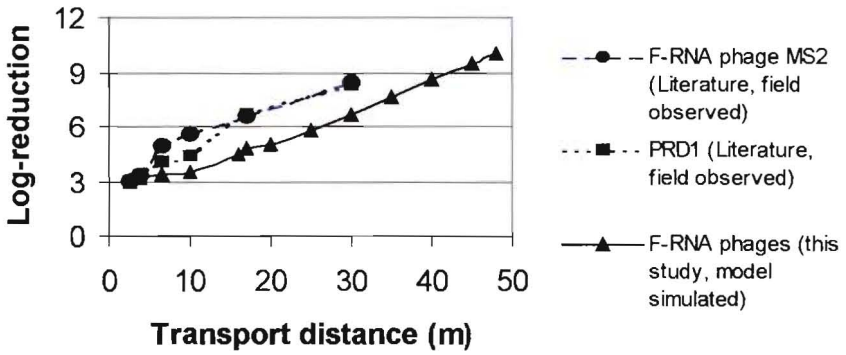

Fig.6.3 Comparison of viral reduction observed in the field experiment (Schijven et al. 1999) and those simulated in this study

The linear correlation between log-reduction and transport distance indicated above was also shown in the field data reported by Stewart and Reneau (1982). In a saturated coastal sandy soil where the water table rises to flood the disposal trench of the septic tank effluent, Stewart and Reneau (1982) observed that the travel of faecal coliforms

shows a reduction from 3 x 10^6 cfu/100 ml in the trench to 1.1 x 10^5 cfu/100ml 150 mm from the edge of the trench (i.e 1.4-log reduction), 2.9 x 10^4 cfu/100 ml 3 m from the trench (i.e. 2-log reduction), and 1.1 x 10^3 cfu/100 ml at 12 to 13 m distance (i.e. 3.4-log reduction). Using the removal rate of faecal coliforms determined in this study (13.60 per day), we could obtain a 3.6-log reduction in faecal coliform concentration at 12 m travel distance, which was similar to the result of Stewart and Reneau (1982) at the equivalent distance.

Sensitivity analysis and limitations of model simulation

Compared to other model input parameters listed in Table 6.3, the ratio of longitudinal dispersivity/distance (consequently the dispersivities), ε, and removal rates of the microbial indicators, derived from the column study, are relatively uncertain with respect to their representing the field conditions. In order to examine the sensitivity of these parameters on the simulation results, different values of ε and removal rates for the F-RNA phages were tested to simulate the setback distances that meet DWSNZ and the results are presented in Fig.6.4. Fig.6.4 shows that simulated setback distances increase linearly with increasing ε and increase in a power function with decreasing removal rates. Using a removal rate of 8 per day, the estimated setback distances are 39-65 m for ε = 0.01-0.12. If using ε = 0.06, the estimated setback distances are 28-225 m for a removal rate 1-16 per day. These results imply that the removal rate is much more sensitive than ε to the simulated results and that adequate determination of removal rates of microbial indicators is crucial in delineation of setback distances. In addition, possible variation in the removal rates is larger than that of the ε values. Although setback distances are very sensitive to the removal rate and could vary significantly, the similarity between model-derived results and field-observed results reported in the literature (as discussed above) suggest that the removal rates derived in this study are reasonable.

As the AT123D model deals with homogeneous media and uniform flow, the model results have several limitations. The major limitations are in the impacts of preferential flow paths, pore-size exclusion, and changes in removal rates with time and distance. Setback distances determined in our study may not be sufficient when these processes occur. Virus movement in groundwater beyond 48 m has been found in sandy aquifers in

the literature as reviewed by Yates (1985). In one case, viruses were detected in shallow groundwater 67 m down-gradient of the septic tank source, and in another case, in groundwater 53 m from the source after 12 days introduction into the septic tank. Viral migration in a sandy aquifer up to 400 m has also been noted (Keswick & Gerba 1980; Gerba 1984). However, the removal rates in the pumice sand aquifer in this study was probably greater than for these aquifers. The impacts of preferential flow paths, pore-size exclusion, and changes in removal rates with time and distance on microbial transport in groundwater are discussed below.

(a) Impact of preferential flow paths

As described previously, the groundwater velocity (7 m/day) used in the model was derived from the highest hydraulic conductivity and the highest gradient measured in the field. Although the value of 7 m/day is higher than the typical groundwater velocities in the pumice sand aquifers, groundwater could possibly move even faster through preferential flow paths (e.g., structural cracks, poorly sealed bores, zones of higher permeability, and areas where pumice sand aquifer overlays fractured bedrock). Therefore, the 48 m setback distance determined from the model simulations, based on the homogeneous aquifer and uniform flow, may not be sufficient when preferential flow paths are present. However, matrix flow, rather than preferential flow (or bypass flow), is considered to be the predominant flow in porous pumice sand aquifers.

(b) Velocity enhancement due to pore-size exclusion

In the model simulation, as a conservative approach, pathogens were assumed to travel with the same velocity as the average groundwater velocity (i.e $R = 1$, or $K_d = 0$). This approach did not consider the impact of possible velocity enhancement in microbial transport. Micro-organisms are sometimes found to travel faster than the average groundwater velocity in certain aquifer systems (often in heterogeneous media such as clayey soils, alluvial gravels, fractured media, and karst).

Generally, the degree of size-exclusion is positively related to microbial size, i.e. bacteria move faster than viruses (Sinton et al. 2000). However, although viruses are small in size, they could be attached to large organic particles in the septic tank/sewage

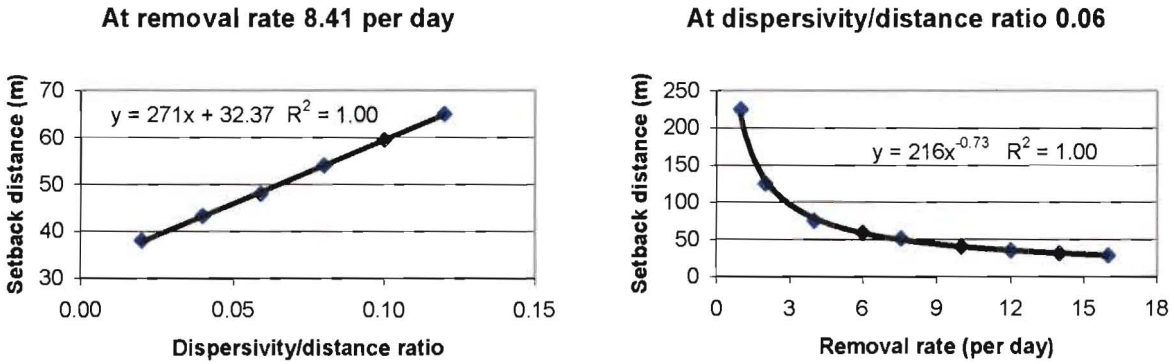

Fig. 6.4. Effects of dispersivity/distance ratio and removal rate on simulated setback distances that meet the Drinking-Water Standards For New Zealand (Ministry of Health 2000)

effluent and hence could possibly travel even faster than bacteria, as found in the studies of Pang et al. (1996) and Sinton et al. (1997). In this study, large organic particles are likely to be filtered out more rapidly in the pumice sand aquifer, and the impact would be much less than observed in the above studies. Velocity enhancement is not often observed in sand aquifers since they are more homogeneous than most other aquifers. However, it can still happen when heterogeneity and preferential flow paths are present. As the pumice sand aquifer material investigated in this study was not very uniform, velocity enhancement could occur in certain circumstances.

(c) Temporal and spatial change of removal rates

Due to the limited data available, we used a constant removal rate in the model simulation and were unable to consider change in removal rates with time and distance. It is known that the efficiencies of filtration tend to decrease with time and distance due to deposits of suspended solids and filtered material causing clogging near the input source. Consequently, a filter layer develops, which further reduces the diameter of pores available for microbial movement. It is also known that removal occurs most significantly in the first few metres near the contaminant source and tends to decline with distance (Schijven & Hassanizadeh 2000). Hence, model simulations using a removal rate determined from the 1-m column system may have overestimated the removal of micro-organisms and thus underestimated the setback distance. Unfortunately, there is no information available to make such an adjustment. To obtain reliable removal rates, a field tracer experiment with a much longer distance and time is needed, which was beyond the budget of this study.

(d) Mixing of different source water

On the one hand, the above model-estimated distances may be insufficient in the occurrence of preferential flow paths, pore-size exclusion, and change in removal rates with time. On the other hand, the estimated distances may be too conservative, as it was assumed that the near-shore bathing-water is all from groundwater. In reality, the quality of bathing water is largely determined by the quality of lake water, which is recharged by not only the groundwater, but also from surface run-off and rainfall etc. Mixing of different source waters would significantly change the microbial concentrations in

bathing water. However, modelling the quality of lake water was beyond the scope of this study.

6.4. Conclusions and implications

Our experimental results suggest that the faecal coliforms, *E. coli*, and F-RNA phages were sorbed in the pumice sand aquifer material investigated. Compared to the die-off rates for the sorbed microbes, the die-off rates for the free microbes in the groundwater alone were much lower and contributed little to the total removal. After travelling through a 1-m pumice sand column, the bacteria had a 4-log reduction and the phages a 3-log reduction. The results of our experiments suggest that the removal of the bacteria was predominately by filtration (87-88%) followed by die-off (12-13%), while removal of the phages was almost equally contributed from both die-off (45%) and filtration (55%). We assumed that filtration also encompassed irreversible sorption.

Model-derived results, based on using the worst-case values, suggest that the minimum setback distance to meet the RWQG of < 126 *E. coli*/100 m is 16 m. This distance allows a 5-log reduction in bacterial concentrations. However, model-estimated viral concentration in the groundwater 16 m downstream is 312,000 times above the DWSNZ. If using this criterion, warning should be given for the consequence of any accidental ingestion of lake-water, since as little as one organism could cause infection for some viruses. If the DWSNZ are used, the minimum setback distance is 48 m. This distance allows a 10-log reduction in viral concentrations.

The above results were consistent with the results observed in a few field studies reported in the literature under similar conditions. This suggests that input values for the model parameters, particularly the removal rates, were close to reality. However, the above distances may not be sufficient if preferential flow paths, pore-size exclusion effects in microbial transport, or changes in removal rates with time/distance occur. On the other hand, the above estimated distances may be too conservative as it has been assumed that the near-shore bathing-water is all from groundwater.

As the worst-case values were used in the model simulations, these distances may be applicable for other lakeshores in pumice sand aquifers with groundwater velocities less than 7 m/day. The setback distance of 48 m may be applicable for a lake that is used for drinking water supply. Pumice sand aquifers are a common aquifer type in the Bay of Plenty and Waikato regions. The above model-estimated distances are greater than the setback distances defined by Environment B.O.P and Environment Waikato (Table 6.1). One exception is that Environment Waikato uses a-30 m distance for surface water bodies, same as drinking water bores. The 30-m distance may be sufficient for preventing bacterial contamination but may not be sufficient for preventing viral contamination.

Although setback distances are site-specific, the methods and many model parameter values are transferable. However, experimental work is needed to determine the removal rate of a selected microbial indicator in a particular groundwater system. As the removal rate is a very sensitive parameter in model simulations, adequate determination of removal rates of the microbial indicator is crucial in delineation of setback distances. Unfortunately, little information is available in the literature on removal rates of micro-organisms. The most available information in the literature are die-off rates in groundwater measured in the laboratory without involving aquifer material. These die-off rates are generally much lower than their relevant removal rates. Consequently, the determined setback distances based on die-off rates of free microbes would be unnecessarily large. Removal of microorganisms is not only by die-off but also by filtration and sedimentation, which are important processes, particularly for bacteria.

Acknowledgements

We thank Mr. David Ray of the National Institute of Water & Atmospheric Research Ltd. for his collaboration in the project and Mr. Graham Timpany for his assistance in the field sampling. This study was a sub-contract to the National Institute of Water & Atmospheric Research Ltd. and funded by the Rotorua District Council.

6.5. Additional study

Contribution of diffusion, interception and settling to filtration

In the publication, we concluded that for the column experiments with no microbial growth, clogging was not due to microbes, but rather due to large colloids in the septic tank effluent. For the colloidal particles with diameters greater than 8% of the media grain size, straining (a removal mechanism for large particles) could be significant (McDowell-Boyer et al., 1986). Consequently it could cause clogging. However, we did not characterise these large colloidal particles, although there were some evidences of their existence in the effluent introduced.

Straining of the microbes through the column was unlikely, as the size of the microbial indicators were 0.16% and 0.003% of the sand grain size for faecal bacteria and F-RNA phages, respectively. According to McDowell-Boyer et al. (1986), bacteria and viruses are unlikely to be filtered by straining in sand and gravel aquifers, except when they are attached to other much larger particles. This conclusion is also supported by the fact that the calculated surface coverage of the microbes in the column is negligible compared to the sand surface area. In this section, we will further investigate this by analysing the individual contributions to microbial filtration of the mechanisms of diffusion, interception and settling. This analysis will be based upon the contributions of the three filtration mechanisms to the single collector efficiency, η (included in Eq. 6.2).

Harvey and Garabedian (1991) define η as the rate at which colloidal particles strike a single porous media grain divided by the rate at which the particles move toward the grain. η is a function of the physical properties of both the porous media and the colloid particles. The total collector efficiency η is the sum of collector efficiencies due to diffusion, interception and settling (sedimentation), as expressed below:

$$\eta = \eta_D + \eta_I + \eta_G \qquad (6.14)$$

$$\text{in which } \eta_D = 0.9\left[\frac{k_B T}{\mu d_p dv}\right]^{2/3} \quad \eta_I = 1.5\left[\frac{d_p}{d}\right]^2 \quad \eta_G = \frac{(\rho_p - \rho) g d_p^2}{18\mu v} \tag{6.15}$$

where

η_D = collection due to Brownian diffusion (dimensionless),

η_I = collection due to interception (dimensionless),

η_G = collection due to settling (dimensionless),

k_B = 1.38x10^{-23} (kg(m/s)^2/K) is the Boltzmann constant,

T = absolute temperature (K),

μ = water viscosity (kg/m/s),

d_p = colloidal particle diameter (m),

d = average diameter of the porous media grain (m),

v = pore-water velocity (m/s),

ρ_p = colloidal density (kg/m^3),

ρ = water density (kg/m^3),

g = gravitational constant (m/s^2).

Eq. 6.14 suggests that filtration is not related to hydrodynamic dispersion (there is no hydrodynamic dispersion term in the above equations).

The room temperature for the column experiments was about 20 °C, hence T =20+273 = 293 K and μ =1.01x10^{-3} kg/m/s. F-RNA phages have a mean diameter of d_p=0.0255 μm (2.55 x10^{-8} m). Faecal bacteria have the shape of rods with a mean length of 3.3 μm and a mean diameter of 0.65 μm. As the colloid-filtration model assumes both colloids and collector particles are spherical, let us model the bacteria using a sphere of equivalent volume, so the diameter of an equivalent sphere (d_p) would be 1.28 μm. The pumice sand used has an average grain size of d = 0.80 mm (8.0 x 10^{-4} m). The pore-water velocity through the column is v = 1.55x10^{-5} m/s (1.34 m/day) for the Continuous Source Experiment. The elevation of our laboratory is approximately sea level, and at sea level g = 9.806 m/s^2. We assume F-RNA phages have the same density as water ρ_p = ρ=1.000 kg/l (1000 kg/m^3). Wan et al. (1995) investigated 25 subsurface bacterial strains, and

found the average buoyant density of bacteria is 1.088 kg/l (1090 kg/m^3). Using these known parameter values, the calculated values for η_D, η_I and η_G are shown in Table 6.7.

The above results suggest that diffusion is the dominant collection mechanism for F-RNA phages; while for faecal bacteria, settling (sedimentation) dominates and diffusion is of lesser importance. Filtration by interception is negligible for both faecal bacteria and F-RNA phages. This supports the results of negligible surface cover compared with the sand surface area as presented in the publication. Harvey and Garabedian (1991) also comment that as the size of the bacteria is much smaller than the aquifer medium grain size, the contribution of physical interception is expected to be insignificant.

Table 6.7. Results of single collector efficiency, η, describing filtration of microbes in the pumice sand column for the Continuous-Source Experiment

	F-RNA phages	Faecal bacteria
η_g	0.00E+00	5.01E-03
η_I	1.52E-09	3.83E-06
η_D	4.89E-02	3.59E-03
η	4.89E-02	8.60E-03
η_G/η	0.00	0.58
η_I/η	0.00	0.00
η_D/η	1.00	0.42

Chapter 7

Discussion

7.1. Introduction

In the previous chapters, we have discussed some important processes and mechanisms of contaminant transport, such as the scale-dependence of dispersion (Chapter 2), interaction of sorption and degradation (Chapter 3), chemical and physical nonequilibrium transport (Chapters 4 and 5), the effect of pore-water velocity on chemical nonequilibrium transport (Chapter 4), sorption/desorption of heavy metals (Chapter 4), non-linear sorption (Chapter 4), mobility and degradation of pesticides (Chapters 3 and 5), as well as die-off and filtration of microbes (Chapter 6). A few approaches to modelling these processes have been presented; for example, a scale-dependent dispersion model (Chapter 2), a method of temporal moments (Chapter 3), and two-region/site models (Chapters 4 and 5) were applied to analyse data.

In this chapter, we will discuss the above topics further and provide linkage between the chapters. We will also extend our discussions to some other important issues in contaminant transport that are relevant to the previous chapters. In addition, we will provide a few applications of the study, raise questions for further study, identify problems and gaps in current research, and offer some ideas for future research.

The important contaminant transport processes and mechanisms as well as modelling issues are discussed in the following sections.

7.2. Advection and velocity related transport issues

Advection is described mathematically by the term $v\frac{\partial C}{\partial x}$ (Eqs. 2.1, 3.1, 4.1, 6.1). Advection involves chemical/microbial transport due to the bulk movement of the groundwater and is the primary mechanism responsible for contaminant migration in aquifers. Under advective flow, a dissolved contaminant travels at the same velocity as the average groundwater. Advection plays a crucial role in contaminant transport through

preferential flow paths, transport of colloids (such as natural organic matter, macromolecule, and microbes) and colloid-facilitated transport of relatively immobile contaminants (e.g. heavy metals, some pesticides and hydrocarbons, and some other organic contaminants).

7.2.1. Preferential flow

Contaminants (both solutes and colloids) travel more rapidly through preferential flow (through macropores and fractures) than through uniform flow. There are two major reasons for this: (a) migration occurs along pathways with relatively high hydraulic conductivity, and, therefore, relatively high groundwater velocity (b) much of the sorptive capacity of the medium is bypassed. In the worst situation, the measured transport through preferential flow paths can be visualised as piston flow.

Under saturated conditions, preferential transport becomes more pronounced at high flow velocities. Laboratory column studies by van Genuchten et al. (1974), Schwarzenbach and Westall (1981) indicate that departures from uniform transport become significant for velocities $\geq$ 1 m/day. In field conditions, groundwater flow velocities are >1 m/day in coarse grain aquifer media (e.g. coarse sand, alluvial gravel, fractured rocks), and < 1 m/day in fine grain media (e.g. sand and silt, and consolidated media). Therefore contaminant transport through coarse aquifer media is often under the influence of preferential flow, and in some cases (e.g. fractured media) it is the dominating process in contaminant migration.

We have previously investigated preferential flow paths at the Burnham experimental site using tracer experiments, a resin bag method, and borehole dilution tests (Pang et al. 1998). As the majority of the work presented in this thesis is based on laboratory studies, preferential flow is not our focus in this study.

7.2.2. Mean and maximum groundwater velocity

As demonstrated in our field studies (Sinton et al., 1997; Pang et al., 1998; Pang and Close 1999c; Sinton et al., 2000), colloids can travel faster than the mean pore-water velocity provided that there are large enough interconnected pores. Therefore, transport of colloids could provide information on the possible maximum contaminant velocities. In most of the current literature, groundwater velocities (i.e. pore-water velocities) are determined from nonreactive solute tracers (e.g. ^3H_2O, Br, and Cl). As solutes travel through all interconnected pores within aquifer media, the groundwater velocities determined from nonreactive solute tracers represent the average values. In contrast, colloids are excluded from small pores due to their larger sizes and travel through interconnected large pores (i.e. size exclusion). Thus, the groundwater velocities determined from the colloids will be larger than the average velocities determined from the nonreactive solute tracers and often close to the maximum groundwater velocity. The extent of the difference in velocities will depend on the size of the colloids, as well as the pore size distribution of the porous medium. For risk analysis and design of monitoring programs, a conservative approach would be to consider the maximum groundwater velocities so that "worst case" contamination events, with regard to extent of contaminant transport, can be better predicted and managed.

As colloidal transport is predominately determined by advection, colloids may be used in field experiments to quantify maximum groundwater velocities, as shown in a study by McKay and Cherry (1993). The transport velocity of microbes can be a few (e.g. Bales et al. 1989; Artinger et al. 2002) or even several orders of magnitude (McKay and Cherry 1993) greater than nonreactive tracers. A comprehensive review of the use of microbes as groundwater tracers is given by Keswick et al. (1982). Colloidal particles have much lower diffusion coefficients than molecular solutes (McKay et al, 2000). Hence, the difference in velocity between a colloidal tracer and a nonreactive solute tracer is not only due to size exclusion (as noted previously) but could also be due to diffusion of the dissolved solutes into the matrix porosity.

According to Puls et al. (1991), particles with diameters of 0.1-2.0 μm may constitute the most mobile size fraction in porous media and particles with diameters greater than 1 μm may actually move faster than the average groundwater flow velocities in porous media due to size exclusion. Therefore, we could use non-sorbing and non-degradable colloidal tracers (such as spores, beads, micro-spheres, and fluorescent dyed silica colloids) with size of 1-2 μm to characterise the maximum groundwater flow velocity and trace preferential flow paths in the field experiments. For example, Pang et al. (1998) used *B. subtilis* spores (size 0.8 μm × 1.5-1.8 μm) in a tracer experiment at the Burnham alluvial gravel aquifer. They found the groundwater velocities determined from the spores could be up to 1.33 times faster than those estimated from Cl (or rhodamine WT).

7.2.3. Velocity enhancement in size/anion exclusion

The phenomenon discussed above in Section 7.2.2, that the mean velocity of colloidal transport could be greater than the mean pore water velocity, is referred to as 'velocity enhancement'. The most likely causes for velocity enhancement are size exclusion and also possibly anion exclusion. We have defined size exclusion previously. Anion exclusion may occur when contaminants and media matrixes are both negatively charged, which is often the case. Size exclusion is normally related to colloids and colloid-facilitated transport while anion exclusion can occur with both colloids and solutes. However, compared to size exclusion, few studies have reported in the literature on experimentally observed anion exclusion. Besides, the magnitude of anion exclusion effect is expected to be much smaller than size exclusion. Velocity enhancement in colloidal transport due to size exclusion is more likely to occur in large pore aquifers and heterogeneous media, such as alluvial gravel and fractured rocks. Velocity enhancement has not been shown for the transport of microbes though the pumice sand column (Chapter 6) but has been shown in our field studies with alluvial gravel (Sinton et al., 1997; Pang et al., 1998; Pang and Close 1999c; Sinton et al., 2000).

In both exclusion processes, some colloids/anions are excluded from a part of the pore volume. Therefore the pore volume for colloidal/anionic transport is smaller than the pore volume determined from a nonreactive tracer. For a unit volume of aquifer material, this would lead to a lower porosity for colloidal/anionic transport than for the nonreactive tracer. For size exclusion, as colloids travel through a narrower range of large pore sizes, the dispersivity for describing colloid transport is much smaller than for solute transport. This is reflected in the much sharper and narrower BTCs of colloids than those of nonreactive solute tracers. This is illustrated in Fig. 7.1 and is also clearly shown in our previous field studies in an alluvial gravel aquifer (Pang et al., 1998 & 1999a; Sinton et al., 2000). The above discussions suggest that different dispersivity and effective porosity from those of nonreactive solutes should be used for modelling colloidal transport.

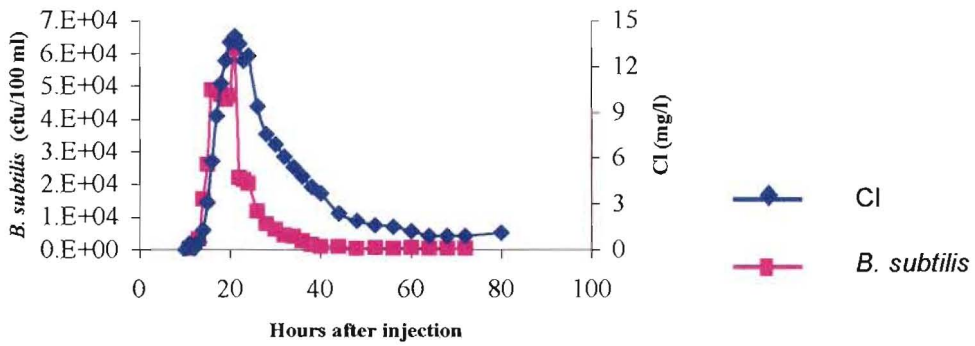

Fig. 7.1 Comparison of BTCs of *B. subtilis* and Cl in well 14 in the May 1995 Experiment carried out at the Burnham Site (Pang et al. 1998).

For velocity enhancement, the ratio of mean pore-water velocity to mean contaminant transport velocity is less than one. This ratio of water to contaminant velocity has been quantified using a 'retardation factor', R, i.e. R = pore-water velocity /contaminant transport velocity (Goltz and Robert, 1987). We would suggest that for velocity enhancement, R is better to be called 'velocity ratio' as the contaminant is not retarded. When a contaminant is retarded, R is defined as $R = 1 + \phi K_d / \theta$ for linear sorption (e.g. Eq. 4.9) and $R = 1 + \phi K n C^{n-1} / \theta$ for non-linear sorption (Eq. 4.21). However, when a contaminant is not retarded, these definitions are meaningless, as neither K_d nor K values can be negative.

Although having said this, if a model (e.g. CXTFIT) requires the input of pore-water velocity and does not require the input of K_d, the model-derived R-value for a contaminant is actually the velocity ratio. If $R<1$, it implies the contaminant moves faster than the conservative tracer, i.e. velocity enhancement. Others also report that the apparent R-values can be less than one (van Genuchten 1981; Bales et al., 1991; Artinger et al., 2002).

We could argue that the definition of $R = 1 + \phi K_d / \theta$ might be interpreted as $R = \theta/\theta + \phi K_d / \theta$ for solutes as the solutes sample the entire pore volume, but $R = \theta_{colloid} / \theta + \phi K_d / \theta$ for colloids as colloids go through only a fraction of the pore volume. As indicated above, porosity of the aquifer media for colloidal transport is smaller than that for solutes, thus $\theta_{colloids}/\theta$ is always <1. Since the colloids are not in the excluded volume, they are not sorbed to aquifer material. Hence, K_d =0 and $R = \theta_{colloids}/\theta$ <1. For velocity enhancement, R would actually measure the ratio of pore space sampled by the colloids ($\theta_{colloids}$) to total pore space (or pore space sampled by a solute) (θ), and the value of $(1-R) = (\theta-\theta_{colloids})/\theta = \theta_{ex}/\theta$ represents the fraction of pores from which colloids were excluded. For example, an R-value of 0.75 suggests that, on average, the colloids are excluded from about 25% of the total pore space.

The above hypothesis is similar to one presented by van Genuchten (1981). As indicated by van Genuchten (1981), in the case of anion exclusion $(1-R)$ can be viewed as the relative anion exclusion volume. That is, $1-R = \theta_{ex}/\theta$, where θ_{ex}/θ represents the relative anion exclusion volume. As $\theta = \theta_{excluded} + \theta_{passed}$, from $1-R=\theta_{ex}/\theta$ we get $R = 1-\theta_{ex}/\theta = (\theta-\theta_{ex})/\theta = \theta_{passed}/\theta$. This is analogous to our interpretation of $R = \theta_{colloids}/\theta$ for size exclusion. Note that for anion exclusion, there is also no sorption (i.e. K_d =0).

As $R = \theta_{colloids}/\theta$ for velocity enhancement, we can estimate the porosity of the medium that is accessible by the colloids from $\theta_{colloids} = R\theta$. It might be possible to determine $\theta_{colloids}$ independently using some empirical relationships (e.g. based upon the medium particle size distribution and colloidal size etc.). This would be an interesting and novel topic. From the

pore-size exclusion concept, we would expect that R would decrease with increasing heterogeneity of the aquifer media (because of a wider particle size distribution) and colloidal size. Hence the degree of velocity enhancement increases.

Summarising 32 data sets of $R<1$ obtained from our previous field experiments with different microbes and flow velocities in heterogeneous alluvial gravel (D_{50}=13-20 mm), the mean $\theta_{microbes}$ value is 0.15 (0.03-0.19) and mean R value is 0.80 (0.49-0.97). These values are lower than the mean $\theta_{microbes}$ = 0.33 (0.27-0.35) and mean R =0.95 (0.83-0.99) obtained from 62 data sets of $R<1$ for the uniform pea gravel (D_{50}=6 mm) in the 8-m long column using different microbes. The following microbes were used in both field and long column experiments: *E. coli* (size 1.5 × < 6 μm), *B. subtilis* spores (0.8 × 1.5-1.8 μm), F-RNA phages and MS2 (0.026 μm). Yeast (6 × 8.5 μm) was also used in the column experiments. The smaller variations of $\theta_{microbes}$ and R values for the pea gravel indicates that $\theta_{microbes}$ and R are comparatively consistent in homogenous media and does not change much with flow rate and species.

As colloids are larger than most solutes and electrically charged, they can be subject to both size- and anion-exclusion. It is expected that for large particle colloids (e.g. spores, bacteria), size-exclusion is more important, while for small particle colloids (e.g. viruses), both processes could be important. When size- and anion-exclusion occur concurrently, they are difficult to model separately.

To my knowledge, no study has been reported in the literature regarding the impact of transport distance on velocity enhancement. It is expected that with increasing transport distance, the degree of heterogeneity increases and, hence, velocity enhancement increases (i.e. R decreases). This is evident in our Burnham field data for individual microbial species as shown in Fig. 7.2. This inverse R-X relationship is in contrast with the positively correlated R-X relationship when $R>1$ (sorption without velocity enhancement). For transport of sorbing solutes, it is found that the retardation factor, R, increases with time and plume displacement distance (Roberts et al., 1986; Burr et al., 1994).

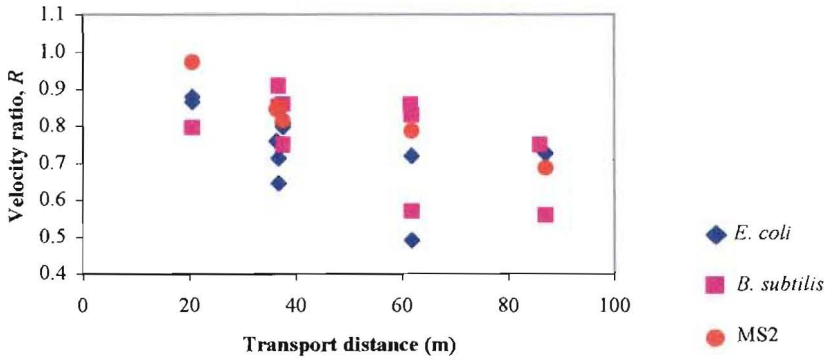

Fig. 7.2. Relationship between velocity ratio and transport distance for velocity enhancement observed in microbial transport through the alluvial gravel aquifer at the Burnham Experimental Site (using original data of Pang et al., 1998 and Sinton et al., 2000).

Another gap in the current literature is that the impact of pore-water velocity on velocity enhancement has not been reported. When examining the effect of pore-water velocity on velocity enhancement, the transport distance should be fixed. From *E. coli* data obtained from an 8-m long pea gravel column (Sinton et al., 2002), we could see that the velocity ratio, R, tends to increase with increasing pore-water velocity at a given distance as shown in Fig. 7.3. This is in contrast to the commonly observed inverse R-v relationship when $R>1$, which was observed in Chapter 4. From the above relationships, there seems to be a relationship such as the one illustrated in Fig. 7.4. When R>1, contaminant is sorbed. Then sorption decreases with increasing pore-water velocity and R value decreases toward one. This is because at high V, non-equilibrium processes become important and less residence time is available for solutes to access the sorption sites. In contrast, when $R<1$, velocity enhancement occurs for the contaminant transport and with increasing pore-water velocity, the degree of velocity enhancement reduces and the value of R approaches unity. This behaviour may be explained by the relation between mobile water fraction and velocity. From 53 BTCs obtained from field experiments, Pang and Close (1999a) observed that with increasing pore-water velocity, the fraction of mobile water increases. Thus, the mean groundwater velocity measured using a solute increases, as the impact of diffusion into

immobile water regions becomes less. Hence, the difference between colloidal velocity and mean groundwater velocity is reduced, bringing the R-values closer to one.

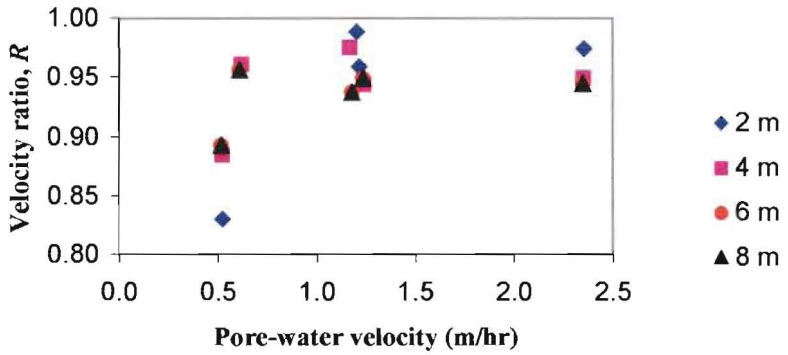

Fig. 7.3. Relationship between velocity ratio and pore-water velocity for velocity enhancement observed in microbial transport through an 8 m long pea gravel column (data from Sinton et al., 2002).

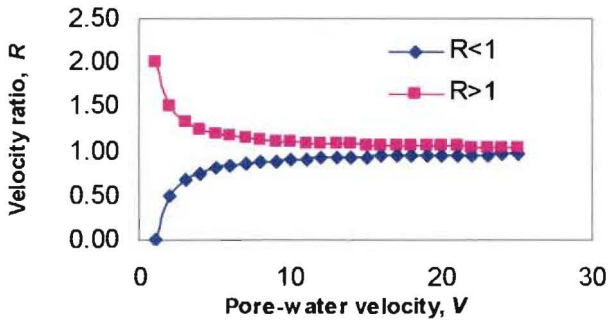

Fig. 7.4. Conceptual relationship between pore-water velocity (v) and velocity ratio (R).

7.2.4. Colloid-facilitated transport

Transport of a sorbing contaminant could be dramatically enhanced by colloids. Colloids are particles with diameters less than 10 μm (Stumm and Morgan, 1981). When attached to colloidal particles, the behaviour of the contaminant will be influenced by transport of the colloids as its sorption coefficient is not only a function of the aquifer material but also the

colloids. Sometimes the contaminant could travel with the colloids at a velocity greater than the average groundwater velocity (Pang and Close, 1999c). It is also possible to simultaneously have velocity enhancement due to exclusion of colloids attached along with retardation due to sorption of unattached contaminants onto aquifer material, so that overall, R would be greater than 1. An example of this is shown in the study of Pang and Close (1999c) for bacterial-facilitated Cd transport: although Cd was attached to *B. subtilis* and travelled with the bacteria much faster than it would travel as an unattached molecule, some Cd was still sorbed on aquifer media.

Colloid-facilitated transport may have important implications in the design of monitoring programs, risk analysis, and operation of remediation scheme. It may be more important in some instances to know the time of arrival of the first 0.1 or 1 percent of the contaminant at monitoring or receptor wells, rather than knowing when the centre of mass arrives. However, monitoring programs and model predictions generally do not consider facilitated transport.

In a field study, Pang and Close (1999c) found that the relative importance of colloid-facilitated transport was higher closer to the source and main flow-line and decreased with increasing transport distance and offset from the main flow-line. When close to the contaminant source, the majority of the contaminant was transported with the colloids, while further down gradient the fraction of contaminant that was affected by colloid-facilitated transport reduced considerably and could be ignored.

When colloid-facilitated transport is involved, two or more peaks often appear in the BTC of the sorbing, relatively immobile contaminant, as shown in Fig. 7.5. The first peak appears to be associated with the colloids and the second peak is believed to represent non-facilitated transport of the dissolved contaminant. Sometimes the fraction of contaminant affected by colloid-facilitated transport is so dominant that the second peak of much lower concentration may be masked. Other times, the fraction of contaminant affected by colloid-

facilitated transport is so small (even though concentrations may be high) that we could misjudge the first peak as analytic error or cross contamination of the samples.

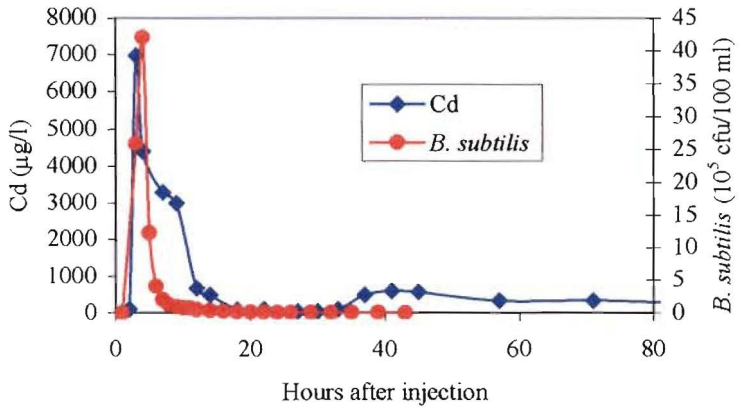

Fig. 7.5 Transport of Cd under the influence of *B. subtilis* in well 2 of the Burnham Experimental Site, 20 m down gradient of the injection well. (from Pang and Close, 1999c)

Previously, we have investigated bacteria-facilitated Cd transport through alluvial gravel at a field scale (Pang and Close, 1999c). In the natural environment, there are many types of colloids. Organic colloids include bio-colloids (such as bacteria, spores, fungi, algae, viruses), macromolecules (such as high molecular weight polymers, humic substances, pulp fibers, proteins), and nonaqueous-phase liquids (such as oil droplets or detergent micelles). Inorganic colloids include clays, metal oxides, and inorganic precipitates in the sub-micrometer size range. It should be noted that viruses are larger than dissolved contaminants but are at the lower end of the colloidal size distribution (Sim and Chrysikopoulos 1998). Hence, they can behave like either solutes and/or colloids. Natural organic matter, if abundant in the solid phase, would increase sorption of the contaminants onto the aquifer material; but if abundant in the liquid phase as colloids, would facilitate transport of the contaminants.

As facilitated transport is a phenomenon that has important effects on groundwater contaminant transport, a future survey of colloids and natural organic matter in groundwater throughout New Zealand is recommended.

7.3. Dispersion

Dispersion is an important attenuation mechanism that results in the dilution of a contaminant. In the 1-D constant dispersion models, dispersion is expressed by the partial derivative $D\frac{\partial^2 C}{\partial X^2}$ (Eqs. 3.1, 4.1, 6.1). In the scale-dependent dispersion model, dispersion is described by $\frac{\partial}{\partial X}\left(\varepsilon X V \frac{\partial C}{\partial X}\right)$ as shown in Eq. 2.1. In the following sections, we will discuss a few important issues related to dispersion.

7.3.1. Scale-dependent dispersion and modelling approach

As indicated in Chapter 2, in the current literature it is generally held true that the reason dispersivity increases with increasing distance, ultimately approaching an asymptotic value, is because aquifer heterogeneity increases with increasing distance. Therefore, it is commonly recommended that a medium-dependent constant dispersivity be used for large-scale problems. Gelhar and Axness (1983) provided the following theoretical equation for calculating the asymptotic longitudinal dispersivity:

$$\alpha_l = \sigma_Y^2 L / \gamma^2$$

where α_l is the asymptotic longitudinal dispersivity (L), σ_Y is the variance of the log-transformed hydraulic conductivity, L is the correlation length in the mean direction of flow (L), and γ is a flow factor. Dagan (1982) also represented a similar theoretical equation except that Dagan considered γ being one. An example of predicting the asymptotic longitudinal dispersivity using the above theoretical equation could be found in Domenico and Schwartz (1998). A limitation is that characterisation of the statistical properties of a medium requires considerable hydraulic conductivity data, which practically are not available.

Very high values of longitudinal dispersivity (up to 10,000 m) have been reported for large-scale field problems (up to 100,000 m), in a review by Gelhar et al. (1992). In Chapter 2, we have challenged the above theory that scale-dependence of dispersion could occur only in heterogeneous media and questioned the existence of an asymptotic value. A theoretical explanation is given in the additional study of Chapter 2 to explain that scale-dependent dispersion could be observed in homogenous media and that dispersivity could increase with distance boundlessly, based upon the theory of Hunt (1999).

The theory of Hunt (1999) is perhaps the only one that could be found in the current literature for interpreting how scale-dependent dispersion could possibly occur in homogenous media. Although scale-dependent dispersion in homogenous media has been reported by other researchers (e.g., Zhang et al., 1994), it is typically explained as "homogenous media are not truly homogenous". The behaviour of the data presented in Chapter 2 could be the result of a combination of things such as the significance of scale dependency, the sensitivity/resolution of the observations, and the scale at which the material can be considered homogeneous. The pea gravel used in the column was angular. Tests in clear containers showed that the gravel packed more tightly than rounded stones, with many narrow gaps between the particles. Therefore, the pea gravel used in the column may not be truly homogenous. Perhaps a better way to test scale-dependent dispersion in homogenous media is to use glass beads with the same diameter.

It should be noted that scale-dependent dispersion is a phenomenon that has typically been observed in saturated zone transport and may not be applicable in the unsaturated zone. The dispersivity generally increases with distance for transport in groundwater, especially when layers are parallel to the flow direction. For vertical transport in the vadose zone, where (variably saturated) flow is often perpendicular to (horizontal) layers, dispersion may not always be scale dependent (Dr. van Genuchten, personal communication, 2001).

Although a scale-dependent dispersion model (SDM) may be superior to a constant dispersion model (CDM) for predicting contaminant concentrations in many cases, CDM may be equally good for certain cases, such as those shown in Chapter 2, where transport is over a fixed distance. The CDM simulations do not predict observed concentrations well when a single dispersivity is used over different transport distances, such as shown in the study of Sinton et al. (2000).

CDM provides a good estimate for a single location. However, when it is used for predicting contaminant concentrations at various locations, we need to run the CDM for each individual location using a different dispersivity for each location. This approach is applied in Chapter 6 in a model prediction of microbial concentrations down gradient of a septic tank. AT123D, which is a three-dimensional constant dispersion model, is used for the prediction. However, the constant value of dispersivity for each point was calculated from $\alpha_x = \varepsilon X$, where ε is the constant ratio of dispersivity to distance derived from column experiments and X is the distance downstream.

The SDM developed in Chapter 2 could be applied to sorbing and degrading solutes, though the application presented in Chapter 2 is limited to a conservative tracer, tritiated water. After publishing this paper, we have used the solutions in analysing Br (conservative tracer) and rhodamine WT (non-conservative tracer) data obtained from a full-header-tank injection experiment conducted in our homogenous artificial aquifer filled with coarse sand. The artificial aquifer has a dimension of 9.54 m x 4.7 m x 2.6 m, and the detailed information is given by Close et al. (2002). The preliminary results suggest that (a) a similar pattern to that reported in Chapter 2 is found: at shorter distances (1.5, 3.5 and 5.5 m) ε value decreases with distance and at larger distances (7.5 and 9.5 m), it becomes relatively constant; and (b) results obtained from the SDM are similar to those obtained from CXTFIT for individual sampling locations. However, presentation of artificial aquifer data is not in the scope of this thesis.

A prediction for the field situation needs a 3-D model, but the SDM developed in this study is only a 1-D model. Hunt (1998) has developed a 3-D SDM but it does not consider sorption and degradation. Perhaps in the future, a 3-D scale-dependent dispersion model could be developed. Also the basic transport equation presented in Chapter 2 does not include degradation in the sorbed phase. We may wish to incorporate this in the updated solutions.

The SDM presented in Chapter 2 has caught the attention of some researchers. To my knowledge, our published data have been used in the forthcoming publications of Dr. Ninghu Su at Queensland University of Technology and Dr. Graham Sander at Griffith University, as well as Dr. Earl Bardsley at Waikato University. In their papers, they also compared their results, using different models, with ours.

7.3.2. 'Apparent dispersion' caused by the presence of 'immobile water zones'

As mentioned in Chapter 2 (Section 7.2.1), in an equilibrium model, dispersion is a combination of hydrodynamic dispersion and molecular diffusion. Hydrodynamic dispersion is a result of variations in velocity across pore openings, different pore size distributions and the tortuous nature of the pore channels. When there is a wide pore-size distribution, some water moves very fast and some moves much slower than the average groundwater velocity, resulting in high dispersion. Molecular diffusion is the tendency of molecules to migrate towards regions of low concentration as a result of the random Brownian motion of the molecules. In general, hydrodynamic dispersion increases with increasing flow velocity, but molecular diffusion is unaffected by velocity. Therefore, in a static system, diffusion is important. With increasing average flow velocity, hydrodynamic dispersion increases to the point that at high velocities, diffusion may be unimportant and could be ignored.

However, ignoring diffusion at high velocities is not always appropriate. If there are a large number of very small stagnant or dead-end pores in the porous medium, then solute molecules can slowly diffuse in and out of these pores, affecting transport and causing tailing

of the solute BTC even at higher velocities. This 'apparent dispersion' caused by solute diffusion into stagnant or dead-end pores is one basis for the mobile/immobile water models (i.e. two-region models), which model diffusive solute exchange between mobile and immobile water zones as a first-order process. This diffusion is described by two parameters: (1) β, the solute capacity ratio of the mobile (equilibrium) and immobile (nonequilibrium) regions, which for a nonsorbing solute represents the fraction of mobile water; and (2) ω, the first-order mass transfer coefficient, quantifying the rate of solute transport between the two regions.

Unlike molecular diffusion described in equilibrium models, which is unaffected by velocity, the 'apparent diffusion' described in two-region models (TRM) as caused by mass transfer between the two regions, and is affected by velocity. They are two different processes. It is found that both β and ω, which describe 'apparent diffusion', change with pore-water velocity (Brusseau et al., 1994; Pang and Close, 1999a). Two-region models will be discussed further in Section 7.4.2.

Although fundamentally not appropriate, an equilibrium model could use an unrealistically high dispersion value to incorporate the effect of the 'apparent diffusion' caused by the presence of immobile water zones in order to simulate tailing in some BTCs. As dispersion is the only explanation for the spreading of a BTC in equilibrium models, the D values estimated from equilibrium models are generally higher than those estimated from TRM. In TRM, in addition to the dispersion coefficient, spreading and tailing are also affected by β and ω. Goltz and Roberts (1986) indicated that D values estimated from BTC data using an equilibrium model can be 50% greater than the D values estimated using a TRM.

The asymmetry and spreading of a BTC can be measured by the Peclet number, as shown in Eq. 5.6, $P=vL/D$, i.e. the ratio of advection to dispersion. A low value of Peclet number indicates a high degree of spreading and asymmetry. In equilibrium models, non-equilibrium effects between mobile and immobile water are modelled approximately as an additional macroscopic dispersion process. Valocchi (1985) derived an expression for the effective

Peclet number, P_e, for the use in the equilibrium model in terms of two-region model parameters:

$$1/P_e = (1/P_m) + (1-\beta)^2/\omega$$

The above non-dimensional equation could be applied for both sorption and non-sorbing solutes. For a non-sorbingsolute, Parker and Valocchi (1986) expressed D of an equilibrium model that includes both dispersion and the effect of rate-limited sorption:

$$D = \varphi D_m + \frac{(1-\varphi)^2(\theta_m V_m)^2}{\alpha\theta}$$

where $\varphi = \theta_m/\theta$, the fraction of mobile water, and α is the first-order kinetic rate coefficient in the TRM. The subscript m refers to mobile water zone. It should be noted that the equation of Parker and Valocchi (1986) is actually a dimensional form of the equation of Valocchi (1985) for non-sorbing solutes.

7.3.3. Relationship with other parameters

Usually, dispersivity is regarded as a physical property of the porous medium and should be constant (Bouwer, 1978). However, this assumption is questionable. At very slow velocities, molecular diffusion can be important. Molecular diffusion is dependent on the physical and chemical properties of the solute molecule and the solvent itself, rather than on the physical properties of the porous medium. At high velocities, physical nonequilibrium often occurs, and hence, 'apparent diffusion' becomes significant as discussed in Section 7.3.2. This effect is incorporated in the dispersivity.

Brusseau (1993) observed that dispersivity is velocity dependent for solute transport in aggregated soils. Pang and Close (1999a) also found that dispersivity decreases with increasing pore-water velocity under nonequilibrium conditions, and, from 53 field BTC data obtained from the Burnham alluvial gravel aquifer, they found there is an empirical

relationship between the two: log α_x = 0.39-1.08 log$V$ with P=0.000 and r =0.61 (Pang and Close, 1998).

Solute size also has an influence on solute dispersivity. Brusseau (1993) commented that dissimilar size solutes might have different dispersivities. As discussed in Section 7.2.3, colloids tend to have smaller dispersivities than solutes. This could also be reflected in α_x/α_y and α_x/α_z ratios. From our unpublished field data obtained from the Burnham Experimental site, the α_x/α_y =14 ratio determined from bacterial tracers is slightly lower than that of solute tracers (α_x/α_y =16, see Pang and Close 1999a).

Dispersivity might be affected by reactive transport (such as sorption). Sorption may increase dispersivity in two ways: (a) because of the presence of nonequilibrium conditions, the effects of diffusion-limited sorption in immobile water zones show up in the form of a higher dispersivity, as discussed in the previous section; and (b) the solute ions have more inclination to be close to solid surface and, therefore, have more tortuous flow paths than conservative tracers which may stay away from particle surfaces and have a smoother pathway.

Klotz et al. (1980) found that dispersivity values increase with mean grain diameter of the aquifer material. This agrees with our observation. At the same transport distance (2 m) and similar pore-water velocities, dispersivity determined for the alluvial gravel column (particle size < 100 mm and 92% > 2 mm) at 20 m/day is 0.82 m (Pang and Close, 1999b) and that for the pea gravel column (particle size 5-7 mm) at 34 m/day is 0.02 m (Chapter 2). However, the much smaller dispersivity of the pea gravel compared to the alluvial gravel is probably related more to the fact that the pea gravel is more uniform.

The apparent relationship described above between dispersivity and other parameters (e.g. pore-water velocity) could be indicators of missing processes that should be included in the model.

7.4. Nonequilibrium transport

7.4.1. Rate-limited processes

In Chapters 4 and 5, we have investigated nonequilibrium transport of heavy metals and pesticides, respectively. Nonequilibrium transport refers to transport that is impacted by kinetic (i.e. rate-limited) physical and/or chemical processes due to different time-scales between processes. Physical nonequilibrium occurs when the time-scale for advection is faster than the time-scale for mass transfer between mobile and immobile regions (Goltz and Oxley, 1991). Chemical nonequilibrium occurs when the system hydraulic residence time is relatively shorter than its chemical reaction time (e.g. sorption, film diffusion, or intra-particle diffusion). Transport with a nonequilibrium component causes observed BTCs to exhibit early breakthrough and long tails, both of which cannot be adequately described by traditional local-equilibrium models.

In a natural groundwater system, equilibrium is often not reached for some transport processes due to complex and non-ideal natural processes. Heterogeneity in hydraulic properties (e.g. hydraulic conductivity and porosity, preferential flow, rate-limited diffusion) and chemical properties (e.g. organic carbon, clay content, ion exchange, hysteretic sorption etc) can contribute to the different time scales between processes.

As aquifer hydraulic properties are mostly heterogeneous in the field, physical nonequilibrium is often reflected in field data, for example as shown in the study of Pang and Close (1999a). Physical nonequilibrium is often the dominating factor for solute transport in field conditions. By analysing Borden aquifer experiments, Brusseau et al., (1991) indicated that solute transport was affected primarily by aquifer heterogeneity and that chemical nonequilibrium was of only of secondary significance. In contrast, physical nonequilibrium tends to be insignificant and often absent in uniformly packed laboratory columns (e.g. Chapter 4; Langner et al., 1998; Pang and Close, 1999b; Casey et al., 2000).

Chemical nonequilibrium could be reflected in both field and laboratory data. For a reactive contaminant, field data often contain both physical and chemical nonequilibrium components, and it is difficult to distinguish the individual contributions of each. However, the physical nonequilibrium component in the field can be determined using a nonreactive tracer. Similarly, a laboratory study using a homogeneously packed column allows study of chemical non-equilibrium processes alone.

7.4.2. Nonequilibrium transport models

Modelling nonequilibrium transport is a valuable tool for the design of remediation operations and monitoring programs. Under nonequilibrium conditions, contaminant concentrations during the release of a contaminant at a particular time will be higher than those under equilibrium conditions. If rate-limited processes are not considered, a remediation system may fail to achieve desired standards of groundwater treatment.

Some nonequilibrium models have been developed to consider processes for which equilibrium is reached quickly as well as rate-limited processes for which equilibrium is reached only slowly. These models hypothesise the existence of mobile and immobile water regions, or instantaneous and kinetic sorption sites. In two-region models, aquifer heterogeneity is idealised as two regions: one in which the velocity is zero, the other where velocity is the average pore velocity, with partitioning of solutes between the two liquid regions governed by first-order mass transfer. When a solute pulse passes through the medium, the bulk of the solute will go through the mobile water zone, and only a small portion of the solute will diffuse into the immobile water zone. After a while, the bulk of solute will have moved through the mobile water zone, and the solute in the immobile water zone slowly diffuses back to the mobile water zone, driven by the concentration gradient. This mass exchange between mobile and immobile water regions causes the commonly observed "tailing" phenomenon in concentration breakthrough curves. Therefore, the sharp front of a BTC can be described by solute transport through the mobile water, and the long tail by solute exchange with immobile water. Similarly, chemical nonequilibrium can be

explained by the two-site concept. Sorption on one type of site is assumed to be instantaneous while on other sites it is assumed to be slow. Desorption of solute from the slow sites back into the flowing water results in BTC tailing.

Based on the above discussion, we can see that in the two-region model there is an assumption that there is no kinetic sorption, and all sorption sites are instantaneous in both mobile and immobile water zones. This assumption is valid for solute transport with equilibrium sorption. In contrast, the two-site model assumes that there is no immobile water region, and solute transport is all through mobile water zone for both instantaneous sites and kinetic sites. This assumption may be reasonable for homogeneously packed columns with uniform hydraulic properties. Although the assumptions are different, both the two-region and two-site models, if expressed in dimensionless form (Eq. 5.3), are mathematically identical (Toride et al., 1995).

In the publications of Chapters 4 and 5, two-site models are used to simulate transport of reactive solutes. The additional study of Chapter 5 shows that when the physical non-equilibrium component is dominant in an aquifer system, two-region models could be used to simulate transport of reactive solutes and the results are very similar to those obtained from the two-site model. This approach is reasonable for analysing the data presented in Chapter 5. From Chapter 3 we could see that rate-limited sorption is generally not very significant for transport of rhodamine WT and pesticides through a pumice sand column, and some BTCs obtained in the field (Chapter 4) are similar to those of conservative tracers. Brusseau and Srivastava (1997) also demonstrated that rate-limited mass transfer processes had relatively small influence on the transport of the organic solutes in the Borden aquifer. Perhaps this could explain why a two-region model could well describe transport of organic solutes in the Borden aquifer, as demonstrated by Goltz and Roberts (1986). However, when the physical nonequilibrium component is not significant in an experimental system, such as shown in Chapter 4, the two-site model is conceptually the most appropriate tool for describing transport of reactive solutes.

Although equilibrium models could capture some degree of tailing by using a high apparent dispersion coefficient or Peclet number as described in Section 7.3.2, nonequilibrium models are considered to be more fundamentally correct for interpretation of asymmetry and tailing in BTCs. In nonequilibrium models, spreading and asymmetry of BTCs may be explained by processes other than dispersion. The parameters β and ω quantify the degree of nonequilibrium existing in the system, and with decreasing β and/or ω values the degree of nonequilibrium increases. The ω value is the ratio of hydrodynamic residence time to sorption reaction time (Brusseau et al., 1991) as shown in Eq. 4.5. From Eq. 4.5, we could see that with decreasing pore-water velocity, the value of ω increases, thus the degree of nonequilibrium reduces. This may explain why equilibrium models are often adequate for describing transport at slow velocities, e.g. transport of some pesticides as presented in Chapter 3.

It should be noted that due to simplifications of the two-region/site models, there are some limitations of these models. Although the assumptions upon which the models are based sound physically reasonable, the assumed conditions are, in fact, gross simplifications of reality. For example, in reality, there is a wide range of pore sizes rather than two zones. The 'mobile water zone' and 'immobile water zone' actually represent relatively permeable and less permeable zones, respectively, and solute transfer between the zones is not strictly a diffusive process. Groundwater velocity is a function of hydraulic gradient, and the 'mobile water' and 'immobile water' fractions are functions of the gradient and groundwater velocity. This is evidenced by the fact that the fraction of mobile water has been shown experimentally to change with groundwater velocity (Pang and Close, 1999a). The nonequilibrium parameters, ω and β, are hypothetical parameters and are difficult to measure experimentally. To some degree, these parameters are fitting parameters that cannot be explicitly measured. As a further development, dual-porosity model replaces the completely stagnant region with a less permeable pore system, in which water is still mobile but with different characteristic coefficient or flow mechanisms (Chen and Wagenet, 1992; Gerke and van Genuchten, 1993). In more recent work, probability distributions are used to

simultaneously consider heterogeneity in both hydraulic properties and the local solute physical/chemical reactions (Chen, 1994; Chen and Wagenet, 1995 & 1997).

7.4.3. Differentiating between physical and chemical nonequilibrium

As stated previously, conventional nonequilibrium models do not simultaneously consider both two-regions and two-sites in modelling transport of a reactive solute (two-region models exclude kinetic sorption and two-site models exclude the immobile water zone). Thus, these models do not distinguish the separate effects of physical and chemical nonequilibrium processes on transport of reactive solutes, as indicated in Chapter 5. However, contaminant transport in field conditions is likely to be affected by both components. We have suggested in Chapter 5 that to identify the individual components, more nonequilibrium parameters need to be considered in a model, and independent measurement/estimation of some nonequilibrium parameters is required.

More complex multifactor non-ideality models have been developed recently (Hu and Brusseau, 1996; Srivastava and Brusseau, 1996). These models incorporate simultaneously multiple non-ideality factors and account explicitly for both physical and chemical heterogeneity (e.g. spatially variable hydraulic conductivity and spatially variable rate-limited sorption). Hence it is possible to quantify the relative contributions of physical and chemical factors on reactive-solute transport. As more parameters are involved in these models, in order to reduce the uncertainty of model prediction, independent measurement/estimation of many parameter values using site-specific information is required. Using case studies, Brusseau (1998) reviewed the specific issue of using calibration for model evaluation and data analysis of reactive-solute transport.

7.5. Sorption/desorption

Often there is some confusion with the use of the terms sorption and adsorption. Technically, the two terms have different definitions. Sorption describes all reversible

associations of chemical with solids. Adsorption describes the condensation of chemical on a surface or pores by physical or chemical bonding forces. The use of the term "adsorption" suggests a known, specific surface interaction. As the nature of most interactions between contaminants and porous media is likely to be unknown, and may involve both absorption into organic material associated with the aquifer solids as well as adsorption, "sorption" is a better, more general, term to use.

7.5.1. Reversibility

When we assume equilibrium sorption (either linear or non-linear), we are assuming that the rates of sorption and desorption are fast (and assumed instantaneous) in comparison with other processes of interest, while kinetic or rate-limited sorption means that the sorption/desorption process is slow compared to other processes of interest. For both equilibrium and nonequilibrium processes, if there are no irreversible processes involved (e.g. degradation, die-off, filtration, precipitation etc.) in the system, the total mass recovered for a sorbing contaminant in the effluent of a column experiment should finally reach 100% if one waits long enough to get a complete BTC. Examples of reversible kinetic sorption/desorption can be found in Chapter 4. Although sorption/desorption of Cd and Pb was kinetic, as suggested from the results of flow interruptions, the total masses of Cd at the high- and intermediate-flows and of Pb at the intermediate flow were fully recovered.

For some organic contaminants, sorption/desorption is not fully reversible, and the amount sorbed is greater than the amount-desorbed. This process is called hysteretic sorption/desorption. It should be noted that although sorption hysteresis is "non-reversible" it is not necessarily irreversible. Irreversible means that there is some solute that once sorbed, never desorbs (that is, when $C = 0$, $S > 0$). Hysteretic sorption means that the amount sorbed may be different, depending on whether you are on the sorption or desorption leg of the isotherm (thus, for a single C, there are two or more S values). It is possible, though, to have a hysteretic sorption/desorption isotherm that is not irreversible (so that when C goes to 0, S also goes to 0).

Hysteretic sorption/desorption isotherms, combined with advection/dispersive transport, have been shown to simulate BTCs with long tails (van Genuchten et al., 1974; van Genuchten and Cleary, 1982). A transport model incorporating hysteretic sorption/desorption isotherms is expressed as (Hornsby and Davidson, 1973; van Genuchten et al., 1974; Wood and Davidson, 1975; and van Genuchten et al., 1977):

$$\frac{\partial C}{\partial t} = D\frac{\partial^2 C}{\partial x^2} - V\frac{\partial C}{\partial x} - \frac{\phi}{\theta}\frac{\partial S}{\partial t}$$

$$S = K_{ads} C^{n_{ads}} \qquad \frac{\partial C}{\partial t} > 0$$

$$S = K_{des} C^{n_{des}} \qquad \frac{\partial C}{\partial t} < 0$$

where $K_{des} = K_{ads} C_{\max}^{n_{ads} - n_{des}}$

Goltz (1986) developed a Crank-Nicolson finite difference approximating of the above non-linear equations. In the finite difference model of Goltz (1986), parameters of K_{ads}, n_{ads}, n_{des}, can be solved from the zeroth and first spatial moments. This approach is experimentally validated in the study of Goltz (1986).

It should be noted that kinetic sorption could be sometimes misjudged as irreversible sorption if not enough time is allowed to reach equilibrium. Constant pH, redox potential, concentration, and reaction rates may indicate when equilibrium is reached. If the retardation factor determined from a column experiment is the same as that determined from a batch test, we could say that the system has reached equilibrium, as a batch test is assumed to measure equilibrium sorption. If the retardation factor determined from a column experiment increases with decreasing flow velocity (such as shown in Chapter 4), the system has not reached equilibrium and is still under nonequilibrium conditions. Equilibrium is indicated when a decrease in flow velocity does not lead to a further increase in the retardation factor.

7.5.2. Linearity

A linear sorption isotherm is generally assumed to describe both equilibrium and nonequilibrium sorption (such as in the models used in this thesis), so that the retardation factor R is constant, independent of contaminant concentration. However, for many contaminants, sorption is non-linear at high concentrations. Therefore when using non-linear isotherm parameter values to calculate the retardation factor, the non-linear isotherm must first be linearized. Two linearization methods, described by van Genuchten (1981), are introduced in the additional study of Chapter 4.

How low the concentration range should be to assume linear sorption is dependent on the type of chemical and aquifer material. For example, in the study of Pang and Close (1999b), rhodamine WT sorption was linear for concentrations < 60 mg/l, but for Cd it was only linear for concentrations <1 mg/l. For clay and organic matter, isotherms are often linear for wide concentration ranges. As indicated in the additional study of chapter 4 for non-linear sorption, when the Freundlich exponent constant n <1, the retardation factor decreases with increasing concentrations; while when n > 1, the retardation factor increases with increasing concentrations.

For most studies reported in the literature, non-linear sorption isotherms are determined from batch tests. In the additional study of Chapter 4, we have presented an innovative method (Clothier et al., 1996) to determine a non-linear sorption isotherm from column data. I suggest testing this method in the future using a non-degradable contaminant. To do this, batch tests should be first conducted to obtain values of the non-linear equilibrium partition coefficient K and Freundlich exponent constant n. Three column experiments are then carried out using the lowest, mean, and highest concentrations as used in the batch tests, respectively. To avoid the influence of nonequilibrium transport, the three experiments must be performed under the same, low flow rate. As the degree of nonequilibrium transport is positively related to flow rate and inversely related to homogeneity, a low flow rate and a

homogenous fine-grain porous medium would be desirable. At true equilibrium conditions, the retardation factor, R, should be the same whether calculated from batch or column data. However, if the column system is influenced by nonequilibrium transport, the R-value of column data will be smaller than that of the batch data.

7.5.3. Sorbents (organic carbon, clay content, oxides, microbes)

It is often assumed that sorption by soils and aquifer media is due to organic matter with a well-defined relationship $K_d = K_{oc} \times OC$, in which K_{oc} is the organic carbon distribution coefficient and OC is the fraction of organic carbon content in the medium. However, from the study presented in Chapter 5, we found that K_d values for pesticides would be underestimated if only considering OC as the sole sorbent in a pumice sand aquifer. We believe that allophane clay in pumice sand aquifer material has also played an important role in pesticide sorption. The alluvial gravel used in this study (Chapter 4) contains only 0.04% of OC, and we expect that such a low level of OC would have little influence on contaminant sorption. Instead, the iron oxide coating on the gravel surface probably plays the most important role in contaminant sorption in the alluvial gravel investigated. The clay mineral content is also very low in the material, so it should also have little influence on contaminant sorption. Bacteria can also act as a sorbent for aqueous contaminants. On the other hand, if the bacteria are immobile, sorption of contaminants onto bacterial particles would enhance retardation (Matthess and Pekdegers, 1985; Malard et al., 1994).

The above discussions suggest that the overall sorption of a contaminant onto aquifer material is influenced by a combination of organic matter content, clay content, oxides, and even microbes. It may be possible in the future to develop an empirical relationship between sorption and organic matter, clay, oxides, and microbial content. Some individual relationships have been quantified. Hinton and Close (1998) have defined a Langmuir isotherm for Pb sorption onto iron oxides coating on the same alluvial gravel used in this study. A Langmuir isotherm is also defined for the sorption of Arsenic onto Fe_2O_3 colloids (Puls et al., 1991). A lot of work has been performed on the relationship between oxides or

organic matter and contaminant sorption. However, relatively few studies have been done on the relationship between clays and contaminant sorption, as it is more difficult to study.

7.6. Irreversible removal processes

A contaminant would not be permanently removed from groundwater through sorption/desorption unless an irreversible process is involved. We have discussed irreversible sorption in Section 7.5.1. Other irreversible processes include degradation for organic contaminants, die-off (or inactivation) for microbes, decay for radionuclides, filtration for colloids, and precipitation for heavy metals.

Degradation, die-off, and decay can usually modelled as first-order processes. Concentration reduction of colloids through filtration is also regarded as a first-order process (Matthess et al. 1988). However, when the sites available for deposition of the colloids are nearly filled, filtration may be described as a second-order process, with the filtration rate a function of both the concentration of the colloids and the deposition sites (personal communication, Dr. Joe Ryan, University of Colorado, 2000). For a process A + B $\Rightarrow$ C, zeroth, first, and second order kinetics with respect to A are expressed as: $d[A]/dt = -k$, $d[A]/dt = -k\,[A]$, and $d[A]/dt = -k\,[A]\,[B]$, respectively.

It is often reasonable to use a first-order total removal rate to encompass all possible first-order removal processes. This approach is used in Chapter 5 for modelling the reduction of pesticides through degradation, irreversible sorption, complexation and filtration for the pesticides sorbed into particles and colloids. It is also used in Chapter 6 for modelling reduction of microbes through die-off and filtration.

By assuming first-order removal, we are assuming concentration is reduced exponentially with time. For uniform flow through a column, where time and distance are linearly related, concentration is reduced exponentially with distance for first-order removal. For example, filtration of colloids is a first-order process so that, $C = C_0 \exp(-f X)$, in which f is the filter

factor (L^{-1}), X is the distance travelled (L), C_o is the initial concentration of a colloidal suspension, and C is the observed concentration at travel distance X (Iwasaki 1937). This equation has the same form as the die-off equation (Eq. 6.11) except that t is replaced with X. As described in the additional study of Chapter 6, filtration includes Brownian diffusion, interception, and sedimentation. Wan et al. (1995) comment that sedimentation of colloids is also a first-order process with respect to distance. In the study of Schijven (2001), removal rate coefficient in unit time (λ) is converted to removal rate coefficient in unit distance (f), i.e the filter factor, by divided by the pore-water velocity V, i.e. $f = \lambda/V$.

7.6.1. Degradation and die-off

Degradation rates for organic contaminants or die-off rates for microbes in the dissolved and sorbed phases are generally not equal. Most information available in the literature is related to degradation/die-off rates in the liquid phase, and much less information is available for the rates in the sorbed phase.

Faster degradation of organic contaminants in the liquid phase than in the solid phase has been found in some porous media with aged organic contaminants (Zhao and Voice, 2000; Alexander, 2000). This is believed that as the organic contaminants are "aged" in the soil and aquifer media, they become progressively less available for uptake by organisms, for exerting toxic effects, and for biodegradation. However, this is not always the case for organic contaminants that are not aged in porous media. An example of this is the pesticide degradation in pumice sand aquifer material discussed in Chapter 5. Degradation of organic contaminants is dependent on many factors, such as the availability of oxygen, nutrients, and carbon sources, and on the composition, size, and activity level of the microbial community. Variations in these factors in the liquid and solid phases would lead to variations in degradation rates in the two phases.

Degradation of organic contaminants could be due to either biological or/and chemical reactions. Most studies reported in the literature focus on biodegradation. However, for

aquifer media with low microbial activity (such as fractured rocks and alluvial gravel), biodegradation may not be significant. For example, Pang and Close (1999d) found that in alluvial gravel aquifer material, 88% of degradation of atrazine was chemical and only 12% was biological.

Similar to organic degradation, whether microbial die-off is greater in the liquid phase or in the solid phase varies with system conditions. Higher die-off rates of viruses in the liquid phase have been reported by Hurst et al. (1980), Reddy et al. (1981), Gerba (1984), Yates & Yates (1988), and Yates & Ouyang (1992). In contrast, higher die-off rates in the solid phase are found in the studies of Blanc & Nasser (1996), Schijven & Hassanizadeh (2000), and in our study in Chapter 6. From available data, the difference in viral die-off rates between the two phases is generally a few fold, while for bacteria it could be much greater (as shown in Chapter 6).

7.6.2. Filtration

In Eq. 6.1, colloid filtration is incorporated as a component of the irreversible attachment term into a transport model that considers advection, dispersion, reversible sorption, first-order die-off, and irreversible attachment. Two different forms of the reversible sorption term could be used in the transport model: a linear, instantaneous sorption/desorption term or a first-order kinetic sorption/desorption term (Harvey and Garabedian, 1991). In Chapter 6, we assumed linear equilibrium and only presented the first approach. The second approach has been used in many studies reported in the literature for modelling microbial transport (Bales et al., 1991; McCaulou et al., 1994; McCaulou et al., 1995; Morley et al., 1998, Chu et al., 2000). The reversible kinetic sorption/desorption of microbes is often described as attachment/detachment. Both attachment and detachment are assumed to be first-order processes with the rate of detachment typically assumed to be much slower than the attachment rate.

7.6.3. Interaction between reversible sorption and irreversible reduction

The moment solutions presented in chapter 3 suggest an inverse relationship between degradation rate and the temporal first moment. Increasing the degradation rate reduces concentrations in the BTC tail, resulting in a shift of the BTC centre-of-mass to the left. As the first moment is used to calculate the retardation factor (a parameter related to sorption), the above relationship shows that the degradation rate is directly related to sorption that would be calculated based upon BTC centre-of-mass. Although the moment solutions in Chapter 3 assume first-order degradation, other first-order irreversible removal processes (e.g. die-off, filtration, irreversible sorption) will have the same effect.

How sensitive is the impact of irreversible removal on the shift of centre-of-mass in a BTC? Let us study how the standardised first moment, μ_1, varies with removal rate λ for a transport time scale dt=50 hours for 1-D transport of a non-sorbing contaminant (Fig. 7.6). Table 7.1 shows that only when $1/\lambda \leq dt$ is the left-shift significant, as suggested from the significantly reduced μ_1 values. An example is illustrated in Fig. 7.7. With increasing λ, the height of a BTC is more reduced and the centre-of-mass is more shift to the left.

The above finding suggests that if we use a model that does not incorporate an irreversible removal process but the contaminant is in fact being removed by some mechanism, we would overestimate the contaminant transport velocity or underestimate its retardation.

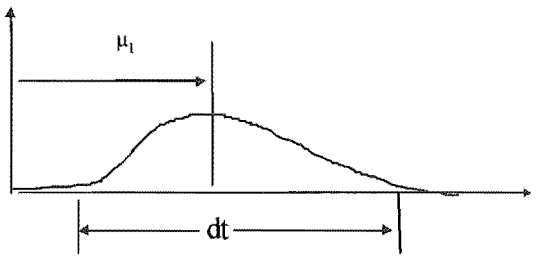

Fig. 7.6. Schematic illustration of transport scale and centre-of-mass in a BTC. Note that the transport time scale *dt*, is defined empirically (e.g. minimum concentration of the BTC = 5% peak concentration).

Table 7.1.

Left shift of centre-of-mass, as indicated from first moment μ_1, in the BTC of a non-sorbing contaminant (R=1)

dt (h)	λ (per h)	1/λ (h)	μ_1 (h)
50	0		15.59
50	0.0001	10000	15.58
50	0.001	1000	15.55
50	0.01	100	15.25
50	0.02	50	14.94
50	0.1	10	12.97
50	1	1	6.73
50	10	0.1	2.35

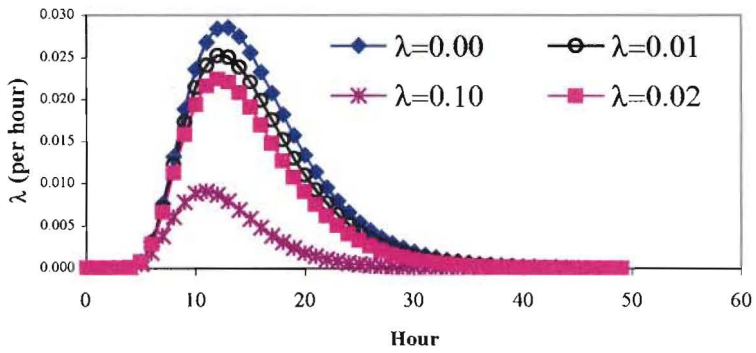

Fig. 7.7. Effect of removal rate on centre-of-mass in a BTC of a non-sorbing contaminant.

This finding that only when $1/\lambda \leq dt$ is the left-shift significant may explain what we have observed in our field rhodamine WT data. Pang and Close (1999) analysed the mass recovery of rhodamine WT data presented by Pang et al. (1998) for a field experiment carried out at the Burnham Experimental Site. They found that although rhodamine WT and the conservative tracer Cl displayed almost identical BTCs (e.g. shown in Fig. 7.8), the relative mass recovery of WT down gradient in comparison to Cl was 90% at 21 m and 82% at 37 m. It is believed that the removal rate of the dye is very small relative to the time step, thus the centre of mass in its BTCs is not affected.

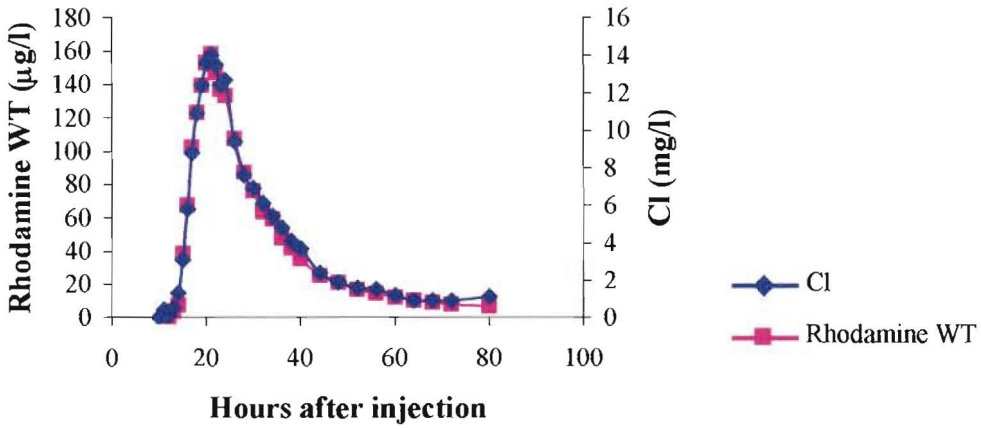

Fig. 7.8. BTCs of Cl and rhodamine WT in well 14 (62 m down gradient of the injection well) at Burnham Experimental Site (from Pang et al. 1998).

7.6.4. Effect of sorption on degradation

The common Advection-Dispersion Equation (ADE) with linear equilibrium sorption and first-order reduction is given by (as mentioned in Chapters 2, 3, and 6)

$$R\frac{\partial c}{\partial t} = D\frac{\partial^2 c}{\partial x^2} - V\frac{\partial c}{\partial x} - \lambda c$$

The same transport equation is presented in CXTFIT manual. In the manual, λ is called combined first-order rate coefficient, and is defined as

$$\lambda = \lambda_l + \frac{\rho_b K_d}{\theta}\lambda_s$$

For linear equilibrium sorption, as $R = 1 + \frac{\rho_b K_d}{\theta}$, we then have $\lambda = \lambda_l + (R-1)\lambda_s$.

However, when looking at the relationship between sorption and degradation, we should not look at only $\lambda = \lambda_l + (R-1)\lambda_s$ but also from the ADE.

Dividing R at both sides of the ADE, we obtain

$$\frac{\partial c}{\partial t} = \frac{D}{R}\frac{\partial^2 c}{\partial x^2} - \frac{V}{R}\frac{\partial c}{\partial x} - \frac{\lambda}{R}c = \frac{D}{R}\frac{\partial^2 c}{\partial x^2} - \frac{V}{R}\frac{\partial c}{\partial x} - \left(\frac{\lambda_l - \lambda_s}{R} + \lambda_s\right)c$$

From this equation, we can see when $\lambda_s < \lambda_l$, effective degradation decreases with increasing sorption, and when $\lambda_s < \lambda_l$, effective degradation increases with increasing sorption. Both situations could happen as described in Section 7.6.1.

7.7. Some issues related to modelling

7.7.1 Temporal moment analysis

The method of temporal moments (MOM) could provide an additional useful means of parameter estimation for contaminant transport. In previous studies reported in the literature, moment solutions are only used for estimating pore-water velocities and dispersion coefficients. Sorption and degradation are two important processes in the transport of many organic contaminants, and often we wish to estimate retardation factors (or sorption coefficients) and degradation rates. However, to our knowledge, the only published MOM solutions considering solute transport undergoing both sorption and degradation are given by Das and Kluitenberg (1996).

Adapting solutions of Das and Kluitenberg (1996), Chapter 3 formulates simple equations for calculating the first-order degradation rate constant and retardation factor based on temporal moments of experimental breakthrough data. As far as we know, the paper reproduced in Chapter 3 represents the first attempt to test the method of Das and Kluitenberg (1996) with experimental data. The method is satisfactorily verified using both column experimental data from our laboratory and some additional data from the literature. The results agree well with curve-fitting results from CXTFIT.

Using these formulas, we could determine transport parameters from time moments of measured concentration breakthrough curves. These experimental moments characterise BTCs based on the distribution of the data and are independent of any transport model. As these formula are derived from solutions of a transport model, one does not have to know the analytical solution to the transport equation (Valocchi, 1985) when calculating the transport parameters. MOM always gives unique results, while curve-fitting could give multiple results if there are more than two parameters to be estimated. As stated in Chapter 3, the main advantage of the MOM is that it is another tool to estimate parameters, and that it appears to do a better job of fitting the tail.

However, the MOM has some disadvantages and difficulties: (1) To ensure the accuracy of the moment analysis, it requires complete BTCs and, thus, relatively frequent data collection. In practice, however, truncated BTCs are more often obtained due to limited experimental time and analytical costs, (2) MOM is inaccurate when the BTC exhibits significant tailing (Maloszewski et al. 1994), and (3) High order moments are difficult to calculate accurately (Leij and Dane, 1992). Hence, the accuracy of a dispersion coefficient estimate, which is largely based on the second moment, would be lower than that for pore-water velocity, which is largely based on the first moment. As a result, the curve fitting approach is generally more accurate in comparison to time moment analysis (Leij and Dane, 1992; Maloszewski et al. 1994; Pang et al. 1998).

The moment solutions represented in Chapter 3, as well as most other examples of time moment analysis reported in the literature, are restricted to 1-D equilibrium transport. A modified method of moments developed by Goltz and Roberts (1987) allows for analysis of 3-D equilibrium transport using time moments from concentration breakthrough data. However the MOM of Goltz and Roberts (1987) does not consider concurrence of sorption and degradation. It may be possible in the future to look into developing 3-D moments that incorporate concurrent sorption and degradation.

Currently, work is ongoing to develop 3-D moment solutions for nonequilibrium transport considering sorption, degradation, and mass exchange between two regions/sites. It is anticipated that these solutions may be applied to data obtained from field experiments conducted by our laboratory. The preliminary results show that the moment solutions can be used to obtain transport parameter values similar to those obtained using N3DADE model of Leij and Toride, (1997), a 3-D nonequilibrium transport model. However, this additional work is beyond the scope of this current study.

Temporal moments are limited for analysing concentration breakthrough over time. Thus MOM is appropriate for analysing column data and field data collected from a limited number of sampling points over time. However, for analysing concentration breakthrough over space, spatial moments are needed. Similar to temporal moments, spatial moments have been used to obtain groundwater solute transport characteristics (Freyberg, 1986; Garabedian et al. 1991). Unlike temporal moments, determination of spatial moments requires a large number of multilevel sampling points to obtain accurate results for the contamination plume. This method may be useful for analysing data obtained from our artificial aquifers in the future.

An application of the MOM formula presented in Chapter 3 is the analysis of Br (conservative tracer) and rhodamine WT (non-conservative tracer) data obtained from a full-header-tank injection experiment conducted in our homogenous artificial aquifer. Similar to the results reported in Chapter 3 (Table 3.1), the MOM gives slightly lower values for the pore-water velocity and degradation rate and slightly higher values for the dispersion coefficient and retardation factor than those obtained from CXTFIT curve fitting. However, presentation of artificial aquifer data is beyond the scope of this thesis.

7.7.2. Measure of goodness-of-fit for inverse modelling

In inverse modelling (used in all chapters), parameter values are varied arbitrarily to best describe the observed data, and different parameter sets can yield very similar curves. Sometimes, the optimised results with a very high r^2 value and 95% confidence intervals of

the model estimation are not realistic, while realistic results could be associated with lower r^2 values and confidence intervals. Good knowledge of the experimental system is required to judge the best results and choose reasonable initial estimates and estimate constraints.

Likewise, the minimum sum of squared residuals (SSR) between data and model estimate does not necessarily represent the best model fit. For example, the Scale Dependent Dispersion Model (SDM) did not fit the experimental data when using minimum SSR as the sole fitting criteria. Comparing of results from the method of moments (MOM) and CXTFIT curve fitting (which minimizes SSR) is also not necessarily appropriate. Both MOM and curve fitting are two different ways of estimating parameters using different criteria – one matches moments and one minimizes SSR. By definition of least squares curve fitting, fitting will always result in a lower SSR than MOM. However, this does not mean that the curve fitting results are "better" than the MOM results. In fact, as was found in Chapter 3, the MOM results better described BTC tailing than the CXTFIT results. This depends on whether the model fits or is appropriate for the data. Note, though, that minimizing SSR might be an appropriate criterion to use when comparing two (or more) models that each attempts to minimize the SSR between data and model fits.

7.7.3. Model optimisation

Apart from SDM, inverse modelling used in this thesis is performed by PEST and CXTFIT. The former is a model-independent optimisation package and the latter is a transport model built with a least-square optimisation option. Compared to PEST, the optimisation package of the CXTFIT has two disadvantages:

(1) It gives the same weighting to all observations. Often a BTC contains more data of low concentration measurements than data of high concentration measurements. This could result in noisy data of low concentrations (e.g. tritium BTCs shown in Chapter 2) being significant and downplaying the important high concentration peak of the BTC.

(2) It is unable to consider relationships between parameters, and assumes all fitting parameters are independent of each other. In fact, parameters might be related and it would be advantageous to reduce the number of fitting parameters by defining a relationship between two parameters (i.e., two degradation rates in two-region/site models).

In contrast PEST allows the user to assign different weights to different observations and can linearly relate two parameters. If the relationship between two parameters is not linear, a pre-processor may be used to define more complex relationships. It is possible that the models in CXTFIT can be coupled with PEST, in order to apply the CXTFIT nonequilibrium models while still taking advantage of the benefits of using PEST (e.g. weighting data and defining parameter dependencies).

Chapter 8

Summary and conclusions

In the publications prepared for this study, we have

(1) developed and experimentally verified solutions for a 1-D scale-dependent dispersion model,

(2) experimentally verified solutions for the temporal moments that consider the interplay of sorption and first-order reduction,

(3) examined the effects of pore-water velocity on chemical nonequilibrium transport of Cd, Zn and Pb through alluvial gravel columns,

(4) investigated attenuation and transport of atrazine, hexazinone and procymidone under field conditions through a volcanic pumice sand aquifer,

(5) and determined setback distances between septic tanks and the shoreline of Lake Okareka for a worst-case scenario, based on transport and attenuation of microbial indicators (*E. coli* and F-RNA phages) in a pumice sand aquifer.

We have also carried out some additional work that is relevant to the studies presented in the publications, including

(1) a theoretical explanation for scale-dependent dispersion in homogenous media,

(2) derivation of theoretical MOM solutions,

(3) introduction of a few methods related to non-linear equilibrium sorption (presentation of transport equation and retardation factor, linearization of non-linear sorption isotherms, determination of a non-linear sorption isotherm using column data, estimation of a retardation factor without using a transport model, and differentiation of tailings caused by non-linear equilibrium sorption and rate-limited sorption),

(4) the use of a two-region model to simulate transport of reactive solutes,

(5) and the determination of the individual contributions of diffusion, interception and settling to filtration.

Lastly we have discussed some important issues in contaminant transport, many of which are not included in the publications and the additional studies. In the discussion, we have indicated some gaps in current research and offered ideas for future research. These issues are:

- contaminant migration through preferential flow,
- characterisation of maximum groundwater velocity using colloids
- velocity enhancement in size/anion exclusion,
- facilitated transport of immobile contaminants by mobile colloids,
- 'apparent dispersion' caused by the presence of 'immobile water zones',
- the relationship between dispersivity and other transport parameters,
- rate-limited processes,
- hypothesises and limitations of nonequilibrium transport models,
- multifactor non-ideality models for differentiating physical and chemical nonequilibrium,
- sorption reversibility and linearity, as well as interaction with irreversible removal processes,
- and some issues related to modelling (e.g. measure of goodness-of-fit and optimisation).

The solutions for a scale-dependent dispersion model (SDM) developed in this study provide a useful new analytical method to solve scale-dependent dispersion problems, which are generally solved by numerical algorithms. The study suggests that the use of a constant dispersivity/distance ratio in a transport model is more appropriate than the use of a constant dispersivity. A SDM is superior to a constant dispersion model (CDM) in predicting contaminant concentrations at multiple locations. When using a CDM to predict contaminant concentrations at multiple locations, the model has to be run separately for each location by varying dispersivity to consider scale-dependent dispersion. Using the theory of Hunt (1999), we have theoretically explained that scale-dependent dispersion could also happen in homogenous media and that dispersivity could increase with distance without bound. Supported with other literature data, we doubt if there would be an asymptotic dispersivity value at a large distance. Scale-dependent dispersion is an important mechanism that needs to be taken into account when designing monitoring programs and experiments.

The formula presented in this study for temporal moment solutions that consider concurrent sorption and first-order reduction allows calculation of a retardation factor and first-order reduction rate using breakthrough data. The solutions suggest that the retardation factor is

inversely related to the first-order reduction rate. Therefore, if we use a model that does not incorporate an irreversible removal process when the contaminant is in fact being removed by some mechanism, we would either overestimate the contaminant transport velocity or underestimate its retardation. To ensure the accuracy of the moments obtained from the breakthrough data, the analysis requires complete breakthrough curves and relatively frequent data collection.

Transport of Cd, Zn and Pb through alluvial gravel columns was dominated by first-order rate-limited sorption and desorption. Pore-water velocity played a very important role in this process. With increasing pore-water velocity, sorption and desorption rates increases, more sorption sites are in equilibrium phases, and the metals are less retarded. Model results suggest that Cd and Zn behave similarly, while Pb is much more strongly sorbed.

Sorption of Cd, Zn and Pb is also non-linear at equilibrium conditions. When a non-linear sorption isotherm is incorporated into a transport equation, the retardation factor (R) is concentration dependent and either decreases or increases with concentration. As it is difficult to model when R is not a constant, most models deal with linear equilibrium sorption so that R is a constant. If using non-linear isotherm parameter values to calculate concentration independent R-values, the non-linear isotherm must first be linearized. Two linearization methods of van Genuchten (1981) are discussed in this study. Non-linear sorption isotherms are traditionally determined from batch tests but could be also determined from data using method of Clothier et al. (1996). When breakthrough of a non-degradable contaminant reaches a steady state (outflow concentration = inflow concentration), retardation factor could be estimated from mass sorbed or desorbed without the use of a model or the method of time moments. Non-linear equilibrium sorption could also cause some tailing of BTCs. The best way to ascertain the controlling process, either by non-linear equilibrium sorption or rate-limited sorption, is to perform a flow interruption during the experiments.

In uniformly packed column systems, physical nonequilibrium is often absent. However, physical nonequilibrium is often the dominating process for contaminant transport in field conditions. Transport of atrazine and procymidone at field conditions in a pumice sand aquifer was influenced by both physical and chemical nonequilibrium. For hexazinone, the the chemical nonequilibrium component was negligible, and a two-region physical nonequilibrium model could well describe the field transport of hexazinone in pumice sand aquifer. Hexazinone was the most mobile and underwent little mass reduction, while procymidone was the least mobile and underwent the greatest mass reduction. The mobility of atrazine was similar to that of a commonly used dye tracer, rhodamine WT. Hence, rhodamine WT could be used as a sorbing tracer in a monitoring program to delimit the appearance of atrazine in pumice sand groundwater. The experimental results indicate that allophane (a clay mineral) has also played an important role in pesticide sorption in the pumice sand aquifer. Our finding of much greater total reduction rates than degradation rates suggests that reduction of pesticides observed in the field tracer experiment were caused not only by degradation but also by other irreversible processes. Hence, the use of laboratory-determined degradation rates could underestimate the reduction of pesticides under field conditions.

Based on the transport of the microbial indicators, *E. coli* and F-RNA phases, in a pumice sand column, and worst-case values for aquifer properties and effluent discharge, model-estimated setback distances between septic tanks and the shoreline of Lake Okareka were determined. These were 16 m to satisfy the Recreational Water Quality Guidelines for *E. coli* (< 126 per 100 ml), and 48 m to meet the Drinking-Water Standards For New Zealand for enteric virus (<1 per 100 L). The distance of 16 m allows a 5-log reduction in bacterial concentrations, while the distance of 48 m allows a 10-log reduction in viral concentrations. These distances may be applicable for other lakeshores in pumice sand aquifers with groundwater velocities less than 7 m/day.

Bacterial removal in a pumice sand column was predominately through filtration (87-88%) and the remainder through die-off (12-13%), while viral removal was by both die-off (45%)

and filtration (55%). Filtration of bacteria was mainly through sedimentation and secondarily through diffusion, while diffusion was the only determinant for filtration of F-RNA phages. Die-off rates of microbes were found to be much lower than their total removal rates. Consequently, the determined setback distances based on die-off rates would be unnecessarily large.

Colloid and colloid-facilitated transport has important implications in the characterisation of aquifer hydraulic properties, risk analysis and design of monitoring programs. Colloids (such as bacteria, spores, viruses, high molecular weight polymers, humic substances etc.) could travel faster than the mean pore-water velocity (i.e., velocity enhancement) and thus would provide information on the possible maximum contaminant velocities and preferential flow. Colloids are larger than solutes and hence are susceptible to pore-size exclusion. Since colloids are excluded from part of the pore volume in aquifer media, aquifer porosity and dispersivity for colloid transport are relatively smaller than for solute transport. Our Burnham field data show that with increasing transport distance, velocity enhancement tends to increase. This is probably a result of increasing heterogeneity with transport distance (hence the difference between colloid velocity and mean pore-water velocity increases). This is also probably related to the fact that the colloids are filtered in the smaller pores and hence the remainders go faster in the large pores at grater distances. The data from our 8-m long column suggest that velocity enhancement tends to decrease with increasing pore-water velocity. This is probably because increasing pore-water velocities reduces the difference between colloidal velocity and mean pore-water velocity, as the colloidal velocity is the maximum groundwater velocity, it is relatively constant.

In this study we have calibrated a number of transport models with observed data. Contaminant attenuation and transport in selected aquifer systems have been characterized with descriptive parameters (e.g. dispersivity, sorption coefficient, retardation factor, degradation rate, die-off rate, filtration rate, mass transfer rates, etc.). We believe that these experimentally established parameter values and some of the methods presented could be very useful to others (e.g. government agencies, regional authorities, and consultants) for

various purposes (e..g., research, management, planning, design of monitoring programs, risk analysis, and consulting). We have also identified some gaps in the current literature, and the ideas presented in this thesis could be beneficial for planning future research.

Notations

Chapter 2:

c	contaminant concentration in liquid phase (M/L^3)
c_o	source concentration (M/L^3)
C^*	dimensionless concentration
C_1, C_2, C_3	constants generated from integration in 2.A5-2.A7
D	mechanical dispersion coefficient constant used in the CDM (L^2/T)
D_o	molecular diffusion coefficient (L^2/T)
f	transform function defined in Eq. 2.20
K_d	partitioning coefficient (L^3/M) in Eq. 2.43
L	unspecified length (L)
n	integer number used in Eq. 2.39
p	transform variable in 2.A5
P	probability of significance in statistic analysis
R	retardation factor
S	concentration in the solid phase (M/M) in Eq. 2.43
t	time (T)
t_0	time duration of the pulse (T)
t^*	dimensionless time defined above Eq. 2.35
T	transformed dimensionless time
V	average pore-water velocity (L/T)
x	longitudinal distance (L)
X	dimensionless length
y	dummy integration variable used in 2.A7

Greek symbols:

α_x	dispersivity (L)
β	transform variable defined in Eqs. 2.20 and 2.21
ε	dispersivity/distance ratio used in the SDM (L/L)
λ	first-order degradation rate (T^{-1})
λ^*	dimensionless degradation rate
θ	dummy integration variable used in 2.A6
τ	dummy integration variable
τ^*	dimensionless integration variable
φ	transform function defined by Eq. 2.6
ψ	transform function included in Eq. 2.11
Ψ	transform function defined above Eq. 2.16
η	porosity of the medium (L^3/ L^3) in Eq. 2.43
μ	degradation rate in the solid phase (T^{-1}) in Eq. 43
ρ_b	bulk density of the medium (M/L^3) in Eq. 2.43

Functions and formula:

erfc	complementary error function
$F(\varepsilon)$	Stirling's asymptotic formula defined in Eq. 2.37
Γ	gamma function
γ	incomplete gamma function

Chapter 3:

A	cross-sectional area of the column (L^2)

c	contaminant concentration (M/L^3)
$C(x, s)$	dimensionless concentration in the Laplace domain
D	dispersion coefficient (L^2/T)
K_d	sorption distribution coefficient (L^3/M)
Q	flow rate (L^3/T)
R	retardation factor
s	Laplace transform variable (dimensionless)
t	time (T)
t_0	pulse duration (T)
V_c	contaminant effective velocity (L/T)
V	average pore-water velocity (L/T)
x	longitudinal distance (L)
λ	combined first-order degradation rate constant (T^{-1}) that accounts for degradation of solute in both liquid and solid phases
λ_l	first-order degradation rate constant in the liquid phase (T^{-1})
λ_s	first-order degradation rate constant in the solid phase (T^{-1})
θ	porosity of the porous material (L^3/L^3)
ρ_b	bulk density of the porous material (M/L^3)
ρ_s	solid density (M/L^3)

Chapter 4:

C	solute concentration in solution (M/L^3)
C_o	initial concentration (M/L^3)
D	dispersion coefficient (L^2/T)
f	fraction of instantaneous sorption sites
k_1	first-order sorption rate coefficient (T^{-1})
k_2	first-order desorption rate coefficient (T^{-1})
K	non-linear equilibrium partition coefficient (L^3/M)

K_d	partition coefficient for linear sorption (L^3/M)
K_{p1}	equilibrium partition coefficient for the instantaneous sites (L^3/M)
K_{p2}	equilibrium partition coefficient for the kinetic sites (L^3/M)
L	characteristic length (L)
m	the mass of the aquifer material in the column (M)
m_{ads}	mass sorbed (M)
m_{des}	mass desorbed (M)
n	Freundlich exponent constant
R	retardation factor
S	sorbed concentration (M/M)
S_1	sorbed concentration on instantaneous sites (M/M)
S_2	sorbed concentration on kinetic sites (M/M)
t	time after injection (T)
T	residence time (T)
V	pore-water velocity (L/T)
x	transport distance (L)
W	column volume (L^3)
α	rate of mass transfer (T^{-1})
ω	mass transfer coefficient
β	partitioning coefficient between the equilibrium and non-equilibrium phases
ϕ	bulk density of the aquifer material (M/L^3)
θ	porosity of the aquifer material (L^3/L^3)

Chapter 5:

A	cross-sectional area of the measuring volume perpendicular to the direction of the flow (L^2)
c	concentration of the solute (M/L^3)
C	normalised resident concentration (dimensionless)

D_x, D_y D_z	dispersion coefficients in the x, y, z directions (L^2/T^1), respectively
K_d	distribution coefficient (L^3/M)
L	characteristic length (L)
M_{re}	relative mass recovery
MRF	mass recovery of a tracer (M/M)
M_o	initial mass injected (M)
P_x, P_y, P_z	Peclet numbers in the x, y, z directions
R	retardation factor
t	time since injection (T)
T	normalised time
U	normalised first-order reduction term
v	pore-water velocity (L/T)
x, y z	spatial coordinates (L)
X, Y Z	dimensionless distances in x, y and z directions
β	partition coefficient between the equilibrium and non-equilibrium phases
θ	effective porosity of the aquifer material (L^3/L^3)
ω	mass transfer coefficient
ρ_b	bulk density of the aquifer material (M/L^3)

Chapter 6:

$A_{microbe}$	surface area of the microbe (L^2)
c	contaminant concentration in the liquid phase (M/L^3)
c_o	inflow concentration (M/L^3)
d_c	average diameter of grain size (L)
D	dispersion coefficient (L^2/T)
D	average diameter of the porous media grain (L)
d	diameter of the microbe (L)
d_p	colloidal particle diameter (L)

g	gravitational constant (L/T^2)
L	length of the microbe (L)
k_{att}	first-order filtration (or attachment) rate coefficient (T^{-1})
k_B	Boltzmann constant ($kg(m/s)^2/K$)
K_d	sorption partitioning coefficient (L^3/M)
n	total number of sand particles
Q	flow rate (L^3/T)
R	retardation factor
S	contaminant concentration in the solid phase (M/M)
t	time (T)
T_o	duration of the pulse (T)
T	solute temperature (K)
v	mean pore-water velocity (L/T)
W	column volume (L^3)
W_p	volume of the each sand particles (L^3)
X	longitudinal distance (L)
α	collision efficiency
λ	first-order total removal rate (T^{-1})
θ	porosity (L^3/L^3)
Φ	mean diameter of the sand particle (L)
μ	combined die-off rate (T^{-1})
μ_l	first-order die-off rate for the free microbes (T^{-1})
μ_s	first-order die-off rate for the sorbed microbes (T^{-1})
η	single collector efficiency
η_D	collection by Brownian diffusion (dimensionless)
η_I	collection by interception (dimensionless)
η_G	collection by settling (dimensionless)
ρ	water density (M/L^3)
ρ_b	bulk density (M/L^3)

ρ_p	colloidal density (M/L^3)
ρ_s	particle density of the sand (M/L^3)

Chapter 7:

C_o	initial concentration in the liquid phase (M/L^3)
C	concentration at travel distance X (M/L^3)
D	dispersion coefficient constant (L^2/T)
D_{50}	mean particle size (L)
dt	transport scale (T)
f	filter factor (L^{-1})
K	non-linear equilibrium partition coefficient (L^3/M)
K_{oc}	organic carbon distribution coefficient (L^3/M)
K_d	linear sorption partitioning coefficient (L^3/M)
k_f	forward sorption rate constants (T^{-1})
k_r	reverse sorption rate constants (T^{-1})
n	Freundlich exponent constant
OC	fraction of organic carbon content
P_e	effective Peclet number
R	retardation factor for retarded contaminant and velocity ratio for velocity enhancement
S	contaminant concentration in the solid phase (M/M)
V	mean pore water velocity (L/T)
X	transport distance (L)
α_x, α_y, α_z	dispersivity in the x, y, z directions (L), respectively
α	firs-order kinetic rate coefficient (T^{-1})
β	partitioning coefficient between the equilibrium and non-equilibrium phases

ε	dispersivity/distance ratio (L/L)
ϕ	fraction of mobile water bulk density of the porous material
λ	first-order removal rate (T^{-1})
μ_1	standardised first moment (T)
θ	total porosity of the porous material (L^3/L^3)
$\theta_{excluded}$	porosity of the porous material that colloids are excluded (L^3/L^3)
θ_{passed}	porosity of the porous material that colloids could travel (L^3/L^3)
ρ_b	bulk density (M/L^3)

Some frequently used abbreviations and specific terminology in this thesis

SDM	scale-dependent dispersion model
CDM	constant dispersion model
ADE	advection-dispersion equation
BTC	concentration breakthrough curve
MOM	method of temporal moments
TRM	two-region nonequilibrium model
TSM	two-site nonequilibrium model

Equilibrium sorption: implies that sorption occurs instantaneously, and can be described by either a linear ($S = K_d C$) or non-linear ($S = KC^n$) isotherm. Concentration breakthrough curves generated under linear equilibrium sorption are relatively symmetric.

Nonequilibrium sorption: implies that sorption (either linear or non-linear) is a slow process (relative to other transport processes, like convection), so that the assumption of instantaneous sorption is inappropriate. For a linear isotherm, nonequilibrium (or rate-limited) sorption/desorption may be mathematically described by

$$\frac{\partial S}{\partial t} = \frac{\theta}{\rho_b} k_1 C - k_2 S$$

where k_1 and k_2 are first-order sorption and desorption rate constants (T^{-1}), respectively. Concentration breakthrough curves generated under nonequilibrium sorption are relatively asymmetric and contain significant tailing.

Adsorption: describes the condensation of chemical on surface or pores by physical or chemical bonding forces. The use of "adsorption" suggests a known, specific surface interaction.

Sorption: describes all reversible associations of chemical with solids. As the nature of most interactions between contaminants and porous media is likely to be unknown, "sorption" is a better term to use than adsorption.

Linear sorption: sorption increases linearly with concentration ($S = K_d C$). For linear equilibrium sorption, the retardation factor is a constant ($R = 1 + K_d \rho_b / \theta$).

Non-linear sorption: sorption increases nonlinearly with concentration ($S = KC^n$). For non-linear equilibrium sorption, the retardation factor increases or decreases with concentration ($R = 1 + \rho_b K n C^{n-1} / \theta$).

Reversible sorption: means that all sorbed chemical will be eventually desorbed from geological solids under certain conditions (e.g. flushing, change pH). Both equilibrium sorption and nonequilibrium sorption are typically assumed to be reversible processes.

Irreversible sorption: means that a fraction of sorbed chemical is permanently sorbed and never desorbs.

Hysteretic sorption: the sorption and desorption isotherms are not coincident, and the amount sorbed is greater than the amount-desorbed. It is possible to have a hysteretic sorption/desorption isotherm that is reversible.

Equilibrium model: a transport model that assumes sorption is an instantaneous process with respect to advection.

Nonequilibrium transport: refers to transport that is impacted by kinetic (i.e. rate-limited) physical and/or chemical processes due to different time-scales between processes. A breakthrough curve obtained from nonequilibrium transport is asymmetric with tailing.

Physical nonequilibrium: occurs when the time-scale for advection is faster than the time-scale for mass transfer between mobile and immobile regions (Goltz and Oxley, 1991). It is a result of heterogeneity in hydraulic properties (e.g. hydraulic conductivity and porosity, preferential flow, rate-limited diffusion, etc.).

Chemical nonequilibrium: occurs when the system hydraulic residence time is relatively shorter than its chemical reaction time (e.g. sorption, film diffusion, or intra-particle diffusion). It is a result of kinetic sorption, or kinetic ion exchange, or hysteretic sorption.

Nonequilibrium model: considers rate-limited processes for which equilibrium is reached slowly. It may also contain processes for which equilibrium is reached quickly. These models hypothesise the existence of mobile and immobile water regions, or instantaneous and kinetic sorption sites.

Non-ideal transport: transport affected by physical or chemical nonequilibrium or where the sorption isotherm is non-linear and/or hysteretic.

Two-region model: idealises aquifer heterogeneity as two regions: one in which the velocity is zero, the other where velocity is the average pore velocity, with partitioning of solutes between the two liquid regions governed by first-order mass transfer. The two-region model assumes that there is no kinetic sorption, and all sorption sites are instantaneous in both mobile and immobile water zone.

According to van Genuchten, 1981), a two-region model for transport of a sorbing contaminant could be expressed as:

$$R_m \frac{\partial C_m}{\partial t} + \frac{\theta_{im} R_{im}}{\theta_m} \frac{\partial C_{im}}{\partial t} = D_x \frac{\partial^2 C_m}{\partial x^2} - v_m \frac{\partial C_m}{\partial x}$$

$$R_{im} \frac{\partial C_{im}}{\partial t} = \frac{\alpha}{\theta_{im}} (C_m - C_{im})$$

in which $R_m = 1 + \frac{f \rho_b K_d}{\theta_m}$ $\quad R_{im} = 1 + \frac{(1-f) \rho_b K_d}{\theta_{im}}$ $\quad \theta = \theta_m + \theta_{im}$

where the subscripts *m* and *im* refer to mobile and immobile regions, respectively.

Two-site model: assumes that sorption on one type of site is instantaneous (S_1) while on the other type of site sorption is assumed to be kinetic (rate-limited) (S_2). The two-site model assumes that there is no immobile region, and solute transport is all through mobile water for both instantaneous sites and kinetic sites. A two-site sorption/desorption model could be expressed by the following:

$$\frac{\partial C}{\partial t} + \frac{\rho_b}{\theta} \left(\frac{\partial S_1}{\partial t} + \frac{\partial S_2}{\partial t} \right) = D \frac{\partial^2 C}{\partial x^2} - V \frac{\partial C}{\partial x}$$

$$\frac{\partial S_1}{\partial t} = K_{p1} \frac{\partial C}{\partial t}$$

$$\frac{\partial S_2}{\partial t} = \frac{\theta}{\rho_b} k_1 C - k_2 S_2$$

References

Aislabie, J., Smith, J., Fraser, R., McLeod, M. 2001. Leaching of bacterial indicators of faecal contamination through four New Zealand soils. Aust. J. Soil Res. 39: 1397-1406.

Akratanakul, S., Boersma, L., Klock, G.O. 1983. Sorption processes in soils as influenced by pore water velocity: 2. Experimental results. Soil Sci. 135(6): 331-341.

Alexander, M. 2000. Aging, bioavailability, and overestimation of risk from environmental pollutants. Environ. Sci. Tech. 34(20): 4259-4265.

Al-Hashimi, A., Evans, G.J., Cox, B. 1994. Contaminants mobility in acid-generating wastes/subsoil systems. J. Environ. Sci. Health, Part A: Environ. Sci. Eng., A29(4): 745-752.

APHA(American Public Health Association). 1998. *Standard methods for the examination of water and wastewater*, 20th ed. APHA, AWWA, WPCF, Washington, D.C.

Aral, M.M., Liao, B. 1996. Analytical solutions for two-dimensional transport equation with time-dependent dispersion coefficients. J. Hydrol. Eng. 1 (1): 20-32.

Aris, R. 1958. On the dispersion of linear kinematic waves, Proc. R. Soc. London, Ser. A, 245: 268-277.

Artinger, R., Rabung, T., Kim, J.I., Sachs, S., Schmeide, K., Heise, K.H., Bernhard, G., Nitsche,H. 2002. Humic colloid-borne migration of uranium in sand columns. J. Contam. Hydrol. 58: 1-12.

AS/NZS 1547. 2000. *On-site domestic-wastewater management. Standards New Zealand.*

Bales, R.C., Li, S., Maguire, K.M., Yahya, M.T., Gerba, C.P., Harvey, R.W. 1995. Virus and bacteria transport in a sandy aquifer, Cape Cod, MA. Ground Water 33: 653-661.

Bales, R.C., Hinkle, S.R., Kroeger, T.W., Stocking, K. 1991. Bacteriophage adsorption during transport through porous media: chemical perturbations and reversibility. Environ. Sci. Technol. 25: 2088-2095.

Bales, R.C., Gerba, C.P., Grondin, G.H., Jensen, S.L. 1989. Bacteriophage transport in sandy soil and fractured tuff. Appl. Environ. Microbiol. 55: 2061-2067.

References:

Bajracharya, K., Barry, D.A. 1997. Non-equilibrium solute transport parameters and their physical significance: numerical and experimental results. J. Contam. Hydrol. 24: 185-204.

Bajracharya, K., Tran, Y.T., Barry, D.A. 1996. Cadmium adsorption at different pore water velocities. Geoderma 73 (3-4): 197-216.

Bitton, G., Farrah, S.R., Ruskin, R.H., Butner, J., Chou, Y.G. 1983. Survival of pathogenic and indicator organisms in groundwater. Ground Water 21: 405-410.

Bitton, G. 1980: *Introduction to Environmental Virology.* John Wiley & Sons, New York, pp. 1-28.

Blanc, R., Nasser, A. 1996. Effect of effluent quality and temperature on the persistence of viruses in soil. Water Sci. Technol. 33: 237-242.

Bouchard, D.C., Wood, A.L., Campbell, M.L., Nkedi-Kizza, P., Rao, P.S.C. 1988. Sorption nonequilibrium during solute transport. J. Contam. Hydrol 2 (3): 209-223.

Bouwer, H. 1978. Groundwater Hydrology. McGraw-Hill.

Brusseau, M.L., Srivastava, R. 1999. Nonideal transport of reactive solutes in heterogeneous porous media: 4. Analysis of the Cape Cod natural-gradient filed experiment. Water Resour. Res. 35 (4): 1113-1125.

Brusseau, M.L., 1998. Non-ideal transport of reactive solutes in heterogeneous porous media: 3. Model testing and data analysis using calibration versus prediction. J. of Hydro. 209: 147-165.

Brusseau, M.L., Hu, Q., Srivastava, R. 1997. Using flow interruption to identify factors causing nonideal contaminant transport. J. Contam. Hydrol. 24: 205-219.

Brusseau, M.L., Srivastava, R. 1997. Nonideal transport of reactive solutes in heterogeneous porous media: 3. Quantitative analysis of the Borden natural-gradient experiment. J. Contam. Hydrol. 28: 115-155.

Brusseau, M.L., Gerstl, Z., Augustijn, D., Rao, P.S.C. 1994. Simulating solute transport in an aggregated soil with the dual-porosity model: measured and optimized parameter values. J. Hydrol. 163: 187-193.

References:

Brusseau, M.L. 1993. The influence of solute size, pore-water velocity, and intraparticle porosity on solute dispersion and transport in soil. Water Resour. Res. 29: 1071-1080.

Brusseau, M.L. 1992a. Nonequilibrium transport of organic chemicals: the impact of pore-water velocity. J. Contam. Hydrol. 9(4): 353-368.

Brusseau, M.L. 1992b. Transport of rate-limited sorbing solutes in heterogeneous porous media: application of a one-dimensional multifactor nonideality model to field data. Water Resour. Res. 28 (9): 2485-2497.

Brusseau, M.L., Larsen, T., Christensen, T.H. 1991. Rate-limited sorption and non-equilibrium transport of organic chemicals in low organic carbon aquifer materials. Water Resour. Res. 27: 1137-1145.

Brusseau, M.L., Rao, P.S.C. 1989. Sorption nonideality during organic contaminant transport in porous media. Critical Rev. Environ. Control 19: 33-99.

Brusseau, M.L., Rao, P.S.C., Jessup, R.E., Davidson, J.M. 1989. Flow interruption: a method for investigating sorption non-equilibrium. J. Contam. Hydrol. 4: 223-240.

Burr, D.T., Sudicky, E.A., Naff, R.L. 1994. Non-reactive and reactive solute transport in three dimensional heterogeneous porous media – mean displacement, plume spreading and uncertainty. Water Resour. Res. 30: 791-815.

Casey, F.X.M., Ong, S.K., Horton, R. 2000. Degradation and transformation of trichloroethylene in miscible-displacement experiments through zerovalent metals. Environ. Sci. Technol. 34 (23): 5023-5029.

Chen, C., Wagenet, R.J. 1997. Description of atrazine transport in soil with heterogeneous nonequilibrium sorption. Soil, Sci. Soc. Amer. J. 61: 360-371.

Chen, C., Wagenet, R.J. 1995. Solute transport in porous media with sorption-site heterogeneity, Environ. Sci. Tech. 29: 2725-2734.

Chen, W. 1994. Solute Nonequilibrium Transport in Heterogeneous Porous Media. A Unified Probability Distribution Approach. Ph.D dissertation, Cornell University.

Chen, C., Wagenet. R.J. 1992. Simulation of water and chemicals in macropore soils: Part 1. Representation of the equivalent macropore influence and its effect on soil-water flow. J. Hydrol. 130: 105-126.

References:

Cho, C.M. 1971. Convective transport of ammonium with nitrification in soil. Can. J. Soil. Sci. 51: 339-350.

Chu, Y., Jin, Y., Yates, M.V. 2000. Virus transport through saturated sand columns as affected by different buffer solutions. J. Environ. Qual. 29: 1103-1110.

Close, M.E., Pang, L., Bright, J.B., Manning, M. 2002. Modelling contaminant transport in groundwater using artificial aquifer: 2. Characterisation of hydraulic and adsorption properties. In preparation.

Close, M., Rosen, M.R. 2001. 1998/99 national survey of pesticides in groundwater using GCMS and ELISA. N. Z. J. Mar. Freshwater Res. 35: 205-219.

Close, M., Pang, L., Magesan, G., Stewart, M. 1999. Field study of pesticide leaching in an allophanic soil in New Zealand - model simulations using GLEAMS. Workshop Proceedings on Environmental Aspects of Pesticide Use. 15-16 November, Hamilton. p. 16.

Close, M.E. 1995. National survey of pesticides in groundwater. Institute of Environmental Science and Research, Technical Report No. CSC 94/55. 22 p.

Clothier, B.E., Magesan, G.N., Heng, L., Vogeler, I. 1996. In situ measurement of the solute adsorption isotherm using a disc permeameter. Water Resour. Res. 32 (4): 771-778.

Dagan, G. 1982. Stochastic modelling of groundwater flow by unconditional and conditional probabilities. 2, the solute transport. Water Resour. Res. 18 (4): 835-848.

Daily, J.W., Harleman, D.R.F. 1966. Fluid dynamics. Addison-Wesley publishing Company, Inc. 454 pp.

Das, B.S., Kluitenberg, G.J. 1996. Moment analysis to estimate degradation rate constants from leaching experiments. Soil Sci. Am. J. 60: 1724-1731.

Debartolomeis, J., Cabelli, V.J. 1991. Evaluation of an *Escherichia coli* host strain for enumeration of F male-specific bacteriophages. Appl. Environ. Microbiol. 57: 1301-1305.

De Marsily, G. 1986. Quantitative hydrogeology: Groundwater hydrology for engineers. Academic Press, San Diego, California.

References:

De Smedt, F., Wierenga, P.J. 1984. Solute transport through columns of glass beads. Water Resour. Res. 20: 225-232.

Dizer, H., Filip, Z., Lopez, J.M., Milde, G., Nasser, A., Seidel, K. 1985. Laboversuche zur persistenz und zum transportverhalten von viren. Umweltbundesamt Materialien 2185: 20-26.

Doherty, J., Brebber, L., Whyte, P. 1994. PEST Model-independent Parameter Estimation. Oxley, Australia: Watermark Computing.

Domenico, P.A., Schwartz, F.W. 1990. Physical and chemical hydrogeology. John Wiley & Sons, Inc. 824 pp.

Domenico, P.A., Schwartz, F.W. 1998. Physical and chemical hydrogeology. John Wiley & Sons, Inc.

Domenico, P.A., Robbins, G.A. 1984. A dispersion scale effect in model calibration and field tracer experiments. J. Hydrol. 70: 123-132.

ECAN. 1999. Groundwater modelling of viral and bacterial transport from on-site sewage disposal. Report No. U99/86. Prepared for the Canterbury Regional Council (now Environment Canterbury) by Pattle Delamore Partners Ltd.

Espinoza, C., Valocchi, A.J. 1998. Temporal moments analysis of transport in chemically heterogeneous porous media. J. Hydrol. Eng. 3 (4): 276-284.

Feitje, L. 1991. General authorisation for sewage effluent disposal. Technical support document. Canterbury Regional Council.

Fetter, C.W. 1993. Contaminant hydrogeology. Macmillan Publishing Co., New York, 71-109.

Freeze, R.A., Cherry, J.A. 1979. Groundwater. Prentice-Hall, Inc, Englewood Cliffs, New Jersey, 604 pp.

Freyberg, D.L. 1986. A natural gradient experiment on solute transport in a sand aquifer. 2. Spatial moments and the advection and dispersion of nonreactive tracers. Water Resour. Res. 22 (13): 2031-2046.

Fuller, C.C., Davis, J.A. 1987. Processes and kinetics of Cd^{2+} sorption by a calcareous aquifer sand. Geochim. Cosmochim. Acta. 51 (6): 1491-1502.

References:

Gamerdinger, A.P., Dowling, K.C., Lemley, A.T., 1993. Miscible displacement and theoretical techniques for simultaneous study of pesticide sorption and degradation during transport. Sorption and Degradation of Pesticides and Organic Chemicals in Soil. SSSA Special Publication vol. 32. Soil Society of America Society of Agronomy, 677 S. Segoe Road, Madison, WI 53711, USA.

Gamerdinger, A.P., Wagent, R.J., van Genuchten, M.Th. 1990. Application of two-site/two-region models for studying simultaneous nonequilibrium transport and degradation of pesticides. Soil Sci. Soc. Am. J. 54: 957-963.

Garabedian, S.P., LeBlanc, D.R., Gelhar, L.W., Celia, M.A. 1991. Large-scale natural gradient tracer test in sand and gravel, Cape Cod, Massachusetts. 2. Analysis of spatial moments for a nonreactive tracer. Water Resour. Res. 27 (5): 911-924.

Gelhar, L.W., Axness, C.L. 1983. Three-dimensional stochastic analysis of macrodispersion in aquifers. Water Resour. Res.19 (1): 161-180.

Gerba, C.P. 1984. Microorganisms as groundwater Tracers. In: Bitton, G. and Gerba, C.P. (eds), *Groundwater Pollution Microbiology*, John Wiley and Sons, Inc., New York. pp. 225-234.

Gerke, H.H., van Genuchten, M.T. 1993. A dual-porosity model for simulating the preferential movement of water and solutes in structured porous media. Water Resour. Res., 29: 305-319.

Gerritse, R.G., Singh, R. 1988. The relationship between pore-water velocity and longitudinal dispersivity of Cl^-, Br^-, and D_2O in soils. J. Hydrol. 4: 173-180.

Goltz, M.N., Bouwer, E.J., Huang, J. 2001. Transport issues and bioremediation modeling for the in situ aerobic cometabolism of chlorinated solvents. Biodegradation 12: 127-140.

Goltz, M.N.; Oxley, M.E. 1991. Analytical modeling of aquifer decontamination when transport is affected by rate-limited sorption. Water Resour. Res. 27(4): 547-556.

Goltz, M.N., Roberts, P.V. 1987. Using the method of moments to analyze three-dimensional diffusion-limited solute transport from temporal and spatial perspectives. Water Resour. Res. 23(8): 1575-1585.

Goltz, M.N., Roberts, P.V., 1986. Three-dimensional solutions for solute transport in an infinite medium with mobile and immobile zones. Water Resour. Res. 22: 1139-1148.

Goltz, M.N. 1986. Three-dimensional analytical modeling of diffusion-limited solute transport. Ph.D dissertation. Environmental Engineering and Science, Stanford University, Stanford, USA.

Goyal, S.M., Gerba, C.P. 1979. Comparative adsorption of human enteroviruses, simian rotavirus, and selected bacteriophages to soils. Appl. Environ. Microbiol. 38: 241-247.

Gunn, I. 2001. Septic tank and soakage system separation distances a review. Unpublished document. Environ UniServices Ltd. Auckland.

Hadfield, J.C., Nicole, D.A., Thompson, M.A. 1999. A summary of groundwater investigations at the Rukuhia pesticide research site. Environment Waikato Internal Series Report 1999/3. Hamilton, New Zealand, pp 33.

Harvey, R.W., Garabedian, S.P. 1991. Use of colloid filtration theory in modeling movement of bacteria through a contaminated sandy aquifer. Environ. Sci. Technol. 25: 178–185.

Havelaar, A.H. 1993. Bacteriophages as models of enteric viruses in the environment. ASM News 59: 614-619.

Havelaar, A.H., van Olphen, M., Drost, Y. 1993. F-Specific RNA bacteriophages are adequate model organisms for enteric viruses in fresh water. Appl. Environ. Microbiol. 59: 2956-2962.

Hildebrand, F.B. 1976. Advanced calculus for applications. Second edition, Prentice-Hall, Englewood Cliffs, New Jersey, 733 pp.

Hinton, C., Close, M. 1998. Lead adsorption onto aquifer gravel using batch experiments and XPS. In: Arehart, G.B. & Hulston, J.R. (Eds.), Water-Rock Interaction, Balkema, Rotterdam, pp.939-942.

Hinz, C., Selim, H. 1994. Transport of zinc and cadmium in soils: experimental evidence and modelling approaches. Soil Sci. Soc. Am. J., 58: 1316-1327.

References:

Hornsby, A.G.; Davidson, J.M. 1973. Solution and adsorbed fluometuron concentration distribution in a water-saturated soil: experimental and predicated evaluation. Soil Sci. Soc. Am. Proc., 37, 823-828.

Hu, Q., Brusseau, M.L. 1996. Transport of rate-limited sorbing solutes in an aggregated porous medium: a multiprocess non-ideality approach. J. Contam. Hydrol. 24: 53-73.

Huang, K., van Genuchten, M.T., Zhang, R. 1996. Exact solutions for one-dimensional transport with asymptotic scale-dependent dispersion. Appl. Math. Modelling 20: 298-308.

Hunt, B. 1999a. Variable dispersion coefficients in one-dimensional contaminant transport problems. Proceedings of the International Conference on Water, Environment, Ecology, Socio-economics and Health Engineering, Hydraulic Modelling, Edited by V.P. Singh, I. W. Seo and J.H. Sonu, Oct. 18-21, Seoul National University, Seoul, Korea, 191-202.

Hunt, B. 1999b. Dispersion model for mountain streams. J. Hydrol. Eng. 125(2): 99-105.

Hunt, B. 1998. Contaminant source solutions with scale-dependent dispersivities. J. Hydrol. Eng. 3 (4): 268-275.

Hurst, C.J., Gerba,. C.P., Cech, I. 1980. Effects of environmental variables and soils characteristics on virus survival in soil. Appl. Environ. Microbiol. 40: 1067-1079.

IAWPRC. 1991. Review Paper: Bacteriophages as model viruses in water quality control. Water Research 25: 529-545.

Iwasaki, T. 1937. Some notes on sand filtration. Journal of the American Water Works Association 29: 1591-1602.

Jacobsen, O.H., Leij, F.J., van Genuchten, M.Th. 1992. Parameter determination for chloride and tritium transport in undisturbed lysimeters during steady flow. Nordic Hydrology 23: 89-104.

Jayawardena, A.W., Lui, P.H. 1984. Numerical Solution of the Dispersion Equation Using a Variable Dispersion Coefficient; Method and Applications. Hydrological Sciences Journal 29 (3): 293-309.

Jernlas, R. 1990. Mobility in sandy soils of four pesticides with different water solubility. Acta Agriculturae Scandinavica 40: 325-340.

Jin, Y., Yates, M.V., Thompson, S.S., Jury, W.A. 1997. Sorption of viruses during flow through saturated sand columns. Environ. Sci. Technol. 31: 548-555.

Johnson, W.P., Blue, K.A., Logan, B.E., Arnold, R.G. 1995. Modelling bacterial detachment during transport through porous media as a residence-time- dependant process. Water Resour. Res. 31: 2649-2658.

Jury, W.A., Roth, K. 1990. Transfer function and solute movement through soil: Theory and applications. Birhauser, Basel, Switzerland, 226 pp.

Karickhoff, S.W., Morris, K.R. 1985. Sorption dynamics of hydrophobic pollutants in sediment suspensions. Environ. Toxicol. Chem. 4: 469-479.

Keswick, B.H. 1984. Sources of groundwater pollution. In: Bitton, G. and Gerba, C.P. (eds), *Groundwater Pollution Microbiology*. John Wiley and Sons, Inc., New York. pp. 39-64.

Keswick, B.H., Gerba, C.P., Secor, S.L., Cech, I. 1982. Survival of enteric viruses and indicator bacteria in groundwater. J. Environ.l Sci. Health, Part A, 17 (6): 903-912.

Keswick, B.H., Gerba, C.P. 1980. Viruses in groundwater. Environ. Sci. Technol. 14: 1290-1297.

Klint, M., Arvin, E., Jensen, B.K. 1993. Degradation of the pesticides mecoprop and atrazine in unpolluted sandy aquifers. J. Environ. Qual. 22: 262-266.

Klotz, D., Seiler, K.P., Moser, H., Neumaier, F. 1980. Dispersivity and velocity relationship from laboratory and field experiment. J. Hydrol. 45: 169-184.

Kookana, R.S., Naidu, R., Tiller, K.G. 1994. Sorption non-equilibrium during cadmium transport through soils. Aust. J. Soil Res. 32: 635-651.

Kookana, R.S., Schuller, R.D., Aylmore, L.A.G. 1993. Simulation of simazine transport through soil columns using time-dependent sorption data measured under flow conditions. J. Contam. Hydrol. 14: 93-115.

Kučera, E. 1965. Contribution to the theory of chromatography: linear nonequilibrium elution chromatography. J. Chromatogr. 19: 237-248.

Lallemand-Barres, P., Peaudecerf, P., 1978. Recherche des relations entre las valeur de la dispersivite macroscopique d'un milieu aquifere, ses autres caracteristiques et les conditions de mesure, Bulletin, Bureau de Recherches Geologiques et Minieres, Sec. 3/4: 277-284.

Langner, H.W., Inskeep, W.P., Gaber, H.M., Jones, W.L., Das, B.S., Wraith, J.M. 1998. Pore water velocity and residence time effects on the degradation of 2,4-D during transport. Environ. Sci. Technol. 32 (9): 1308-1315.

Lee, L.S., Rao, P.S.C., Brusseau, M.L., Ogwada, R.A. 1988. Nonequilibrium sorption of organic contaminants during flow through columns of aquifer materials. Environ. Toxicol. Chem. 7(10): 779-793.

Leij, F.J., Toride, N. 1997. N3DADE: A computer program for evaluating non-equilibrium three-dimensional solute transport in porous media. Research report no. 143. Riverside, California: U.S. Salinity Laboratory, Agricultural Research Service, U.S. Department of Agriculture.

Leij, F.J., Dane, J.H. 1992. Moment method applied to solute transport with binary and ternary exchange. Soil Sci. Soc. Am. J. 56 (3): 667-674.

Levy, J., Chesters, G. 1995. Simulation of atrazine and metabolite transport and fate in a sandy-till aquifer. J. Contam. Hydrol. 20: 67-88.

Li, Y., Ghodrati, M. 1995. Transport of nitrate in soils as affected by earthworm activities. J. Environ. Qual. 24: 432-438.

Logan, J.D. 1996. Solute transport in porous media with scale-dependent dispersion and periodic boundary conditions. J. Hydrol. 184(3-4): 261-276.

Magesan, G., Lee, B., Close, M., Hadfield, J. 1999. Field study of pesticide leaching in an allophanic soil in New Zealand - site characteristics and experimental results. Workshop Proceedings on Environmental Aspects of Pesticide Use. 15-16 November, Hamilton. p. 15.

Mallard, F., Reygrobellet, J.L., Soulie, M. 1994. Transport and retention of fecal bacteria at sewage-polluted fractured rock sites. J. Environ. Qual. 23: 1352-1363.

Maloszewski, P., Benischke, R., Harum, T., Zojer, H., 1994. Estimation of solute transport parameters in heterogen groundwater system of a karstic aquifer using artificial

tracer experiments. Water Down Under 94, vol. 2, 105-111, part A. The Institute of Engineers, Australia, Barton.

Mandal, B., Hazra, G.C. 1997. Zinc adsorption in soils as influenced by different soil management practices. Soil Sci. 162 (10): 713-721.

Maraqa, M.A., Wallace, R.B., Voice, T.C. 1999. Effects of residence time and degree of water saturation on sorption nonequilibrium parameters. J. Contam. Hydrol. 36(1-2): 53-72.

Martin, G.N., Noonan, M.J. 1977. Effects of domestic wastewater disposal by land irrigation on groundwater quality of the Central Canterbury Plains. Water and soil Technical Publication No.7, Ministry of Works and Development, Wellington, New Zealand. 25 p.

Matthess, G., 1994. Fate of pesticides in aquatic environments. In: Börner, H (Ed.), Chemistry of Plant Protection. Pesticides in Ground and Surface Water, vol. 9. Springer, Berlin, pp. 192-246.

Matthess, G., Pekdeger, A., Schroeter, J. 1988. Persistence and transport of bacteria and viruses in groundwater - a conceptual evaluation. J. Contam. Hydrol. 2: 171-188.

Matthess, G., Pekdeger, A. 1985. Survival and transport of pathogenic bacteria and viruses in groundwater. In *Ground Water Quality*. (ed. C.H. Ward, W. Giger, and P.L. McCarty), 472-482. Wiley and Sons, New York, NY.

McCaulou, D.R., Bales, R.C., Arnold, R.G. 1995. Effect of temperature-controlled motility on trnsport of bacteria and microsheres through saturated sediment. Water Resour. Res. 31: 271-280.

McCaulou, D.R., Bales, R.C., McCarthy, J.F. 1994. Use of short-pulse experiments to study bacteria transport through porous media. J. Contam. Hydrol. 15: 1-14.

McDowell-Boyer, L.M., Hunt, J.R., Sitar, N. 1986. Particle transport through porous media. Water Resour. Res. 22(13): 1901-1921.

McKay, L.D., Senford, W.E., Strong, J.M., 2000. Field-scale migration of colloid tracers in a fractured shale saprolite. Ground Water 38: 139-147.

McKay, L.D., Cherry, J.A. 1993. A field example of bacteriophage as tracers of fracture flow. Environ. Sci. Technol. 27: 1075-1079.

Mcleod, M., Aislabie, J., Smith, J., Fraser, R., Roberts, A., Taylor, M. 2001. Viral and chemical tracer movement through contrasting soils. J Environ. Qual. 30(6): 2134-2140.

Miller, J.J., Foroud, N., Hill, B.D., Lindwall, C.W. 1995. Herbicides in surface runoff and groundwater under surface irrigation in southern Alberta. Can. J. Soil Sci./Rev. Can. Sci. Sol 75: 145-148.

Ministry of Health. 2000. Drinking-Water Standards for New Zealand 2000. Compiled by: National Drinking-Water Standards Review Expert Working Group. 130 p.

Ministry for the Environment. 1999. Recreational Water Quality Guidelines: Guidelines for the Management of Waters used for Fresh Water Recreation and Recreational Shellfish-Gathering. Published by the Ministry for the Environment, Wellington, New Zealand.

Mishra, S., Parker, J.C. 1989. Analysis of solute transport with a hyperbolic scale dependent dispersion model. Hydro. Processes 4(1): 45-57.

Molz, F.J., Güven, O., Melville, J.G. 1983. An examination of scale-dependent dispersion coefficients. Ground Water 21 (6): 715-725.

Moore, R.S., Taylor, D.H., Reddy, M.M.M., Sturman, L.S. 1982. Adsorption of reovirus by minerals and soils. Appl. Environ. Microbiol. 44: 852-859.

Morley, L.M., Hornberger, G.M., Mills, A.L., Herman, J.S. 1998. Effects of transverse mixing on transport of bacteria through heterogenous porous media. Water Resour. Res. 34 (8): 1901-1908.

Nasser, A., Tchorch, Y., Fattal, B. 1993. Comparative Survival of *E. coli*, F+Bacteriophages, HAV and Poliovirus 1 in Wastewater and Groundwater. Water Sci. Technol. 28: 401-407.

Pang, L., Davies, H., Hall, C., Stanton, G. 2001. Setback distance between septic tanks and bathing shores of Lake Okareka. Prepared as part of an investigation by NIWA for the Rotorua District Council. ESR Client Report CSC0110. 93 p.

Pang, L., Close, M.E. 1999a. Field-scale physical nonequilibrium transport in an alluvial gravel aquifer. J. Contam. Hydrol. 38(4): 447-464.

Pang, L., Close, M.E. 1999b. Nonequilibrium transport of Cd in alluvial gravels. J. Contam. Hydrol. 36: 185-206.

Pang, L., Close, M.E. 1999c. A field study of nonequilibrium and facilitated transport of Cd in an alluvial gravel aquifer. Ground Water 37 (5): 785 -792.

Pang, L., Close, M.E., 1999d. Attenuation and transport of atrazine and picloram in an alluvial gravel aquifer. New Zealand Journal of Marine and Freshwater Research 33 (2): 279-291.

Pang, L., Close, M.E. 1998. Field-scale physical nonequilibrium transport in an alluvial gravel aquifer: effects on β, α, and α_x. Institute of Environmental Science and Research, PO Box 29181, Christchurch, New Zealand. Technical report No. TR9804, 31 pp.

Pang, L., Close, M.E., Noonan, M. 1998. Rhodamine WT and Bacillus subtilis transport through an alluvial gravel aquifer. Ground Water 36(1): 112-122.

Pang, L., Close, M.E., Sinton, L.W. 1996. Protection zones of the major water supply springs in the Rotorua District. Institute of Environmental Science and Research, Technical report No. CSC 96/7. 77 p.

Parker, J.C., Valocchi, A.J. 1986. Constraints on the validity of the equilibrium and first order kinetic transport models in structured soils. Water Resour. Res. 22: 399-407.

Pekdeger, A., Isenbeck, M., Schroter, J., Taylor, T., Fic, M. 1988. Parameters for modelling the transport of cadmium as influenced by the chemical properties of ground water and aquifer material. Groundwater Flow and Quality Modelling. Reidel, Boston. pp. 423-438.

Peterson, H.G., Boutin, C., Freemark, K.E., Martin, P.A. 1997. Toxicity of hexazinone and diquat to green algae, diatoms, cyanobacteria and duckweed. Aquat. Toxicol. 39: 111-134.

Pickens, J.F., Grisak, G.E. 1981a. Modelling of scale-dependent dispersion in hydrogeologic systems. Water Resour. Res. 17(6): 1701-1711.

Pickens, J.F., Grisak, G.E. 1981b. Scale-dependent dispersion in a stratified granular aquifer. Water Resour. Res. 17(4): 1191-1211.

Pieper, A.P., Ryan, J.N., Harvey, R.W., Amy, G.L., Illangasekare, T.H., Metge, D.W. 1997. Transport and recovery of bacteriophage PRD1 in a sand and gravel aquifer: effect of sewage-derived organic matter. Environ. Sci. Technol. 31: 1163-1170.

Powelson, D.K., Gerba, C.P. 1994. Virus removal from sewage effluents during saturated and unsaturated flow through soil columns. Water Research 28: 2175-2181.

Ptacek, C.J., Gillham, R.W. 1992. Laboratory and field measurements of non-equilibrium transport in the Borden aquifer, Ontario, Canada. J. Contam. Hydrol. 10 (2): 119-158.

Ptak, T., Schmid, G. 1996. Dual-tracer transport experiments in a physically and chemically heterogeneous porous aquifer: effective transport parameters and spatial variability. J. Hydrol. 183 (1-2): 117-138.

Ptak, T., Teutsch, G. 1994. Forced and natural gradient tracer tests in a highly heterogeneous porous aquifer: instrumentation and measurements. J. Hydrol. 159: 79-104.

Puls, R.W., Powell, R.M., Clark, D.A., Paul, C.J. 1991. Facilitated transport of inorganic contaminants in ground water: Part II. colloidal transport. Environmental Research Brief, USEPA, EPA/600/M91/040. 12 pp.

Rajagopolan, R., Tien, C. 1976. Trajectory analysis of deep-bed filtration with the sphere-in-cell porous media model. AICh J. 22: 523-533.

Rajaram, H., Gelhar, L.W. 1993. Plume scale-dependent dispersion in heterogeneous aquifers – 1. Lagrangian analysis in a stratified aquifer. Water Resour. Res. 29 (9): 3249-3260.

Ray, D., Gibbs, M., Turner, S., Timany, G. 2000. Septic tanks leachate study for Rotorua Lakes. Prepared for Rotorua District Council. NIWA Client Report: RDC00205/2. 74 p.

Rijnaarts, H.H.M., Norde, W., Bouwer, E.J., Lyklema, J., Zehnder, A.J.B. 1996. Bacterial deposition in porous media related to the clean bed collision efficiency and to substratum blocking by attached cells. Environ. Sci. Technol. 30 (10): 2869-2876.

Ritter, W.F. 1990. Pesticide contamination of ground water in the United States - a review. J. Environ. Sci. Health 25. Part B: Pesticides, food contaminants and agricultural wastes: 1-29.

Roberts, P.V., Goltz, M.N., Mackay, D.M., 1986. A natural gradient experiment on solute transport in a sand aquifer, 3 , Retardation estimates and mass balances for organic solutes. Water Resour. Res. 22: 2047-2058.

Roco, M.C., Khadilkar, J., Zhang, J. 1989. Probabilistic approach for transport of contaminants through porous media. International Journal for Numerical Methods in Fluids 9 (12): 1431-1451.

Rose, J.B., Gerba, C.P. 1991. Use of risk assessment for development of microbial standards. Water Sci. Technol. 24 (2): 29-34.

Rubin, Y., Cushey, M.A., Wilson, A. 1997. The moments of the breakthrough curves of instantaneously and kinetically sorbing solutes in heterogeneous geologic media: prediction and parameter inference from field measurements. Water Resour. Res. 33(11): 2465-2481.

Sabatini, D.A.; Austin, T.A.L. 1991. Characteristics of rhodamine WT and fluorescein as adsorbing groundwater-water tracers. Ground Water 29: 341-349.

Schijven, J.F. 2001. Virus removal from groundwater by soil passage. Modeling, Field and Laboratory Experiments. PhD thesis. Civil Engineering and Geosciences, Delft University of Technology, Netherlands. 264 p. Printed by Ponsen & Looijen B.V., Wageningen. ISBN 90-646-4046-7.

Schijven, J.F., Hassanizadeh, S.M. 2000. Removal of viruses by soil passage: overview of modeling, processes, and parameters. Critical Reviews in Environmental Science and Technology 30(1): 49-127.

Schijven, J.F., Hoogenboezem, W., Hassanizadeh, S.M., Peters, J.H. 1999. Modelling Removal of Bacteriophages MS2 and PRD1 by Dune Infiltration at Castricum, The Netherlands. Water Resour. Res. 35: 1101-1111.

Schulin, R., Wierenga, P.J., Flühler, H., Leuenberger, J. 1987. Solute transport through a stony soil. Soil Sci. Soc. Am. J. 51: 36-42.

References:

Schwarzenbach, R.P., Westall, J. 1981. Transport of nonpolar organic compounds from surface water to groundwater: laboratory sorption studies. Environ. Sci. Technol. 15: 1360-1367.

Selim, H.M., 1989. Predication of contaminant retention and transport in soils using multireaction models. Environ. Health Perspect. 39: 69-75.

Shimojima, E., Sharma, M.L. 1995. The influence of pore water velocity on transport of sorptive and non-sorptive chemicals through an unsaturated sand. J. Hydrol. 164 (1-4): 239-261.

Sinclair, J.L., Lee, T.R. 1992. Biodegradation of atrazine in subsurface environments. United States Environmental Protection Agency, Environmental Research Brief, EPA/600/S-92/001. 8 p.

Singh, P., Kanwar, R.S. 1991. Preferential solute transport through macropores in large undisturbed saturated soil columns. J. Environ. Qual. 20: 295-300.

Sinton, L.W., Pang, L., Close, M.E., Noonan, M.J., Hall, C.H., Braithwaite, R.R. 2002. Relative transport and attenuation of bacteria and bacteriophages in an 8 m column of saturated, pea gravel. In preparation.

Sinton, L.W., Noonan, M.J., Finlay, R.K., Pang, L., Close, M.E. 2000. Relative reductions in bacterial and bateriophage concentrations in an alluvial gravel aquifer. N. Z. J. Mar. Freshwater Res. 34 (1): 175-186.

Sinton, L.W., Finlay, R.K., Pang. L., Scott, D.M. 1997. Transport of bacteria and bacteriophages in irrigated effluent into and through an alluvial gravel aquifer. Water, Air and Soil pollution 98 (1-2): 17-48.

Sinton, L.W. 1986. Microbial contamination of alluvial gravel aquifers by septic tank effluent. Water, Air, & Soil Pollution 28: 407-425.

Sim, Y., Chrysikopoulos, C.V. 1998. Three-dimensional analytical models for virus transport in saturated porous media. Transport in Porous Media 30: 87-112.

Sobsey, M.D., Shields, P.A., Hauchmann, F.H., Hazard, R.L., Caton, L.W. 1986. Survival and transport of hepatitis A virus in soils, groundwater, and wastewater. Water Sci. Technol. 18: 97-106.

Spurlock, F.C., Huang, K., van Genuchten, M.Th. 1995. Isotherm nonlinearity and nonequilibrium sorption effectsd on transport of fenuron and monuron in soil columns. Environ. Sci. Technol. 29: 1000-1007.

Srivastava, R., Brusseau, M.L. 1996. Nonideal transport of reactive solutes in heterogenous porous media, 1. Numerical model developement and moments analysis. J. Contam. Hydrol., 24(2): 117-143.

Stewart, L.W., Reneau, Jr.R.B. 1982. Movement of faecal coliform bacteria from septic tank effluent through coastal plain soils with high seasonal fluctuating water tables. Proceedings of the Third National Symposium on Small Community Sewage Treatment Chicago, December. 1981. pp. 319-327.

Stumm, W., Morgan, J.J. 1981. Aquatic chemistry. John Wiley & Sons, Inc. 780 pp.

Su, N., Sander, G.. 2002. Similarity Solutions of the Generalised Fokker-Planck Equation with Time and Scale-Dependent Dispersivity for Solute Transport in Fractal Porous Media. Submitted to Journal of Applied Mathematics.

The ARS Pesticide Properties Database, www.arsusda.gov/rsml/ppdb.html, as at May 2000.

Thorpe, H.R., Burden, R.J., Scott, D.M. 1982. Potential for contamination of the Heretaunga Plains Aquifers. *Water and Soil Technical Publication No.24*, 148 p.

Tomlin, C. (ed) 1994. The Pesticide Manual. The British Crop Protection Council & the Royal Society of Chemistry. 1341 pp.

Toride, N., Leij, F.J., van Genuchten, M.Th., 1995. The CXTFIT code for estimating transport parameters from laboratory or field. Version 2.0. U.S. Dep. Agric., Res. Rept. no. 138, 121 pp.

USEPA (United States Environmental Protection Agency). 1991. *Test methods for Escherichia coli in drinking waters.* United States Environmental Protection Agency. EPA-600/4-91/016.

USPHS. 1958. Manual of Septic Tank Practice. US Department of Health Education and Welfare, USPHS Publication No. 526, Bureau of State Services, Division of Sanitary Engineering Services.

References:

Valocchi, A.J. 1986. Effect of radial flow on deviations from local equilibrium during sorbing solute transport through homogenous soils. Water Resour. Res. 22(12): 1693-1701.

Valocchi, A.J. 1985. Validity of the local equilibrium assumption for modeling sorbing solute transport through homogenous soils. Water Resour. Res. 21(6): 808-820.

van Genuchten, M.Th., Alves, W.J., 1982. Analytical solutions of the one-dimensional convective-dispersive solute transport equation. U.S. Dep. Agrc. Tech. Bull. 1661, 151pp.

van Genuchten, M.Th., 1981. Non-equilibrium transport parameters from miscible displacement experiments. US Dep. Agric., Res. Rept., No. 119, 88 pp.

van Genuchten, M.Th.; Wierenga, P.J.; O'Connor, G.A. 1977. Mass transfer studies in sorbing porous media: III. Experimental evaluation with 2,4,5-T. Soil Sci. Soc. Am. Proc., 41, 278-285.

van Genuchten, M.Th.; Davidson, J.M.; Wierenga, P.J. 1974. An evaluation of kinetic and equilibrium equations for the prediction of pesticide movement through porous media. Soil Sci. Soc. Am. Proc., 38, 29-35.

Wan, J., Tokunaga, T.K., Tsang, C-F. 1995. Bacterial sedimentation through a porous medium. Water Resour. Res. 31 (7): 1627-1636.

Wauchope, R.D., Butter, T.M., Hornsby, A.G., Augustijn-Bechers, P.W.M., Burt, J.P. 1992. The SCS/ARS/CES Pesticide Database for environmental decision making. Reviews of Environmental Contamination and Toxicology. Vol. 123. Spring-Verlag. 164 pp.

Wheatcraft, S.W., Tyler, S.W. 1988. Explanation of Scale-Dependent Dispersivity in Heterogeneous Aquifers Using Concepts of Fractal Geometry. Water Resour. Res. 24 (4): 566-578.

Wilczak, A., Keinath, T.M. 1993. Kinetics of sorption and desorption of copper (II) and lead (II) on activated carbon. Water Environ. Res. 65(3): 238-244.

Wood, M., Harold, J., Johnson, A., Hance, R. 1991. The potential for atrazine degradation in aquifer sediments. in Pesticides in Soils and Water: Current Perspectives, ed by Walker A, British Crop Protection Council Monograph No 47, pp 175-182.

References:

Wood, A.L.; Davidson, J.M. 1975. Fluometuron and water content distributions during infiltration: measured and calculated. Soil Sci. Soc. Am. Proc., 39, 820-825.

Yahya, M.T., Galsomies, L., Gerba, C.P., Bales, R.C. 1993. Survival of Bacteriophages MS2 and PRD1 in Groundwater. Water Sci. Technol. 27: 409-412.

Yao, K.M., Habibian, M.T., O'Melia, C.R. 1971. Water and waste water filtration: concepts and applications. Environ. Sci. Technol. 5: 1105-1112.

Yates, M.V., Ouyang, Y. 1992. VIRTUS, a model of virus transport in unsaturated soils. Appl. Environ. Microbiol. 58: 1609-1616.

Yates, M.V., Yates, S.R. 1988. Virus survival and transport in groundwater. Water Sci. Tech. 20: 301-307.

Yates, M.V. 1985. Septic Tank Density and Groundwater Contamination. Ground Water 23: 586-591.

Yates, M.V., Gerba, C.P., Kelly, L.M. 1985. Virus persistence in groundwater. Appl. Environ. Microbiol. 49 (4): 778-781.

Yates, S.R. 1992. An analytical solution for one-dimensional transport in porous media with an exponential dispersion function. Water Resour. Res. 28(8): 2149-2154.

Yates, S.R. 1990. An analytical solution for one-dimensional transport in heterogeneous porous media. Water Resour. Res. 26(10): 2331-1338.

Yeh, G.T. 1981. AT123D: Analytical transient one-, two-, and three-dimensional simulation of waste transport in the aquifer system. ORNL-5602. Oak Ridge National Laboratory, Oak Ridge, Tennessee, 88 p.

Young, D.F., Ball, W.P. 2000. Column experimental design requirements for estimating model parameters from temporal moments under nonequilibrium conditions. Adv. Water Resour. 23: 449-460.

Yu, C., Warrick, A.W., Conklin, M.H. 1999. A moment method for analyzing breakthrough curves of step inputs. Water Resour. Res. 35(11): 3567-3572.

Zhang, R., Huang, K., Xiang, J. 1994. Solute movement through homogeneous and heterogeneous soil columns. Advances in Water Resources 17 (5): 317-324.

Zhao, X., Voice, T.C. 2000. Assessment of bioavailability using a multicolumn system. Environ. Sci. Technol. 34(8): 1506-1512.